BioMed Research International

New Biomaterials in Drug Delivery and Wound Care

Guest Editors: Šeila Selimović, Francesco Piraino, Robert Gauvin, and Hojae Bae

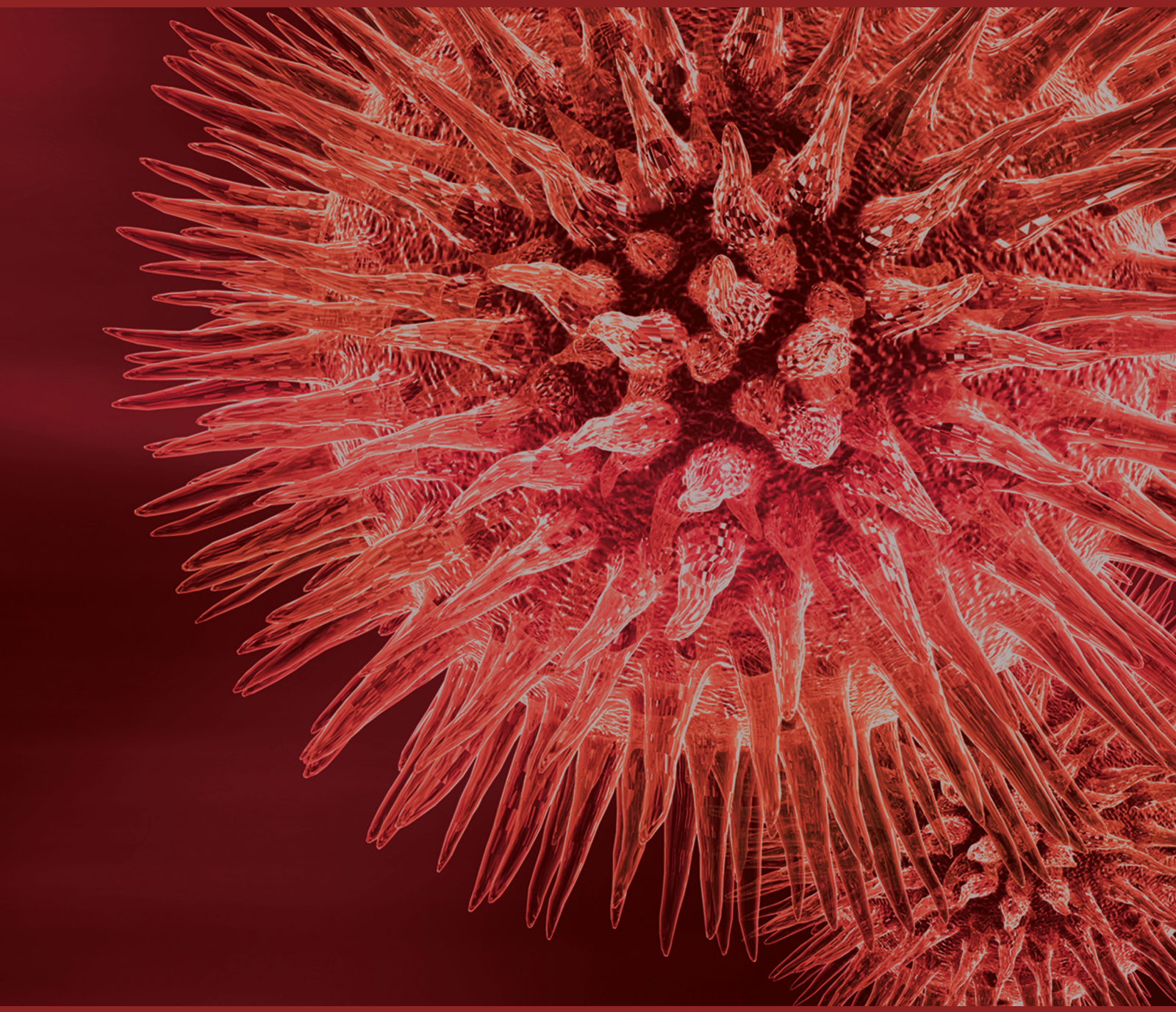

New Biomaterials in Drug Delivery and Wound Care

BioMed Research International

New Biomaterials in Drug Delivery and Wound Care

Guest Editors: Šeila Selimovic, Francesco Piraino, Robert Gauvin, and Hojae Bae

Contents

New Biomaterials in Drug Delivery and Wound Care, Šeila Selimović, Francesco Piraino, Robert Gauvin, and Hojae Bae
Volume 2015, Article ID 320496, 2 pages

Macrophage-Targeting Gene Delivery Using a Micelle Composed of Mannose-Modified Lipid with Triazole Ring and Dioleoyl Trimethylammonium Propane, Ichiki Fukuda, Shinichi Mochizuki, and Kazuo Sakurai
Volume 2015, Article ID 350580, 8 pages

A Current View of Functional Biomaterials for Wound Care, Molecular and Cellular Therapies, Francesco Piraino and Šeila Selimović
Volume 2015, Article ID 403801, 10 pages

Bone Regeneration from PLGA Micro-Nanoparticles, Inmaculada Ortega-Oller, Miguel Padial-Molina, Pablo Galindo-Moreno, Francisco O'Valle, Ana Belén Jódar-Reyes, and Jose Manuel Peula-García
Volume 2015, Article ID 415289, 18 pages

Naturally Occurring Extracellular Matrix Scaffolds for Dermal Regeneration: Do They Really Need Cells?, A. M. Eweida and M. K. Marei
Volume 2015, Article ID 839694, 9 pages

Custom-Made Antibiotic Cement Nails in Orthopaedic Trauma: Review of Outcomes, New Approaches, and Perspectives, Marcin K. Wasko and Rafal Kaminski
Volume 2015, Article ID 387186, 12 pages

Twelve-Month Results of a Single or Multiple Dexamethasone Intravitreal Implant for Macular Edema following Uncomplicated Phacoemulsification, Solmaz Abdolrahimzadeh, Vito Fenicia, Maurizio Maurizi Enrici, Pasquale Plateroti, Dora Cianfrone, and Santi Maria Recupero
Volume 2015, Article ID 362564, 6 pages

A Comparison of the Process of Remodeling of Hydroxyapatite/Poly-D/L-Lactide and Beta-Tricalcium Phosphate in a Loading Site, Hiroyuki Akagi, Hiroki Ochi, Satoshi Soeta, Nobuo Kanno, Megumi Yoshihara, Kenshi Okazaki, Takuya Yogo, Yasuji Harada, Hajime Amasaki, and Yasushi Hara
Volume 2015, Article ID 730105, 14 pages

Chitosan and Its Potential Use as a Scaffold for Tissue Engineering in Regenerative Medicine, Martin Rodríguez-Vázquez, Brenda Vega-Ruiz, Rodrigo Ramos-Zúñiga, Daniel Alexander Saldaña-Koppel, and Luis Fernando Quiñones-Olvera
Volume 2015, Article ID 821279, 15 pages

Potential of Newborn and Adult Stem Cells for the Production of Vascular Constructs Using the Living Tissue Sheet Approach, Jean-Michel Bourget, Robert Gauvin, David Duchesneau, Murielle Remy, François A. Auger, and Lucie Germain
Volume 2015, Article ID 168294, 10 pages

***In Vitro* Evaluation of Scaffolds for the Delivery of Mesenchymal Stem Cells to Wounds**, Elizabeth A. Wahl, Fernando A. Fierro, Thomas R. Peavy, Ursula Hopfner, Julian F. Dye, Hans-Günther Machens, José T. Egaña, and Thilo L. Schenck
Volume 2015, Article ID 108571, 14 pages

Hindawi Publishing Corporation
BioMed Research International
Volume 2015, Article ID 320496, 2 pages
http://dx.doi.org/10.1155/2015/320496

Editorial

New Biomaterials in Drug Delivery and Wound Care

Šeila Selimović,[1] Francesco Piraino,[2] Robert Gauvin,[3] and Hojae Bae[4]

[1]*American Association for the Advancement of Science, Arlington, VA 22202, USA*
[2]*Institute of Bioengineering, School of Engineering, École Polytechnique Fédérale de Lausanne, 1015 Lausanne, Switzerland*
[3]*Quebec Center for Functional Materials and Department of Surgery, Faculty of Medicine, Université Laval, Quebec City, QC, Canada G1V 0A6*
[4]*Department of Bioindustrial Technologies, College of Animal Bioscience and Technology, Konkuk University, Seoul 05029, Republic of Korea*

Correspondence should be addressed to Francesco Piraino; francesco.piraino@epfl.ch

Received 9 September 2015; Accepted 10 September 2015

Biological organisms evolve within specific conditions and constraints in their environment, giving rise to elegant and efficient strategies for fabricating materials that often outperform man-made materials of similar composition. Synthesizing and engineering novel bioinspired materials with similar characteristics require in-depth understanding of the properties, composition, and hierarchical organization of biological materials. These biomaterials are becoming increasingly incorporated into the medical sector, for example, as transport vehicles in drug delivery or as skin and soft tissue substitutes in wound management.

In this view, several investigators have been invited to contribute original research findings and reviews that could stimulate continuing efforts to understand new biomaterials with direct clinical applications in the interconnected fields of wound care, drug encapsulation, and transport. This special issue is divided into categories based on the following key words: stem cells, bone tissue engineering, functional biomaterials, scaffolds, and implants.

In the category of stem cells, J.-M. Bourget et al. evaluated the potential use of mesenchymal stem cells (MSCs) isolated from bone marrow-derived MSCs and umbilical cord blood-derived MSCs for blood vessel engineering. Their results reinforce the versatility of the self-assembly approach since they demonstrate that it is possible to recapitulate a contractile media layer from MSCs, without the need of exogenous scaffolding material. E. A. Wahl et al. compared the behavior of human adipose-derived MSCs seeded on four different biomaterials that are awaiting or have already received Food and Drug Administration approval to determine a suitable regenerative scaffold for delivering these cells to dermal wounds and increasing wound healing potential.

In the category of bone tissue engineering, I. Ortega-Oller et al. reported the use of nano- and/or microparticles of poly(lactic-co-glycolic acid) (PLGA) as a delivery system of the bone morphogenetic protein 2. R. Ramos-Zúñiga et al. concentrated on the intrinsic properties offered by chitosan and its use in tissue engineering, considering it as a promising alternative for regenerative medicine as a bioactive polymer. M. K. Wasko and R. Kaminski performed a systematic review of current evidence of antibiotic cement nails (ACNs) in orthopedic trauma and provided an up-to-date analysis of the indications, operative technique, failure mechanisms, complications, outcomes, and outlooks for the ACNs use in long bone infection.

In the category of functional biomaterials, F. Piraino and Š. Selimović discussed approaches in tissue engineering and regenerative medicine to address stages characterizing the mammalian response to tissue injury through the application of biomaterials. They also reviewed molecular therapies with particular attention to drug delivery methods and gene therapies. Finally, they examined cellular treatments and provided an outlook on the future of drug delivery and wound care biomaterials. I. Fukuda et al. synthesized two types of mannose-modified lipids with different stereoisomer (α-mannose and β-mannose). Their delivery system to

macrophages may overcome the problems for gene therapy and could be potentially used for treatment of immune diseases involved in macrophages.

In the category of scaffolds, A. M. Eweida and M. K. Marei reviewed the online published literature for the studies that performed extracellular matrix (ECM) revitalization believing that, in chronic and difficult-to-heal wounds, revitalizing the ECM scaffolds would be beneficial to overcome the defective host tissue interaction. H. Akagi et al. evaluated the utility of a hydroxyapatite (HA) and poly-DL-lactide (PDLLA) scaffold compared to β-tricalcium phosphate, at a loading site as a new bioresorbable scaffold.

Finally in the category of implants, S. Abdolrahimzadeh et al. evaluated the effectiveness of one or two intravitreal injections of a sustained release dexamethasone implant in patients with persistent macular edema following uncomplicated phacoemulsification. They observed a statistically significant improvement of mean central foveal thickness and best corrected visual acuity with one or two intravitreal dexamethasone implants over 12 months.

By collecting these papers, we hope to enrich our readers and researchers in the field of biomaterials in drug delivery and wound care. We believe that new biomaterials will be an important part of future drug delivery and wound care research activities.

Acknowledgments

We thank the authors participating in the present special issue.

Šeila Selimović
Francesco Piraino
Robert Gauvin
Hojae Bae

Hindawi Publishing Corporation
BioMed Research International
Volume 2015, Article ID 350580, 8 pages
http://dx.doi.org/10.1155/2015/350580

Research Article

Macrophage-Targeting Gene Delivery Using a Micelle Composed of Mannose-Modified Lipid with Triazole Ring and Dioleoyl Trimethylammonium Propane

Ichiki Fukuda,[1] Shinichi Mochizuki,[1] and Kazuo Sakurai[1,2]

[1]*Department of Chemistry and Biochemistry, The University of Kitakyushu, 1-1 Hibikino, Wakamatsu-ku, Kitakyushu, Fukuoka 808-0135, Japan*
[2]*NexTEP, Japan Science and Technology Agency, 4-1-8 Honcho, Kawaguchi, Saitama 332-0012, Japan*

Correspondence should be addressed to Kazuo Sakurai; sakurai@kitakyu-u.ac.jp

Received 9 March 2015; Accepted 28 May 2015

Academic Editor: Hojae Bae

Gene carriers with cell specific ligand molecules are needed for the treatment of several diseases. Mannose is known to be recognized and incorporated into the cells through mannose recognition lectins that are exclusively expressed on macrophages. In this study, we synthesized two types of mannose-modified lipids with different stereoisomer (α-mannose and β-mannose). To make a complex with plasmid DNA (pDNA), termed "lipoplex," we prepared a two-component micelle made from cationic lipid; dioleoyltrimethylammoniumpropane (DOTAP); and mannose-modified lipid (D/α-Man or D/β-Man). The prepared D/α-Man lipoplexes were able to bind to one of the α-mannose lectins concanavalin A (ConA) immobilized on gold substrate in the quartz-crystal microbalance sensor cell. D/β-Man lipoplexes did not show any frequency changes. These results indicate that the mannose residues were exposed on the lipoplexes, leading to not only the binding to ConA but also the prevention of nonspecific interactions with proteins. Both lipoplexes showed high transfection efficiencies to RAW264.7 cells which have several kinds of mannose lectins. This delivery system to macrophages may overcome the problems for gene therapy and may be used for the treatment of immune diseases involved in macrophages.

1. Introduction

The development of targeted cellular gene delivery systems is an important research theme for clinical applications of gene therapies. Although nonpathogenic viral vectors such as retroviruses and lentiviruses are mainly used, nonviral alternatives have been studied because of their advantages of safety and low manufacturing costs [1]. The most commonly used synthetic gene carriers are cationic lipids and polymers, which can form complexes with negatively charged plasmid DNA (pDNA) via electrostatic interactions. One of the greatest obstacles to overcome before they can be used in human therapy is their low uptake efficiency into the target cells because of a lack of cellular selectivity. To this end, cationic carriers are modified with various compounds to improve pDNA accumulation in the target cells. A typical example is attaching a carbohydrate as a ligand molecule. Some cells express lectins, which are carbohydrate-binding proteins that exhibit high specificity for sugar molecules. The relationships between carbohydrates and cells with lectin have been exploited for cell-specific drug delivery, such as galactose for hepatocytes [2–5], hyaluronic acid for liver sinusoidal endothelial cells [6, 7], and mannose for macrophages [8, 9].

Macrophages are immune cells that play an important role in immune system regulation. As proinflammatory cytokines secreted by macrophages are related to the pathogenesis of various inflammatory diseases such as acute hepatitis [10] and ulcerative colitis [11, 12], inhibiting such cytokines is beneficial for patients. Mannose-recognizing lectins are exclusively expressed on macrophages; they recognize glycoproteins with mannose, *N*-acetylglucosamine, and fucose residues and subsequently internalize them [13, 14]. Several studies have focused on mannose residues as a pilot molecule for targeting macrophages.

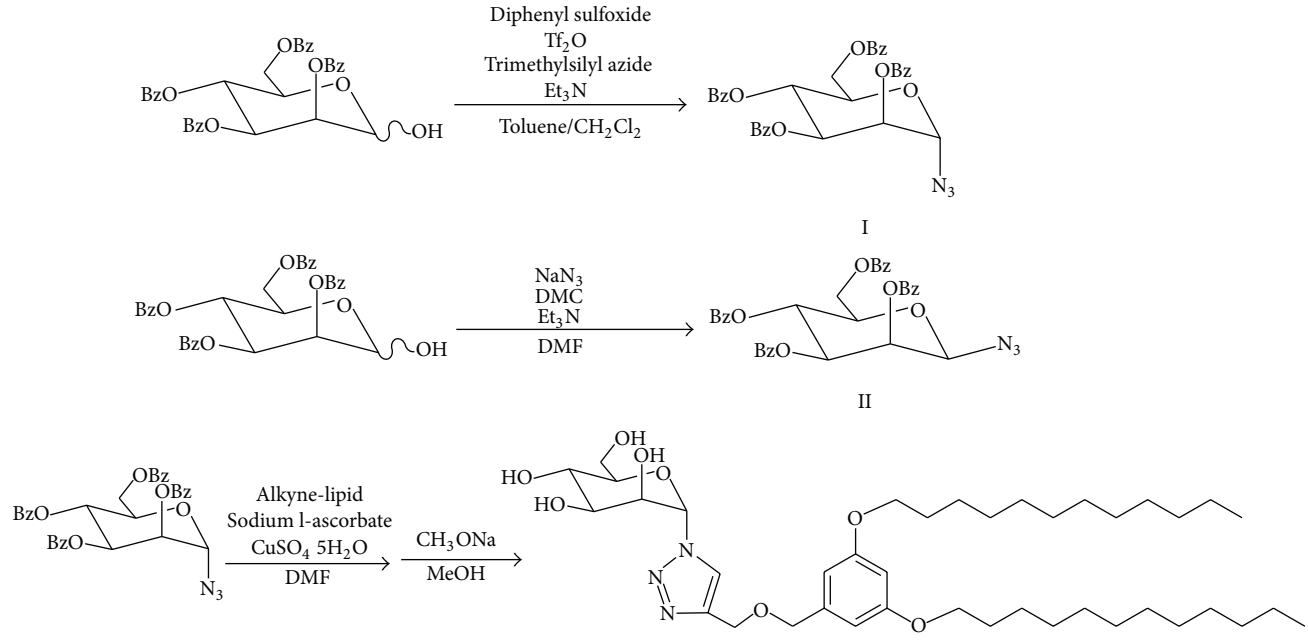

Scheme 1: Synthetic route of α-mannose- or β-mannose-modified lipid through click chemistry.

We previously reported a series of lipids with an aromatic linker connected with amine or amidine that can be used as transfection reagents with better efficiency and lower cytotoxicity than conventional reagents [15, 16]. Analysis of the hydrophobic moieties that induce high transfection efficiency by altering the alkyl chain lengths and the positions revealed that lipids with an amino residue attached to C12 in the meta-meta position exhibit the highest efficiencies [16]. In addition, lipids can form stable micelles at low concentrations as a result of hydrophobic interactions among aromatic rings and 2 alkyl chains as well as π-π stacking derived from aromatic rings. After synthesizing galactose-modified lipids, evaluation of the transfection efficiencies for hepatocytes with asialoglycoprotein receptor (ASGPR), which recognizes galactose and *N*-acetylgalactosamine residues on glycoproteins, revealed that the complexes comprising galactose-modified lipids, cationic lipids, and pDNAs exhibited ASGPR-dependent gene expression [5].

In the present study, we synthesized mannose-modified lipids with an aromatic ring with C12 in the meta-meta position. The mannose-modified lipids were mixed with cationic lipids to form complexes with DNA, termed "lipoplexes," and their transfection efficiencies in macrophages were evaluated.

2. Materials and Methods

2.1. Materials. 3,5-Dihydroxybenzaldehyde, potassium carbonate, propargyl bromide, and RPMI-1640 medium were purchased from Wako Pure Chemical Industries, Ltd., (Osaka, Japan). 1-Bromododecane, sodium borohydride, so dium hydride, 2,3,4,6-tetra-O-benzoly-D-mannopyranose, trifluoromethanesulfonic anhydride, diphenyl sulfoxide, N,N-dimethylformamide, trimethylsilyl azide, and 2-chloro-1,3-dimethylimidazolium chloride were purchased from Tokyo Chemical Industry Co., (Tokyo Japan). Sodium methoxide was purchased from Kanto Chemical Co., (Tokyo Japan). Copper(II)sulfate pentahydrate was purchased from Sigma-Aldrich (St. Louis, MO).

2.2. Synthesis of the Mannose-Modified Lipid (Scheme 1). 2,3,4,6-Tetra-O-benzoly-D-mannopyranose and diphenyl sulfoxide were mixed in solution of dichloromethane and toluene (dichloromethane : toluene = 1 : 3) at molar ratio of 1 : 1 and stirred at −78°C for 10 minutes. The reactant was added to trifluoromethanesulfonic anhydride at molar ratio of 1 : 1.3 and stirred at −45°C for 30 minutes. The reactant was added to trimethylsilyl azide at molar ratio of 1 : 5 and stirred at −45°C for 30 minutes, followed by −20°C for 2.5 hours [17]. The reaction mixture was extracted with ethyl acetate and purified compound I by silica gel chromatography using a mixture of ethyl acetate and hexane (ethyl acetate : hexane = 1 : 3) as a mobile phase.

2,3,4,6-Tetra-O-benzoly-D-mannopyranose, 2-chloro-1,3-dimethylimidazolium chloride, sodium azide, and triethylamine were mixed in solution of N,N-dimethylformamide at molar ratio of 1 : 10 : 10 : 3 and stirred at 0°C for 2 hours [18]. The reaction mixture was extracted with ethyl acetate and purified compound II by silica gel chromatography using a mixture of ethyl acetate and hexane (ethyl acetate : hexane = 2 : 3) as a mobile phase.

The compound I or compound II was an attached aromatic ring with C12 in the meta-meta position as shown in Scheme 1 in a similar manner to our previous report [5]. The obtained mannose-modified lipid was identified by ^{1}H NMR.

2.3. Preparation of the Lipoplex Composed of Mannose-Modified Lipid/Cationic Lipid Micelle and pDNA. We mixed the mannose-modified lipid and dioleoyltrimethylammoniumpropane (DOTAP; Sigma-Aldrich) at the same molar ratio and dissolved them in chloroform and vacuum dried. Each mixture was dissolved in water and added to the pDNA encoding luciferase (pGL3-Control Vector; Promega, Madison, WI) at the indicated N/P ratios (i.e., the cation/anion charge ratio, $[\text{cationic amino group}]_{\text{DOTAP}}/[\text{anionic phosphate group}]_{\text{nucleic acid}}$) and incubated for 1 hour. To confirm the complexation, the mixtures were separated by 1% agarose gel electrophoresis. DNA was stained with ethidium bromide and the image was obtained using a PharosFX (Bio-Rad, Richmond, CA).

2.4. ζ Potential and Size Measurements. We prepared the lipoplexes at indicated N/P ratios in 150 mM NaClaq, where we fixed DOTAP concentration at 0.3 mM. The zeta potentials and hydrodynamic radiuses were measured with a Nano-ZS (Malvern Instruments, Malvern, UK) at 25°C. The refractive index was 1.59.

2.5. Small-Angle X-Ray Scattering (SAXS) Measurement. SAXS measurements from the lipoplexes were carried out at BL40B2 SPring-8 with a 0.7 m camera using a Rigaku imaging plate (30 × 30 cm, 3000 × 3000 pixels) as a detector. The wavelength of the beam was 1.0 Å, and the exposure time was 300 seconds. The obtained two dimensional image was circularly averaged to give an intensity $I(q)$ versus q plots, where q is the magnitude of the scattering vector defined by $q = 4\pi \sin\theta/\lambda$ with the scattering angle of 2θ. The concentration of mannose-modified lipids was 3 mM.

2.6. Interaction between Concanavalin A (ConA) and Lipoplexes. ConA (Wako) was immobilized on gold substrate in the quartz-crystal microbalance (QCM) sensor cell (AFFINIX QN μ; INITIUM, Inc., Tokyo, Japan) at 10 μg/mL for 1 h at r.t. After blocking with 1% BSA in PBS for 1 h, the sensor cell was filled with 500 μL of 10 mM HEPES containing 2 mM $CaCl_2$ adding the samples at 36 μg/mL and measuring the frequency changes at 25°C.

2.7. Gene Transfection. RAW264.7 cells were seeded at 2.0×10^4 cells in a 96-well microplate and incubated at 37°C under 5% CO_2. The cells were cultured in RPMI-1640 containing 10% FBS and 100 U/mL penicillin and 0.1 mg/mL streptomycin. After 24 hours, the cells were transfected with the pDNA at 0.2 μg/mL using the lipoplexes or Lipofectamine 2000 (Invitrogen, Carlsbad, CA). In brief, on the day of transfection, the wells were replaced with fresh medium without serum and added the lipoplexes at the indicated N/P ratio. After 6 hours, the wells were replaced with fresh medium containing serum. After 48 hours, the cells were washed with PBS twice adequately and then lysed with a lysis buffer from the luciferase assay kit (Promega). After adding luciferin, the luciferase activity in an aliquot of the cell lysate was measured with a luminescence plate reader (Wallac 1420; Perkin Elmer, Wellesley, MA). The protein concentration of each well lysate was determined with a standard protein assay (Dojindo, Kumamoto, Japan). The luciferase activity in each sample was normalized to the luminescence intensity per microgram of protein.

3. Results

3.1. Lipoplex Preparation and Characterization. As the 2 prepared kinds of mannose-modified lipids (Scheme 1) have no cationic charge, they are unable to form a complex with pDNA via electrostatic interactions. In addition, the mannose-modified lipids themselves cannot form micelles in aqueous solution owing to their low solubility. In our previous study, we added the cationic lipid DOTAP to sugar-modified lipids with the same features to compensate for the deficits described above [5]. In fact, the mixture of DOTAP with sugar-modified lipid was dispersed in aqueous solution, forming lipoplexes with pDNA. Therefore, we added DOTAP to mannose-modified lipid at the same molar ratio; thus, we prepared binary micelles comprising DOTAP and α-mannose- or β-mannose-modified micelles, which were designated D/α-Man and D/β-Man, respectively. After mixing pDNA with D/α-Man, D/β-Man, or DOTAP at the indicated N/P ratios, lipoplex formation was examined by agarose gel electrophoresis (Figure 1). With DOTAP, there were no free pDNA bands observed at N/P > 2. The same results were obtained for the mixtures of pDNA with D/α-Man and D/β-Man micelles, indicating that the addition of mannose-modified lipids does not disturb lipoplex formation or galactose- or glucose-modified lipids. Therefore, D/α-Man and D/β-Man form stable complexes at N/P > 2.

The hydrodynamic radii and ζ potentials of the resultant lipoplexes were measured at various N/P ratios. The hydrodynamic radii were almost all ~100 nm and they exhibited a small polydispersity at all N/P ratios (Figure 2 and Supplementary Table 1 available online at http://dx.doi.org/10.1155/2015/350580). Supplementary Figure 1 shows the histograms of the lipoplexes at N/P = 2. All lipoplexes exhibited a single peak. These results indicate that the lipoplexes were dispersed without forming large aggregates. The ζ potentials of all samples increased with the increasing N/P ratio, plateauing at N/P = 3. The ζ potentials of all micelles exhibited around −40 mV (data not shown), which is consistent with the plateaued values. In particular, they changed drastically from a negative to a positive charge between N/P 1 and 2. The positive charge at N/P = 2 means that all pDNA was covered by cationic compounds, which is consistent with the complete complex formation at N/P = 2 (Figure 1). The ζ potentials of D/α-Man and D/β-Man lipoplexes were lower than those of DOTAP lipoplexes at N/P = 2 even at the same concentration of DOTAP. The ζ potential is related to the electrical charge at the interface between a solid surface and its liquid medium and does not reflect the total charge of the entire particle [19]. Therefore, these results suggest that both lipoplexes express the mannose residues on the surface, resulting in low ζ potential. The high positive ζ potentials at N/P > 3 can be attributed to the excessive feed of D/α-Man and D/β-Man micelles against pDNA. As high ζ

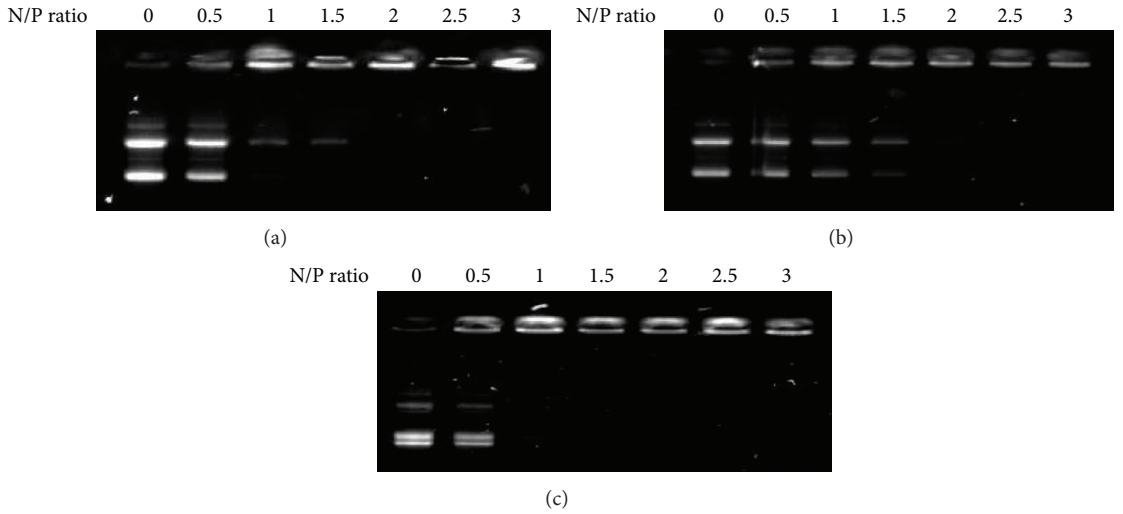

Figure 1: Confirmation of the complexation between pDNA and D/α-Man (a), D/β-Man (b), or DOTAP (c) micelles at indicated N/P ratios.

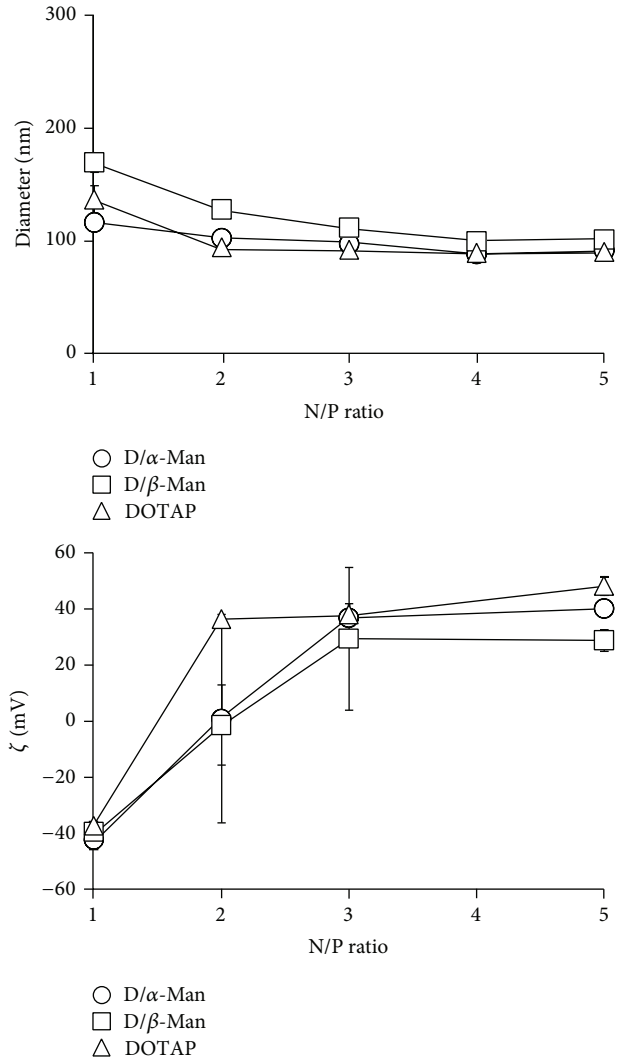

Figure 2: Diameters and ζ potentials for the lipoplexes determined with dynamic light scattering measurements.

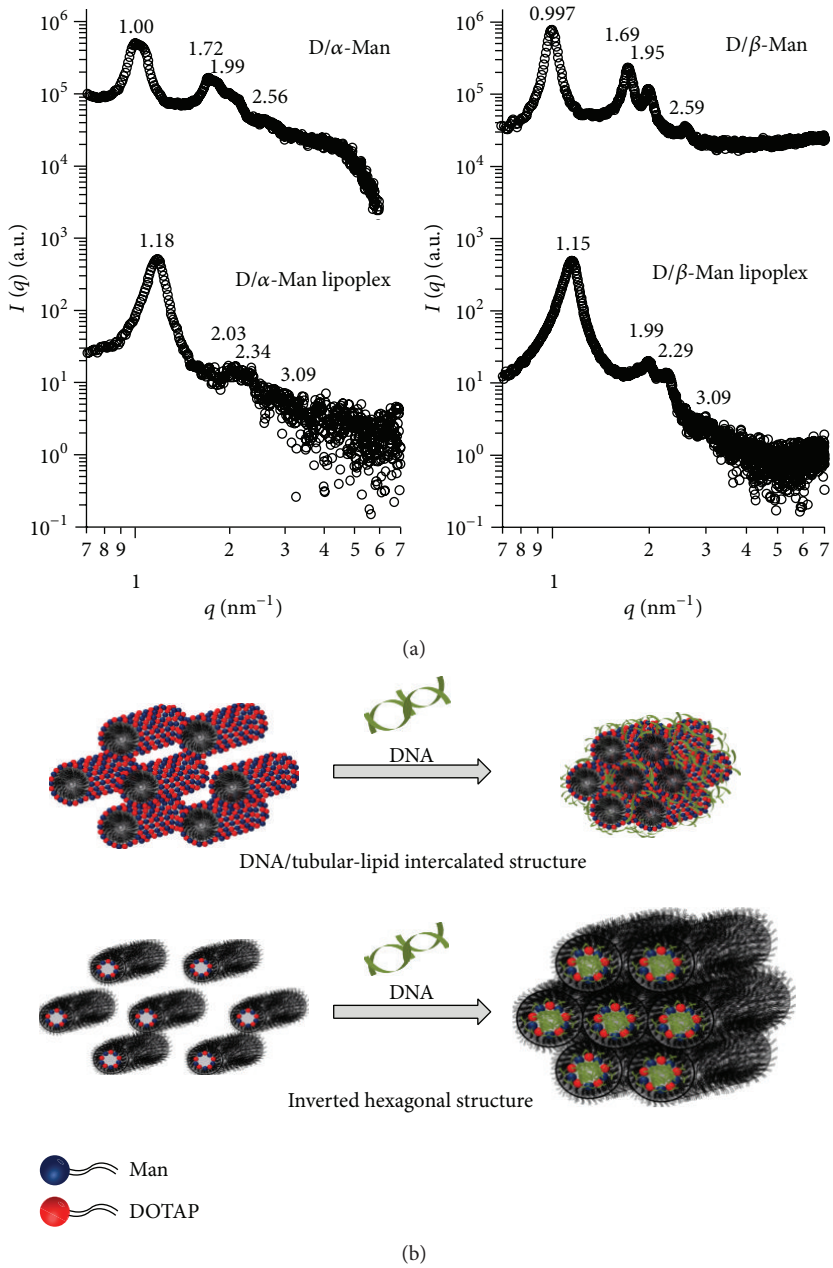

Figure 3: SAXS profiles of D/α-Man and D/β-Man micelles before and after complexation with pDNA at N/P = 2 (a) and the schematic illustration showing the structure of D/α-Man and D/β-Man lipoplexes (b).

potential might lead to nonspecific cellular uptake because of the electrostatic interaction between cellular membranes and lipoplexes, we used lipoplexes at N/P = 2 for all subsequent examinations.

Safinya et al. propose a relationship between the supramolecular structure of lipoplexes and their transfection efficiency with use of SAXS [20–23]. They state that the addition of pDNA causes most cationic lipids to undergo structural transition and that some form hexagonally packed cylinders including inverted hexagonal [21] and DNA/tubular-lipid intercalated structures [22]. Therefore, we examined the structures of D/α-Man and D/β-Man before and after complexation with pDNA by using SAXS (Figure 3(a)). All samples exhibited sharp diffraction peaks, indicating the formation of ordered structures. The positions satisfied the relation of $1:\sqrt{3}:2:\sqrt{7}$, indicating that the micelles and lipoplexes formed a hexagonally packed cylindrical structure [24]. For both types of micelles, the addition of pDNA did not alter hexagonal packing, but the peak positions were shifted to the wider angle side. The intercylinder distances determined from the peak positions for D/α-Man, D/β-Man, D/α-Man lipoplexes, and D/β-Man lipoplexes were 7.25, 7.28, 6.15, and 6.31 nm, respectively. These results indicate that negatively charged pDNA reduces or cancels electrostatic

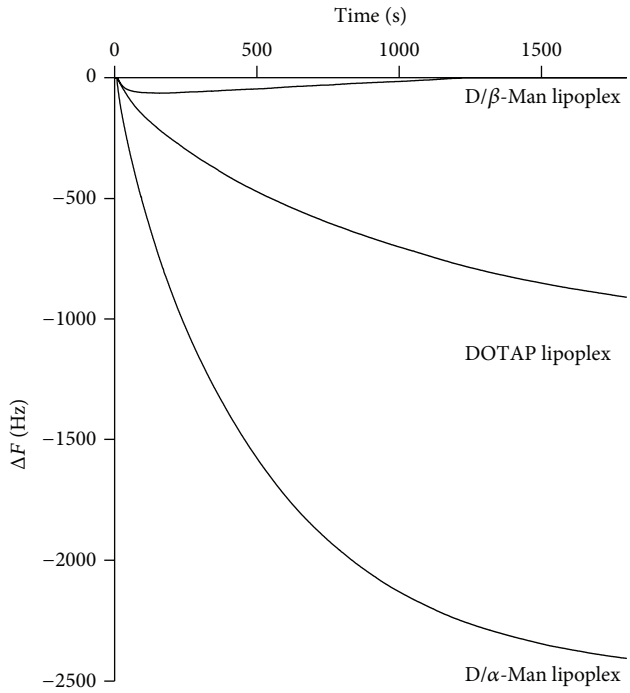

Figure 4: Time courses of frequency changes of ConA immobilized QCM in response to addition of the lipoplexes (N/P = 2).

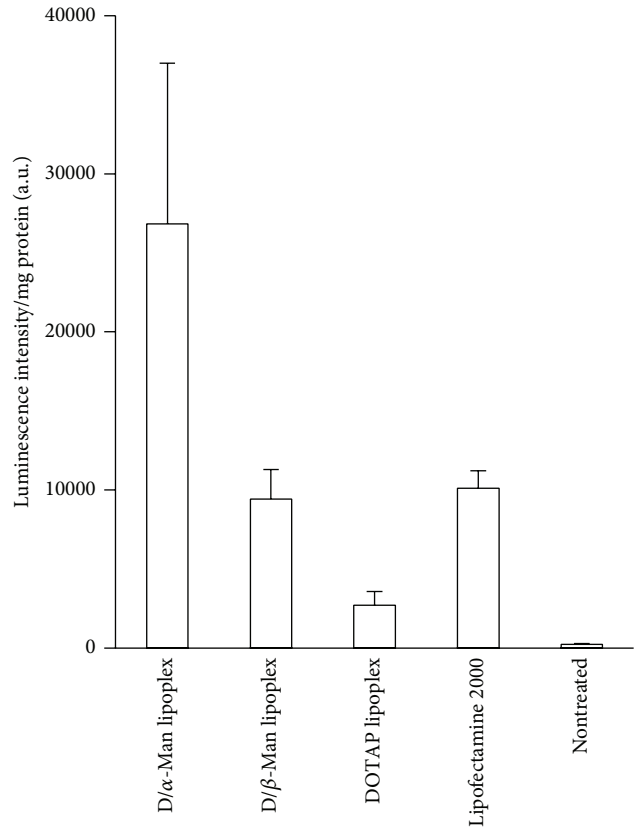

Figure 5: Transfection efficiencies for the lipoplexes at N/P = 2. Data represent the mean ± S.D. of triplicate wells.

repulsions between adjoining tubular lipids through intercalation, resulting in contracted cylinder distance; this implies that both lipoplexes adopt a DNA/tubular-lipid intercalated packing (Figure 3(b)).

In summary, at N/P = 2, D/α-Man, and D/β-Man, lipoplexes have the same characteristics including particle size, surface charge, and inner structure in which tubular lipids and pDNA are hexagonally packed within the particles.

3.2. Binding of D/α-Man and D/β-Man Lipoplexes to ConA. We previously reported that lipoplexes comprising galactose-modified lipids, DOTAP, and pDNA bound to ASGPR resulted in strong gene expression in HepG2 cells containing ASGPRs. In the present study, we examined the binding of D/α-Man and D/β-Man lipoplexes to mannose-recognition proteins with QCM. QCM measures the decrease in the frequency of a quartz-crystal immersed in solutions, which is directly related to the increase in mass due to the surface adsorption of guest molecules onto the resonator. ConA was used as a model protein because it is a lectin that recognizes α-D-mannosyl and α-D-glucosyl groups [25]. Figure 4 shows that the QCM frequency changes when equal masses of D/α-Man, D/β-Man, or DOTAP lipoplexes were added to the QCM cell. The addition of D/α-Man lipoplexes rapidly decreased the frequency, whereas the addition of D/β-Man lipoplexes did not. The addition of DOTAP lipoplexes slightly decreased the frequency, albeit a smaller extent than D/α-Man lipoplexes. DOTAP lipoplexes, which have strong cationic characteristics, are considered to nonspecifically bind or adsorb to ConA or bovine serum albumin coated on the sensor cell via electrostatic interactions. These results indicate that the mannose moieties in the lipoplexes are exposed to the surface. β-mannose on the lipoplexes shields the cationic characteristic of DOTAP and prevents nonspecific binding, whereas α-mannose not only exhibited the same effect as β-mannose but also was definitely recognized and bound to the binding site.

3.3. Gene Expression Efficiency. We subsequently examined gene expression efficiency in murine macrophage RAW264.7 cells. D/α-Man lipoplexes induced the highest gene expression, which was 3 times higher than that induced by Lipofectamine 2000 (Figure 5). D/β-Man lipoplexes induced gene expression to the same level as that of Lipofectamine 2000. Meanwhile, DOTAP lipoplexes induced much lower gene expression than D/α-Man and D/β-Man lipoplexes. These results suggest that D/α-Man and D/β-Man lipoplexes can induce gene expression in macrophages with the aid of mannose-modified lipid; in particular, the gene expression was strongly dependent on α-mannose compared to β-mannose.

4. Discussion

Carriers with cell-specific ligand molecules can be critical for efficient targeted gene delivery. Because sugar is guaranteed to have high specificity for its particular lectin, sugar

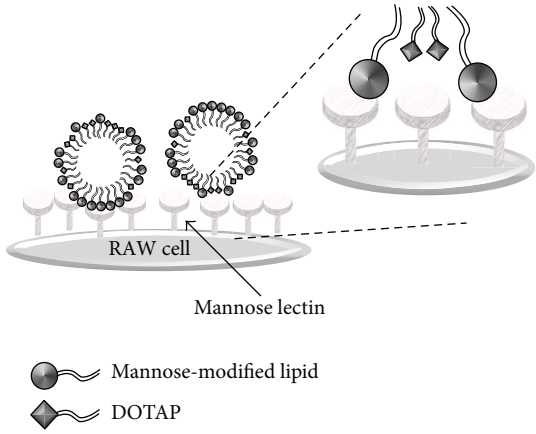

Figure 6: The schematic illustration showing the configurational relationship between mannose-modified lipids and DOTAP in the micelles.

modification is a useful strategy for the abovementioned purpose. Furthermore, for some lectins, the affinity of their ligands increases with the valence of sugar residues. Lee et al. demonstrate that multivalent glycosides simultaneously bind to receptors, enhancing affinity in comparison to monovalent glycosides [26, 27]; this phenomenon is known as the "cluster effect." Only cationic lipids or polymers can be used to bind pDNA to carriers. The N/P ratio is one of the factors that determine transfection efficacy. Although the lipoplexes with a high N/P ratio can easily interact with cellular membranes, they can simultaneously exhibit strong cellular toxicity. Lipoplexes with sugars on their surface can be used to resolve this dilemma, because they can be recognized by lectins even at low N/P ratios.

We prepared 2 types of stereoisomeric mannose-modified lipids as ligands for mannose lectin and generated micelles by mixing DOTAP for pDNA binding. The lipoplexes bound to the mannose lectin ConA (Figure 4) and induced high transfection efficiency in RAW264.7 cells (Figure 5). These results strongly indicate that mannose residues can be exposed to the surface of lipoplexes. Considering its molecular structure, DOTAP bends greatly because of the *cis*-double bonds in the alkyl chains. The linear length of DOTAP is shorter than that of mannose-modified lipids. Therefore, most DOTAP is considered to be located internally in the micelles (Figure 6), decreasing the ζ potential of D/α-Man and D/β-Man lipoplexes compared to that of DOTAP lipoplexes (Figure 2) as well as preventing nonspecific proteins interactions (Figure 4).

We prepared micelles by mixing mannose-modified lipids and DOTAP at the same molar ratio. Fortunately, the lipoplexes exhibited mannose-dependent gene expression, suggesting that the configurations between mannoses and their density on the lipoplexes are sufficient for recognition by lectins. Their configurations are mainly dominated by the mannose-modified lipid content in micelles and can be easily controlled by changing the mixing ratio between mannose-modified lipids and DOTAP. Therefore, it is possible to optimize lipoplexes for inducing further transfection efficiency.

Macrophages have several kinds of mannose lectins such as CD206 (mannose receptor) [28, 29], CLEC4E [30, 31], and CLEC12A [32, 33]. Although some lectins are known to mainly recognize α-mannose, fucose, and high mannose with a mixture of α- and β-linkages, the recognition of other lectins remains unknown [14]. RAW cells may express mannose lectins that preferentially recognize α-mannose, resulting in higher transfection efficiency of D/α-Man lipoplexes than D/β-Man lipoplexes (Figure 5).

In conclusion, lipoplexes comprising equimolar amounts of pDNA and D/α-Man exhibit good transfection efficiency at N/P = 2. Although D/α-Man and D/β-Man lipoplexes do not differ with respect to size, surface charge, or supramolecular structure, they distinctly differ with respect to ConA recognition, indicating the exposure of mannose residues on these lipoplexes. Both lipoplexes exhibited high gene expression, which may be dependent on the expression level of mannose lectins on RAW cells. Therefore, the present study suggests that our lipoplexes with mannose residues can be used in the treatment of macrophage-related diseases.

Disclosure

All SAXS measurements were carried out at SPring-8 40B2 (2013A1207).

Conflict of Interests

The authors declare that there is no conflict of interests regarding the publication of this paper.

References

[1] S. Kawakami, Y. Higuchi, and M. Hashida, "Nonviral approaches for targeted delivery of plasmid DNA and oligonucleotide," *Journal of Pharmaceutical Sciences*, vol. 97, no. 2, pp. 726–745, 2008.

[2] G. Y. Wu and C. H. Wu, "Receptor-mediated in vitro gene transformation by a soluble DNA carrier system," *Journal of Biological Chemistry*, vol. 262, no. 10, pp. 4429–4432, 1987.

[3] M. Hashimoto, M. Morimoto, H. Saimoto, Y. Shigemasa, and T. Sato, "Lactosylated chitosan for DNA delivery into hepatocytes: the effect of lactosylation on the physicochemical properties and intracellular trafficking of pDNA/chitosan complexes," *Bioconjugate Chemistry*, vol. 17, no. 2, pp. 309–316, 2006.

[4] J. C. Perales, G. A. Grossmann, M. Molas et al., "Biochemical and functional characterization of DNA complexes capable of targeting genes to hepatocytes via the asialoglycoprotein receptor," *The Journal of Biological Chemistry*, vol. 272, no. 11, pp. 7398–7407, 1997.

[5] M. Sakashita, S. Mochizuki, and K. Sakurai, "Hepatocyte-targeting gene delivery using a lipoplex composed of galactose-modified aromatic lipid synthesized with click chemistry," *Bioorganic & Medicinal Chemistry*, vol. 22, no. 19, pp. 5212–5219, 2014.

[6] S. Asayama, M. Nogawa, Y. Takei, T. Akaike, and A. Maruyama, "Synthesis of novel polyampholyte comb-type copolymers consisting of a poly(L-lysine) backbone and hyaluronic acid side chains for a DNA carrier," *Bioconjugate Chemistry*, vol. 9, no. 4, pp. 476–481, 1998.

[7] Y. Takei, A. Maruyama, A. Ferdous et al., "Targeted gene delivery to sinusoidal endothelial cells: DNA nanoassociate bearing hyaluronan-glycocalyx," *The FASEB Journal*, vol. 18, no. 6, pp. 699–701, 2004.

[8] M. Hashimoto, M. Morimoto, H. Saimoto et al., "Gene transfer by DNA/mannosylated chitosan complexes into mouse peritoneal macrophages," *Biotechnology Letters*, vol. 28, no. 11, pp. 815–821, 2006.

[9] K. Un, S. Kawakami, M. Yoshida et al., "The elucidation of gene transferring mechanism by ultrasound-responsive unmodified and mannose-modified lipoplexes," *Biomaterials*, vol. 32, no. 20, pp. 4659–4669, 2011.

[10] M. Leist, F. Gantner, S. Jilg, and A. Wendel, "Activation of the 55 kDa TNF receptor is necessary and sufficient for TNF- induced liver failure, hepatocyte apoptosis, and nitrite release," *Journal of Immunology*, vol. 154, no. 3, pp. 1307–1316, 1995.

[11] D. K. Podolsky, "Inflammatory bowel disease," *The New England Journal of Medicine*, vol. 347, no. 6, pp. 417–429, 2002.

[12] R. J. Xavier and D. K. Podolsky, "Unravelling the pathogenesis of inflammatory bowel disease," *Nature*, vol. 448, no. 7152, pp. 427–434, 2007.

[13] R. Townsend and P. Stahl, "Isolation and characterization of a mannose/N-acetylglucosamine/fucose-binding protein from rat liver," *Biochemical Journal*, vol. 194, no. 1, pp. 209–214, 1981.

[14] T. B. H. Geijtenbeek and S. I. Gringhuis, "Signalling through C-type lectin receptors: shaping immune responses," *Nature Reviews Immunology*, vol. 9, no. 7, pp. 465–479, 2009.

[15] K. Koiwai, K. Tokuhisa, R. Karinaga et al., "Transition from a normal to inverted cylinder for an amidine-bearing lipid/pDNA complex and its excellent transfection," *Bioconjugate Chemistry*, vol. 16, no. 6, pp. 1349–1351, 2005.

[16] S. Mochizuki, Y. Kamikawa, K. Nishina et al., "Relationship between DNA-transfection efficiency and chemical structures of aromatic cationic lipids," *Bulletin of the Chemical Society of Japan*, vol. 85, no. 3, pp. 354–359, 2012.

[17] K. D. Bodine, D. Y. Gin, and M. S. Gin, "Synthesis of readily modifiable cyclodextrin analogues via cyclodimerization of an alkynyl-azido trisaccharide," *Journal of the American Chemical Society*, vol. 126, no. 6, pp. 1638–1639, 2004.

[18] T. Tanaka, H. Nagai, M. Noguchi, A. Kobayashi, and S.-I. Shoda, "One-step conversion of unprotected sugars to beta-glycosyl azides using 2-chloroimidazolinium salt in aqueous solution," *Chemical Communications*, no. 23, pp. 3378–3379, 2009.

[19] A. V. Delgado, F. González-Caballero, R. J. Hunter, L. K. Koopal, and J. Lyklema, "Measurement and interpretation of electrokinetic phenomena," *Journal of Colloid and Interface Science*, vol. 309, no. 2, pp. 194–224, 2007.

[20] K. Ewert, N. L. Slack, A. Ahmad et al., "Cationic lipid-DNA complexes for gene therapy: understanding the relationship between complex structure and gene delivery pathways at the molecular level," *Current Medicinal Chemistry*, vol. 11, no. 2, pp. 133–149, 2004.

[21] I. Koltover, T. Salditt, J. O. Rädler, and C. R. Safinya, "An inverted hexagonal phase of cationic liposome-DNA complexes related to DNA release and delivery," *Science*, vol. 281, no. 5373, pp. 78–81, 1998.

[22] K. K. Ewert, H. M. Evans, A. Zidovska, N. F. Bouxsein, A. Ahmad, and C. R. Safinya, "A columnar phase of dendritic lipid-based cationic liposome-DNA complexes for gene delivery: hexagonally ordered cylindrical micelles embedded in a DNA honeycomb lattice," *Journal of the American Chemical Society*, vol. 128, no. 12, pp. 3998–4006, 2006.

[23] F. Yeh, E. L. Sokolov, A. R. Khokhlov, and B. Chu, "Nanoscale supramolecular structures in the gels of poly (diallyldimethylammonium chloride) interacting with sodium dodecyl sulfate," *Journal of the American Chemical Society*, vol. 118, no. 28, pp. 6615–6618, 1996.

[24] F. Yeh, E. L. Sokolov, A. R. Khokhlov, and B. Chu, "Nanoscale supramolecular structures in the gels of poly(diallyldimethylammonium chloride) interacting with sodium dodecyl sulfate," *Journal of the American Chemical Society*, vol. 118, no. 28, pp. 6615–6618, 1996.

[25] M. Schwarz, L. Spector, A. Gargir et al., "A new kind of carbohydrate array, its use for profiling antiglycan antibodies, and the discovery of a novel human cellulose-binding antibody," *Glycobiology*, vol. 13, no. 11, pp. 749–754, 2003.

[26] Y. C. Lee, R. R. Townsend, M. R. Hardy et al., "Binding of synthetic oligosaccharides to the hepatic Gal/GalNAc lectin. Dependence on fine structural features," *The Journal of Biological Chemistry*, vol. 258, no. 1, pp. 199–202, 1983.

[27] R. T. Lee, P. Lin, and Y. C. Lee, "New synthetic cluster ligands for galactose/N-acetylgalactosamine-specific lectin of mammalian liver," *Biochemistry*, vol. 23, no. 18, pp. 4255–4261, 1984.

[28] J. Zhang, J. Zhu, X. Bu et al., "Cdc42 and RhoB activation are required for mannose receptor-mediated phagocytosis by human alveolar macrophages," *Molecular Biology of the Cell*, vol. 16, no. 2, pp. 824–834, 2005.

[29] J. L. Miller, B. J. M. DeWet, L. Martinez-Pomares et al., "The mannose receptor mediates dengue virus infection of macrophages," *PLoS Pathogens*, vol. 4, no. 2, article e17, 2008.

[30] S. Yamasaki, E. Ishikawa, M. Sakuma, H. Hara, K. Ogata, and T. Saito, "Mincle is an ITAM-coupled activating receptor that senses damaged cells," *Nature Immunology*, vol. 9, no. 10, pp. 1179–1188, 2008.

[31] S. Yamasaki, M. Matsumoto, O. Takeuchi et al., "C-type lectin Mincle is an activating receptor for pathogenic fungus, Malassezia," *Proceedings of the National Academy of Sciences of the United States of America*, vol. 106, no. 6, pp. 1897–1902, 2009.

[32] A. S. J. Marshall, J. A. Willmen, H.-H. Lin, D. L. Williams, S. Gordon, and G. D. Brown, "Identification and characterization of a novel human myeloid inhibitory C-type lectin-like receptor (MICL) that is predominantly expressed on granulocytes and monocytes," *Journal of Biological Chemistry*, vol. 279, no. 15, pp. 14792–14802, 2004.

[33] C. H. Chen, H. Floyd, N. E. Olson et al., "Dendritic-cell-associated C-type lectin 2 (DCAL-2) alters dendritic-cell maturation and cytokine production," *Blood*, vol. 107, no. 4, pp. 1459–1467, 2006.

Hindawi Publishing Corporation
BioMed Research International
Volume 2015, Article ID 403801, 10 pages
http://dx.doi.org/10.1155/2015/403801

Review Article

A Current View of Functional Biomaterials for Wound Care, Molecular and Cellular Therapies

Francesco Piraino[1] and Šeila Selimović[2]

[1]*Institute of Bioengineering, School of Engineering, École Polytechnique Fédérale de Lausanne, 1015 Lausanne, Switzerland*
[2]*American Association for the Advancement of Science, Washington, DC 20520, USA*

Correspondence should be addressed to Francesco Piraino; francesco.piraino@epfl.ch

Received 18 March 2015; Revised 20 August 2015; Accepted 23 August 2015

Academic Editor: Tetsuji Yamaoka

The intricate process of wound healing involves activation of biological pathways that work in concert to regenerate a tissue microenvironment consisting of cells and external cellular matrix (ECM) with enzymes, cytokines, and growth factors. Distinct stages characterize the mammalian response to tissue injury: hemostasis, inflammation, new tissue formation, and tissue remodeling. Hemostasis and inflammation start right after the injury, while the formation of new tissue, along with migration and proliferation of cells within the wound site, occurs during the first week to ten days after the injury. In this review paper, we discuss approaches in tissue engineering and regenerative medicine to address each of these processes through the application of biomaterials, either as support to the native microenvironment or as delivery vehicles for functional hemostatic, antibacterial, or anti-inflammatory agents. Molecular therapies are also discussed with particular attention to drug delivery methods and gene therapies. Finally, cellular treatments are reviewed, and an outlook on the future of drug delivery and wound care biomaterials is provided.

1. Introduction

Tissue repair and wound healing are complex physiological processes in which the damaged tissue repairs itself after an injury, such as a superficial cut, internal bleeding, or excision of a tumor. The wound healing process is generally divided into the sequential, but partially overlapping phases (Figure 1) of hemostasis (clotting to stop bleeding), inflammatory response (removal of bacteria and tissue debris from the site of damage), proliferation (cell division to regenerate the tissue, angiogenesis, and matrix deposition), and remodeling (cellular apoptosis and matrix realignment in the newly generated tissue) [1]. The wound healing response involves direct cell-to-cell and cell-matrix communication, in addition to the indirect communication between different cell types *via* soluble molecules. These interactions can be enhanced or accelerated by the strategic delivery of hormones, hemostatic agents, anti-inflammatory drugs, angiogenesis-inducing compounds, and cell growth factors.

The specifics of a therapeutic approach depend on the type of wound and tissue properties. For example, wounds can be incisional (closed) or excisional (open), acute (result of a cut or a gunshot) or chronic (due to a long-term infection or underlying disease). In the latter case, the wound healing process is disrupted. Both superficial and internal wounds can be treated with a number of dressings, which range from topical pharmaceutical formulations as well as gauzes and synthetic dressings to modern materials like hydrocolloids, hydrogels and foams, and biomaterials. The type of wound dictates the choice of drug and drug delivery vehicle to aid the tissue repair process: a dressing might be chosen for its ability to absorb exudates from the wound or to degrade and release a biopolymer used in the proliferation stage. Another material might prove a better drug delivery vehicle, while yet another one would be better suited to encapsulating cell growth factors. Last, but not least, factors affecting the choice of treatment also include cost, ease of handling, and the ability to accelerate the healing process.

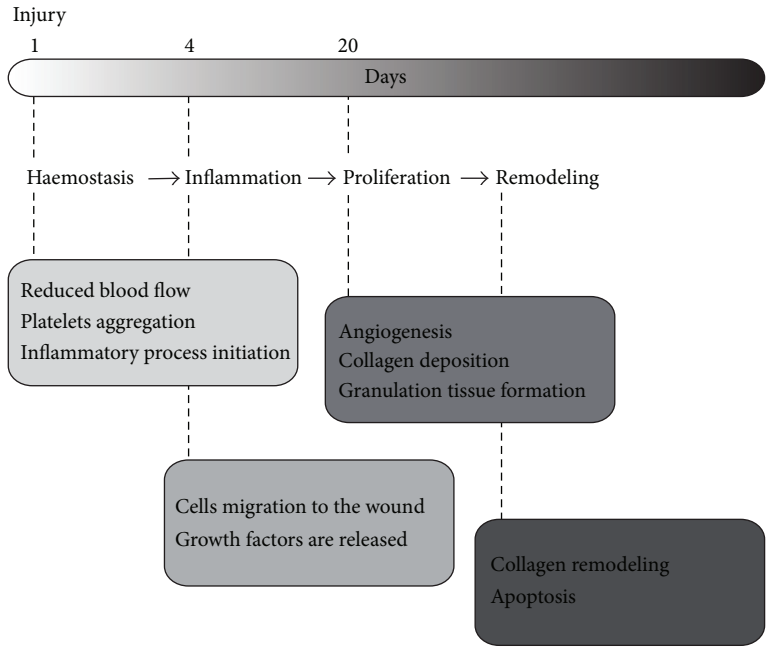

Figure 1: Overview of the wound healing process. The injury is immediately followed by hemostasis, which is characterized by reduced blood flow, platelet aggregation, and initiation of the inflammatory process. During the inflammation response, cells migrate to the wound and release growth factors. In a later stage of the wound healing process, the proliferation stage, angiogenesis is followed by deposition of collagen and the formation of granulation tissue. Finally, collagen fibers align in the remodeling stage and cells that have fulfilled their wound healing function enter apoptosis.

In this review, we focus on wound healing processes in adult tissue (as opposed to fetal tissue) and introduce a number of molecules that play key roles in these processes. We then discuss interactions between tissues and biomaterials, such as requirements for biomaterial-based dressings. Finally, we address molecular and cellular therapies for treatment of external and internal wounds.

2. The Natural Wound Healing Process

2.1. Hemostasis. Hemostasis involves a series of processes that work together to stop the bleeding from a wound. In intact blood vessels, endothelial cells secrete the coagulation inhibitor thrombomodulin and produce prostacyclin and nitric oxide to prevent aggregation of platelets [2]. In case of an injury to a blood vessel, endothelial cells switch to producing von Willebrand factor (vWF) in order to jump start hemostasis. Concurrent with this process is vasoconstriction in order to limit the amount of blood leaving the damaged vessel and is followed by the formation of a platelet plug that blocks the break in the vessel. The last step in hemostasis is the formation of a fibrin clot through production of plasma factor VII (FVII) [3, 4] and prothrombin. Fibrin is a type of collagen fiber and is produced around the platelet plug, anchoring it in place [5]. White and red blood cells become entrapped in the fibrin structure, a process called blood coagulation. Both the platelet plug and fibrin clot serve to seal the physical hole in the blood vessel until the tissue is healed.

2.2. Inflammatory Response. In the inflammation phase, interleukins, a type of cytokine, are activated. Interleukin 6 (IL-6) [6] stimulates macrophage activation and chemotaxis of monocytes, and interleukin 8 (IL-8) [7] encourages neovascularization and proliferation of neutrophils. The different types of leukocytes are responsible for countering pathogens and for degrading the damaged tissue and creating new, healthy tissue. The remaining stages of the wound healing response are particularly sensitive to an abnormal increase or reduction in leukocyte activity.

2.3. Proliferation. In the proliferation stage, macrophages and neutrophils release chemoattractants to draw fibroblasts to the wound site and enable synthesis and remodeling of the extracellular matrix (ECM) [8]. Cellular migration is aided by the production of hyaluronic acid (HA), which absorbs water and lends the tissue the ability to resist deformation [9].

2.4. Remodeling. Collagen is the most abundant structural protein in the human ECM. Collagen Type I predominates and is upregulated by decorin in wound healing [10]. The production of disorganized and strongly cross-linked Type I collagen structures leads to fibrosis or scars, new tissue that is visually distinct from the surrounding, undamaged tissue.

Remodeling of the ECM is also facilitated by proteases such as tissue-derived inhibitors (TIMPs) and matrix metalloproteinases (MMPs), for example, collagenase [8]. The formation of scars is marked by increased TIMP-1 [11] and

TIMP-3 [12] activity. In general, scarring is accompanied by a lower MMP to TIMP expression ratio, as a slow collagen turnover leads to increased protein accumulation. Plasminogen is another protease central to wound repair [13]. When activated to plasmin, it promotes fibrinolysis, preventing the fibrin clot from growing and ultimately degrading it.

Transforming growth factor-betas are a family of cytokines involved in many parts of the cell cycle: cell growth, proliferation, differentiation, and apoptosis [14]. They serve as chemotactic for fibroblasts, stimulating production of collagen Type I. Concurrently, TGF-β also decreases MMP expression, leading to the accumulation of collagen. In case of an injury to the tissue, expression of TGF-β is upregulated by signaling factors like decorin, fibromodulin, and hypoxia-inducible factor-1-alpha (HIF-1-alpha). With respect to cutaneous wounds, TGF-β signaling in keratinocytes is reduced, leading to accelerated reepithelization of the wound [15].

Two additional growth factors that enhance fibrosis are the platelet-derived growth factor (PDGF) [16, 17] and fibroblast growth factor (FGF) [18]. PDGF serves as a fibroblast chemoattractant and its expression increases during the formation of fibrotic tissue. FGF is actually a collection of multiple cytokines such as keratinocyte growth factors, which are expressed more strongly in wound repair than in healthy tissue.

Lastly, a cytokine that signals endothelial cells to enter the mitotic stage is the vascular endothelial growth factor (VEGF) [19]. Noteworthy, the expression of VEGF is increased in nonfibrotic wounds compared to scar wounds.

3. Interactions between Tissues and Biomaterials

3.1. Functional Requirements of Wound Repair Biomaterials. Hydrogel-based dressings for skin wounds provide a barrier between the wound and the external environment, thus preventing infection and absorbing exudates (such as water, plasma, and red blood cells). Similarly, biomaterials used for internal wounds should repel or damage microbes and other infectious agents, be hydrophilic and sufficiently porous to absorb exuded liquids, and/or have a large enough swelling factor to fill any voids within the damaged tissue. In order to prevent an inflammatory response to the hydrogel itself, the material should be biologic and degradable on a time scale comparable to the wound healing process (on the order of days) [20, 21]. In addition, hydrogels can serve as delivery vehicles for drugs and other wound healing compounds and can be manipulated to allow for controlled release of these components in both space and time [22, 23]. Hence, the cellular response at a wound site can be controlled and significantly accelerated by providing hemostatic, immunomodulatory, antibiotic, angiogenesis, and cell growth agents as regulated by hydrogel carriers.

Medical dressings are engineered to fulfill one or several functions: stem bleeding by helping to seal the wound, absorb plasma, blood, and other exuded fluids, debride the wound by removing foreign objects from the site, protect the affected area from pathogens, and aid the granulation or improve epithelization. Depending on the goal of the treatment, the dressing can be designed to control the moisture content of the wound, prevent an infection, or maintain the optimal microenvironment (such as pH and temperature). The treatment goal then dictates the design parameters of the biological dressing, such as hydrophilicity (dressing can be either hydrophilic or hydrophobic to control the rate of fluid passage from the wound), porosity and swelling ratio (to allow an encapsulated drug to diffuse into the wound), and degradation (to release the biomaterial into the wound and aid the tissue regeneration).

More specifically, advanced wound therapies focus, among others, on either preventing ECM damage by delivering specific proteins to the wound site or enabling ECM synthesis through various growth factors or autologous proteins. For example, ECMs contained in hydrogel-based dressings can allow cellular adhesion and thus aid tissue regeneration.

The goals listed above can be achieved with a number of bioactive hydrogels, such as those based on collagen, HA, chitosan, alginate, or elastin, or also multiarm (poly)ethylene glycol (PEG) precursors. For example, certain molecules from the ECM can be tethered to hydrogels such as PEG to render them bioactive [24]. Such bioactive hydrogels have been shown to be cytocompatible and do not provoke significant inflammatory responses, but they nonetheless provide useful physical and chemical characteristics to support the tissue regeneration process [20, 25]. For example, alginate-based dressings usually have large swelling ratios and are capable of absorbing large exudate volumes in wounds [26]. In addition, they can also be applied to dry wounds after a treatment with saline. Collagen, being the main structural protein in various connective tissues, is a prime candidate for dressings providing ECM structures [27]. Next, chitin and chitosan are known for their adhesive, but also antibacterial and fungicidal properties. This makes both polymers useful for wound dressings in any form ranging from fibers and membranes to larger scaffolds and hydrogels [28, 29]. Hyaluronan, another chief component of the ECM, is also associated with ECM remodeling and contributes to cell proliferation [9, 30]. For example, some dressings used for chronic wound treatment utilize hyaluronan-based scaffolds, with fibronectin connected to the protein to aid the migration of cells into the wound. Finally, elastin is a load-bearing and a greatly stretchable protein in connective tissue that helps, for example, skin reestablish its barrier function after an injury [31]. Elastin also helps induce ECM synthesis, cell migration, and production of proteases.

Aside from their native properties, various biomaterials can be used to deliver functional molecules to the wound site, including therapeutics. For example, alginate and PEG are easily functionalized using chemical conjugation methods [32], while poly(lactic-*co*-glycolic acid) (PLGA) based materials [33, 34] can be used for controlled release of molecules embedded into the biomaterial scaffold. Stromal cell-derived factor (SDF, a set of cytokines that activate leukocytes), VEGF, and PDGF can be encapsulated into PLGA capsules and released over time to induce endothelial cell migration and vessel formation or to stabilize blood vessels and ultimately

induce angiogenesis. As a result, PLGA finds applications in sutures and implants due to its degradation properties.

By functionalizing biomaterials or tuning their physical properties, it is possible to design novel wound healing materials with optimal antibacterial, anti-inflammatory, and adhesive properties. To induce desired hemostatic processes, glycoproteins such as the vWF can be encapsulated into the biomaterials scaffolds [35]. In addition, anti-inflammatory molecules can be delivered to the wound site encapsulated in calcium alginate gels [26]. Finally, the antibacterial properties of some biomaterials dressings can be boosted by encapsulating antibacterial agents such as vancomycin [36] and amoxicillin [37] into the scaffolds and hydrogels.

3.2. Biomaterials Interactions at the Surface. The surface interaction between biomaterials and the damaged tissue occurs at various length scales, from the organ (millimeters to centimeters) and tissue scale (millimeters) to the scale of individual cells (micrometers) and proteins (nanometers) [38, 39]. A tissue or part of an organ can be in contact with a biomaterial-based ECM or dressing for weeks, and in the case of organs even up to months or years, and the interactions are based on physical contact, tissue ingrowth, and chemical bonding. The smaller the tissue component, the shorter the interaction time: individual cells interact with a biomaterial for days or weeks *via* integrin, while individual proteins (such as glycosaminoglycans (GAGs)) interact through secondary bonding and hydrophobic interactions on time scales as short as seconds and minutes. Among the physical and mechanical interaction mechanisms are the entanglement of macromolecules and interdigitation of the ECM with the physical biomaterial structure, for example, pores. The main chemical type of interaction is ionic, covalent, or metallic, and it can be accompanied by hydrogen bonding and van der Waals and hydrophobic interactions.

Biomaterial surfaces can induce changes in cell phenotype, including the cell morphology, development, or biochemical properties. Knowing this, various properties of biomaterial-based dressings can be engineered to facilitate an optimal tissue regeneration rate. For example, the pore size of a scaffold can serve to regulate the migration speed of cells: the smaller the average pore size, the lower the fibroblast migration speed in collagen-GAG scaffolds [40]. Nonetheless, it has been shown that other cells, such as prostate cancer cells, migrate faster than fibroblasts through the same scaffold. In addition, a decrease in pore diameter is linked to an increase in the specific biomaterial surface, offering a greater density of binding sites for cell attachment.

Using collagen as an example, one can delay the biomaterial degradation by tuning the degree of crosslinking, grafting GAG molecules onto collagen fibers, and preserving the native polymer structure (or avoiding the premature degradation of collagen into gelatin) [41]. Noteworthy, it has been showed that the melting of the quaternary collagen structure can reduce thrombosis by inhibiting platelet clotting and decrease the inflammatory response [42]. In general, biomaterial scaffolds (regeneration templates) can lose their activity if their chemical composition, quaternary protein structure, pore size, and rate of degradation are outside of the optimal range.

4. Molecular Therapies

4.1. Drug Delivery Methods. Most therapeutics are administered orally, in the form of aerosols, liquids, capsules, or tablets, such that they enter the circulatory system through the gut lining (or, in the case of aerosols, through the lung). Intravascular and intramuscular injections are another often used transportation method that allows the circulatory system to transport the drug throughout the body, including to the wound site [43–46]. In the case of external or open wounds, dressings can also contain bioactive agents that are embedded into the biomaterial scaffold. In general, drug delivery devices rely on their specifically designed physical and chemical properties (described earlier) to transport the drug and ultimately deliver the appropriate bioactive agent at the appropriate time to the site of interest, the wound site. The therapeutics or bioactive agents range from small-molecule drugs to antibodies, proteins, plasmid DNA, and oligonucleotides. Noteworthily, drug delivery devices do not only deliver molecules to the wound site, but can also control the presentation of the encapsulated agents. One example is the use of genetically modified cells that are engineered to express various growth factors or cytokines, a common approach in gene therapy.

4.2. Gene Therapy. Gene therapy is a research field focusing on genetic modification of cells for therapeutic purposes. This discipline has developed approaches for permanent or transient cellular transformation. The concept of gene therapy arose during the 1970s when Friedmann and Roblin proposed guidelines for the gene therapy in humans [47]. Since then, gene therapy for wound treatments has mainly been represented in experiments with animal wound models [48]. Nevertheless, the development of new gene therapy protocols for treatment of a wide array of monogenetic as well as multifactorial diseases has continued and lately Margolis and coworkers reported the results of the first clinical trial in humans for gene therapy in wound healing [49].

The cellular events driving regenerative processes are strongly regulated by complex molecular mechanisms. Manipulation of these mechanisms at the genetic level offers several advantages over exogenous application of substances.

In vivo or *in vitro* methodologies can be employed to convey genes to the tissue of interest [50]. In the first approach, the cells are isolated, cultured, and genetically modified *in vitro* and subsequently implanted into the tissue as illustrated in Figure 2. Although laborious, the method enables selective gene transfer to the specific targeted cell type. The efficiency of the transfection can be quantified and the risk of systemic contamination can be reduced by automation. Furthermore, the risks of detrimental effects related to systemic vector administration are avoided. The second approach includes direct delivery of the gene to the targeted cell. Vectors may be directed to the site of tissue repair by topical application, injection or carried by biomaterial scaffolds. The limitations

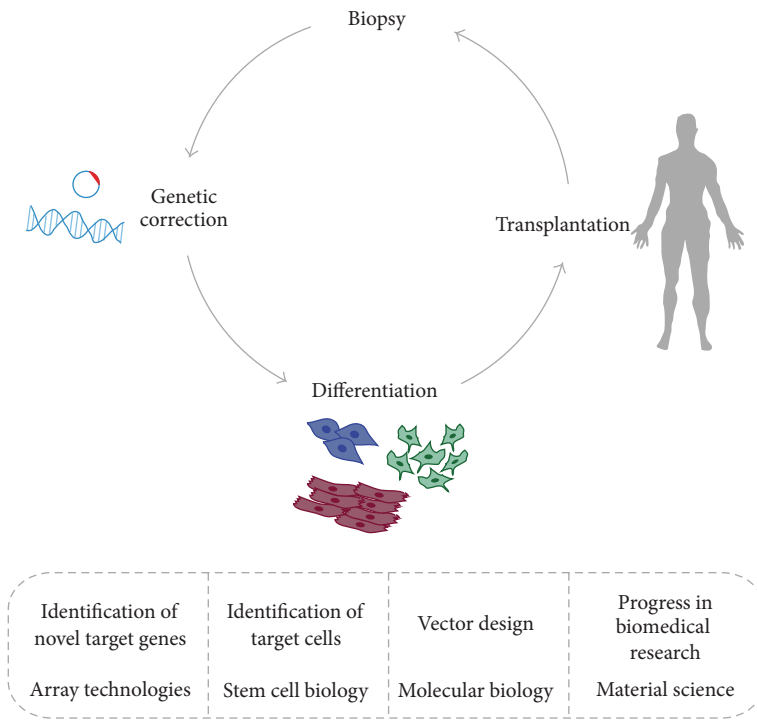

FIGURE 2: Genetic modifications for patient-specific therapy. This technique can be divided into three main phases. First, a biopsy is performed and cells are expanded *in vitro*. Second, a gene is introduced into these cells. Finally, the genetically engineered cells are transplanted to the patient. The dashed box reports the different research fields involved in this type of approach.

of this method are the low transfection efficiency and the lack of complete specificity. The selection of an appropriate delivery system is vital for effective gene therapy. The cells must be able to take up the transgene and express the product within a specific time period in a required amount. Moreover, any gene delivery technology should be nontoxic, atraumatic and should not evoke immune responses [51].

The various delivery systems can be categorized into biological, physical, and chemical techniques. Biological methods are additionally classified into viral and nonviral methods. Viral methods use viruses as vectors for delivery of the genetic material to the recipient cell. Nonviral biological vectors may be bacteria, bacteriophages, virus-like particles, or biological liposomes. The nonbiological methods for gene delivery may be physical and chemical. The transgenes to be delivered are incorporated into closed circular DNA molecules called plasmids. Electroporation, ultrasound, needle injection, or hydrodynamic delivery engages a physical force to deliver the transgene into the cell. Chemical approaches use natural or synthetic substances as transgene carriers.

The increased understanding of the complex molecular mechanisms that regulate cells participating in tissue repair has laid a foundation for therapeutic interventions with the purpose of enhancing wound healing. Such therapies could be applied to increase the rate of wound healing and enhance the quality of newly formed tissue in wounds complicated by delayed or insufficient healing. Furthermore, molecular mechanisms could be manipulated to prevent excessive scarring in fibrotic conditions such as hypertrophic scars and keloids. In this context, gene therapy offers several advantages over direct administration of peptide factors. Peptides delivered to the wound environment are highly susceptible to proteolytic degradation, lowering the effective dose. Furthermore, sequestration by the wound matrix may prevent binding to receptors at the surfaces of cells. Gene therapy allows sustained and regulated secretion of factors in their proper spatial and temporal context. This aspect is particularly important as growth factors may have different effects depending on cell type, concentration, and other simultaneous signals from soluble factors, adhesion molecules, and matrix components.

Growth factor genes have been widely used in experimental gene therapy to enhance wound healing. The most commonly used approach has been to overexpress genes that stimulate reepithelialization [52] or angiogenesis [53–56].

Gene therapy has shown great promise in the experimental setting as a way to enhance wound healing. Clinical trials are underway to assess the safety of various gene therapy protocols in human subjects. Further development will, however, be needed to bring gene therapy from the experimental setting to established clinical practice. To achieve this, several issues will have to be addressed. Technologies for gene delivery will have to be further improved to achieve cell-type specific and efficient transformation without eliciting an immune response or provoking toxic reactions. Gene therapy in wound healing should not be limited to the overexpression of single growth factors with the aim to accelerate tissue

repair. The identification of new target genes will be an important step to increase the possibilities for quantitatively as well as qualitatively enhanced wound healing. In particular the targeting of genes coding for intracellular factors may become a way to increase the therapeutic specificity. Furthermore, simultaneous delivery of several transgenes, and at different time-points, will increase the possibilities to stimulate several events, acting in concert to enhance healing.

5. Cellular Therapies

Usually wound management involves examining the cause of injury and letting the body to recover. The emergence of regenerative medicine coupled with an increased understanding of the cellular and biochemical factors involved in wound repair has provided new therapeutic options which aim to alter the wound microenvironment facilitating regeneration.

5.1. Biomaterials for Cell Therapies. Polymers originating from biological sources are usually divided into nucleotide, protein and poly(amino acid), and polysaccharide and poly(hydroxyalkanoate). Biopolymers have been investigated for the preparation of biomaterials for a range of applications. However, biomaterial scaffolds from biopolymers often require improved mechanical properties, control of porosity, and optimized processing for practical use, regenerative medicine. Many studies concerning the preparation and application of biopolymer-based scaffolds have been conducted. Table 1 reports references for some biopolymers.

The development of cellular therapies for wound repair dates back more than 30 years with the publication of the first successful protocols for the culture of keratinocytes [57]. Eventually, small sheets of cells were developed [58]. Since these early efforts, a better understanding of the wound healing process, coupled with advances in cell culture techniques and the development of *in vitro* bioreactor systems, has led to the creation of more complex tissue engineered constructs.

Current constructs lack the functional sensory nerves. Melanocytes have been used to repopulate burn scars and for the treatment of vitiligo [59], but they have yet to be included in a commercial skin substitute. A significant limitation has been the limited viability of allogeneic cells used in the majority of tissue engineered skin equivalents and the high cost and limited shelf life associated with using autologous cells. Skin needs to be capable of regeneration, growth, and adaptation to the wound site. Cell persistence is therefore an important consideration in developing new skin substitutes. While the objective of cellular therapies is to create a substitute for skin *in vitro* that can integrate into the engraftment site *in vivo*, an alternative approach is to engineer a biocompatible, resorbable matrix that can recruit the native tissue cells to the injured site and facilitate wound healing. Control of the wound microenvironment is a critical aspect of this wound healing approach. As has been demonstrated with the currently available living skin equivalents, the delivery of ECM components and growth factors, and not necessarily the delivery of cells, to the site of injury appears to have the most beneficial effect [60]. Recent discoveries in stem cell biology and regenerative medicine have emphasized a strategy that may be more productive than the traditional cell-centric approach. By providing the correct microenvironmental niche, it may be possible to promote wound regeneration *in situ*.

Table 1: A selection of biopolymers used in wound healing.

Biologically derived polymers	References
Poly(hydroxyalkanoate)s	[80]
Poly[(R)-3-hydroxybutyrate]	[81–83]
Worm silk	[84]
Spider silk	[85]
Collagen	[27, 41, 42, 86]
Elastin	[31, 87–90]
Resilin	[91–93]
Keratin/chitosan	[94]
Cellulose	[95]

5.2. Stem Cells for Wound Healing. Treatment of nonhealing wounds has remained difficult in spite of the better understanding of pathophysiologic principles. Early data suggest the use of multipotent stem cells in order to accelerate wound healing. Until recently, research has mostly been focused on bone marrow-derived mesenchymal stem cells; still adipose-derived stem cells (ADSCs) and those derived from hair follicles gain more and more interest for potential application for the restoration of various injured tissues.

Stem cells are considered able to differentiate and have a lengthy self-renewal capacity [61, 62]. These properties have raised the hope that human embryonic stem cells (hESCs) can be valuable for the treatment of various injuries [63]. Notwithstanding their exceptional potential, the use of embryonic stem cells remains debated in scientific and political circles. To circumvent ethical issues, Yamanaka and coworkers created pluripotent somatic cells by direct reprogramming and generated pluripotent stem cells from human somatic cells that were analogous to hESCs [64, 65]. Therefore, stem cells derived from adult sources could potentially be similar to embryonic stem cells. The opportunity to regenerate injured tissues is opening the way to new cures that require strict assessment in preliminary clinical trials.

Encouraging findings from stem cell-based treatments in postinfarction myocardial repair [66] have led to the application of similar strategies in order to treat skin wounds [67–70]. Nonetheless, stem cells use seems beneficial over diffusible factors because stem cells can interact with their wound microenvironment [71]. Conversely, despite the above-mentioned improvement in wound healing using various stem cell lines, several issues need to be pondered before administering stem cells to patients. For example, stem cells functionality decreases with age; thus, older patients may not present the perfect population as donors [72]. Also, the risk of immunological rejection upon transplant or transfusion must be considered in case of using stem cells from allogenic sources. The mode of stem cells delivery is

another frequently discussed issue. Ideally, stem cells should keep their multipotency until administered in order to boost engraftment [70].

In conclusion, wound healing necessitates a sound combination of cell migration and proliferation, in addition to ECM deposition, angiogenesis, and remodeling. A variety of sources have been exploited to isolate stem cells for wound healing. Still, additional efforts are necessary in order to solve the many questions on stem cells' clinical application.

6. Conclusion and Outlook

Over the past decades, extraordinary advances and improved understanding in medicine, materials science, and engineering have led to great achievements in drug delivery and wound healing. In addition, microfluidic technologies have shown unparalleled advantages for biomaterials synthesis and for design of drug delivery systems based on cells. Furthermore, generation of concentration gradients of biochemical molecules [73] and within hydrogels [74, 75] plays a key role in tissue morphogenesis as well as in wound healing, bacterial invasion, and immune response. Microfluidics can additionally offer integrated structures to resemble the *in vivo* cellular environment. The transition from 2D to 3D cell culture has developed as a growing number of studies have established meaningful changes in the morphology, migration, differentiation, and viability of cells between 3D and 2D. Hence, efforts have been made to produce 3D platforms to mimic the *in vivo* microenvironment [76–78]. Based on these events, we expect that in the future integrated microfluidic devices for wound care will be able to monitor all the vital signs of the healing process, such as oxygen levels and temperature, and make adjustments when needed and communicate the information to health professionals on- or off-site [79].

Challenges, however, still exist. For example, gene delivery technologies will require further improvement to enable cell-type specific and efficient transformation without provoking an immune response. Ideally, both cellular and acellular treatments should enable delivery and spatiotemporal control of multiple molecules at the wound site without requiring intervention from a medical professional. Finally, the identification of new target genes as well as new biomaterial compounds with multiple tunable characteristics will be vital to a major step forward in wound healing treatments. Thus, future investigation in this path will be of tremendous relevance for translational medicine and therapeutics applications.

Conflict of Interests

No competing financial interests exist for either author.

References

[1] G. C. Gurtner, S. Werner, Y. Barrandon, and M. T. Longaker, "Wound repair and regeneration," *Nature*, vol. 453, no. 7193, pp. 314–321, 2008.

[2] A. S. Colwell, M. T. Longaker, and H. P. Lorenz, "Mammalian fetal organ regeneration," *Advances in Biochemical Engineering/Biotechnology*, vol. 93, pp. 83–100, 2005.

[3] P. Golino, "The inhibitors of the tissue factor: factor VII pathway," *Thrombosis Research*, vol. 106, no. 3, pp. V257–V265, 2002.

[4] B. Osterud and S. I. Rapaport, "Activation of factor IX by the reaction product of tissue factor and factor VII: additional pathway for initiating blood coagulation," *Proceedings of the National Academy of Sciences of the United States of America*, vol. 74, no. 12, pp. 5260–5264, 1977.

[5] H. F. Dvorak, V. S. Harvey, P. Estrella, L. F. Brown, J. McDonagh, and A. M. Dvorak, "Fibrin containing gels induce angiogenesis. Implications for tumor stroma generation and wound healing," *Laboratory Investigation*, vol. 57, no. 6, pp. 673–686, 1987.

[6] P. C. Heinrich, I. Behrmann, S. Haan, H. M. Hermanns, G. Müller-Newen, and F. Schaper, "Principles of interleukin (IL)-6-type cytokine signalling and its regulation," *Biochemical Journal*, vol. 374, no. 1, pp. 1–20, 2003.

[7] A. E. Koch, P. J. Polverini, S. L. Kunkel et al., "Interleukin-8 as a macrophage-derived mediator of angiogenesis," *Science*, vol. 258, no. 5089, pp. 1798–1801, 1992.

[8] N. S. Greaves, K. J. Ashcroft, M. Baguneid, and A. Bayat, "Current understanding of molecular and cellular mechanisms in fibroplasia and angiogenesis during acute wound healing," *Journal of Dermatological Science*, vol. 72, no. 3, pp. 206–217, 2013.

[9] W. Y. J. Chen and G. Abatangelo, "Functions of hyaluronan in wound repair," *Wound Repair and Regeneration*, vol. 7, no. 2, pp. 79–89, 1999.

[10] S. P. Reese, C. J. Underwood, and J. A. Weiss, "Effects of decorin proteoglycan on fibrillogenesis, ultrastructure, and mechanics of type I collagen gels," *Matrix Biology*, vol. 32, no. 7-8, pp. 414–423, 2013.

[11] C. Ries, "Cytokine functions of TIMP-1," *Cellular and Molecular Life Sciences*, vol. 71, no. 4, pp. 659–672, 2014.

[12] R. Basu, J. Lee, J. S. Morton et al., "TIMP3 is the primary TIMP to regulate agonist-induced vascular remodelling and hypertension," *Cardiovascular Research*, vol. 98, no. 3, pp. 360–371, 2013.

[13] A. Godier and B. J. Hunt, "Plasminogen receptors and their role in the pathogenesis of inflammatory, autoimmune and malignant disease," *Journal of Thrombosis and Haemostasis*, vol. 11, no. 1, pp. 26–34, 2013.

[14] M. Pakyari, A. Farrokhi, M. K. Maharlooei, and A. Ghahary, "Critical role of transforming growth factor beta in different phases of wound healing," *Advances in Wound Care*, vol. 2, no. 5, pp. 215–224, 2013.

[15] K. W. Finnson, S. McLean, G. M. Di Guglielmo, and A. Philip, "Dynamics of transforming growth factor beta signaling in wound healing and scarring," *Advances in Wound Care*, vol. 2, no. 5, pp. 195–214, 2013.

[16] J. E. Glim, F. B. Niessen, V. Everts, M. van Egmond, and R. H. J. Beelen, "Platelet derived growth factor-CC secreted by M2 macrophages induces alpha-smooth muscle actin expression by dermal and gingival fibroblasts," *Immunobiology*, vol. 218, no. 6, pp. 924–929, 2013.

[17] T. Burnouf, H. A. Goubran, T.-M. Chen, K.-L. Ou, M. El-Ekiaby, and M. Radosevic, "Blood-derived biomaterials and platelet growth factors in regenerative medicine," *Blood Reviews*, vol. 27, no. 2, pp. 77–89, 2013.

[18] H.-X. Shi, C. Lin, B.-B. Lin et al., "The anti-scar effects of basic fibroblast growth factor on the wound repair in vitro and in vivo," *PLoS ONE*, vol. 8, no. 4, Article ID e59966, 2013.

[19] A. Nauta, C. Seidel, L. Deveza et al., "Adipose-derived stromal cells overexpressing vascular endothelial growth factor accelerate mouse excisional wound healing," *Molecular Therapy*, vol. 21, no. 2, pp. 445–455, 2013.

[20] G. Stynes, G. K. Kiroff, W. A. J. Morrison, and M. A. Kirkland, "Tissue compatibility of biomaterials: benefits and problems of skin biointegration," *ANZ Journal of Surgery*, vol. 78, no. 8, pp. 654–659, 2008.

[21] D. F. Williams, "There is no such thing as a biocompatible material," *Biomaterials*, vol. 35, no. 38, pp. 10009–10014, 2014.

[22] Y. Qiu and K. Park, "Environment-sensitive hydrogels for drug delivery," *Advanced Drug Delivery Reviews*, vol. 64, supplement, pp. 49–60, 2012.

[23] I. Tokarev and S. Minko, "Stimuli-responsive porous hydrogels at interfaces for molecular filtration, separation, controlled release, and gating in capsules and membranes," *Advanced Materials*, vol. 22, no. 31, pp. 3446–3462, 2010.

[24] J. Zhu, "Bioactive modification of poly(ethylene glycol) hydrogels for tissue engineering," *Biomaterials*, vol. 31, no. 17, pp. 4639–4656, 2010.

[25] R. Edwards and K. G. Harding, "Bacteria and wound healing," *Current Opinion in Infectious Diseases*, vol. 17, no. 2, pp. 91–96, 2004.

[26] A. D. Augst, H. J. Kong, and D. J. Mooney, "Alginate hydrogels as biomaterials," *Macromolecular Bioscience*, vol. 6, no. 8, pp. 623–633, 2006.

[27] G. Vaissiere, B. Chevallay, D. Herbage, and O. Damour, "Comparative analysis of different collagen-based biomaterials as scaffolds for long-term culture of human fibroblasts," *Medical and Biological Engineering and Computing*, vol. 38, no. 2, pp. 205–210, 2000.

[28] R. Jayakumar, M. Prabaharan, P. T. Sudheesh Kumar, S. V. Nair, and H. Tamura, "Biomaterials based on chitin and chitosan in wound dressing applications," *Biotechnology Advances*, vol. 29, no. 3, pp. 322–337, 2011.

[29] A. Francesko and T. Tzanov, "Chitin, chitosan and derivatives for wound healing and tissue engineering," in *Biofunctionalization of Polymers and Their Applications*, G. S. Nyanhongo, W. Steiner, and G. Gübitz, Eds., vol. 125 of *Advances in Biochemical Engineering / Biotechnology*, pp. 1–27, Springer, Berlin, Germany, 2011.

[30] A. Yu, H. Niiyama, S. Kondo, A. Yamamoto, R. Suzuki, and Y. Kuroyanagi, "Wound dressing composed of hyaluronic acid and collagen containing EGF or bFGF: comparative culture study," *Journal of Biomaterials Science, Polymer Edition*, vol. 24, no. 8, pp. 1015–1026, 2013.

[31] J. F. Almine, S. G. Wise, and A. S. Weiss, "Elastin signaling in wound repair," *Birth Defects Research Part C—Embryo Today*, vol. 96, no. 3, pp. 248–257, 2012.

[32] S. Zalipsky, "Chemistry of polyethylene glycol conjugates with biologically active molecules," *Advanced Drug Delivery Reviews*, vol. 16, no. 2-3, pp. 157–182, 1995.

[33] D. J. Hines and D. L. Kaplan, "Poly(lactic-co-glycolic) acid–controlled-release systems: experimental and modeling insights," *Critical Reviews in Therapeutic Drug Carrier Systems*, vol. 30, no. 3, pp. 257–276, 2013.

[34] C. M. Hwang, Y. Park, J. Y. Park et al., "Controlled cellular orientation on PLGA microfibers with defined diameters," *Biomedical Microdevices*, vol. 11, no. 4, pp. 739–746, 2009.

[35] G. T. Franzesi, B. Ni, Y. Ling, and A. Khademhosseini, "A controlled-release strategy for the generation of cross-linked hydrogel microstructures," *Journal of the American Chemical Society*, vol. 128, no. 47, pp. 15064–15065, 2006.

[36] H.-W. Kim, J. C. Knowles, and H.-E. Kim, "Hydroxyapatite porous scaffold engineered with biological polymer hybrid coating for antibiotic Vancomycin release," *Journal of Materials Science: Materials in Medicine*, vol. 16, no. 3, pp. 189–195, 2005.

[37] S. Wang, F. Zheng, Y. Huang et al., "Encapsulation of amoxicillin within laponite-doped poly(lactic-co-glycolic acid) nanofibers: preparation, characterization, and antibacterial activity," *ACS Applied Materials & Interfaces*, vol. 4, no. 11, pp. 6393–6401, 2012.

[38] Y.-P. Jiao and F.-Z. Cui, "Surface modification of polyester biomaterials for tissue engineering," *Biomedical Materials*, vol. 2, no. 4, pp. R24–R37, 2007.

[39] K. Rechendorff, M. B. Hovgaard, M. Foss, V. P. Zhdanov, and F. Besenbacher, "Enhancement of protein adsorption induced by surface roughness," *Langmuir*, vol. 22, no. 26, pp. 10885–10888, 2006.

[40] F. J. O'Brien, B. A. Harley, I. V. Yannas, and L. J. Gibson, "The effect of pore size on cell adhesion in collagen-GAG scaffolds," *Biomaterials*, vol. 26, no. 4, pp. 433–441, 2005.

[41] M. L. Jarman-Smith, T. Bodamyali, C. Stevens, J. A. Howell, M. Horrocks, and J. B. Chaudhuri, "Porcine collagen crosslinking, degradation and its capability for fibroblast adhesion and proliferation," *Journal of Materials Science: Materials in Medicine*, vol. 15, no. 8, pp. 925–932, 2004.

[42] R. W. Farndale, J. J. Sixma, M. J. Barnes, and P. G. De Groot, "The role of collagen in thrombosis and hemostasis," *Journal of Thrombosis and Haemostasis*, vol. 2, no. 4, pp. 561–573, 2004.

[43] J. S. Boateng, K. H. Matthews, H. N. E. Stevens, and G. M. Eccleston, "Wound healing dressings and drug delivery systems: a review," *Journal of Pharmaceutical Sciences*, vol. 97, no. 8, pp. 2892–2923, 2008.

[44] N. A. Peppas, J. Z. Hilt, A. Khademhosseini, and R. Langer, "Hydrogels in biology and medicine: from molecular principles to bionanotechnology," *Advanced Materials*, vol. 18, no. 11, pp. 1345–1360, 2006.

[45] N. A. Peppas, P. Bures, W. Leobandung, and H. Ichikawa, "Hydrogels in pharmaceutical formulations," *European Journal of Pharmaceutics and Biopharmaceutics*, vol. 50, no. 1, pp. 27–46, 2000.

[46] L. G. Ovington, "Advances in wound dressings," *Clinics in Dermatology*, vol. 25, no. 1, pp. 33–38, 2007.

[47] T. Friedmann and R. Roblin, "Gene therapy for human genetic disease?" *Science*, vol. 175, no. 4025, pp. 949–955, 1972.

[48] G. F. Pierce and T. A. Mustoe, "Pharmacologic enhancement of wound healing," *Annual Review of Medicine*, vol. 46, pp. 467–481, 1995.

[49] D. J. Margolis, L. M. Morris, M. Papadopoulos et al., "Phase I study of H5.020CMV.PDGF-beta to treat venous leg ulcer disease," *Molecular Therapy*, vol. 17, no. 10, pp. 1822–1829, 2009.

[50] O. M. Tepper and B. J. Mehrara, "Gene therapy in plastic surgery," *Plastic and Reconstructive Surgery*, vol. 109, no. 2, pp. 716–734, 2002.

[51] M. Braddock, C. J. Campbell, and D. Zuder, "Current therapies for wound healing: electrical stimulation, biological therapeutics, and the potential for gene therapy," *International Journal of Dermatology*, vol. 38, no. 11, pp. 808–817, 1999.

[52] K. W. Liechty, M. Nesbit, M. Herlyn, A. Radu, N. S. Adzick, and T. M. Crombleholme, "Adenoviral-mediated overexpression of

platelet-derived growth factor-B corrects ischemic impaired wound healing," *Journal of Investigative Dermatology*, vol. 113, no. 3, pp. 375–383, 1999.

[53] D. J. Margolis, T. Crombleholme, and M. Herlyn, "Clinical protocol: phase I trial to evaluate the safety of H5.020CMV.PDGF-B for the treatment of a diabetic insensate foot ulcer," *Wound Repair and Regeneration*, vol. 8, no. 6, pp. 480–493, 2000.

[54] M. Ailawadi, J. M. Lee, S. Lee, N. Hackett, R. G. Crystal, and R. J. Korst, "Adenovirus vector-mediated transfer of the vascular endothelial growth factor cDNA to healing abdominal fascia enhances vascularity and bursting strength in mice with normal and impaired wound healing," *Surgery*, vol. 131, no. 2, pp. 219–227, 2002.

[55] A. Saaristo, T. Tammela, A. Farkkila et al., "Vascular endothelial growth factor-C accelerates diabetic wound healing," *The American Journal of Pathology*, vol. 169, no. 3, pp. 1080–1087, 2006.

[56] H. Brem, A. Kodra, M. S. Golinko et al., "Mechanism of sustained release of vascular endothelial growth factor in accelerating experimental diabetic healing," *Journal of Investigative Dermatology*, vol. 129, no. 9, pp. 2275–2287, 2009.

[57] J. G. Rheinwald and H. Green, "Serial cultivation of strains of human epidermal keratinocytes: the formation of keratinizing colonies from single cells," *Cell*, vol. 6, no. 3, pp. 331–334, 1975.

[58] H. Green, O. Kehinde, and J. Thomas, "Growth of cultured human epidermal cells into multiple epithelia suitable for grafting," *Proceedings of the National Academy of Sciences of the United States of America*, vol. 76, no. 11, pp. 5665–5668, 1979.

[59] A. B. Lerner, R. Halaban, S. N. Klaus, and G. E. Moellmann, "Transplantation of human melanocytes," *Journal of Investigative Dermatology*, vol. 89, no. 3, pp. 219–224, 1987.

[60] M. Ehrenreich and Z. Ruszczak, "Update on tissue-engineered biological dressings," *Tissue Engineering*, vol. 12, no. 9, pp. 2407–2424, 2006.

[61] A. J. Becker, E. A. McCulloch, and J. E. Till, "Cytological demonstration of the clonal nature of spleen colonies derived from transplanted mouse marrow cells," *Nature*, vol. 197, no. 4866, pp. 452–454, 1963.

[62] I. L. Weissman, "Stem cells: units of development, units of regeneration, and units in evolution," *Cell*, vol. 100, no. 1, pp. 157–168, 2000.

[63] J. A. Thomson, J. Itskovitz-Eldor, S. S. Shapiro, and et al, "Embryonic stem cell lines derived from human blastocysts," *Science*, vol. 282, no. 5391, pp. 1145–1147, 1998.

[64] S. Yamanaka, "Strategies and new developments in the generation of patient-specific pluripotent stem cells," *Cell Stem Cell*, vol. 1, no. 1, pp. 39–49, 2007.

[65] A.-K. Hadjantonakis and V. E. Papaioannou, "The stem cells of early embryos," *Differentiation*, vol. 68, no. 4-5, pp. 159–166, 2001.

[66] L. C. Amado, A. P. Saliaris, K. H. Schuleri et al., "Cardiac repair with intramyocardial injection of allogeneic mesenchymal stem cells after myocardial infarction," *Proceedings of the National Academy of Sciences of the United States of America*, vol. 102, no. 32, pp. 11474–11479, 2005.

[67] W.-S. Kim, B.-S. Park, J.-H. Sung et al., "Wound healing effect of adipose-derived stem cells: a critical role of secretory factors on human dermal fibroblasts," *Journal of Dermatological Science*, vol. 48, no. 1, pp. 15–24, 2007.

[68] S. François, M. Mouiseddine, N. Mathieu et al., "Human mesenchymal stem cells favour healing of the cutaneous radiation syndrome in a xenogenic transplant model," *Annals of Hematology*, vol. 86, no. 1, pp. 1–8, 2007.

[69] Y. J. Wu, L. Chen, P. G. Scott, and E. E. Tredget, "Mesenchymal stem cells enhance wound healing through differentiation and angiogenesis," *Stem Cells*, vol. 25, no. 10, pp. 2648–2659, 2007.

[70] A. M. Altman, N. Matthias, Y. S. Yan et al., "Dermal matrix as a carrier for in vivo delivery of human adipose-derived stem cells," *Biomaterials*, vol. 29, no. 10, pp. 1431–1442, 2008.

[71] D. S. Krause, N. D. Theise, M. I. Collector et al., "Multi-organ, multi-lineage engraftment by a single bone marrow-derived stem cell," *Cell*, vol. 105, no. 3, pp. 369–377, 2001.

[72] S. M. Chambers and M. A. Goodell, "Hematopoietic stem cell aging: wrinkles in stem cell potential," *Stem Cell Reviews*, vol. 3, no. 3, pp. 201–211, 2007.

[73] Š. Selimović, W. Y. Sim, S. B. Kim et al., "Generating nonlinear concentration gradients in microfluidic devices for cell studies," *Analytical Chemistry*, vol. 83, no. 6, pp. 2020–2028, 2011.

[74] F. Piraino, G. Camci-Unal, M. J. Hancock, M. Rasponi, and A. Khademhosseini, "Multi-gradient hydrogels produced layer by layer with capillary flow and crosslinking in open microchannels," *Lab on a Chip*, vol. 12, no. 3, pp. 659–661, 2012.

[75] M. J. Hancock, F. Piraino, G. Camci-Unal, M. Rasponi, and A. Khademhosseini, "Anisotropic material synthesis by capillary flow in a fluid stripe," *Biomaterials*, vol. 32, no. 27, pp. 6493–6504, 2011.

[76] F. Piraino, Š. Selimović, M. Adamo et al., "Polyester μ-assay chip for stem cell studies," *Biomicrofluidics*, vol. 6, no. 4, Article ID 044109, 2012.

[77] Š. Selimović, F. Piraino, H. Bae, M. Rasponi, A. Redaelli, and A. Khademhosseini, "Microfabricated polyester conical microwells for cell culture applications," *Lab on a Chip*, vol. 11, no. 14, pp. 2325–2332, 2011.

[78] S. Lopa, F. Piraino, R. J. Kemp et al., "Fabrication of multi-well chips for spheroid cultures and implantable constructs through rapid prototyping techniques," *Biotechnology and Bioengineering*, vol. 112, no. 7, pp. 1457–1471, 2015.

[79] P. Mostafalu, W. Lenk, M. R. Dokmeci, B. Ziaie, A. Khademhosseini, and S. Sonkusale, "Wireless flexible smart bandage for continuous monitoring of wound oxygenation," in *Proceedings of the 10th IEEE Biomedical Circuits and Systems Conference (BioCAS '14)*, pp. 456–459, October 2014.

[80] Y. Doi, S. Kitamura, and H. Abe, "Microbial synthesis and characterization of poly(3-hydroxybutyrate-co-3-hydroxyhexanoate)," *Macromolecules*, vol. 28, no. 14, pp. 4822–4828, 1995.

[81] S. Kusaka, H. Abe, S. Y. Lee, and Y. Doi, "Molecular mass of poly[(R)-3-hydroxybutyric acid] produced in a recombinant *Escherichia coli*," *Applied Microbiology and Biotechnology*, vol. 47, no. 2, pp. 140–143, 1997.

[82] S. Kusaka, T. Iwata, and Y. Doi, "Properties and biodegradability of ultra-high-molecular-weight poly[(*R*)-3-hydroxybutyrate] produced by a recombinant *Escherichia coli*," *International Journal of Biological Macromolecules*, vol. 25, no. 1–3, pp. 87–94, 1999.

[83] T. Iwata, M. Fujita, Y. Aoyagi, Y. Doi, and T. Fujisawa, "Time-resolved X-ray diffraction study on poly[(R)-3-hydroxybutyrate] films during two-step-drawing: generation mechanism of planar zigzag structure," *Biomacromolecules*, vol. 6, no. 3, pp. 1803–1809, 2005.

[84] L. F. Drummy, D. M. Phillips, M. O. Stone, B. L. Farmer, and R. J. Naik, "Thermally induced α-helix to β-sheet transition in renegated silk fibers and films," *Biomacromolecules*, vol. 6, no. 6, pp. 3328–3333, 2005.

[85] J. Sirichaisit, V. L. Brookes, R. J. Young, and F. Vollrath, "Analysis of structure/property relationships in silkworm (*Bombyx mori*) and spider dragline (*Nephila edulis*) silks using raman spectroscopy," *Biomacromolecules*, vol. 4, no. 2, pp. 387–394, 2003.

[86] M. Pollock and R. E. Shadwick, "Relationship between body-mass and biomechanical properties of limb tendons in adult mammals," *American Journal of Physiology*, vol. 266, no. 3, pp. R1016–R1021, 1994.

[87] B. B. Aaron and J. M. Gosline, "Elastin as a random-network elastomer: a mechanical and optical analysis of single elastin fibers," *Biopolymers*, vol. 20, no. 6, pp. 1247–1260, 1981.

[88] N. Annabi, S. M. Mithieux, P. Zorlutuna, G. Camci-Unal, A. S. Weiss, and A. Khademhosseini, "Engineered cell-laden human protein-based elastomer," *Biomaterials*, vol. 34, no. 22, pp. 5496–5505, 2013.

[89] N. Annabi, A. Tamayol, S. R. Shin, A. M. Ghaemmaghami, N. A. Peppas, and A. Khademhosseini, "Surgical materials: current challenges and nano-enabled solutions," *Nano Today*, vol. 9, no. 5, pp. 574–589, 2014.

[90] N. Annabi, Š. Selimović, J. P. Acevedo Cox et al., "Hydrogel-coated microfluidic channels for cardiomyocyte culture," *Lab on a Chip*, vol. 13, no. 18, pp. 3569–3577, 2013.

[91] T. Weis-Fogh, "Thermodynamic properties of resilin, a rubber-like protein," *Journal of Molecular Biology*, vol. 3, no. 5, pp. 520–531, 1961.

[92] K. Bailey and T. Weis-Fogh, "Amino acid composition of a new rubber-like protein, resilin," *Biochimica et Biophysica Acta*, vol. 48, no. 3, pp. 452–459, 1961.

[93] T. Weisfogh, "Molecular interpretation of elasticity of resilin, a rubber-like protein," *Journal of Molecular Biology*, vol. 3, no. 5, pp. 648–667, 1961.

[94] T. Tanabe, N. Okitsu, A. Tachibana, and K. Yamauchi, "Preparation and characterization of keratin-chitosan composite film," *Biomaterials*, vol. 23, no. 3, pp. 817–825, 2002.

[95] S. Sun, J. R. Mitchell, W. MacNaughtan et al., "Comparison of the mechanical properties of cellulose and starch films," *Biomacromolecules*, vol. 11, no. 1, pp. 126–132, 2010.

Hindawi Publishing Corporation
BioMed Research International
Volume 2015, Article ID 415289, 18 pages
http://dx.doi.org/10.1155/2015/415289

Review Article

Bone Regeneration from PLGA Micro-Nanoparticles

Inmaculada Ortega-Oller,[1] Miguel Padial-Molina,[1] Pablo Galindo-Moreno,[1] Francisco O'Valle,[2] Ana Belén Jódar-Reyes,[3] and Jose Manuel Peula-García[3,4]

[1] *Department of Oral Surgery and Implant Dentistry, University of Granada, 18011 Granada, Spain*
[2] *Department of Pathology, School of Medicine and IBIMER, University of Granada, 18012 Granada, Spain*
[3] *Biocolloid and Fluid Physics Group, Department of Applied Physics, University of Granada, 18071 Granada, Spain*
[4] *Department of Applied Physics II, University of Málaga, 29071 Málaga, Spain*

Correspondence should be addressed to Jose Manuel Peula-García; jmpeula@uma.es

Received 27 March 2015; Accepted 4 June 2015

Academic Editor: Hojae Bae

Poly-lactic-co-glycolic acid (PLGA) is one of the most widely used synthetic polymers for development of delivery systems for drugs and therapeutic biomolecules and as component of tissue engineering applications. Its properties and versatility allow it to be a reference polymer in manufacturing of nano- and microparticles to encapsulate and deliver a wide variety of hydrophobic and hydrophilic molecules. It additionally facilitates and extends its use to encapsulate biomolecules such as proteins or nucleic acids that can be released in a controlled way. This review focuses on the use of nano/microparticles of PLGA as a delivery system of one of the most commonly used growth factors in bone tissue engineering, the bone morphogenetic protein 2 (BMP2). Thus, all the needed requirements to reach a controlled delivery of BMP2 using PLGA particles as a main component have been examined. The problems and solutions for the adequate development of this system with a great potential in cell differentiation and proliferation processes under a bone regenerative point of view are discussed.

1. Introduction

Bone regeneration is one of the main challenges facing us in the daily clinic. Immediately after a tooth extraction, normal biological processes remodel the alveolar bone limiting in some cases the possibility of future implant placement. Different strategies for the preservation of that bone have been explored in recent years. Other conditions, such as trauma, tumor resective surgery, or congenital deformities, require even higher technical and biological requirements to generate the necessary bony structure for the occlusal rehabilitation of the patient. To overcome these anatomical limitations in terms of bone volume, different approaches have been proposed to either improve the implant osteointegration or to augment the bone anatomy where it will be placed [1, 2]. Autogenous bone graft is still considered the "gold standard" due to its osteogenic, osteoconductive, and osteoconductive properties [3, 4]. However, it also presents several limitations including the need for a second surgery, limited availability, and morbidity in the donor area [5]. Therefore, other biomaterials such as allogeneic grafts, with osteoconductivity and osteoinductive capacities [6, 7], and xenogeneic grafts [8, 9] and alloplastic biomaterials [10], with osseoconductive potential, were proposed. All these materials, although acceptable, are not suitable in many conditions and usually require additional consideration in the decision process [11]. Additionally, the bone quantity and quality that can be obtained with these materials are often limited.

The use of bioactive molecules, alone or in combination with the previously described materials, has, therefore, become a major area of interest thanks to their high potential. When using this kind of procedures, it is important to consider (1) the delivery method and (2) the molecule itself. Bioactive molecules can be transported into the defect area as a solution or a gel, embedded in sponges, adhered to solid scaffolds and, more recently, included in particles of different sizes. Using these methods, PDGF (platelet-derived growth

factor), FGF (fibroblast growth factor), IGF (insulin growth factor), Runx2, Osterix (Osx), LIM domain mineralization protein (LMP), BMP (bone morphogenic protein) and, more recently, periostin have been proposed as potential candidates for regeneration procedures within the oral cavity, including bone and periodontal tissues [12, 13]. These molecules have been tested alone or in combination with stem cells [14] using several *in vitro* and *in vivo* strategies [15].

Consequently, within the context of this review, we intend to review the delivery methods of bioactive molecules with the purpose of bone regeneration, with a particular focus on polymeric nano/microparticles, especially those with PLGA as main component, to encapsulate the growth factor BMP-2. An overview of the biological functions of bone morphogenetic proteins and an analysis of the different parameters affecting the physicochemical properties of these systems are presented. Synthesis method, particle size and morphology, use of stabilizers and their incidence in the colloidal stability, protective function, and surface functionality will be discussed. In addition, we explore the different strategies that can be used to optimize the encapsulation efficiency and release kinetics, main parameters that determine the correct development of polymeric carriers used in tissue-engineered bone processes.

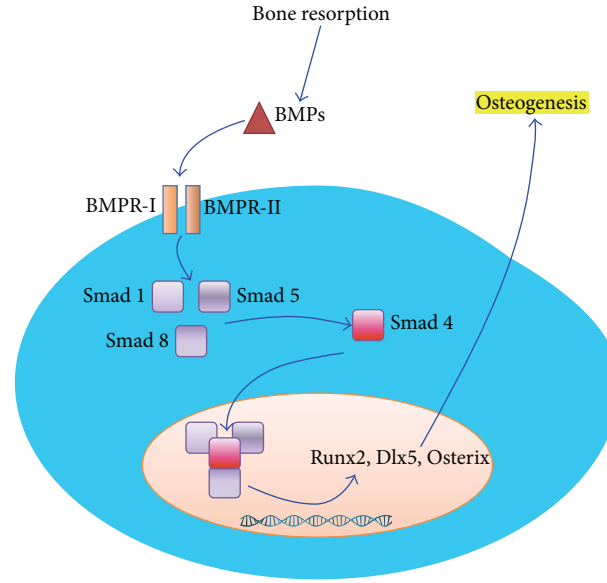

Figure 1: Schematic representation of the main BMP molecular pathway to osteogenesis. BMPs interact with cell surface receptors I and II to activate Smads 1, 5, and 8. These activated Smads activate Smad 4. All together as a protein complex activate Runx2, Dlx5, and Osterix.

2. BMPs: Action and Regulation

For bone regeneration, in particular, bone morphogenetic growth factors (BMP) are probably the more tested group of molecules. Since 1965, when Urist [16] showed that the extracted bone BMPs could induce bone and cartilage formation when implanted in animal tissue, an increasing number of reports have tested its *in vivo* application and biological foundation when used in bone defects [17–19]. BMPs are members of the TGF-β superfamily of proteins [20]. The BMP family of proteins groups more than 20 homodimeric or heterodimeric morphogenetic proteins, which functions in many cell types and tissues, not all of them being osteogenic [21]. BMPs can be divided into 4 subfamilies based on their function and sequence, being BMP-2, BMP-4, and BMP-7 the ones with osteogenic potential [21]. The actions of BMPs include chondrogenesis, osteogenesis, angiogenesis, and extracellular matrix synthesis [22]. Within this family of proteins, BMP-2 has been the most studied. It has osteoinductive properties that promote the formation of new bone by initiating, stimulating, and amplifying the cascade of bone formation through chemotaxis and stimulation of proliferation and differentiation of the osteoblastic cell lineage [5, 17, 19, 20]. The absence of it, as studied in knockout models, leads to spontaneous fractures that do not heal with time [23]. In fact, other models have demonstrated that the absence of either BMP-4 [24] or BMP-7 [25] do not lead to bone formation and function impairment which demonstrate the compensatory effect produced by BMP-2 alone [26].

Many cell types in bone tissue produce BMPs, including osteoprogenitor cells, osteoblasts, chrondrocytes, platelets, and endothelial cells. This secreted BMP is then stored in the extracellular matrix where it mostly interacts with collagen type IV [27]. During the repair and remodeling processes, osteoclast resorptive activity induces the release of BMPs to the medium so that they are suspended and can interact with nearby cells to initiate the subsequent osteogenic process [28].

A BMP in the extracellular matrix binds to cell surface receptors BMPR-I and BMPR-II and activates the Smad cytoplasmic proteins or the MAPK pathway [29]. When BMPR-I is activated, BMPR-II is recruited and activated as well [30]. The activation of the complexes BMPR-I and BMPR-II leads to the activation of several Smads (1, 5, and 8) that also activate Smad 4 and they all form protein complexes that are transported into the nucleus where Runx2, Dlx5, and Osterix genes (important in osteogenesis) are activated [26, 27] (Figure 1). Similarly, when the MAPK pathway is activated, it leads to induction of Runx2 transcription and, therefore, to bone differentiation [31]. A number of extracellular and intracellular antagonists have also been described, including noggin, chordin, and gremlin or Smads 6, 7, and 8b, respectively [32].

2.1. Clinical Use of BMP-2. Today, the BMP-2 is commercially available under different brand names and concentrations. It usually consists of a collagen absorbable sponge embedded with recombinant human BMP-2. In 2002, it was approved by the FDA as an alternative of autogenous bone grafting in anterior lumbar interbody fusion [33]. Later, in 2007, the FDA approved the use of rhBMP-2 as an alternative for autogenous bone grafting in the increase of the alveolar crest defects associated with the tooth extraction maxillary sinus pneumatization [33].

Beside the applications in spine clinical studies, where very high concentrations are used (AMPLIFY, rhBMP-2, 40 mg), clinical studies have supported its use in the oral

cavity. BMPs have been used in periodontal regeneration, bone healing, implant osteointegration, oral surgery with orthodontic purposes, bone pathology sequel repair, distraction osteogenesis, and endodontic reparative surgery [28, 34]. However, it has shown more promising results in cases where only bone tissue is to be regenerated, including preimplant site development, sinus lift, vertical and horizontal ridge augmentation, and dental implant wound healing [35]. In this sense, it has been shown that the use of rhBMP-2 induced the formation of bone suitable for placement of dental implants and their osteointegration [36]. Furthermore, it appears that the newly formed bone has similar properties to the native bone and is, therefore, capable of supporting denture occlusal forces [37]. In the particular case of sinus lifting, where bone deficiency is greater and, therefore, supportive therapies can be more helpful, a recent meta-analysis found a total of 3 human studies and 4 animal trials (Table 1) [38]. In summary, the included studies concluded that rhBMP-2 induces new bone formation with comparable bone quality and quantity of newly formed bone to that induced by autogenous bone graft. In some cases, even higher bone quality and quantity have been reported [39].

Conversely, recent studies report severe complications after its use [61]. Even more, high doses have also associated with carcinogenic effects, which led the authors to emphasize the need for better guidelines in BMP clinical use [62]. Not so drastic, recent studies are highlighting the negative side effects and risks of its application, making high emphasis on potential bias of nonreproducible industry sponsored research, especially when used in spinal fusion [44, 63, 64]. The use of rhBMP-2 has been shown to increase the risks for wound complications and dysphagia with high effectiveness and harms misrepresentation through selective reporting, duplicate publication, and underreporting [44]. Specifically in oral bone regenerative applications, a report in sinus lift concluded that the use of BMP-2 promotes negative effects on bone formation when combined with anorganic bovine bone matrix versus anorganic bovine bone alone [41], in contrast with previous reports and reviews [38]. Taking together this information, it can be concluded that it is of extreme importance to be careful with the clinical use of new products, avoiding off-label applications. It is also important to highlight the need for more and better clinical research.

To overcome these limitations, new strategies, such as the use of *ex vivo* BMP-2-engineered autologous MSCs [65], encapsulation of the protein in different biomaterials, or delivery by gene therapy, are being explored in recent years.

The development of these technologies is based on some biological facts. *In vitro* effects of BMPs are observed at very low dosages (5–20 ng/mL), although current commercially available rhBMPs are used in large dosages (up to 40 mg of some products) [28]. This is probably due to an intense proteolytic consumption during the early postsurgical phases. It is important to know the proper sequence of biological events that lead to normal tissue healing. Then, this knowledge can be used to intervene at the specific time frame where our therapy is intended to act [15]. Effective bone formation, as described above, is a sequential process. Therefore, the inductive agent should be delivered at a maintained concentration during a timeframe. In this sense, as in many other processes in medicine, it has been recently demonstrated that long-term release of BMP-2 is more effective than short-term over a range of doses [51]. It is also important to note that the role of other molecular pathways and crosstalk between the different components playing in bone regeneration is not perfectly understood yet, and, therefore, more research has to be conducted.

What is known so far, in summary, is that BMPs, specifically BMP-2, is of utility for promoting bone regeneration [28]. However, the currently FDA-approved BMP-2 delivery system (INFUSE, Medtronic Sofamor Danek, Inc.) presents important limitations [66]. Firstly, protein is quickly inactivated. Therefore, its biological action disappears, maybe even before the blood clot that forms after the surgery is being organized. Second, the recombinant protein is delivered in an absorbable collagen sponge. Thus, the distribution of the BMP in a liquid suspension embedded into a collagen sponge makes it impossible to be certain that the protein is reaching the ideal target. Therefore, where, when, and for how long a dose of BMP-2 is reached (determined by the delivery method) are important factors. Because of that, new forms of BMP-2 delivery are being developed. These new technologies have to guarantee a higher half-life of the protein and a stepped release, to increase the effects on the desired cell targets. The biotechnology opens the door to be able to provide a solution to these limitations.

Biodegradable nanoparticles (nanospheres and nanocapsules) have developed as a promising important tool for the delivery of macromolecules via parenteral, mucous, and topical applications [67–70]. Well-established biodegradable polymers such as poly(acid D, L-lactic) or poly(D, L-lactic-co-glycolic) have been widely used in the preparation of nanoparticles in recent decades because of its biocompatibility and full biodegradability [71]. However, it is known that certain macromolecules, such as proteins or peptides, may lose activity during their encapsulation, storage, delivery, and release [72]. To overcome this problem, the addition of stabilizers such as oxide polyethylene (PEO) or the coencapsulation with other macromolecules and its derivatives seem to be a promising strategy.

3. Polymeric Colloidal Particles to Encapsulate Hydrophilic Molecules

Generally, polymeric colloidal particles are hard systems with a homogeneous spherical shape composed by natural or synthetic polymers. In order to encapsulate hydrophilic molecules as proteins or nucleic acids, it is necessary to optimize the polymeric composition and the synthesis method. In this process, a high encapsulation efficiency, maintenance of the biological activity of the encapsulated biomolecule, and obtaining of an adequate release pattern have to be achieved [73–75]. Several delivery systems of BMP2 (and other growth factors, GFs) using polymeric particles have been described in the literature. Most of them are microparticulated systems using the biocompatible and biodegradable PLGA copolymer as main component [76, 77]. Taking into account the incorporation of BMP2 to the carrier system, encapsulation

Table 1: Summary of clinical and animal studies using BMP-2 for sinus floor elevation (adapted from [38]). The included studies overall concluded that rhBMP-2 induces new bone formation with comparable bone quality and quantity of newly formed bone to that induced by autogenous bone graft.

Reference	Study design	Follow-up (months)	Species (subjects)	Core biopsy harvesting (months)	Graft material	% Newly formed bone	Bone height gain (mm)	Bone width gain (mm)	Bone density (mg/mL)	Immune response	Histology
Boyne et al. 2005 [37]	RCT	52	Human (48)	6–11	0.75 mg/mL rhBMP-2/ACS	NA	11.29	Crest: 2.02 Midpoint: 8.54 Apical: 11.86	84	None	NA
					1.50 mg/mL rhBMP-2/ACS		0.47	Crest: 1.98 Midpoint: 7.80 Apical: 10.78	134		
					Autogenous bone graft; autogenous bone graft + allogeneic bone graft		10.16	Crest: 4.66 Midpoint: 10.17 Apical: 10.56	350		
Triplett et al. 2009 [40]	RCT	58	Human (160)	6	1.50 mg/mL rhBMP-2/ACS	NA	7.83 ± 3.52	NA	200	None	Rich vascular marrow space high in cellular content
					Autogenous bone graft (iliac crest, tibia or oral cavity); autogenous bone graft + allogeneic bone graft		9.46 ± 4.11		283		Osteoclasts still present; higher fibrous tissue
Kao et al. 2012 [41]	Prospective	6–9	Human (22)	6–9	rhBMP-2/ACS + ABB	16.04 ± 7.45	NA	NA	NA	None	Fewer ABB particles; less newly formed bone (woven and mature bone structure)
					ABB	24.85 ± 5.82					More ABB particles remaining; higher newly formed bone (woven and matured bone structure)
Nevins et al. 1996 [36]	Prospective	12	Goat (6)	12	rhBMP-2/ACS	NA	NA	NA	NA	None	Dense isolated trabeculae and bone marrow; osteoblast and osteoclasts; no cortical bone
					ACS/Buffer						Collagenous connective tissue; no evidence of inflammation; no neo-osteogenesis
Hanisch et al. 1997 [42]	RCT	24	Nonhuman primate (12)	24	rhBMP-2/ACS ACS	NA	6.0 ± 0.3 2.6 ± 0.3	NA	14.4 ± 2.9 13.9 ± 4.6	NA	Newly formed bone indistinguishable from residual bone
Wada et al. 2001 [43]	Prospective	8	Rabbit (10)	8	rhBMP-2/ACS	22.4 ± 4.4	NA	NA	NA	NA	Cortical bone formation in both groups; trabeculae with clear lamellar structure were embedded in fatty marrow
					Autogenous bone graft (iliac crest)	21.9 ± 4.5					
Lee et al. 2013 [39]	Prospective	8	Mini-pig (8)	8	rhBMP-2/ACS	NA	9.3 ± 0.5	NA	51.9 ± 3	NA	Newly formed cancellous bone; new bone continuous with resident bone; woven bone in fibrovascular and fatty marrow
					Autogenous bone graft (iliac crest)		8.6 ± 0.7		32.9 ± 2.5		Irregular and variable bone among different subjects

NA: not available; RCT: randomized clinical trial; ACS: absorbable collagen sponge; ABB: anorganic bovine bone.

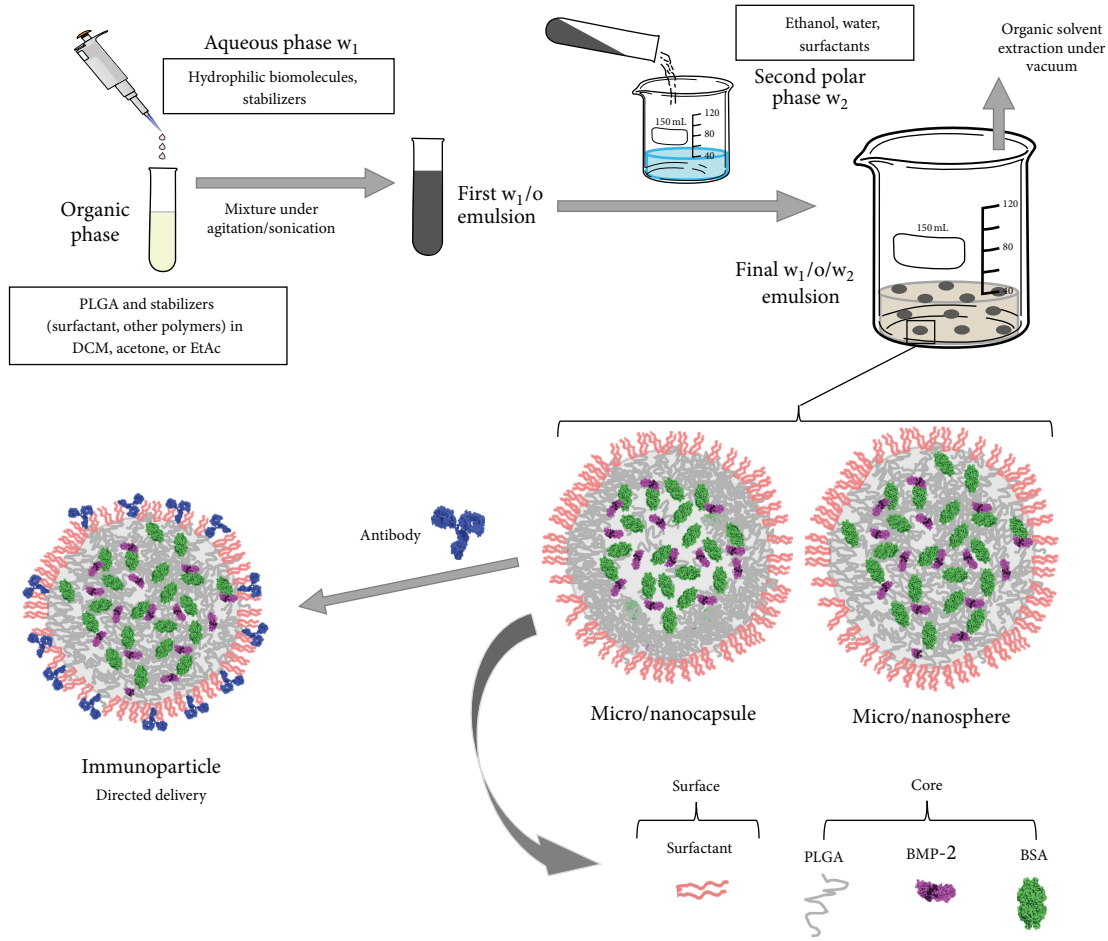

FIGURE 2: Double emulsion procedure (water/oil/water emulsion, $W_1/O/W_2$) to obtain PLGA micro/nanoparticles. Depending on the synthesis conditions (stabilizers, solvents and mixing procedure) it is possible to obtain micro-nanospheres with a uniform matrix or micro-nanocapsules with a core-shell structure. Immunoparticles used for directed delivery can be obtained by attaching specific antibody molecules on the particle surface.

is preferred to absorption because the growth factors are more protected against environmental factors in the medium and may have better control over the delivery and release to achieve the desired concentrations in specific site and time [78].

Normally, if the GFs are related with bone regeneration processes, nano-microparticles are trapped in a second system as hydrogels or tissue engineering scaffolds, which also play an important role in the release profile of GFs from these particles [78]. The nano-microparticles have allowed the development of multiscale scaffold, thereby facilitating control of the internal architecture and adequate patterns of mechanical gradients of cells and signaling factors [79].

All steps, from the synthesis method and its characteristics, the encapsulation process, or the final surface modification for a targeted delivery, determine the characteristics of these systems and their main goal: the controlled release of bioactive GFs.

3.1. Synthesis Methods. It is possible to found several procedures to encapsulate hydrophilic molecules as proteins or nucleic acids in polymeric nano/microparticles. Phase separation [80] or spray drying [81] techniques have been reported to encapsulate hydrophilic molecules. However, in the case of proteins, the most normally used procedure to encapsulate them into PLGA micro- and nanoparticles is the double-emulsion (water/oil/water, W/O/W) solvent evaporation technique [75, 82]. A schematic description of this technique is presented in Figure 2. In a general way, PLGA is dissolved in an organic solvent and emulsified, using mechanical agitation or sonication, with water containing an appropriate amount of protein. Thus, a primary water/oil (W/O) emulsion is obtained. In the second phase, this emulsion is poured into a large polar phase leading to an immediate precipitation of the particles as a consequence of the polymer shrinkage around droplets of the primary emulsion. This phase may be composed of a water solution of a stabilizer (surfactant) or ethanol-water mixtures [83, 84]. After stirring, the organic solvent is rapidly extracted by evaporation under vacuum. A wide list of different modifications have been tested in this procedure in order to obtain a micro/nanocarrier system with adequate colloidal stability, high encapsulation efficiency, adequate bioactivity, and, finally, a long-time release profile with low "initial burst."

The goal is to avoid a high amount of protein (>60%) being released very quickly (24 hours), which is one of the biggest problems of a controlled release system [76].

3.2. Organic Solvent. Hans and Lowman show different examples of organic solvents used in multiple emulsion processes. Normally, dichloromethane (DMC), ethyl acetate, acetone and their mixtures can be used [82]. In the first step, a good organic solvent with low water solubility to facilitate the emulsification process and low boiling point for an easy evaporation would be the election. However, the structure of the encapsulated protein molecules can be affected and denaturation processes and loss of biological activity appear when they interact with a typical organic solvent as DMC [73]. Ethyl acetate, on the other hand, exerts less denaturating effects with a lower incidence on the bioactivity of the encapsulated proteins [85].

Other important factors related with the organic solvent are their physical properties that affect how the polymer tails self-organize in the shell of the emulsion droplets and modify the nanoparticle morphology and the encapsulation efficiency [86]. In this way, a higher water solubility of the organic solvent, that is, ethyl acetate, favors a rapid solvent removal. Additionally, the solvent removal rate can be controlled by adjusting the volume of the polar phase as well as the shear stress during the second emulsification step. An increase of these two parameters increases the diffusion rate of ethyl acetate from primary microparticles to outer aqueous phase, resulting in their rapid solidification [87]. It also enhances the encapsulation efficiency and minimizes the contact-time between protein molecules and organic solvent [88], obtaining at the same time a lower burst effect and a slower drug release from the microparticles [87].

3.3. Particle Size and Morphology. Particle size is an important parameter and one of the main goals of the delivery polymeric system. Microspheres, from a few micrometers up to 100 μm, are suitable for oral delivery, mucosal adhesion, or inside scaffold use, that is, for bone regeneration. Nanoscale dimension of the carrier offers enhanced versatility when compared with particles of larger size. This is due to the fact that they have higher colloidal stability, improved dispersibility and bioavailability, more reactive surface and also, can deliver proteins or drugs inside and outside of the corresponding cells [89]. BMP2 promotes bone formation and induces the expression of other BMPs and initiates the signaling pathway from the cell surface by binding to two different surface receptors [22]. Therefore, the BMP2 carrier particles must release it into the extracellular medium. Since cellular intake of PLGA nanoparticles is very fast, the intaking process can be limited by an increase in size from nano- to microparticles [90]. However, the interaction between particles and cells is strongly influenced by particle size. If cell internalization is desired, the particle must be comprised in the submicron scale at an interval between 2 and 500 nm [91]. Moreover, this size is needed for a rapid distribution after parenteral administration in order to reach different tissues through different biological barriers. In addition, the intake by macrophages is minimized with a diameter of nanoparticles under 200 nm and even smaller [82, 92]. As discussed by Yang et al. [93], slight modifications of the synthesis procedure can suppose drastic effects on the size or particle morphology and, therefore, in the protein encapsulation efficiency and kinetic release.

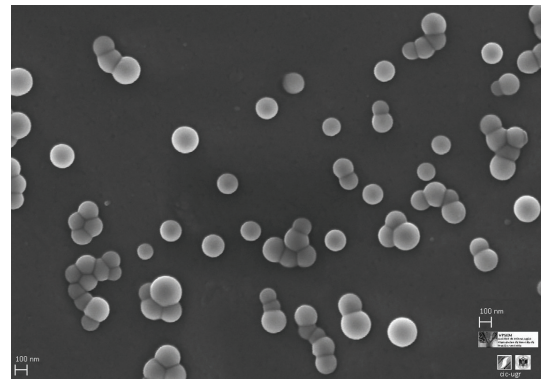

Figure 3: Scanning electron microscopy (SEM) photography of PLGA nanoparticles obtained by a double emulsion emulsification procedure. This system with spherical shape, low polydispersity, and nanoscopic scale shows the intended properties for an adequate physiological distribution and cell internalization.

In double emulsion processes, the first emulsification step largely determines the particle size while the second emulsification step, characterized by the solvent elimination and polymer precipitation, mainly affects the particle morphology [86]. However, the use of surfactant solutions as the polar medium of the second emulsification process and the volume ratio between organic and polar phases in this step has shown an important influence in the final size [94]. Therefore, the correct election of the organic solvent, the polymer concentration, the addition of surfactant, and the emulsification energy allow controlling the size of the system.

The incorporation of poloxamers (F68) in the organic solvent of the primary emulsification helps to increase the colloidal stability of the first dispersion by being placed at the water/oil interface. This reduces the particle size in comparison with pure PLGA nanoparticles in which the only stability source comes from electric charge of the carboxyl groups of the PLGA [95]. It is normal to obtain spherical micro/nanospheres with a polymeric porous core. A typical SEM micrograph of PLGA nanoparticles obtained by W/O/W emulsion using a mixture of organic solvents (DCM/acetone) and ethanol/water as second polar medium is shown in Figure 3, in which the spherical shape and uniform size distribution are the main characteristics. The outer polymeric shell in the second emulsification step pushed the water droplets to the inner core according to their solidification process [96]. This process allows producing particles like capsules with a core-shell structure in which the inner core has a low polymer density. Figure 4 shows a typical core-shell structure in which the polymer precipitates and shrinks around the water droplets during the solvent change of the second phase and the subsequent organic solvent evaporation process [97]. In this case, the process of

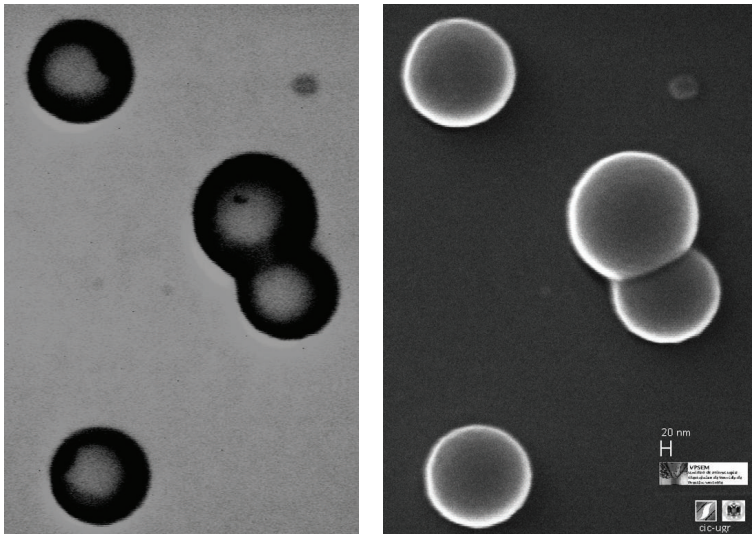

(a) (b)

Figure 4: PLGA/poloxamers188 blend nanoparticles. (a) Scanning transmission electron microscopy (STEM) photography; (b) scanning electron microscopy (SEM) photography. STEM technique allows the analysis of the nanoparticle structure with an internal region with a low polymer density, which is representative of nanocapsules with core-shell structure.

solidification of the polymer is influenced and determined by the miscibility of the organic solvent with the second polar phase and the removal rate.

The polymeric shell often presents channels or pores as a consequence of the inner water extrusion due to osmotic forces. This can reduce the encapsulation efficiency and favors a fast initial leakage with the unwanted "burst release" [93]. This modification of internal structure of the particles is usually indicated assigning the term "nanosphere" to the system with a core consisting of a homogeneous polymer matrix. The bioactive agent is dispersed within them, while the core-shell structure would be similar to a "nanocapsule" where the biomolecule is preferably in the aqueous cavity surrounded by the polymeric shell [78] (see Figure 2).

3.4. Stabilizer Agents

3.4.1. Colloidal Stability. The double emulsion method normally requires the presence of stabilizers in order to confer colloidal stability during the first emulsification step, to prevent the coalescence of the emulsion droplets, and, later, to maintain the stability of the final nano/microparticles [98]. Polyvinyl alcohol (PVA) and PEO derivate as poloxamers (also named pluronics) have been used in most cases [83, 94]. Others include natural surfactants, such as phospholipids [99, 100]. In some cases, it is possible to avoid surfactants if the particles have an electrostatic stability contribution, that is, from the uncapped end carboxyl groups of the PLGA molecules [101].

As it has been previously commented, PVA and poloxamers have shown their efficiency in synthetizing both nano- and microparticles, affecting not only the stability of the systems but also their size and morphology. Thus, a size reduction effect has been found using PVA in the external water phase, affecting at the same time the surface porosity, mainly in microsized particles [94]. A comparative study between this and phospholipids (di-palmitoyl phosphatydilcholine, DPPC) as stabilizers showed that DPPC could be a better emulsifier than PVA to produce nano- and microparticles. With this method, a much lower amount of stabilizer was needed to obtain a similar size. In the same study, a higher porosity on the particle surface for the PVA emulsified nanospheres was shown [99].

On the other hand, the combination of PLGA with poloxamers has shown positive effects for the nano- and microsystems in terms of stability [102]. The use of these surfactants in the first or second steps of the W/O/W emulsion procedure leads to different situations. Thus, if poloxamers are blended with PLGA in the organic phase of the primary emulsification, an alteration of the surface roughness is obtained. However, if these are added in the inner water phase, an increase of porosity is found [83]. In addition, their inclusion in the polar phase of the second emulsification step also generates hydrophilic roughness surfaces. A quantification of this is shown in Figure 5, in which the electrophoretic mobility of both PLGA pure and PLGA/pluronic F68 nanoparticles is measured as a function of the pH of the medium. The observed dependence with this parameter is a consequence of the weak acid character of the PLGA carboxyl groups. When poloxamer molecules are present at the interface, a systematic reduction of mobility was found as a consequence of the increase in the surface roughness. The hydrophilic surfactant chains spread out towards the solvent originating a displacement of the shear plane and the consequent mobility reduction [95, 101].

The final PLGA particle size is primarily controlled by electrostatic forces and is not significantly affected by the presence or nature of poloxamer stabilizers [101]. The recognition of the nanocarriers by the mononuclear phagocytic system (MPS) can be significantly altered if the surface of

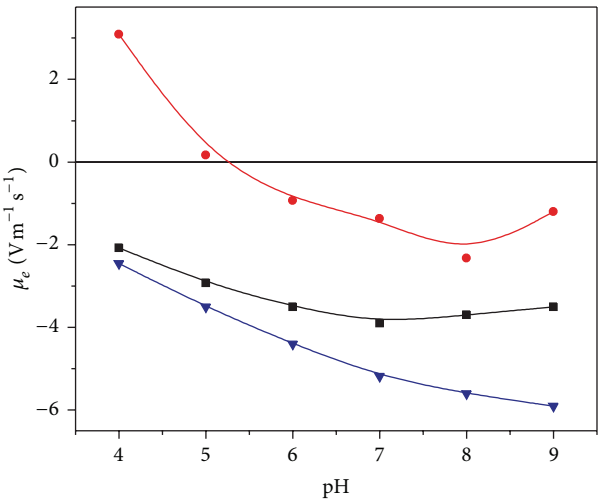

FIGURE 5: Electrophoretic mobility versus pH for PLGA nanoparticles with different characteristics. (▼) PLGA, (■) PLGA/poloxamer188 blend, and (•) PLGA covered by Immuno-γ-globulin. The different surface composition affects the electrokinetic behaviour of bare nanoparticles. Surface charge values were screened by the presence of nonionic surfactant as poloxamers, or, in a higher extension, by the presence of antibody molecules attached on the surface.

colloidal particles is modified by using PEO block copolymer of the poloxamer molecules. The steric barrier given by these surfactant molecules prevents or minimizes the adsorption of plasma protein and decreases the recognition by macrophages [103]. The size of microspheres is also unaffected by the coencapsulation of poloxamers. The system containing poloxamer-PLGA blends drive to an inner structure displaying small holes and cavities in relation with microspheres of pure PLGA with a compact matrix-type structure [83].

Microparticles formulated by poloxamer in the second polar medium have completely different surface than the PVA ones, almost without pores [94]. A comparison between different poloxamers shows that the hydrophilic-lipophylic balance (HBL) of the surfactant plays a crucial role determining the surfactant-polymer interactions and controlling the porosity and roughness of the nano-microparticles [83, 104].

In a similar manner to surfactants, polymer characteristics, like the hydrophobicity grade, the molecular weight or the hydrolysis degradation rate, can strongly influence the particle morphology. Therefore, the polymer composition of the particles greatly affects its structure and properties. This is why it is usual to use other polymers in order to modify the behavior and application of the particles. In this way, polyethylene glycol (PEG) of different chain length is frequently used to modify the surface characteristics. With PEG, particles are more hydrophilic and with rougher surfaces which affects the MPS action by increasing the circulating-time and half-life *in vivo*, like the presence of PEO chains [105]. Additionally, PEG chains also provide colloidal stability via steric stabilization. Pegylated-PLGA nano- or microparticles can be normally obtained by using in the synthesis method PLGA/PEG di- and triblock copolymers [58, 59, 75]. Natural polymers as chitosan, besides modifying the hydrophobicity-hydrophilicity ratio of the surface, also confer them a mucoadhesive character [106].

3.4.2. Encapsulation Efficiency and Bioactivity. Furthermore, the use of stabilizers (surfactants or polymers) also influences the encapsulation efficiency and the protein stability. In fact, for the W/O/W solvent evaporation process, the chlorinated organic solvent used for the first emulsification could degrade protein molecules encapsulated in this step if they come into contact with the organic/water interface, causing their aggregation or denaturation [107]. The polymer-protein interaction, the shear stress for the emulsification process, and the pH reduction derived from PLGA polymer degradation can also produce the same situation with the subsequent loss of biological activity of the encapsulated biomolecules. Different strategies to prevent it have been used. For example, an increase of the viscosity around protein molecules can help to isolate them from their microenvironment [108]. In this way, viscous products, such as starch, have been used to prevent protein instability [109]. These authors coencapsulate BMP2 with albumin inside starch microparticles using other biodegradable polymer, poly-ε-caprolactone, instead of PLGA. The BMP2 retained its bioactivity. Despite a low encapsulation rate, beside an initial burst followed by an uncompleted release, the amount of BMP2 needed at the beginning was lower [109]. The combination of PEO surfactants with PLGA (blended in the organic phase) can also preserve the bioactivity of microencapsulated proteins [110] or nucleic acids [84].

However, in most cases, the coencapsulation of GFs with other biomolecules was the preferred strategy. Thereby, serum albumins (SA) have shown the capacity to limit the aggregation-destabilization of several proteins incited by the water/organic solvent interface of the primary emulsification process [111, 112]. White et al. encapsulated lysozyme inside PLGA-PEG microparticles. In addition to the protective function, they also observed an important increase of the entrapment efficiency when human SA was coencapsulated with lysozyme and BMP2 [59]. d'Angelo et al. used heparin as stabilizer because it forms a specific complex with several GFs, stabilizes their tridimensional structure, and promotes their bioactivity. An encapsulation efficiency of 35% was increased to 87% using bovine SA as a second stabilizer to encapsulate two natural proangiogenic growth factors inside PLGA-poloxamer blended nanoparticles. The *in vitro* cellular assays showed the preservation of the biological activity of GFs up to one month [56].

The use of more hydrophilic surfactants (poloxamers) or polymers (PEG) in the inner water phase or blended with PLGA in the organic phase of the primary emulsion reduces the interaction of encapsulated proteins with the hydrophobic PLGA matrix. This prevents disrupting the structure of the protein molecules and helps, at the same time, to neutralize the acidity generated by the hydrolytic degradation of the PLGA [113]. In some cases, the combination of several stabilizers, such as poloxamers, trehalose, and sodium bicarbonate, has been shown to preserve the integrity

of encapsulated proteins but it also reduces the encapsulation efficiency [114].

As a general rule, encapsulation efficiency increases with the size of the particles [82]. Additionally, the adequate stabilization of the primary emulsion by amphiphilic polymers and a rapid solidification (precipitation) of polymer in the second step are favorable parameters for enhancing protein entrapment efficiency in the W/O/W emulsion technique [87].

The tendency of BMP2 to interact with hydrophobic surfaces may decrease the loss of encapsulated protein during the extraction of the solvent phase. This favors a higher entrapment but it lowers the later extraction [58]. An optimal protein encapsulation is obtained when pH of the internal and external water phases is near the isoelectric point of the protein [92]. Blanco and Alonso [83] observed a reduction in the protein encapsulation efficiency when poloxamer was coencapsulated in the primary emulsion. This highlights the main role played by the protein-polymer interaction in the encapsulation efficiency and the later release process. However, too much emulsifier may also result in a reduction of the encapsulation efficiency [99]. Therefore, an equilibrium between the emulsification powder of the surfactant and their concentration is needed.

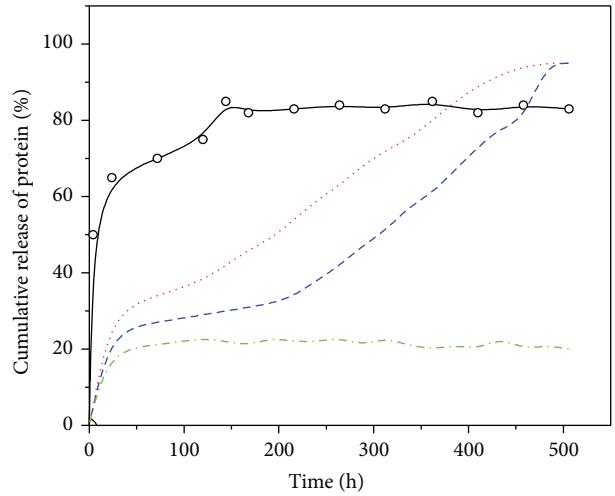

Figure 6: Release profiles. (○) BSA release from PLGA nanoparticles with high initial burst release; (red dots line) biphasic model combining a moderate initial burst and a subsequent sustained release; (blue dash line) triphasic model with a lag of release between both initial and sustained release phases; (dash-dot green line) incomplete release.

3.5. Release Profile. The release profile represents one of the most important characteristics of a nano/micro particulate carrier system since their development has a main final objective: the adequate release of the encapsulated bioactive molecules to reach the desired clinical action.

The release pattern of protein encapsulated in PLGA micro/nanoparticles can present different behavior. It is possible to find a continuous release when the diffusion of the biomolecule is faster than the particle erosion. This process involves a continuous diffusion of the protein from the polymer matrix before the PLGA particle is degraded in lactic and glycolic acid monomers by hydrolysis [74]. A biphasic release characterized by an initial burst at or near the particle surface followed by a second phase in which protein is progressively released by diffusion has also been described. The second phase can be enhanced by bulk erosion of PLGA shell and matrix which results in an important increase of pores and channels [75]. A third triphasic release profile has been found when a lag release period occurs after initial burst and until polymer degradation starts [115]. Finally, it is possible to obtain an incomplete protein release as a consequence of additional factors related with the protein-polymer interaction or protein instability. Figure 6 illustrates the different release profiles previously described. The optimal carrier system should be capable of releasing a controlled concentration gradient of growth factors in the appropriate time, preventing or at least reducing or controlling the initial burst effect [116]. A controlled initial burst followed by a sustained release significantly improves the *in vivo* bone regeneration [117–119].

Giteau et al. [108] present an interesting revision on "How to achieve a sustained and complete release from PLGA microparticles." They begin by analyzing the influence of the release medium and sampling method on the release profile and highlight the significance of the centrifugation cleaning process or the release medium volume. Adjusting to adequate values the centrifugation speed or the buffer volume, it is possible to separate micro/nanoparticles from protein-containing release medium in a very easy way. This allows for stable and reproducible release patterns. On the other hand, to ensure a better protein release profile, modification of the microparticle formulation and microencapsulation process in order to preserve protein aggregation has to be performed. Protein stability has to be maintained by preventing the formation of harmful medium. For example, the synthesis formulation can be modified to use more hydrophilic polymers, since they have been shown to reduce the initial burst and to deliver bioactive proteins over long time periods.

The most relevant strategies are referenced below. Drug release from PLGA nano/microparticles can be controlled by the polymer molecular weight and the relation between monomers (lactide/glycolide) so that an increase in glycolic acid accelerates the weight loss of polymer due to the higher hydrophilicity of the matrix [75]. A mixture of different PLGA nanoparticles obtained using 50 : 50 and 75 : 50 latide/glycolide ratio has shown a great potential for protein drug delivery with a higher initial burst from PLGA 50 : 50. A slow release period has been observed for PLGA 75 : 50 encapsulating a glycoprotein (α-1-antitrypsin) with clinic activity in some pulmonary diseases [60].

On the other hand, a faster erosion of the microspheres with reduction in the PLGA molecular weight due to the facility of water penetration and the subsequent polymer degradation has been described [83]. Schrier et al. working with microspheres prepared by w/o/w using different types of PLGA analyzed the important role of the molecular weight, lactide-glycolide relation, and acid residues [57]. The amount of rhBMP2 adsorbed on the microparticle surface increased

with the hydrophobicity of the polymer. At the same time, the release was in correlation with the degradation profile of the different polymers [57].

Thus, the use of more hydrophilic polymers reduces the hydrophobic protein-polymer interaction. This effect favors a more homogeneous distribution in the polymer matrix and increases the water uptake in the microspheres. Thus, the release rate of rhBMP2 encapsulated in microspheres composed by a PEG-PLGA di-block copolymer is increased with the PEG content of the polymer matrix [58]. A similar result was obtained using PLGA-PEG-PLGA triblock copolymers [59]. In this case, modifying the monomer relation (lactide-glycolide) in the PLGA and increasing the amount of PLGA-PEG-PLGA in the formulations, the release profile of BMP-2 coencapsulated with human SA in microespheres was adjustable. Similarly, the interaction of lysozyme with poloxamer 188 before their encapsulation produces a sustained release over 3 weeks without any burst effect. In the same line, using PLGA-PEG-PLGA as polymer, a sustained release of bioactive lysozime was extended over 45 days when the protein was complexed with poloxamer 188 previously to the encapsulation [120]. However, the presence of PEG300 as an additive of the inner phase of microparticles during the encapsulation process also influences the protein distribution and the release profile. In this case there is a decrease of the initial burst but with less overall release [58].

On the other hand, the use of PLGA-poloxamers blends is useful to obtain a sustained release for more than one month without any incidence in the high initial burst [56, 92]. However, for an encapsulated plasmid inside nanoparticles obtained by PLGA-poloxamer blends, the hydrophobicity of the surfactant allows prolonging the release up to 2 weeks in a controlled manner. Moreover, a complete release was reached for the PLGA-poloxamer blend instead PLGA nanoparticles, in which the maximum release was around 40% [84].

PLGA and poloxamers (pluronic F68) blends can also be used to obtain nanocomposite vesicles by a double emulsion process. These vesicles are suitable for the encapsulation of hydrophobic and hydrophilic molecules. The presence of pluronic affects the colloidal stability of the vesicles and the release pattern of the encapsulated molecules. These vesicles present a wall of 30 nm and the drug is encapsulated in the presence of the poloxamer [121].

Other strategies include the use of different compounds to increase the release time. Thus, BMP2 encapsulated in PLGA-PVA nanoparticles (around 300 nm) showed higher encapsulation efficiency and a short-time release profile with a very high initial burst. However, with the same synthesis procedure (w/o/w) but using PHBV (Poly(3 hydroxybutyrateco-3-hydroxivalerate)), BMP7 loaded nanocapsules had less encapsulation efficiency despite a long-time delivery. Nevertheless, the maximum released amount was lower. This difference in the release profile was due to the difference in hydrophilicity and degradation rates of both polymers [122]. Similarly, PLGA-poloxamer blend nanoparticles were superficially modified by introducing chitosan in the second step of the synthesis. This method showed a sustained release profile for up to 14 days without any initial important burst. In this case, a recombinant hepatitis B antigen was used [106]. Moreover, the use of heparin conjugated with PLGA porous microspheres has also been described to obtain a long-time delivery system reducing at the same time the initial burst. In these systems, heparin was immobilized onto the nano/microparticle surface. The release was controlled by using the binding affinities of heparin to several growth factors including BMP2. In this case, the initial burst was reduced to 4–7% during first day followed by a sustained release of about 1% per day [51–53].

The initial burst release may be attenuated by the fabrication of double-wall microspheres, that is, core-shell microparticles. The presence of a PLA shell reduces the release rate of BSA encapsulated in the PLGA core and extends the duration of the release profile up to two months. Moreover, an increase in the PLA molecular weight influences the rate of particle erosion, which further slows the protein release [123].

The modification of the viscosity in the environment of microparticles additionally influences the release pattern. Viscosity can control the burst at earliest time point and promote a sustained release. This situation has been shown for rhBMP2-PLGA microspheres embedded in a chitosan-thioglycolic acid hydrogel (Poloxamer 407) [124]. Yilgor et al. also incorporated the nanoparticles of their sequential delivery system into a scaffold composed by chitosan and chitosan-PEO [54]. In other work, PLGA/PVA microspheres with encapsulated BMP2 were combined with different composite biomaterials (gelatin hydrogel or polypropylene fumarate). The sustained release of the bioactive molecule was extended over a period of 42 days. *In vivo* results indicate the importance of the composite characteristics. In this case, an enhanced bone formation was obtained when the PLGA microparticles were incorporated into the more hydrophobic matrix (polypropylene fumarate) [125, 126].

Finally, Table 2 summarizes important information about different parameters related to the use of PLGA based nano- or microparticles to encapsulate, transport, and release growth factors (mainly BMP2).

3.6. Gene Therapy for Bone Tissue Engineering: Directed Delivery. In the last years, gene therapy has begun to play a role in bone tissue regeneration becoming an alternative method for the delivery of BMP2 [127, 128]. Thus, the genes encoding a specific protein can be delivered to a specific cell, rather than the proteins themselves. To reach this purpose, an efficient gene vector is necessary. Viral vectors possess the best transfection efficiency but numerous disadvantages, the most notable of them being the risk of mutagenesis. Nonviral vectors elude these problems but with a significant reduction in the transfection rate [129]. Therefore, intracellular delivery of bioactive agents has become the most used strategy for gene therapy, looking for the adequate transfection and consequent expression of the desired protein [79].

PLGA microspheres obtained by a w/o/w double emulsion process have been used by Qiao et al. to entrap plasmid-BMP2/polyethyleneimine nanoparticles. In this case, a sustained release of these nanoparticles until 35 days without initial burst was found resulting in differentiation of osteoblast

Table 2: Nano/microparticles systems to encapsulate GFs, mainly BMP2 growth factor. Most of them are in the microscopic scale and were used to be entrapped into scaffold of different characteristics. PVA has been the more used surfactant-stabilizer. It is possible to find both, encapsulation and surface adsorption of the growth factors with high-moderate efficiency. The use of heparin as stabilizer reduces significantly the initial burst release, favoring a sustained release in the time. The bioactivity of the GF was preserved in most of the systems and coencapsulation with other biomolecules seems to have a similar effect than the use of surfactants as stabilizers.

Polymers	Stabilizer	Size	Encapsulation % EE	Release	Biological activity	Reference
PLGA	PVA	10–20 μm	Adsorbed rhBMP2	20 ng/mL of constant sustained release	Better bone formation after 8 weeks	Fu et al. 2013 [44]
PLGA	PVA	10–100 μm	rhBMP2-BSA 69% (BMP)	Burst (20%) Sustained until 77% (28 days)	BMP2 molecules with bioactivity	Tian et al. 2012 [45]
PLGA 75 : 25	PVA	182 μm	82%	—	Good bone defect repair outcomes within 8–12 weeks	Rodríguez-Évora et al. 2014 [46]
PLGA	PVA	228 μm	60,5%	30% initial burst. Slower release of 4% per week. After 8 weeks 60% released	No loss of bioactivity	Reyes et al. 2013 [47]
PLGA/PEG	No double emulsion synthesis	100–200 μm	Adsorbed BMP2	13% initial burst. Slower release of 0.01–8% per day. After 23 days 70% released	Substantial bone regeneration of the scaffold	Rahman et al. 2014 [48]
Different PLGA	PVA	20–100 μm	30% (uncapped PLGA) 90% (capped PLGA)	26–49% (1 day) Total after 2 weeks	No loss of bioactivity	Lupu-Haber et al. 2013 [49]
PLGA 75 : 25	PVA	5–125 μm	—	Initial burst 30% (1 day) Sustained 35 days	Higher volumes and surface area coverage of new bone	Wink et al. 2014 [50]
PLGA	Heparin	200–800 nm	Adsorbed BMP2 94%	No initial burst. Sustained over 4 weeks	Significant reduction of the BMP2 dose for good bone formation	La et al. 2010 [51]
PLGA	Heparin-Poloxamer	160 nm	Adsorbed BMP2 100%	Initial burst (4–7%) linear profile	Higher matrix mineralization of regenerated bone	Chung et al. 2007 [52]
PLGA	Heparin	100–250 nm	Adsorbed 94%	Initial burst 10% (1 day) 60% after 30 days	No loss of bioactivity Efficacy of administration, amount 50-fold lower	Jeon et al. 2008 [53]
PLGA	PVA	~300 nm	80%	85% initial burst (1 day)	No loss of bioactivity	Yilgor et al. 2009 [54]
PLGA (in rings)	PVA	215 μm	66%	Moderate burst Sustained release over 6 weeks	60% of calvaria defect were healed	Rodríguez-Évora et al. 2013 [55]
PLGA-Poloxamer 188 Blend	Poloxamer	150 nm	FGF-BSA-Heparin 60–80%	40% initial burst (1 day), 60% (30 days)	No loss of bioactivity	d'Angelo et al. 2010 [56]
Different PLGA polymers	PVA	μm order	rhBMP2 adsorption 40–75%	20–80% initial burst (1 day)	—	Schrier et al. 2001 [57]

Table 2: Continued.

Polymers	Stabilizer	Size	Encapsulation % EE	Release	Biological activity	Reference
PLGA/PEG	PVA	37–67 μm	72–99%	33% initial burst (1 day)	Little loss of bioactivity	Lochmann et al. 2010 [58]
PLGA/PLGA-PEG-PLGA	PVA	100 μm	HSA-BMP2 60%	70% initial burst (1 day)	No loss of bioactivity	White et al. 2013 [59]
PLGA	PVA	100–1000 nm	A-1-antitrypsin 90%	30% initial burst (1 day) 50% after 24 days	Biological activity was preserved using BSA and β-cyclodextrine.	Pirooznia et al. 2012 [60]

promoted by the correct transfection of the delivered biofunctional BMP2-DNA [130].

In spite of the general caution with gene therapy, the genetic delivery of BMP2 has the potentiality of a better safety compared with the delivery of large amounts of recombinant protein [131]. Lu et al. specify the urgent need to develop more efficient delivery nanoparticles and transfection methods in order to apply the nonviral vectors in stem cell engineering and bone regeneration. Although enhanced bone formation has been shown in several recent studies using genes such as HIF-1α and miRNAs, new genetic sequences will be discovered and used in bone engineering in the near future that will most likely change our perspective [132].

PLGA nanospheres represent a well-studied biomolecule delivery system that could be applied to cell targeting, in order to enhance the delivery of specific proteins or nucleic acids inside or near the bone engineering reference cells, that is, mesenchymal stem cells [133]. The targeting properties can be supplied by a ligand functionalization strategy: modification of the surface structure of the nanocarrier by conjugating a cell-specific ligand to direct the release of encapsulated biomolecules preferably in close association with the target cells [134]. The use of pegylated nanoparticles with a covalent attachment of different ligands is reported as a potential technique to deliver bone cell-specific biomolecules for bone engineering [135].

Specific antibodies that recognize surface receptors in these cells could be covalently coupled to the surface of PLGA nanoparticles, obtaining "immunonanoparticles." There are several examples of antibody immobilization on surface of PLGA nanoparticles. Kocbek et al. demonstrated the specific recognition of breast tumor cells by a specific monoclonal antibody attached on PLGA fluorescent nanoparticles obtained by W/O/W emulsion process [136]. For the surface covalent attachment, they used a more simple carbodiimide method, which promotes the formation of an amide bond between free carboxylic end groups of PLGA nanoparticles and primary amine groups of the antibody molecule [81]. This procedure can be highly influenced by the presence of stabilizers frequently used to confer colloidal stability to nanoparticles. The electrophoretic mobility of PLGA nanoparticles with an antibody (immuno-γ-globuline anti-human C-reactive protein) covalently attached on the surface is shown in Figure 5. It is necessary to remark the drastic decrease in the mobility values of the antibody-modified nanoparticles with respect to bare PLGA nanoparticles, which could imply low colloidal stability and the subsequent aggregation of the nanosystem. Santander-Ortega et al. proposed a lower antibody loading in which the bare PLGA patches must be coated by a nonionic surfactant in order to obtain immunoreactive stable nanoparticles [95]. Ratzinger et al. indicated that the presence of high poloxamer concentrations decreased the coupling efficiency to carboxylic end groups in PLGA nanoparticles, showing that an equilibrium that combines sufficient stability and the best coupling efficiency is necessary [98]. To prevent this problem, Cheng et al. synthetized carboxyl functionalized PLGA-PEG block copolymer, attaching a specific aptamer to the surface of pegylated nanoparticles via carbodiimide method. In this work, an enhanced drug delivery to prostate tumors has been shown in comparison to equivalent nontargeted nanoparticles [137].

3.7. Scaffolds. The data reported in the literature indicate that PLGA micro/nanoparticles are promising to achieve a sustained, spatial, and temporally controlled delivery of growth factors required for cell growth and cell differentiation. They can be incorporated with cells in solid scaffold or injectable hydrogels [73]. Scaffolds are porous 3D structures normally used to improve tissue-engineered bone [28]. According to Tian et al. [45], a scaffold designed with this objective must have (1) appropriate mechanical strength to support the growth of new bone; (2) appropriate porosity to allow ingrowth of bone-related cells; (3) good biocompatibility allowing the growth of cells on its surface without being rejected by the body; and (4) low toxicity to cells and tissues surrounded and (5) must be able to induce osteogenic differentiation of bone-related stem cells and (6) be biodegradable with nontoxic degradation products that can be eventually replaced by new bone. Additionally, the scaffold for bone regeneration must maintain the delivery or release of BMP (growth factors) "*in situ*" for a long time. In this way, nano/microparticles inside scaffolds are being used to release an adequate flow of these signaling biomolecules and preserve their functional structure [138]. The incorporation of colloidal micro/nanoparticles into fibrous scaffolds adds in the possibility of multiple drugs loading. However, this multidrug system could also involve a decrease of the mechanical properties of the structure and a possible loss of nanoparticles entrapped between the fibers [139].

Considering that the *in vivo* half-life of most biomolecules, especially proteins, is relatively short, it is essential that bioactive scaffolds maintain a desired concentration "*in situ*" to direct tissue regeneration. To do so, an initial release of the encapsulated growth factor in the first hours to quickly get an effective therapeutic concentration followed by a sustained long-time release profile is required [139]. Most of the polymeric particles inserted in scaffold structures are in a micron-scale. The main objective of these microparticles is the protection and temporary control of growth factor delivery. However, given the porosity of these structures, nanoparticles and especially particles of a few microns may become more important since it is possible to design systems with a simple and easy diffusion through the structure. This process could allow the specific recognition of a particular cell type, releasing their encapsulated BMPs in the same environment and helping their differentiation to cell/bone tissue. In any case, the larger-size microspheres might not necessarily be useless for bone regeneration scaffolds. As the microspheres gradually degrade, the space they occupied will be conducive to ingrowth of tissue. In addition to affecting the compression modulus of scaffolds because of their hollow feature, the particle size of microspheres can also influence the release of rhBMP2 [45].

4. Conclusion

The use of polymeric particles using PLGA is a promising system for a spatially and temporally controlled delivery of growth factors that promote cell growth and differentiation in bone engineering and regeneration by means of their incorporation beside cells into solid scaffold or hydrogels.

The PLGA is widely used for its biodegradability and biocompatibility and is approved by FDA and the European Medicines Agency for use in drug delivery systems supplied via parenteral. On the other hand, BMPs are potent growth factors for bone repair and specifically BMP2 shows excellent ability to induce bone formation of adequate quality. The procedure for synthesizing PLGA nano- or microparticles can be modified in their different variables to obtain systems with controlled size, in which it is possible to encapsulate hydrophobic or hydrophilic molecules, with an adequate colloidal stability and the possibility of surface functionalization for targeted delivery.

With this scenario, an optimization of methods and components must balance the structure and morphology of PLGA micro/nanoparticles in order to achieve high encapsulation efficiency of BMP2 and looking for a main goal: control of delivery, reducing the initial burst, and reaching a sustained release profile, preserving the biological activity, and directed to the target cells to minimize the clinical amount needed and allowing a correct bone tissue regeneration.

Conflict of Interests

The authors declare no conflict of interests with any of the products listed in the paper.

Acknowledgments

The authors wish to express their appreciation for the financial support granted by the "Ministerio de Educación y Ciencia" (MEC, Spain), Projects MAT2013-43922-R, and Research Groups no. FQM-115, no. CTS-138, and no. CTS-583 (Junta de Andalucía, Spain). Partial support was also provided by the Andalucía Talent Hub Program from the Andalusian Knowledge Agency, cofunded by the European Union's Seventh Framework Program, Marie Skłodowska-Curie actions (COFUND, Grant Agreement no. 291780) and the Ministry of Economy, Innovation, Science and Employment of the Junta de Andalucía (Miguel Padial-Molina).

References

[1] M. Padial-Molina, P. Galindo-Moreno, and G. Avila-Ortiz, "Biomimetic ceramics in implant dentistry," *Minerva Biotecnologica*, vol. 21, no. 3, pp. 173–186, 2009.

[2] B. Al-Nawas and E. Schiegnitz, "Augmentation procedures using bone substitute materials or autogenous bone—a systematic review and meta-analysis," *European Journal of Oral Implantology*, vol. 7, supplement 2, pp. S219–S234, 2014.

[3] A. Katranji, P. Fotek, and H.-L. Wang, "Sinus augmentation complications: etiology and treatment," *Implant Dentistry*, vol. 17, no. 3, pp. 339–349, 2008.

[4] C. E. Misch, "Maxillary sinus augmentation for endosteal implants: organized alternative treatment plans," *The International Journal of Oral Implantology: Implantologist*, vol. 4, no. 2, pp. 49–58, 1987.

[5] C. Myeroff and M. Archdeacon, "Autogenous bone graft: donor sites and techniques," *The Journal of Bone & Joint Surgery—American Volume*, vol. 93, no. 23, pp. 2227–2236, 2011.

[6] G. Avila, R. Neiva, C. E. Misch et al., "Clinical and histologic outcomes after the use of a novel allograft for maxillary sinus augmentation: a case series," *Implant Dentistry*, vol. 19, no. 4, pp. 330–341, 2010.

[7] S. J. Froum, S. S. Wallace, N. Elian, S. C. Cho, and D. P. Tarnow, "Comparison of mineralized cancellous bone allograft (Puros) and anorganic bovine bone matrix (Bio-Oss) for sinus augmentation: histomorphometry at 26 to 32 weeks after grafting," *The International Journal of Periodontics & Restorative Dentistry*, vol. 26, no. 6, pp. 543–551, 2006.

[8] P. Galindo-Moreno, G. Ávila, J. E. Fernández-Barbero et al., "Evaluation of sinus floor elevation using a composite bone graft mixture," *Clinical Oral Implants Research*, vol. 18, no. 3, pp. 376–382, 2007.

[9] P. Galindo-Moreno, I. Moreno-Riestra, G. Avila et al., "Effect of anorganic bovine bone to autogenous cortical bone ratio upon bone remodeling patterns following maxillary sinus augmentation," *Clinical Oral Implants Research*, vol. 22, no. 8, pp. 857–864, 2011.

[10] S. L. Wheeler, "Sinus augmentation for dental implants: the use of alloplastic materials," *Journal of Oral and Maxillofacial Surgery*, vol. 55, no. 11, pp. 1287–1293, 1997.

[11] S. S. Wallace and S. J. Froum, "Effect of maxillary sinus augmentation on the survival of endosseous dental implants. A systematic review.," *Annals of Periodontology/the American Academy of Periodontology*, vol. 8, no. 1, pp. 328–343, 2003.

[12] M. Padial-Molina and H. F. Rios, "Stem cells, scaffolds and gene therapy for periodontal engineering," *Current Oral Health Reports*, vol. 1, no. 1, pp. 16–25, 2014.

[13] M. Padial-Molina, S. L. Volk, and H. F. Rios, "Periostin increases migration and proliferation of human periodontal ligament fibroblasts challenged by tumor necrosis factor -alpha and *Porphyromonas gingivalis* lipopolysaccharides," *Journal of Periodontal Research*, vol. 49, no. 3, pp. 405–414, 2014.

[14] H. Behnia, A. Khojasteh, M. Soleimani, A. Tehranchi, and A. Atashi, "Repair of alveolar cleft defect with mesenchymal stem cells and platelet derived growth factors: a preliminary report," *Journal of Cranio-Maxillofacial Surgery*, vol. 40, no. 1, pp. 2–7, 2012.

[15] M. Padial-Molina, J. T. Marchesan, A. D. Taut, Q. Jin, W. V. Giannobile, and H. F. Rios, "Methods to validate tooth-supporting regenerative therapies," *Methods in Molecular Biology*, vol. 887, pp. 135–148, 2012.

[16] M. R. Urist, "Bone: formation by autoinduction," *Science*, vol. 150, no. 3698, pp. 893–899, 1965.

[17] P. Boyne and S. D. Jones, "Demonstration of the osseoinductive effect of bone morphogenetic protein within endosseous dental implants," *Implant Dentistry*, vol. 13, no. 2, pp. 180–184, 2004.

[18] E. A. Wang, V. Rosen, J. S. D'Alessandro et al., "Recombinant human bone morphogenetic protein induces bone formation," *Proceedings of the National Academy of Sciences of the United States of America*, vol. 87, no. 6, pp. 2220–2224, 1990.

[19] J. M. Wozney, "The bone morphogenetic protein family and osteogenesis," *Molecular Reproduction and Development*, vol. 32, no. 2, pp. 160–167, 1992.

[20] E. Barboza, A. Caúla, and F. Machado, "Potential of recombinant human bone morphogenetic protein-2 in bone regeneration," *Implant Dentistry*, vol. 8, no. 4, pp. 360–367, 1999.

[21] A. C. Carreira, G. G. Alves, W. F. Zambuzzi, M. C. Sogayar, and J. M. Granjeiro, "Bone morphogenetic proteins: structure, biological function and therapeutic applications," *Archives of Biochemistry and Biophysics*, vol. 561, pp. 64–73, 2014.

[22] J. C. Bustos-Valenzuela, A. Fujita, E. Halcsik, J. M. Granjeiro, and M. C. Sogayar, "Unveiling novel genes upregulated by both rhBMP2 and rhBMP7 during early osteoblastic transdifferentiation of C2C12 cells," *BMC Research Notes*, vol. 4, article 370, 2011.

[23] K. Tsuji, A. Bandyopadhyay, B. D. Harfe et al., "BMP2 activity, although dispensable for bone formation, is required for the initiation of fracture healing," *Nature Genetics*, vol. 38, no. 12, pp. 1424–1429, 2006.

[24] K. Tsuji, K. Cox, A. Bandyopadhyay, B. D. Harfe, C. J. Tabin, and V. Rosen, "BMP4 is dispensable for skeletogenesis and fracture-healing in the limb," *The Journal of Bone and Joint Surgery—American Volume*, vol. 90, supplement 1, pp. 14–18, 2008.

[25] K. Tsuji, K. Cox, L. Gamer, D. Graf, A. Economides, and V. Rosen, "Conditional deletion of BMP7 from the limb skeleton does not affect bone formation or fracture repair," *Journal of Orthopaedic Research*, vol. 28, no. 3, pp. 384–389, 2010.

[26] G. Chen, C. Deng, and Y.-P. Li, "TGF-beta and BMP signaling in osteoblast differentiation and bone formation," *International Journal of Biological Sciences*, vol. 8, no. 2, pp. 272–288, 2012.

[27] M.-C. Ramel and C. S. Hill, "Spatial regulation of BMP activity," *FEBS Letters*, vol. 586, no. 14, pp. 1929–1941, 2012.

[28] A. C. Carreira, F. H. Lojudice, E. Halcsik, R. D. Navarro, M. C. Sogayar, and J. M. Granjeiro, "Bone morphogenetic proteins: facts, challenges, and future perspectives," *Journal of Dental Research*, vol. 93, no. 4, pp. 335–345, 2014.

[29] F. Deschaseaux, L. Sensébé, and D. Heymann, "Mechanisms of bone repair and regeneration," *Trends in Molecular Medicine*, vol. 15, no. 9, pp. 417–429, 2009.

[30] T. D. Mueller and J. Nickel, "Promiscuity and specificity in BMP receptor activation," *FEBS Letters*, vol. 586, no. 14, pp. 1846–1859, 2012.

[31] C. Sieber, J. Kopf, C. Hiepen, and P. Knaus, "Recent advances in BMP receptor signaling," *Cytokine & Growth Factor Reviews*, vol. 20, no. 5-6, pp. 343–355, 2009.

[32] G. Sapkota, C. Alarcón, F. M. Spagnoli, A. H. Brivanlou, and J. Massagué, "Balancing BMP signaling through integrated inputs into the Smad1 linker," *Molecular Cell*, vol. 25, no. 3, pp. 441–454, 2007.

[33] W. F. McKay, S. M. Peckham, and J. M. Badura, "A comprehensive clinical review of recombinant human bone morphogenetic protein-2 (INFUSE Bone Graft)," *International Orthopaedics*, vol. 31, no. 6, pp. 729–734, 2007.

[34] P. Hong, D. Boyd, S. D. Beyea, and M. Bezuhly, "Enhancement of bone consolidation in mandibular distraction osteogenesis: a contemporary review of experimental studies involving adjuvant therapies," *Journal of Plastic, Reconstructive and Aesthetic Surgery*, vol. 66, no. 7, pp. 883–895, 2013.

[35] D. B. Spagnoli and R. E. Marx, "Dental implants and the use of rhBMP-2," *Dental Clinics of North America*, vol. 55, no. 4, pp. 883–907, 2011.

[36] M. Nevins, C. Kirker-Head, M. Nevins, J. A. Wozney, R. Palmer, and D. Graham, "Bone formation in the goat maxillary sinus induced by absorbable collagen sponge implants impregnated with recombinant human bone morphogenetic protein-2," *The International Journal of Periodontics & Restorative Dentistry*, vol. 16, no. 1, pp. 8–19, 1996.

[37] P. J. Boyne, L. C. Lilly, R. E. Marx et al., "De novo bone induction by recombinant human bone morphogenetic protein-2 (rhBMP-2) in maxillary sinus floor augmentation," *Journal of Oral and Maxillofacial Surgery*, vol. 63, no. 12, pp. 1693–1707, 2005.

[38] L. Torrecillas-Martinez, A. Monje, M. A. Pikos et al., "Effect of rhBMP-2 upon maxillary sinus augmentation: a comprehensive review," *Implant Dentistry*, vol. 22, no. 3, pp. 232–237, 2013.

[39] J. Lee, C. Susin, N. A. Rodriguez et al., "Sinus augmentation using rhBMP-2/ACS in a mini-pig model: relative efficacy of autogenous fresh particulate iliac bone grafts," *Clinical Oral Implants Research*, vol. 24, no. 5, pp. 497–504, 2013.

[40] R. G. Triplett, M. Nevins, R. E. Marx et al., "Pivotal, randomized, parallel evaluation of recombinant human bone morphogenetic protein-2/absorbable collagen sponge and autogenous bone graft for maxillary sinus floor augmentation," *Journal of Oral and Maxillofacial Surgery*, vol. 67, no. 9, pp. 1947–1960, 2009.

[41] D. W. K. Kao, A. Kubota, M. Nevins, and J. P. Fiorellini, "The negative effect of combining rhBMP-2 and Bio-Oss on bone formation for maxillary sinus augmentation," *The International Journal of Periodontics & Restorative Dentistry*, vol. 32, no. 1, pp. 61–67, 2012.

[42] O. Hanisch, D. N. Tatakis, M. D. Rohrer, P. S. Wöhrle, J. M. Wozney, and U. M. E. Wikesjö, "Bone formation and osseointegration stimulated by rhBMP-2 following subantral augmentation procedures in nonhuman primates," *The International Journal of Oral & Maxillofacial Implants*, vol. 12, no. 6, pp. 785–792, 1997.

[43] K. Wada, A. Niimi, K. Watanabe, T. Sawai, and M. Ueda, "Maxillary sinus floor augmentation in rabbits: a comparative

histologic-histomorphometric study between rhBMP-2 and autogenous bone," *The International Journal of Periodontics & Restorative Dentistry*, vol. 21, no. 3, pp. 253–263, 2001.

[44] R. Fu, S. Selph, M. McDonagh et al., "Effectiveness and harms of recombinant human bone morphogenetic protein-2 in spine fusion: a systematic review and meta-analysis," *Annals of Internal Medicine*, vol. 158, no. 12, pp. 890–902, 2013.

[45] Z. Tian, Y. Zhu, J. Qiu et al., "Synthesis and characterization of UPPE-PLGA-rhBMP2 scaffolds for bone regeneration," *Journal of Huazhong University of Science and Technology—Medical Science*, vol. 32, no. 4, pp. 563–570, 2012.

[46] M. Rodríguez-Évora, E. García-Pizarro, C. del Rosario et al., "Smurf1 knocked-down, mesenchymal stem cells and BMP-2 in an electrospun system for bone regeneration," *Biomacromolecules*, vol. 15, no. 4, pp. 1311–1322, 2014.

[47] R. Reyes, A. Delgado, R. Solis et al., "Cartilage repair by local delivery of TGF-β1 or BMP-2 from a novel, segmented polyurethane/polylactic-co-glycolic bilayered scaffold," *Journal of Biomedical Materials Research Part A*, 2013.

[48] C. V. Rahman, D. Ben-David, A. Dhillon et al., "Controlled release of BMP-2 from a sintered polymer scaffold enhances bone repair in a mouse calvarial defect model," *Journal of Tissue Engineering and Regenerative Medicine*, vol. 8, no. 1, pp. 59–66, 2014.

[49] Y. Lupu-Haber, O. Pinkas, S. Boehm, T. Scheper, C. Kasper, and M. Machluf, "Functionalized PLGA-doped zirconium oxide ceramics for bone tissue regeneration," *Biomedical Microdevices*, vol. 15, no. 6, pp. 1055–1066, 2013.

[50] J. D. Wink, P. A. Gerety, R. D. Sherif et al., "Sustained delivery of rhBMP-2 by means of poly(lactic-co-glycolic acid) microspheres: cranial bone regeneration without heterotopic ossification or craniosynostosis," *Plastic and Reconstructive Surgery*, vol. 134, no. 1, pp. 51–59, 2014.

[51] W.-G. La, S.-W. Kang, H. S. Yang et al., "The efficacy of bone morphogenetic protein-2 depends on its mode of delivery," *Artificial Organs*, vol. 34, no. 12, pp. 1150–1153, 2010.

[52] Y.-I. Chung, K.-M. Ahn, S.-H. Jeon, S.-Y. Lee, J.-H. Lee, and G. Tae, "Enhanced bone regeneration with BMP-2 loaded functional nanoparticle-hydrogel complex," *Journal of Controlled Release*, vol. 121, no. 1-2, pp. 91–99, 2007.

[53] O. Jeon, S. J. Song, H. S. Yang et al., "Long-term delivery enhances in vivo osteogenic efficacy of bone morphogenetic protein-2 compared to short-term delivery," *Biochemical and Biophysical Research Communications*, vol. 369, no. 2, pp. 774–780, 2008.

[54] P. Yilgor, K. Tuzlakoglu, R. L. Reis, N. Hasirci, and V. Hasirci, "Incorporation of a sequential BMP-2/BMP-7 delivery system into chitosan-based scaffolds for bone tissue engineering," *Biomaterials*, vol. 30, no. 21, pp. 3551–3559, 2009.

[55] M. Rodríguez-Évora, A. Delgado, R. Reyes et al., "Osteogenic effect of local, long versus short term BMP-2 delivery from a novel SPU-PLGA-βTCP concentric system in a critical size defect in rats," *European Journal of Pharmaceutical Sciences*, vol. 49, no. 5, pp. 873–884, 2013.

[56] I. d'Angelo, M. Garcia-Fuentes, Y. Parajó et al., "Nanoparticles based on PLGA: poloxamer blends for the delivery of proangiogenic growth factors," *Molecular Pharmaceutics*, vol. 7, no. 5, pp. 1724–1733, 2010.

[57] J. A. Schrier, B. F. Fink, J. B. Rodgers, H. C. Vasconez, and P. P. DeLuca, "Effect of a freeze-dried CMC/PLGA microsphere matrix of rhBMP-2 on bone healing," *AAPS PharmSciTech*, vol. 2, no. 3, article E18, 2001.

[58] A. Lochmann, H. Nitzsche, S. von Einem, E. Schwarz, and K. Mäder, "The influence of covalently linked and free polyethylene glycol on the structural and release properties of rhBMP-2 loaded microspheres," *Journal of Controlled Release*, vol. 147, no. 1, pp. 92–100, 2010.

[59] L. J. White, G. T. S. Kirby, H. C. Cox et al., "Accelerating protein release from microparticles for regenerative medicine applications," *Materials Science and Engineering C: Materials for Biological Applications*, vol. 33, no. 5, pp. 2578–2583, 2013.

[60] N. Pirooznia, S. Hasannia, A. S. Lotfi, and M. Ghanei, "Encapsulation of alpha-1 antitrypsin in PLGA nanoparticles: in vitro characterization as an effective aerosol formulation in pulmonary diseases," *Journal of Nanobiotechnology*, vol. 10, article 20, 2012.

[61] M. Ronga, A. Fagetti, G. Canton, E. Paiusco, M. F. Surace, and P. Cherubino, "Clinical applications of growth factors in bone injuries: experience with BMPs," *Injury*, vol. 44, supplement 1, pp. S34–S39, 2013.

[62] J. G. Devine, J. R. Dettori, J. C. France, E. Brodt, and R. A. McGuire, "The use of rhBMP in spine surgery: is there a cancer risk?" *Evidence-Based Spine-Care Journal*, vol. 3, no. 2, pp. 35–41, 2012.

[63] E. J. Carragee, E. L. Hurwitz, and B. K. Weiner, "A critical review of recombinant human bone morphogenetic protein-2 trials in spinal surgery: emerging safety concerns and lessons learned," *The Spine Journal*, vol. 11, no. 6, pp. 471–491, 2011.

[64] M. C. Simmonds, J. V. E. Brown, M. K. Heirs et al., "Safety and effectiveness of recombinant human bone morphogenetic protein-2 for spinal fusion: a meta-analysis of individual-participant data," *Annals of Internal Medicine*, vol. 158, no. 12, pp. 877–889, 2013.

[65] V. H.-Y. Chung, A. Y.-L. Chen, L.-B. Jeng, C.-C. Kwan, S.-H. Cheng, and S. C.-N. Chang, "Engineered autologous bone marrow mesenchymal stem cells: alternative to cleft alveolar bone graft surgery," *Journal of Craniofacial Surgery*, vol. 23, no. 5, pp. 1558–1563, 2012.

[66] T. A. Ratko, S. E. Belinson, D. J. Samson, C. Bonnell, K. M. Ziegler, and N. Aronson, *Bone Morphogenetic Protein: The State of the Evidence of On-Label and Off-Label Use*, Agency for Healthcare Research and Quality, Rockville, Md, USA, 2010.

[67] G. Barratt, "Colloidal drug carriers: achievements and perspectives," *Cellular and Molecular Life Sciences*, vol. 60, no. 1, pp. 21–37, 2003.

[68] V. W. Bramwell and Y. Perrie, "Particulate delivery systems for vaccines," *Critical Reviews in Therapeutic Drug Carrier Systems*, vol. 22, no. 2, pp. 151–214, 2005.

[69] N. Csaba, M. Garcia-Fuentes, and M. J. Alonso, "The performance of nanocarriers for transmucosal drug delivery," *Expert Opinion on Drug Delivery*, vol. 3, no. 4, pp. 463–478, 2006.

[70] M. J. Santander-Ortega, T. Stauner, B. Loretz et al., "Nanoparticles made from novel starch derivatives for transdermal drug delivery," *Journal of Controlled Release*, vol. 141, no. 1, pp. 85–92, 2010.

[71] W. Jiang, R. K. Gupta, M. C. Deshpande, and S. P. Schwendeman, "Biodegradable poly(lactic-co-glycolic acid) microparticles for injectable delivery of vaccine antigens," *Advanced Drug Delivery Reviews*, vol. 57, no. 3, pp. 391–410, 2005.

[72] T. R. Shantha Kumar, K. Soppimath, and S. K. Nachaegari, "Novel delivery technologies for protein and peptide therapeutics," *Current Pharmaceutical Biotechnology*, vol. 7, no. 4, pp. 261–276, 2006.

[73] F. Danhier, E. Ansorena, J. M. Silva, R. Coco, A. Le Breton, and V. Préat, "PLGA-based nanoparticles: an overview of biomedical applications," *Journal of Controlled Release*, vol. 161, no. 2, pp. 505–522, 2012.

[74] A. Kumari, S. K. Yadav, and S. C. Yadav, "Biodegradable polymeric nanoparticles based drug delivery systems," *Colloids and Surfaces B: Biointerfaces*, vol. 75, no. 1, pp. 1–18, 2010.

[75] H. K. Makadia and S. J. Siegel, "Poly Lactic-co-Glycolic Acid (PLGA) as biodegradable controlled drug delivery carrier," *Polymers*, vol. 3, no. 3, pp. 1377–1397, 2011.

[76] F. Mohamed and C. F. van der Walle, "Engineering biodegradable polyester particles with specific drug targeting and drug release properties," *Journal of Pharmaceutical Sciences*, vol. 97, no. 1, pp. 71–87, 2008.

[77] G. A. Silva, O. P. Coutinho, P. Ducheyne, and R. L. Reis, "Materials in particulate form for tissue engineering. 2. Applications in bone," *Journal of Tissue Engineering and Regenerative Medicine*, vol. 1, no. 2, pp. 97–109, 2007.

[78] S. Zhang and H. Uludag, "Nanoparticulate systems for growth factor delivery," *Pharmaceutical Research*, vol. 26, no. 7, pp. 1561–1580, 2009.

[79] V. E. Santo, M. E. Gomes, J. F. Mano, and R. L. Reis, "From nano-to macro-scale: nanotechnology approaches for spatially controlled delivery of bioactive factors for bone and cartilage engineering," *Nanomedicine*, vol. 7, no. 7, pp. 1045–1066, 2012.

[80] M.-K. Tran, A. Swed, and F. Boury, "Preparation of polymeric particles in CO_2 medium using non-toxic solvents: formulation and comparisons with a phase separation method," *European Journal of Pharmaceutics and Biopharmaceutics*, vol. 82, no. 3, pp. 498–507, 2012.

[81] B. Ertl, F. Heigl, M. Wirth, and F. Gabor, "Lectin-mediated bioadhesion: preparation, stability and Caco-2 binding of wheat germ agglutinin-functionalized poly-(D,L-lactic-co-glycolic acid)-microspheres," *Journal of Drug Targeting*, vol. 8, no. 3, pp. 173–184, 2000.

[82] M. L. Hans and A. M. Lowman, "Biodegradable nanoparticles for drug delivery and targeting," *Current Opinion in Solid State and Materials Science*, vol. 6, no. 4, pp. 319–327, 2002.

[83] D. Blanco and M. J. Alonso, "Protein encapsulation and release from poly(lactide-co-glycolide) microspheres: effect of the protein and polymer properties and of the co-encapsulation of surfactants," *European Journal of Pharmaceutics and Biopharmaceutics*, vol. 45, no. 3, pp. 285–294, 1998.

[84] N. Csaba, P. Caamaño, A. Sánchez, F. Domínguez, and M. J. Alonso, "PLGA: poloxamer and PLGA:poloxamine blend nanoparticles: new carriers for gene delivery," *Biomacromolecules*, vol. 6, no. 1, pp. 271–278, 2005.

[85] C. Sturesson and J. Carlfors, "Incorporation of protein in PLG-microspheres with retention of bioactivity," *Journal of Controlled Release*, vol. 67, no. 2-3, pp. 171–178, 2000.

[86] I. D. Rosca, F. Watari, and M. Uo, "Microparticle formation and its mechanism in single and double emulsion solvent evaporation," *Journal of Controlled Release*, vol. 99, no. 2, pp. 271–280, 2004.

[87] F. T. Meng, G. H. Ma, W. Qiu, and Z. G. Su, "W/O/W double emulsion technique using ethyl acetate as organic solvent: effects of its diffusion rate on the characteristics of microparticles," *Journal of Controlled Release*, vol. 91, no. 3, pp. 407–416, 2003.

[88] R. Ghaderi and J. Carlfors, "Biological activity of lysozyme after entrapment in poly (d,l-lactide-co-glycolide)-microspheres," *Pharmaceutical Research*, vol. 14, no. 11, pp. 1556–1562, 1997.

[89] H. Wang, S. C. G. Leeuwenburgh, Y. Li, and J. A. Jansen, "The use of micro- and nanospheres as functional components for bone tissue regeneration," *Tissue Engineering Part B: Reviews*, vol. 18, no. 1, pp. 24–39, 2012.

[90] S. Xiong, X. Zhao, B. C. Heng, K. W. Ng, and J. S.-C. Loo, "Cellular uptake of Poly-(D,L-lactide-co-glycolide) (PLGA) nanoparticles synthesized through solvent emulsion evaporation and nanoprecipitation method," *Biotechnology Journal*, vol. 6, no. 5, pp. 501–508, 2011.

[91] L. Y. T. Chou, K. Ming, and W. C. W. Chan, "Strategies for the intracellular delivery of nanoparticles," *Chemical Society Reviews*, vol. 40, no. 1, pp. 233–245, 2011.

[92] M. J. Santander-Ortega, M. V. Lozano-López, D. Bastos-González, J. M. Peula-García, and J. L. Ortega-Vinuesa, "Novel core-shell lipid-chitosan and lipid-poloxamer nanocapsules: stability by hydration forces," *Colloid and Polymer Science*, vol. 288, no. 2, pp. 159–172, 2010.

[93] Y.-Y. Yang, T.-S. Chung, and N. Ping Ng, "Morphology, drug distribution, and in vitro release profiles of biodegradable polymeric microspheres containing protein fabricated by double-emulsion solvent extraction/evaporation method," *Biomaterials*, vol. 22, no. 3, pp. 231–241, 2001.

[94] T. Feczkó, J. Tóth, and J. Gyenis, "Comparison of the preparation of PLGA-BSA nano- and microparticles by PVA, poloxamer and PVP," *Colloids and Surfaces A: Physicochemical and Engineering Aspects*, vol. 319, no. 1–3, pp. 188–195, 2008.

[95] M. J. Santander-Ortega, D. Bastos-González, and J. L. Ortega-Vinuesa, "Electrophoretic mobility and colloidal stability of PLGA particles coated with IgG," *Colloids and Surfaces B: Biointerfaces*, vol. 60, no. 1, pp. 80–88, 2007.

[96] Y.-Y. Yang, H.-H. Chia, and T.-S. Chung, "Effect of preparation temperature on the characteristics and release profiles of PLGA microspheres containing protein fabricated by double-emulsion solvent extraction/evaporation method," *Journal of Controlled Release*, vol. 69, no. 1, pp. 81–96, 2000.

[97] D.-L. Fang, Y. Chen, B. Xu et al., "Development of lipid-shell and polymer core nanoparticles with water-soluble salidroside for anti-cancer therapy," *International Journal of Molecular Sciences*, vol. 15, no. 3, pp. 3373–3388, 2014.

[98] G. Ratzinger, U. Länger, L. Neutsch, F. Pittner, M. Wirth, and F. Gabor, "Surface modification of PLGA particles: the interplay between stabilizer, ligand size, and hydrophobic interactions," *Langmuir*, vol. 26, no. 3, pp. 1855–1859, 2010.

[99] S.-S. Feng and G. Huang, "Effects of emulsifiers on the controlled release of paclitaxel (Taxol) from nanospheres of biodegradable polymers," *Journal of Controlled Release*, vol. 71, no. 1, pp. 53–69, 2001.

[100] J. M. Chan, L. Zhang, K. P. Yuet et al., "PLGA-lecithin-PEG core-shell nanoparticles for controlled drug delivery," *Biomaterials*, vol. 30, no. 8, pp. 1627–1634, 2009.

[101] M. Fraylich, W. Wang, K. Shakesheff, C. Alexander, and B. Saunders, "Poly(D,L-lactide-co-glycolide) dispersions containing pluronics: from particle preparation to temperature-triggered aggregation," *Langmuir*, vol. 24, no. 15, pp. 7761–7768, 2008.

[102] M. J. Santander-Ortega, J. M. Peula-García, F. M. Goycoolea, and J. L. Ortega-Vinuesa, "Chitosan nanocapsules: effect of chitosan molecular weight and acetylation degree on electrokinetic behaviour and colloidal stability," *Colloids and Surfaces B: Biointerfaces*, vol. 82, no. 2, pp. 571–580, 2011.

[103] J. S. Tan, D. E. Butterfield, C. L. Voycheck, K. D. Caldwell, and J. T. Li, "Surface modification of nanoparticles by PEO/PPO block

copolymers to minimize interactions with blood components and prolong blood circulation in rats," *Biomaterials*, vol. 14, no. 11, pp. 823–833, 1993.

[104] C. Bouissou, U. Potter, H. Altroff, H. Mardon, and C. van der Walle, "Controlled release of the fibronectin central cell binding domain from polymeric microspheres," *Journal of Controlled Release*, vol. 95, no. 3, pp. 557–566, 2004.

[105] R. Gref, Y. Minamitake, M. T. Peracchia, V. Trubetskoy, V. Torchilin, and R. Langer, "Biodegradable long-circulating polymeric nanospheres," *Science*, vol. 263, no. 5153, pp. 1600–1603, 1994.

[106] P. Paolicelli, C. Prego, A. Sanchez, and M. J. Alonso, "Surface-modified PLGA-based nanoparticles that can efficiently associate and deliver virus-like particles," *Nanomedicine*, vol. 5, no. 6, pp. 843–853, 2010.

[107] I. Brigger, C. Dubernet, and P. Couvreur, "Nanoparticles in cancer therapy and diagnosis," *Advanced Drug Delivery Reviews*, vol. 54, no. 5, pp. 631–651, 2002.

[108] A. Giteau, M. C. Venier-Julienne, A. Aubert-Pouëssel, and J. P. Benoit, "How to achieve sustained and complete protein release from PLGA-based microparticles?" *International Journal of Pharmaceutics*, vol. 350, no. 1-2, pp. 14–26, 2008.

[109] E. R. Balmayor, G. A. Feichtinger, H. S. Azevedo, M. van Griensven, and R. L. Reis, "Starch-poly-ε-caprolactone microparticles reduce the needed amount of BMP-2," *Clinical Orthopaedics and Related Research*, vol. 467, no. 12, pp. 3138–3148, 2009.

[110] M. J. Santander-Ortega, D. Bastos-González, J. L. Ortega-Vinuesa, and M. J. Alonso, "Insulin-loaded PLGA nanoparticles for oral administration: an in vitro physico-chemical characterization," *Journal of Biomedical Nanotechnology*, vol. 5, no. 1, pp. 45–53, 2009.

[111] L. Meinel, O. E. Illi, J. Zapf, M. Malfanti, H. Peter Merkle, and B. Gander, "Stabilizing insulin-like growth factor-I in poly(D,L-lactide-co-glycolide) microspheres," *Journal of Controlled Release*, vol. 70, no. 1-2, pp. 193–202, 2001.

[112] C. Srinivasan, Y. K. Katare, T. Muthukumaran, and A. K. Panda, "Effect of additives on encapsulation efficiency, stability and bioactivity of entrapped lysozyme from biodegradable polymer particles," *Journal of Microencapsulation*, vol. 22, no. 2, pp. 127–138, 2005.

[113] M. Tobío, S. P. Schwendeman, Y. Guo, J. McIver, R. Langer, and M. J. Alonso, "Improved immunogenicity of a core-coated tetanus toxoid delivery system," *Vaccine*, vol. 18, no. 7-8, pp. 618–622, 1999.

[114] D. K. Malik, S. Baboota, A. Ahuja, S. Hasan, and J. Ali, "Recent advances in protein and peptide drug delivery systems," *Current Drug Delivery*, vol. 4, no. 2, pp. 141–151, 2007.

[115] J. L. Cleland, "Protein delivery from biodegradable microspheres," in *Protein Delivery: Physical Systems*, L. M. Sanders and R. W. Hendron, Eds., pp. 1–41, Plenum Press, New York, NY, USA, 1997.

[116] S. H. Oh, T. H. Kim, and J. H. Lee, "Creating growth factor gradients in three dimensional porous matrix by centrifugation and surface immobilization," *Biomaterials*, vol. 32, no. 32, pp. 8254–8260, 2011.

[117] B. N. Brown, J. E. Valentin, A. M. Stewart-Akers, G. P. McCabe, and S. F. Badylak, "Macrophage phenotype and remodeling outcomes in response to biologic scaffolds with and without a cellular component," *Biomaterials*, vol. 30, no. 8, pp. 1482–1491, 2009.

[118] B. N. Brown, J. M. Freund, L. Han et al., "Comparison of three methods for the derivation of a biologic scaffold composed of adipose tissue extracellular matrix," *Tissue Engineering—Part C: Methods*, vol. 17, no. 4, pp. 411–421, 2011.

[119] B. Li, T. Yoshii, A. E. Hafeman, J. S. Nyman, J. C. Wenke, and S. A. Guelcher, "The effects of rhBMP-2 released from biodegradable polyurethane/microsphere composite scaffolds on new bone formation in rat femora," *Biomaterials*, vol. 30, no. 35, pp. 6768–6779, 2009.

[120] A. Paillard-Giteau, V. T. Tran, O. Thomas et al., "Effect of various additives and polymers on lysozyme release from PLGA microspheres prepared by an s/o/w emulsion technique," *European Journal of Pharmaceutics and Biopharmaceutics*, vol. 75, no. 2, pp. 128–136, 2010.

[121] B. P. Nair and C. P. Sharma, "Poly(lactide-*co*-glycolide)-laponite-F68 nanocomposite vesicles through a single-step double-emulsion method for the controlled release of doxorubicin," *Langmuir*, vol. 28, no. 9, pp. 4559–4564, 2012.

[122] P. Yilgor, N. Hasirci, and V. Hasirci, "Sequential BMP-2/BMP-7 delivery from polyester nanocapsules," *Journal of Biomedical Materials Research—Part A*, vol. 93, no. 2, pp. 528–536, 2010.

[123] Y. Xia, Q. Xu, C.-H. Wang, and D. W. Pack, "Protein encapsulation in and release from monodisperse double-wall polymer microspheres," *Journal of Pharmaceutical Sciences*, vol. 102, no. 5, pp. 1601–1609, 2013.

[124] Y. Fu, L. Du, Q. Wang et al., "In vitro sustained release of recombinant human bone morphogenetic protein-2 microspheres embedded in thermosensitive hydrogels," *Die Pharmazie*, vol. 67, no. 4, pp. 299–303, 2012.

[125] D. H. R. Kempen, L. Lu, T. E. Hefferan et al., "Retention of in vitro and in vivo BMP-2 bioactivities in sustained delivery vehicles for bone tissue engineering," *Biomaterials*, vol. 29, no. 22, pp. 3245–3252, 2008.

[126] D. H. R. Kempen, L. Lu, A. Heijink et al., "Effect of local sequential VEGF and BMP-2 delivery on ectopic and orthotopic bone regeneration," *Biomaterials*, vol. 30, no. 14, pp. 2816–2825, 2009.

[127] H. Nie, M.-L. Ho, C.-K. Wang, C.-H. Wang, and Y.-C. Fu, "BMP-2 plasmid loaded PLGA/HAp composite scaffolds for treatment of bone defects in nude mice," *Biomaterials*, vol. 30, no. 5, pp. 892–901, 2009.

[128] F. Wegman, Y. van der Helm, F. C. Öner, W. J. A. Dhert, and J. Alblas, "Bone morphogenetic protein-2 plasmid DNA as a substitute for bone morphogenetic protein-2 protein in bone tissue engineering," *Tissue Engineering Part A*, vol. 19, no. 23-24, pp. 2686–2692, 2013.

[129] J. Fischer, A. Kolk, S. Wolfart et al., "Future of local bone regeneration—protein versus gene therapy," *Journal of Cranio-Maxillofacial Surgery*, vol. 39, no. 1, pp. 54–64, 2011.

[130] C. Qiao, K. Zhang, H. Jin et al., "Using poly(lactic-co-glycolic acid) microspheres to encapsulate plasmid of bone morphogenetic protein 2/polyethylenimine nanoparticles to promote bone formation in vitro and in vivo," *International Journal of Nanomedicine*, vol. 8, pp. 2985–2995, 2013.

[131] C. H. Evans, "Gene delivery to bone," *Advanced Drug Delivery Reviews*, vol. 64, no. 12, pp. 1331–1340, 2012.

[132] C.-H. Lu, Y.-H. Chang, S.-Y. Lin, K.-C. Li, and Y.-C. Hu, "Recent progresses in gene delivery-based bone tissue engineering," *Biotechnology Advances*, vol. 31, no. 8, pp. 1695–1706, 2013.

[133] T. N. Vo, F. K. Kasper, and A. G. Mikos, "Strategies for controlled delivery of growth factors and cells for bone regeneration,"

Advanced Drug Delivery Reviews, vol. 64, no. 12, pp. 1292–1309, 2012.

[134] W. Ji, H. Wang, J. J. J. P. van den Beucken et al., "Local delivery of small and large biomolecules in craniomaxillofacial bone," *Advanced Drug Delivery Reviews*, vol. 64, no. 12, pp. 1152–1164, 2012.

[135] V. Luginbuehl, L. Meinel, H. P. Merkle, and B. Gander, "Localized delivery of growth factors for bone repair," *European Journal of Pharmaceutics and Biopharmaceutics*, vol. 58, no. 2, pp. 197–208, 2004.

[136] P. Kocbek, N. Obermajer, M. Cegnar, J. Kos, and J. Kristl, "Targeting cancer cells using PLGA nanoparticles surface modified with monoclonal antibody," *Journal of Controlled Release*, vol. 120, no. 1-2, pp. 18–26, 2007.

[137] J. Cheng, B. A. Teply, I. Sherifi et al., "Formulation of functionalized PLGA-PEG nanoparticles for *in vivo* targeted drug delivery," *Biomaterials*, vol. 28, no. 5, pp. 869–876, 2007.

[138] C. Romagnoli, F. D'Asta, and M. L. Brandi, "Drug delivery using composite scaffolds in the context of bone tissue engineering," *Clinical Cases in Mineral and Bone Metabolism*, vol. 10, no. 3, pp. 155–161, 2013.

[139] D. Puppi, X. Zhang, L. Yang, F. Chiellini, X. Sun, and E. Chiellini, "Nano/microfibrous polymeric constructs loaded with bioactive agents and designed for tissue engineering applications: a review," *Journal of Biomedical Materials Research Part B: Applied Biomaterials*, vol. 102, no. 7, pp. 1562–1579, 2014.

Hindawi Publishing Corporation
BioMed Research International
Volume 2015, Article ID 839694, 9 pages
http://dx.doi.org/10.1155/2015/839694

Review Article

Naturally Occurring Extracellular Matrix Scaffolds for Dermal Regeneration: Do They Really Need Cells?

A. M. Eweida[1,2] and M. K. Marei[3]

[1]*Department of Head and Neck Surgery, Faculty of Medicine, University of Alexandria, Alexandria 21111, Egypt*
[2]*Department of Plastic & Reconstructive Surgery, University of Heidelberg, 67071 Ludwigshafen, Germany*
[3]*Tissue Engineering Laboratories, Faculty of Dentistry, University of Alexandria, Alexandria 21111, Egypt*

Correspondence should be addressed to A. M. Eweida; ahmad.eweida@alexmed.edu.eg

Received 2 March 2015; Revised 19 April 2015; Accepted 19 April 2015

Academic Editor: Francesco Piraino

The pronounced effect of extracellular matrix (ECM) scaffolds in supporting tissue regeneration is related mainly to their maintained 3D structure and their bioactive components. These decellularized matrix scaffolds could be revitalized before grafting via adding stem cells, fibroblasts, or keratinocytes to promote wound healing. We reviewed the online published literature in the last five years for the studies that performed ECM revitalization and discussed the results of these studies and the related literature. Eighteen articles met the search criteria. Twelve studies included adding cells to acellular dermal matrix (ADM), 3 studies were on small intestinal mucosa (SIS), one study was on urinary bladder matrix (UBM), one study was on amniotic membrane, and one study included both SIS and ADM loaded constructs. We believe that, in chronic and difficult-to-heal wounds, revitalizing the ECM scaffolds would be beneficial to overcome the defective host tissue interaction. This belief still has to be verified by high quality randomised clinical trials, which are still lacking in literature.

1. Introduction

The extracellular matrix (ECM) is a complex mixture of structural and functional proteins, glycoproteins, and proteoglycans arranged in a unique, tissue specific three-dimensional (3D) ultrastructure. The pronounced effect of ECM scaffolds in supporting tissue regeneration is related mainly to two major characteristics: the maintained 3D structure and the bioactive components. Their natural 3D structure provides structural support and tensile strength, attachment sites for cell surface receptors, and a reservoir for signaling factors that modulate angiogenesis, cell migration, cell proliferation, and orientation in wound healing [1]. The bioactive components include but are not limited to collagen, laminin, fibronectin, glycosaminoglycans, and a various group of growth factors (VEGF: vascular endothelial growth factor, bFGF: basic fibroblast growth factor, EGF: epidermal growth factor, TGF-beta: transforming growth factor-beta, KGF: keratinocyte growth factor, HGF: hepatocyte growth factor, and PDGF: platelet derived growth factor). The presence of such bioactive molecules, together with their native inhibitors, in their preserved natural 3D spatial structure provides a very convenient platform for cells to regenerate [1, 2].

The decellularized dermis of the skin, submucosa of the small intestine and urinary bladder (Figure 1), and the amniotic membrane are of the commonest sources for ECM scaffolds used for tissue regeneration. Various market products were developed from naturally occurring ECM scaffolds and were approved as wound dressing for skin wounds and burns. Alloderm is one of the first approved acellular matrix materials and was extensively investigated in literature. It is processed directly from fresh cadaver skin that is treated with high salt to remove the cellular components. It is then freeze dried, leaving an immunologically inert acellular dermal matrix with intact basement membrane complex. Approved by the FDA, it has been used to treat burns since 1992. Oasis is a product derived from porcine small intestinal submucosa (SIS). It has been studied at Purdue University in West Lafayette, USA, and is now commercially available as wound dressing [3]. Graft Jacket is a cryogenically stored

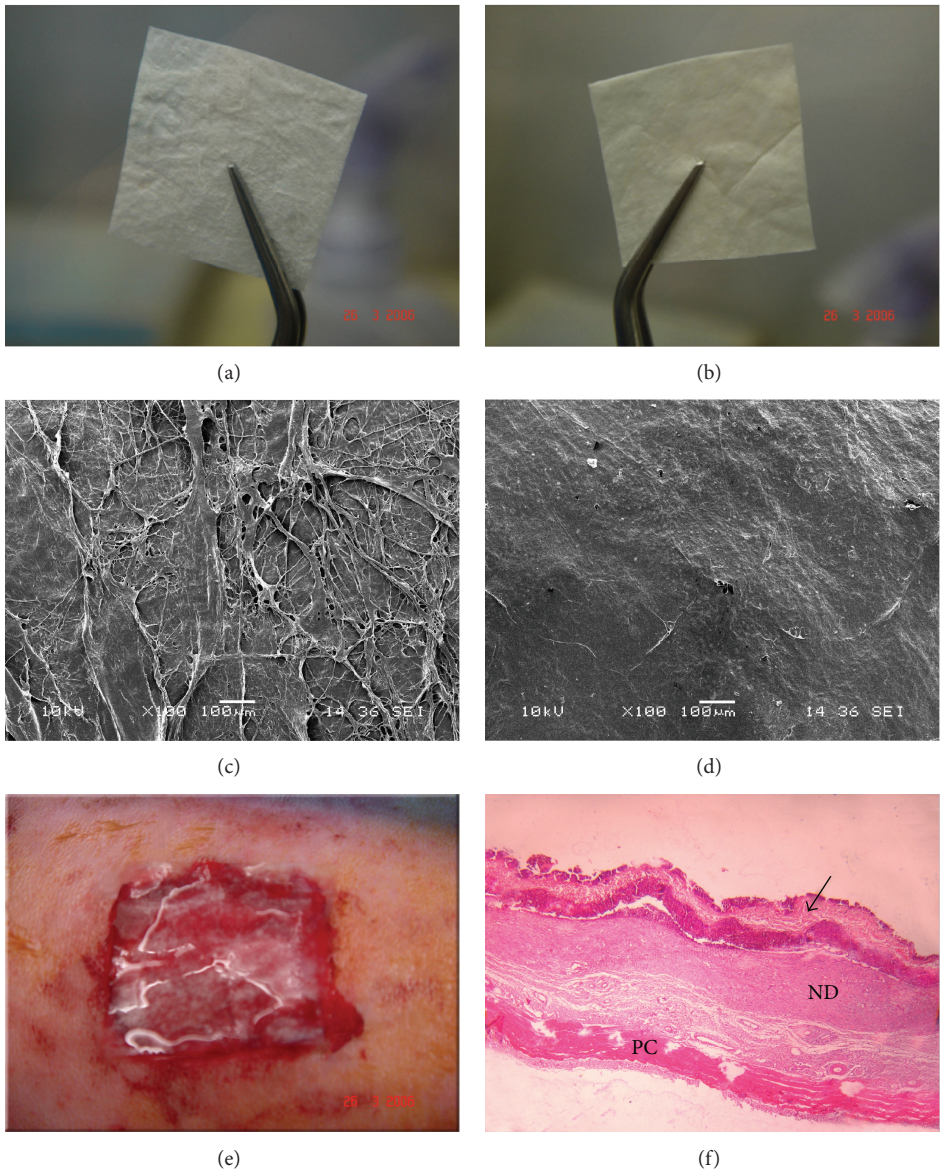

Figure 1: Urinary bladder matrix scaffold. (a) Rough surface. (b) Smooth surface. (c) UBM rough surface (SEM). (d) UBM smooth surface (SEM). (e) Implantation of UBM on full thickness wounds in rabbits (rough surface downwards). (f) H&E section of the wound after 1 week of grafting. Arrow points to the UBM. PC: Panniculus carnosus layer. ND: neodermis. Original magnification ×40.

acellular dermal matrix (ADM) originating from cadaveric skin that is already approved for wound care purposes [4]. Epiflex is a human acellular dermal matrix transplant manufactured from screened consenting donors [5]. Endoform is an approved extracellular matrix created from the submucosa of the sheep fore-stomach, a tissue whose structure is similar to the dermis [6]. MatriStem MicroMatrix (ACell, Columbia, MD, USA) is a recently approved UBM scaffold for wound regeneration [7]. Although proved beneficial for acute and simple wounds the literature lacks high quality clinical evidences that these scaffolds can provide the desirable effects when applied to chronic, difficult-to-heal wounds.

The pathophysiology of chronic wounds and ulcers is usually too complex to be reversed by adding a single factor or cellular component. Chronic ischemic or diabetic wounds as an example are thought to result from the combined comorbidities of neuropathy, vascular deficits, impaired immunity, infection, and repeated tissue trauma, all overlapping to produce a vicious cycle that is very difficult to break [8]. Standard surgical care of such chronic complicated wounds usually fails to match patient's satisfaction and restore the quality of life, and sometimes very complex surgical procedures are required to treat such wounds [9].

Inhibition of extracellular matrix deposition and increased activity of matrix metalloproteinases (MMPs) with concomitant decreased activity of MMP inhibitors were suggested as mechanisms for delayed wound healing in chronic wounds. Regarding the cellular factors; fibroblasts are

usually senescent, keratinocytes show impaired migration, and leukocytes exhibit impaired intracellular killing functions. Recently, an impaired function of the gap junctions has immerged as an additional pathological mechanism leading to impaired wound healing. Associated neuropathy leads to a decreased level of neuropeptides that normally contribute to healing. Neuropathy reduces capillary blood flow and vice versa [10–12]. These complex factors and mechanisms suggest that providing the wound with a new viable "tissue" and "milieu" is mandatory to achieve a significant response.

The ECMs are characterized by early degradation so that a major part of their role depends on the active interaction with the recipient cells and tissue. In difficult-to-heal wounds this interaction is usually defective due to a lack of reaction by recipient cells.

In an attempt to overcome this, a process of introducing cells into the biostatic graft, known as "revitalization," could help these scaffolds perform their function, at least for the early stage after implantation. The grafted cells are usually the recipient's autologous cells (differentiated or stem cells) that are seeded either directly onto the scaffold or after retrieval and propagation in culture [13]. Revitalization of ECM scaffolds with keratinocytes, fibroblasts, or stem cells were shown to improve vascularization, scaffold integration, and cellular proliferation [14–16]. We reviewed the online published literature in the last five years for the studies that performed ECM revitalization and discussed the result of these studies and the related literature.

2. Materials and Methods

A PubMed search was performed for the articles published in English language within the previous 5 years. All the articles related to adding keratinocytes, fibroblasts, or stem cells to naturally occurring ECM scaffolds were included. The following string was used for the online search:

> (urinary bladder matrix OR UBM OR small intestinal mucosa OR SIS OR decellularized skin OR alloderm OR acellular dermal matrix OR oasis OR graftjacket OR endoform OR matristem OR Epiflex) AND (keratinocytes OR fibroblasts OR stem cells) AND (skin regeneration OR skin repair OR skin reconstruction OR wound OR burn) AND (English[lang]) AND ("last 5 years"[PDat] AND (Humans[Mesh] OR Animals[Mesh:noexp]))

3. Results

The search string yielded 121 articles. The articles were filtered according to title, abstract, and full text resulting in 18 articles that met the search criteria. Twelve studies included adding cells to ADM, 3 studies were on SIS, one study was on UBM, one study was on amniotic membrane, and one study included both SIS and ADM loaded constructs. All in vivo studies were experimental and no single clinical study was found. The type of the study and the most relevant results and remarks are summarized in Table 1.

4. Discussion

Although there are no guidelines that clearly recommend the use of ECM scaffolds for wound healing, their benefit in acute wounds and burns has been demonstrated in several clinical studies. The complex mixture of structural and functional proteins, glycoproteins, and proteoglycans retained in its original 3D structure provides the key benefit of using these scaffolds for wound healing. This structure provides a temporary support into which cells can migrate and proliferate in a well-organized and controlled fashion leading to improved wound healing. The suggested mechanisms of wound improvement when applying the ECM scaffolds alone are related to providing a structural support, stimulating angiogenesis, chemotaxis for endothelial cells, and release of growth factors [17, 18].

In case of chronic and difficult-to-heal wounds the challenge is much bigger. The suggested role of ECM scaffolds in improving such wounds is not fully understood. It has been suggested that they would act as a biological cover that modulates the wound environment by reducing the inflammatory activity to promote wound healing [19]. There is currently limited published data that reaches a sufficient level of evidence about the role of ECM scaffolds alone in chronic and difficult-to-heal wounds [3, 20–27].

The positive role of combining ECM scaffolds with stem cells, fibroblasts, or keratinocytes was clearly demonstrated in in vitro and experimental in vivo studies. It is believed that native stem cells play an important role in wound regeneration or healing. GFP-labelled MSCs were found in the skin of non-GFP mice after peripheral injection. This indicates that wounding stimulates MSCs to migrate via chemotaxis to the injury site and differentiate to functional skin cells [28]. Some studies have indicated that wound healing is enhanced through ADSCs that promote human dermal fibroblast proliferation by direct cell-to-cell contact and via a paracrine effect [29].

However, the relation between the efficacy of wound healing and the number of transplanted MSCs does not seem to be a linear one. Yeum et al. [30] have shown that repeated injection of additional MSCs did not increase the number of MSCs participating in wound healing beyond a certain constant maximum amount. The number of MSCs in the wound site remains constant in the range $2\text{-}3 \times 10^5$ from day 1 to day 10. MSCs were not detected after day 10, probably because the role of transplanted MSCs ended thereafter. Lam et al. [31] also could not detect the signals after 12 days postwounding. It was suggested that the stem cells would have been engulfed by macrophages or migrated to other body sites speculating that after the completion of the MSCs' roles, the wound site no longer needs the MSCs as it has recovered completely by 14 days.

Although the effect of stem cells is well documented in promoting wound healing, these cells usually do not survive well when directly transplanted to the wound site. Many studies have shown that a great number of cells die during transplantation and this effect would be diminished if cells were allowed to proliferate in an optimal milieu [32, 33]. Attempts for aiding stem cell survival often involve

Table 1: Studies applying cells to ECM scaffolds in the last 5 years.

Research group	Type of the study	ECM and loaded cells	Results	Remarks
Castagnoli et al. 2010 [57]	Noncomparative in vitro study	Human ADM + human keratinocytes	Preparation and characterization of a new cutaneous biosubstitute made up of alloplastic acellular glycerolized dermis & cultured autologous keratinocytes	(i) No in vivo studies (ii) Proof of principle
Han et al. 2010 [50]	Comparative in vivo study	Porcine ADM + autologous STSG +/− microencapsulated VEGF-expressing fibroblasts	Significant increase in survival & microvessels density in grafts containing microencapsulated VEGF-expressing cells	Cells were injected below the ADM and STSG
Eweida et al. 2011 [52]	Comparative in vivo study	Porcine UBM +/− rabbit keratinocytes	Reduction of early wound contraction and improving wound vascularity	(i) Keratinocytes were transplanted on the rough surface of the UBM (ii) No in vivo cell tracking
Liu et al. 2011 [14]	Comparative in vivo study	Mouse ADSC +/− porcine SIS +/− porcine ADM	Cell loaded ECM scaffolds showed better angiogenesis and early wound closure than cell-free ECM and cell loaded non-ECM scaffolds	The study emphasised the synergistic effect of ECM scaffolds and ADSC on angiogenesis
Lugo et al. 2011 [58]	Noncomparative in vivo study	Human ADM + human keratinocytes	The prevascularized neodermis supported the transplanted keratinocytes leading to a superior wound epithelialization	Keratinocytes were added in fibrin gel one week after implantation of the angiogenic factors-infiltrated ADM
Orbay et al. 2011 [37]	Comparative in vivo study	Rat ADM +/− rat ADSC	The construct enhanced the volume maintenance, vascular density, and collagen content in a subcutaneous soft tissue augmentation model in rats	The SC augmentation model did not address wound healing aspects related to epithelialization
Roessner et al. 2011 [15]	Comparative in vivo study	Human ADM (Epiflex) +/− rat fibroblasts +/− irradiation	Fibroblasts added no significant difference regarding soft tissue volume regeneration. However, a significant increase in wound tensile strength was noted if the transplanted cells were not subjected to irradiation	(i) The ADM was implanted within a deeper tissue defect to replace excised muscles (ii) Due to this special defect design, the increase in wound breaking strength may not be directly related to the physical presence of the seeded implants
Seland et al. 2011 [40]	Comparative in vivo study	Human ADM +/− human keratinocytes (loaded on microcarriers or as single layer or as STSG)	Only the keratinocytes implanted as STSG or loaded on microcarriers had a significant positive effect on epidermal and dermal thickness at 16 & 21 days after transplantation	(i) Keratinocytes were added to the fibrin pretreated wounds fourteen days after the initial transplantation of ADM (ii) In vivo tracking of transplanted cells was performed till the end of the experiment
Huang et al. 2012 [51]	Comparative in vivo study	Mouse ADM +/− human ADSCs	Increased thickness of granulation tissue, improved reepithelialization & wound closure rate, and increased vascular density	(i) ADSCs were seeded on ADM and not directly to the wound bed (ii) In vivo cell tracking was performed till day 14 (iii) VEGF-expressing ASCs could be detected after transplantation
Peramo et al. 2012 [39]	Noncomparative in vitro study	Human ADM (Alloderm) + human keratinocytes (from skin and oral mucosa origins)	In vitro development of human mucocutaneous lip junction equivalent	(i) In vitro proof of principle and was not examined in vivo (ii) Maintaining this delicate transition zone would be challenging in a normal surgical setting
Shi et al. 2012 [16]	Noncomparative in vitro study	SIS + human keratinocytes in a high MMP medium	SIS inhibits the MMP activity and thus promotes keratinocyte migration	The study focuses on the role of the bioactive structure of SIS rather than its scaffolding properties

Table 1: Continued.

Research group	Type of the study	ECM and loaded cells	Results	Remarks
Zajicek et al. 2012 [38]	Noncomparative in vitro study	Porcine ADM (Xe-Derma) + human keratinocytes	The results suggest that the firm natural structure of ADM stimulates proliferation and differentiation of human primary keratinocytes	A concomitant in vivo study involved the application of only the scaffold without adding cells in acute wounds
Deshpande et al. 2013 [44]	Comparative in vitro study	Human ADM + keratinocytes +/− fibroblasts +/− basement membrane	The formation of a well-organized epithelium depends on the presence of intact basement membrane but is independent of the presence of cultured fibroblasts	Exclusively in vitro study
Huang et al. 2013 [59]	Comparative in vivo study	Human keratinocytes +/− cross-linked human acellular amniotic membrane	Combination of keratinocytes with the acellular amniotic membrane significantly reduced wound contraction at 4 weeks than the cells alone	The study did not include a group with the ECM alone
Lam et al. 2013 [31]	Comparative in vivo study	+/− mouse ADSC +/− porcine SIS	(i) In vivo cell tracking revealed a significant increase in stem cell survival and proliferation with SIS (ii) Delivering stem cells on the SIS significantly decreased fibrosis but slightly improved healing, while SIS alone hindered healing as the patch stented the wound open	(i) A splinted excisional wound model was used to simulate human wound healing and minimize healing by contracture (ii) The special splint-wound design and the too early removal of the SIS patch in some groups (2 days) led to unfavorable results in terms of wound healing
Sahin et al. 2013 [48]	Comparative in vivo study	Human ADM +/− rat bMSCs	Increased, adherence, angiogenesis, and vertical vascular penetration of ADM especially if combined with negative pressure dressing therapy	(i) The MSCs were added once & randomly to the wound bed before ADM implantation (ii) The bMSCs were not tracked in vivo (iii) The early adherence of ADM was probably related to early angiogenesis
Yeum et al. 2013 [30]	Comparative in vivo study	SIS +/− mouse bMSCs	Enhanced wound closure and less wound inflammation with bMSCs	(i) bMSCs were repeatedly transplanted every 2 days for 2 weeks (ii) In vivo cell tracking was performed
Bondioli et al. 2014 [60]	Comparative in vitro study	Fibroblasts +/− human ADM	The matrix extract significantly increased the proliferation rate of fibroblasts	Only an in vitro study as part of the characterization of the matrix

ADSC: adipose derived stem cells.
bMSC: bone marrow derived stem cells.
STSG: split thickness skin graft.

codelivery with slow release and survival-promoting gels such as Matrigel or collagen gel. In several in vivo and in vitro studies Matrigel was found to be superior probably due to its basement membrane component [34–36]. Similar studies on SIS have demonstrated that the ECM patch allowed the stem cells to remain localized to the wound area rather than migrate to other regions as evidenced by in vivo cell tracking [31].

Orbay et al. [37] concluded that ADSCs could attach to ADM and decrease its in vivo resorption suggesting that this construct may be a useful tool for soft tissue augmentation with stable long-term results. This effect was thought to be due to stimulatory effects of ADSCs on fibroblasts leading to an indirect increase in the synthesis of collagen and extracellular matrix components.

In an attempt to enhance wound epithelialization, keratinocytes were added to ECM scaffolds in various studies. Based on the in vitro behaviour of the keratinocytes, Zajicek et al. [38] suggested that the ADM promotes wound healing through supporting the growth of patient's own keratinocytes from the adnexa remnants in the wound by providing optimal conditions for their attachment, proliferation, and migration. Peramo et al. [39] proved that Alloderm could also permit the differentiation and stratification of nonkeratinized, buccal mucosa in vitro.

Regarding their effect on the dermal regeneration, Seland et al. [40] have shown that implantation of a single cell layer of keratinocytes to the ADM added nothing to the dermal thickness in the wound healing process. Interestingly keratinocytes loaded on microcarriers showed a significantly

thicker epithelium and neodermis at both 16 and 21 days after grafting compared to the wounds treated with a single layer. This led to the hypothesis that these carriers could act as a facilitator for the dermal regeneration beside their role in transportation and transplantation of autologous keratinocytes.

For the recipient keratinocytes to proliferate and uniformly stratify above/within the ECM, it was traditionally known that an optimal environment would require the presence of fibroblasts [41]. This is probably due to the paracrine interaction between the two cell types [42, 43]. Deshpande et al. have concluded in their in vitro study, however, that the formation of a well-organized epithelium on the acellular dermal matrix depends mainly on the presence of intact basement membrane but is largely independent of the presence of cultured fibroblasts. They have noticed that incorporating fibroblasts in the absence of a basement membrane had no significant effect on the keratinocyte behavior [44]. Other groups have demonstrated an enhanced keratinocyte migration on a sterilized dermis after removal of basement membrane antigens but in the presence of fibroblasts under conditions of normal extracellular calcium concentration [45]. These conditions probably represent the in vivo situation during normal wound healing, when the basement membrane has been traumatically disrupted and fibroblast numbers are upregulated in order to heal the wound [46]. We guess that the solution for these contradictory results is the establishment of a well-standardized in vivo study for the assessment of the definite role of fibroblasts and basement membrane factors.

In chronic and difficult-to-heal wounds, vascularisation of the wound bed is a major concern. If STSG is to be implanted over the ADM, then adequate scaffold neovascularisation would be an essential prerequisite. Neovascularisation of the matrix occurs during the early stages of complete adherence of ADM to the recipient wound bed [47]. Increasing and accelerating this neovascularisation and estimating its timing are thus important for an optimal treatment plan [48]. An enhanced angiogenesis through the application of ECM scaffolds was also suggested as an important factor in decreasing wound fibrosis [31]. Sahin et al. [48] have demonstrated that adding MSCs to the ADM has a significant positive effect on the vascularisation probably due to enhanced secretion of VEGF [49]. Han et al. [50] have also demonstrated that enhancement of ADM engraftment and wound angiogenesis could be achieved by seeding of microencapsulated VEGF-expressing fibroblasts below the scaffold. Huang et al. [51] have also demonstrated that DiI-labeled cells were colocalized with staining for VEGF and vWF (Von Willebrand factor) well 14 days after seeding on ADM and implantation in full thickness wounds, suggesting that the grafted cells might improve angiogenesis via the indirect paracrine effect or contribute to newly formed vasculature. Our research group has also demonstrated an enhanced angiogenic activity with autologous keratinocyte grafting with porcine UBM, which could be attributed to a cross talk between the keratinocyte and endothelial cells and release of angiogenic factors from UBM degradation, or even from the dying keratinocytes after grafting [52].

In difficult-to-heal wounds as in chronic or irradiated wounds, it is always wise to bring new healthy "tissue" to the wound bed. Applying the same concept makes adding cells to the scaffold crucial for wound regeneration in such difficult situations where the wound regeneration capacity is subnormal. Roessner et al. [15] have demonstrated that adding fibroblasts to ADM in irradiated wounds would improve wound healing evidenced by enhanced wound tensile strength. This effect was abolished when the transplanted cells where irradiated in an adjuvant-radiotherapy setting.

In a clinical setting, these difficult-to-heal wounds were almost exclusively treated with cell-loaded non-ECM scaffolds such as Apligraf, Dermagraft, and GammaGraft [53]. From all the available ECM scaffolds, only the SIS (Oasis) and to a lesser extent Graft Jacket have been reported clinically in a considerable number of patients to improve chronic wounds without adding cells [3, 21, 25]. The role of SIS in promoting wound closure was extensively investigated. Shi et al. [16] have demonstrated that MMPs inhibit keratinocyte migration in vitro and that preincubating the MMP solution with SIS could significantly reduce this inhibitory effect. MMPs are important contributors to wound chronicity and are abundantly expressed in chronic ulcers and not in acute wounds [54]. MMPs inhibit keratinocyte migration and degrade fibronectin, growth factors, and other proteins vital to wound healing and thus reducing elevated levels of MMPs in chronic wounds should promote healing [55].

A high quality randomized controlled clinical study comparing the wound healing potential of cell free versus cell loaded ECM scaffolds is unfortunately still lacking. Lev-Tov et al. [56] have introduced a protocol to compare the standard surgical care either alone or with Dermagraft (bioengineered ECM containing living fibroblasts) or with UBM (Oasis). Although Dermagraft is not a naturally occurring ECM scaffold, the data coming out of such a study would be useful in understanding the relative role of ECM and added cells in a clinical context.

We think that in difficult-to-heal wounds adding cells to the ECM scaffolds would enhance their regenerative capacity. In acute and simple wounds, however, the regenerative capacity of the native tissues are usually preserved so that the high costs and time linked to adding autologous cells within good clinical practice guidelines could be avoided as the relative benefit would be negligible. These conclusions are based on our surgical and experimental experiences and still have to be verified by high quality randomised clinical trials.

List of Abbreviations

ADM: Acellular dermal matrix
ADSC: Adipose derived stem cells
bFGF: Basic fibroblast growth factor
bMSC: Bone marrow derived mesenchymal stem cells
EGF: Epidermal growth factor
HGF: Hepatocyte growth factor
KGF: Keratinocyte growth factor
MMP: Matrix metalloproteinases
PDGF: Platelet derived growth factor
STSG: Split thickness skin graft

TGF-beta: Transforming growth factor-beta
UBM: Urinary bladder matrix
VEGF: Vascular endothelial growth factor
vWF: Von Willebrand factor.

Conflict of Interests

The authors declare that there is no conflict of interests regarding the publication of this paper.

References

[1] S. F. Badylak, "The extracellular matrix as a scaffold for tissue reconstruction," *Seminars in Cell and Developmental Biology*, vol. 13, no. 5, pp. 377–383, 2002.

[2] K. Lindberg and S. F. Badylak, "Porcine small intestinal submucosa (SIS): a bioscaffold supporting in vitro primary human epidermal cell differentiation and synthesis of basement membrane proteins," *Burns*, vol. 27, no. 3, pp. 254–266, 2001.

[3] E. N. Mostow, G. D. Haraway, M. Dalsing, J. P. Hodde, and D. King, "Effectiveness of an extracellular matrix graft (OASIS Wound Matrix) in the treatment of chronic leg ulcers: a randomized clinical trial," *Journal of Vascular Surgery*, vol. 41, no. 5, pp. 837–843, 2005.

[4] R. S. Kirsner, G. Bohn, V. R. Driver et al., "Human acellular dermal wound matrix: evidence and experience," *International Wound Journal*, 2013.

[5] E. Rössner, M. D. Smith, B. Petschke et al., "Epiflex A new decellularised human skin tissue transplant: manufacture and properties," *Cell and Tissue Banking*, vol. 12, no. 3, pp. 209–217, 2011.

[6] B. A. Liden and B. C. H. May, "Clinical outcomes following the use of ovine forestomach matrix (endoform dermal template) to treat chronic wounds," *Advances in Skin & Wound Care*, vol. 26, no. 4, pp. 164–167, 2013.

[7] G. J. Kruper, Z. P. VandeGriend, H. S. Lin, and G. F. Zuliani, "Salvage of failed local and regional flaps with porcine urinary bladder extracellular matrix aided tissue regeneration," *Case Reports in Otolaryngology*, vol. 2013, Article ID 917183, 5 pages, 2013.

[8] J. Apelqvist, K. Bakker, W. H. van Houtum, and N. C. Schaper, "Practical guidelines on the management and prevention of the diabetic foot," *Diabetes/Metabolism Research and Reviews*, vol. 24, supplement 1, pp. S181–S187, 2008.

[9] A. M. Eweida, W. Lang, M. Schmitz, and R. E. Horch, "Salvage of a free radial forearm flap by creation of an arteriovenous fistula at the distal arterial pedicle," *Microsurgery*, vol. 33, no. 5, pp. 391–395, 2013.

[10] M. A. M. Loots, E. N. Lamme, J. Zeegelaar, J. R. Mekkes, J. D. Bos, and E. Middelkoop, "Differences in cellular infiltrate and extracellular matrix of chronic diabetic and venous ulcers versus acute wounds," *Journal of Investigative Dermatology*, vol. 111, no. 5, pp. 850–857, 1998.

[11] A. Medina, P. G. Scott, A. Ghahary, and E. E. Tredget, "Pathophysiology of chronic nonhealing wounds," *Journal of Burn Care and Rehabilitation*, vol. 26, no. 4, pp. 306–319, 2005.

[12] A. Mendoza-Naranjo, P. Cormie, A. E. Serrano et al., "Overexpression of the gap junction protein Cx43 as found in diabetic foot ulcers can retard fibroblast migration," *Cell Biology International*, vol. 36, no. 7, pp. 661–667, 2012.

[13] E. Olender, I. Uhrynowska-Tyszkiewicz, and A. Kaminski, "Revitalization of biostatic tissue allografts: new perspectives in tissue transplantology," *Transplantation Proceedings*, vol. 43, no. 8, pp. 3137–3141, 2011.

[14] S. Liu, H. Zhang, X. Zhang et al., "Synergistic angiogenesis promoting effects of extracellular matrix scaffolds and adipose-derived stem cells during wound repair," *Tissue Engineering Part A*, vol. 17, no. 5-6, pp. 725–739, 2011.

[15] E. D. Roessner, S. Thier, P. Hohenberger et al., "Acellular dermal matrix seeded with autologous fibroblasts improves wound breaking strength in a rodent soft tissue damage model in neoadjuvant settings," *Journal of Biomaterials Applications*, vol. 25, no. 5, pp. 413–427, 2011.

[16] L. Shi, S. Ramsay, R. Ermis, and D. Carson, "*In vitro* and *in vivo* studies on matrix metalloproteinases interacting with small intestine submucosa wound matrix," *International Wound Journal*, vol. 9, no. 1, pp. 44–53, 2012.

[17] F. Li, W. Li, S. A. Johnson, D. A. Ingram, M. C. Yoder, and S. F. Badylak, "Low-molecular-weight peptides derived from extracellular matrix as chemoattractants for primary endothelial cells," *Endothelium*, vol. 11, no. 3-4, pp. 199–206, 2004.

[18] J. P. Hodde, R. D. Record, H. A. Liang, and S. F. Badylak, "Vascular endothelial growth factor in porcine-derived extracellular matrix," *Endothelium*, vol. 8, no. 1, pp. 11–24, 2001.

[19] G. Mulder and D. Lee, "A retrospective clinical review of extracellular matrices for tissue reconstruction: equine pericardium as a biological covering," *Wounds*, vol. 21, no. 9, pp. 254–261, 2009.

[20] S. A. Brigido, "The use of an acellular dermal regenerative tissue matrix in the treatment of lower extremity wounds: a prospective 16-week pilot study," *International Wound Journal*, vol. 3, no. 3, pp. 181–187, 2006.

[21] J. A. Niezgoda, C. C. van Gils, R. G. Frykberg, and J. P. Hodde, "Randomized clinical trial comparing OASIS Wound Matrix to Regranex Gel for diabetic ulcers," *Advances in Skin & Wound Care*, vol. 18, no. 5, part 1, pp. 258–266, 2005.

[22] B. R. Martin, M. Sangalang, S. Wu, and D. G. Armstrong, "Outcomes of allogenic acellular matrix therapy in treatment of diabetic foot wounds: an initial experience," *International Wound Journal*, vol. 2, no. 2, pp. 135–165, 2005.

[23] G. Silverstein, "Dermal regeneration template in the surgical management of diabetic foot ulcers: a series of five cases," *Journal of Foot and Ankle Surgery*, vol. 45, no. 1, pp. 28–33, 2006.

[24] C. L. Winters, S. A. Brigido, B. A. Liden, M. Simmons, J. F. Hartman, and M. L. Wright, "A multicenter study involving the use of a human acellular dermal regenerative tissue matrix for the treatment of diabetic lower extremity wounds," *Advances in Skin & Wound Care*, vol. 21, no. 8, pp. 375–381, 2008.

[25] A. Reyzelman, R. T. Crews, J. C. Moore et al., "Clinical effectiveness of an acellular dermal regenerative tissue matrix compared to standard wound management in healing diabetic foot ulcers: a prospective, randomised, multicentre study," *International Wound Journal*, vol. 6, no. 3, pp. 196–208, 2009.

[26] R. H. Demling, J. A. Niezgoda, G. D. Haraway, and E. N. Mostow, "Small intestinal submucosa wound matrix and full-thickness venous ulcers: preliminary results," *Wounds*, vol. 16, no. 1, pp. 18–22, 2004.

[27] M. Romanelli, V. Dini, M. Bertone, S. Barbanera, and C. Brilli, "OASIS wound matrix versus Hyaloskin in the treatment of difficult-to-heal wounds of mixed arterial/venous aetiology," *International Wound Journal*, vol. 4, no. 1, pp. 3–7, 2007.

[28] E. V. Badiavas, M. Abedi, J. Butmarc, V. Falanga, and P. Quesenberry, "Participation of bone marrow derived cells in cutaneous wound healing," *Journal of Cellular Physiology*, vol. 196, no. 2, pp. 245–250, 2003.

[29] W.-S. Kim, B.-S. Park, J.-H. Sung et al., "Wound healing effect of adipose-derived stem cells: a critical role of secretory factors on human dermal fibroblasts," *Journal of Dermatological Science*, vol. 48, no. 1, pp. 15–24, 2007.

[30] C. E. Yeum, E. Y. Park, S.-B. Lee, H.-J. Chun, and G.-T. Chae, "Quantification of MSCs involved in wound healing: Use of SIS to transfer MSCs to wound site and quantification of MSCs involved in skin wound healing," *Journal of Tissue Engineering and Regenerative Medicine*, vol. 7, no. 4, pp. 279–291, 2013.

[31] M. T. Lam, A. Nauta, N. P. Meyer, J. C. Wu, and M. T. Longaker, "Effective delivery of stem cells using an extracellular matrix patch results in increased cell survival and proliferation and reduced scarring in skin wound healing," *Tissue Engineering Part A*, vol. 19, no. 5-6, pp. 738–747, 2013.

[32] C. Fredriksson, G. Kratz, and F. Huss, "Transplantation of cultured human keratinocytes in single cell suspension: a comparative in vitro study of different application techniques," *Burns*, vol. 34, no. 2, pp. 212–219, 2008.

[33] U. Kneser, L. Stangenberg, J. Ohnolz et al., "Evaluation of processed bovine cancellous bone matrix seeded with syngenic osteoblasts in a critical size calvarial defect rat model," *Journal of Cellular and Molecular Medicine*, vol. 10, no. 3, pp. 695–707, 2006.

[34] F. Cao, A. H. Sadrzadeh Rafie, O. J. Abilez et al., "In vivo imaging and evaluation of different biomatrices for improvement of stem cell survival," *Journal of Tissue Engineering and Regenerative Medicine*, vol. 1, no. 6, pp. 465–468, 2007.

[35] I. Kutschka, I. Y. Chen, T. Kofidis et al., "Collagen matrices enhance survival of transplanted cardiomyoblasts and contribute to functional improvement of ischemic rat hearts," *Circulation*, vol. 114, no. 1, supplement, pp. I167–I173, 2006.

[36] D. Philp, S. S. Chen, W. Fitzgerald, J. Orenstein, L. Margolis, and H. K. Kleinman, "Complex extracellular matrices promote tissue-specific stem cell differentiation," *Stem Cells*, vol. 23, no. 2, pp. 288–296, 2005.

[37] H. Orbay, Y. Takami, H. Hyakusoku, and H. Mizuno, "Acellular dermal matrix seeded with adipose-derived stem cells as a subcutaneous implant," *Aesthetic Plastic Surgery*, vol. 35, no. 5, pp. 756–763, 2011.

[38] R. Zajicek, V. Mandys, O. Mestak, J. Sevcik, R. Königova, and E. Matouskova, "Human keratinocyte growth and differentiation on acellular porcine dermal matrix in relation to wound healing potential," *The Scientific World Journal*, vol. 2012, Article ID 727352, 8 pages, 2012.

[39] A. Peramo, C. L. Marcelo, and S. E. Feinberg, "Tissue engineering of lips and muco-cutaneous junctions: *in vitro* development of tissue engineered constructs of oral mucosa and skin for lip reconstruction," *Tissue Engineering Part C: Methods*, vol. 18, no. 4, pp. 273–282, 2012.

[40] H. Seland, C.-J. Gustafson, H. Johnson, J. P. E. Junker, and G. Kratz, "Transplantation of acellular dermis and keratinocytes cultured on porous biodegradable microcarriers into full-thickness skin injuries on athymic rats," *Burns*, vol. 37, no. 1, pp. 99–108, 2011.

[41] B. Coulomb, C. Lebreton, and L. Dubertret, "Influence of human dermal fibroblasts on epidermalization," *Journal of Investigative Dermatology*, vol. 92, no. 1, pp. 122–125, 1989.

[42] J. S. Rubin, D. P. Bottaro, M. Chedid et al., "Keratinocyte growth factor as a cytokine that mediates mesenchymal-epithelial interaction," *EXS*, vol. 74, pp. 191–214, 1995.

[43] N. Maas-Szabowski, A. Shimotoyodome, and N. E. Fusenig, "Keratinocyte growth regulation in fibroblast cocultures via a double paracrine mechanism," *Journal of Cell Science*, vol. 112, no. 12, pp. 1843–1853, 1999.

[44] P. Deshpande, D. R. Ralston, and S. Macneil, "The use of allodermis prepared from Euro skin bank to prepare autologous tissue engineered skin for clinical use," *Burns*, vol. 39, no. 6, pp. 1170–1177, 2013.

[45] C. A. Harrison, M. J. Heaton, C. M. Layton, and S. M. Neil, "Use of an in vitro model of tissue-engineered human skin to study keratinocyte attachment and migration in the process of reepithelialization," *Wound Repair and Regeneration*, vol. 14, no. 2, pp. 203–209, 2006.

[46] C. A. Hernon, C. A. Harrison, D. J. A. Thornton, and S. MacNeil, "Enhancement of keratinocyte performance in the production of tissue-engineered skin using a low-calcium medium," *Wound Repair and Regeneration*, vol. 15, no. 5, pp. 718–726, 2007.

[47] A. K. Wong, B. H. Schonmeyer, P. Singh, D. L. Carlson, S. Li, and B. J. Mehrara, "Histologic analysis of angiogenesis and lymphangiogenesis in acellular human dermis," *Plastic and Reconstructive Surgery*, vol. 121, no. 4, pp. 1144–1152, 2008.

[48] I. Sahin, S. Ozturk, M. Deveci, A. U. Ural, O. Onguru, and S. Isik, "Experimental assessment of the neo-vascularisation of acellular dermal matrix in the wound bed pretreated with mesenchymal stem cell under subatmospheric pressure," *Journal of Plastic, Reconstructive and Aesthetic Surgery*, vol. 67, no. 1, pp. 107–114, 2014.

[49] L. Chen, E. E. Tredget, P. Y. G. Wu, and Y. Wu, "Paracrine factors of mesenchymal stem cells recruit macrophages and endothelial lineage cells and enhance wound healing," *PLoS ONE*, vol. 3, no. 4, Article ID e1886, 2008.

[50] Y.-F. Han, Y.-Q. Han, Y.-G. Pan, Y.-L. Chen, and J.-K. Chai, "Transplantation of microencapsulated cells expressing VEGF improves angiogenesis in implanted xenogeneic acellular dermis on wound," *Transplantation Proceedings*, vol. 42, no. 5, pp. 1935–1943, 2010.

[51] S.-P. Huang, C.-C. Hsu, S.-C. Chang et al., "Adipose-derived stem cells seeded on acellular dermal matrix grafts enhance wound healing in a murine model of a full-thickness defect," *Annals of Plastic Surgery*, vol. 69, no. 6, pp. 656–662, 2012.

[52] A. Eweida, M. Saad, E. Gabr, M. Marei, and M. R. Khalil, "Cultured keratinocytes on urinary bladder matrix scaffolds increase angiogenesis and help in rapid healing of wounds.," *Advances in Skin & Wound Care*, vol. 24, no. 6, pp. 268–273, 2011.

[53] B. D. Lepow, M. Downey, J. Yurgelon, L. Klassen, and D. G. Armstrong, "Bioengineered tissues in wound healing: a progress report," *Expert Review of Dermatology*, vol. 6, no. 3, pp. 255–262, 2011.

[54] M. Vaalamo, M. Weckroth, P. Puolakkainen et al., "Patterns of matrix metalloproteinase and TIMP-1 expression in chronic and normally healing human cutaneous wounds," *British Journal of Dermatology*, vol. 135, no. 1, pp. 52–59, 1996.

[55] D. Telgenhoff and B. Shroot, "Cellular senescence mechanisms in chronic wound healing," *Cell Death and Differentiation*, vol. 12, no. 7, pp. 695–698, 2005.

[56] H. Lev-Tov, C.-S. Li, S. Dahle, and R. R. Isseroff, "Cellular versus acellular matrix devices in treatment of diabetic foot

ulcers: study protocol for a comparative efficacy randomized controlled trial," *Trials*, vol. 14, article 8, 2013.

[57] C. Castagnoli, M. Fumagalli, D. Alotto et al., "Preparation and characterization of a novel skin substitute," *Journal of Biomedicine and Biotechnology*, vol. 2010, Article ID 840363, 11 pages, 2010.

[58] L. M. Lugo, P. Lei, and S. T. Andreadis, "Vascularization of the dermal support enhances wound re-epithelialization by in situ delivery of epidermal keratinocytes," *Tissue Engineering: Part A*, vol. 17, no. 5-6, pp. 665–675, 2011.

[59] G. Huang, S. Ji, P. Luo et al., "Accelerated expansion of epidermal keratinocyte and improved dermal reconstruction achieved by engineered amniotic membrane," *Cell Transplantation*, vol. 22, no. 10, pp. 1831–1844, 2013.

[60] E. Bondioli, M. Fini, F. Veronesi et al., "Development and evaluation of a decellularized membrane from human dermis," *Journal of Tissue Engineering and Regenerative Medicine*, vol. 8, no. 4, pp. 325–336, 2014.

Hindawi Publishing Corporation
BioMed Research International
Volume 2015, Article ID 387186, 12 pages
http://dx.doi.org/10.1155/2015/387186

Review Article

Custom-Made Antibiotic Cement Nails in Orthopaedic Trauma: Review of Outcomes, New Approaches, and Perspectives

Marcin K. Wasko[1] and Rafal Kaminski[2]

[1]*Department of Orthopaedics and Rheumoortopaedics, Prof. A. Gruca Teaching Hospital, Konarskiego 13, 05-400 Otwock, Poland*
[2]*Department of Trauma Surgery and Orthopaedics, Prof. A. Gruca Teaching Hospital, Konarskiego 13, 05-400 Otwock, Poland*

Correspondence should be addressed to Marcin K. Wasko; m.wasko@cmkp.edu.pl

Received 20 February 2015; Revised 18 May 2015; Accepted 20 May 2015

Academic Editor: Francesco Piraino

Since the first description in 2002 by Paley and Herzenberg, antibiotic bone cement nails (ACNs) have become an effective tool in the orthopaedic trauma surgeons' hands. They simultaneously elute high amounts of antibiotics into medullary canal dead space and provide limited stability to the debrided long bone. In this paper, we perform a systematic review of current evidence on ACNs in orthopaedic trauma and provide an up-to-date review of the indications, operative technique, failure mechanisms, complications, outcomes, and outlooks for the ACNs use in long bone infection.

1. Introduction

Musculoskeletal infections remain a challenge for orthopaedic surgeons and infectious disease specialists. Bone provides a unique milieu for bacteria, with low vascularity and turnover rate. Most of the orthopaedic trauma infections are caused by biofilm-forming bacteria [1]. Biofilm consists of hydrated matrix of polysaccharide and protein. Once formed, it protects the microorganism from antimicrobials, opsonization, and phagocytosis, thus contributing to the chronicity of infections [2]. In order to cure biofilm-related infection, four principles formulated by Cierny and Mader must be observed: (a) complete surgical debridement with dead space management, (b) fracture/nonunion stabilization, (c) soft tissue coverage, and (d) adequate antibiotic levels [3]. In healthy bone, local antibiotics' concentrations might be less than 20% of serum levels, as is for most beta-lactams [4]. Their efficacy is further diminished by biofilms, which decrease molecule penetration [5]. With intramedullary infections, the optimal way of debridement is to ream the medullary canal. After reaming, it takes approximately 4 weeks for bone to revascularise [6]. Therefore, even with prolonged antibiotic therapy, local bone tissue remains without bactericidal concentrations, thus not interfering with bacterial growth. Acrylic bone cement is the gold standard for dead space management and the standard carrier for local antibiotic delivery in the management of orthopaedics infections [2, 7]. It delivers high concentrations of the drug locally, even to avascular areas that are inaccessible to systemic antibiotics. Those concentrations are high enough to be effective even against organisms that are resistant to drug concentrations achieved by intravenous supply. At the same time, very low serum antibiotic concentrations are observed and hence the risk for toxicity is considerably diminished [8, 9].

Antibiotic loaded bone cement can be customized intraoperatively to different shapes and forms. In intramedullary infections, antibiotic bone cement nails or antibiotic cement nails (ACNs) are preferable. Figure 1 presents an example of an ACN. They offer local delivery of antibiotics, while filling the dead space and offering stability to the fracture/nonunion site, if present.

The primary objective of this paper is to perform a systematic review of current evidence on ACNs in orthopaedic trauma. The secondary objective was to provide an up-to-date review of the indications, operative technique, failure mechanisms, complications, outcomes, and outlooks for the ACNs use in musculoskeletal infection.

Figure 1: The photo of the prepared intraoperatively *K*-wire-armed, antibiotic loaded cement nail with a syringe (for scale comparison).

2. Materials and Methods

2.1. Search Strategy. To identify relevant papers, we searched Medline database via PubMed interface with no restriction on language or publication date. The search string included word "intramedullary" and one of the following words, "osteomyelitis," "infection," "nail," "nailing," "debridement," and "reaming" and was performed on January 1, 2015. We searched all fields in the Medline database, with no restriction applied to full-text availability. Additionally, we manually reviewed the reference lists of the articles retrieved by database search for potentially missing papers.

The clinical studies selected were original articles on antibiotic cement nails. We excluded all the studies on bone cement use in arthroplasty and spine surgery as well as *in vitro* and *in vivo* studies, although we did not use the "restrict to human studies" filter in PubMed.

Details such as the number of patients, anatomical site, the age of the patients, the preparation and composition of nail, length of follow-up, and final outcome were collected.

3. Results and Discussion

3.1. Search Results. Literature review of antibiotic cement nails cases is given in Table 1. Figure 2 shows search strategy flow diagram. Since detailed discussion of clinical outcomes is beyond the scope of this review, for detailed discussion of clinical outcomes and perspectives on intramedullary infection treatment, including ACNs, we suggest the reader consults an excellent clinical review by Makridis et al. [10].

3.2. Indications for ACNs. The indication for the use of ACN is medullary infection, whatever the cause and presentation. Intramedullary infection is a well-recognized complication of intramedullary nailing for trauma [11]. It spreads along the length of the nail and involves the entire length of bone [12]. Multiple points or also the entire medullary canal is involved in pin tract infections after external fixation [13]. Reported rates of infectious complications after planned conversion from external fixation to intramedullary nailing for the femoral fractures range from 1.7 to 20% [14–18]. Similar problems can occur with lengthening over nails with external fixation and transport over nail [19, 20]. Therefore, the indications for ACN span from long bone fractures with concomitant soft tissue damage, to infected nonunion sequelae of external fixation and haematogenous osteomyelitis.

All these diagnoses share a common trait; there is usually no sequestrum and dead bone is limited to within the medullary canal [21]. However, according to the Cierny principles, after the removal of the intramedullary nail it acts as an avascular noncollapsible dead space that needs to be managed [22]. It could not be managed appropriately with poly(methyl methacrylate) (PMMA) beads strung on elastic wire and introduced into medullary canal, since they do not conform to the dead space shape and their removal becomes increasingly difficult starting already 2 weeks after insertion due to fibrous overgrowth [23]. Rather than using multiple beads on a single wire, Klemm and in another paper Seligson and Klemm used PMMA stick, formed of a PMMA mass attached to a single wire [24, 25]. This construct could be passed around external fixator's pins and its removal was facilitated. Unfortunately, it did not provide any mechanical stability to the fracture/nonunion site. In that scenario, stability is very important to treat the infection and to obtain drainage cessation or lessening [26, 27].

3.3. Contraindications for ACNs. There is one paper stating that, in bone deficits exceeding 6 cm, other alternatives for restoring stability and infection control should be used [34]. There is also an obvious contraindication for the reaming and, thus, the use of nail in people under 16 years of age [28].

3.4. The Role of Local Antibiotics Delivery versus the Role of Debridement. In a 2013 Cochrane review, the authors could not show any significant difference in osteomyelitis recurrence rates after parenteral or oral antibiotic administration [39]. Although it might be due to the fact that only limited and low quality evidence on the subject is available, this might also suggest the importance of surgical debridement as a cure, which is an observation commonly accepted among the orthopaedic surgeons [40]. A prospective trial by Simpson et al. documented the effect of surgical debridement on cure rates. They achieved 100% success with wide excision (clearance margin of 5 mm or more), 28% failure rate with marginal resection, and a total failure with local debulking and intralesional biopsy [41]. The importance of this issue is highlighted by articles describing novel ways to thoroughly debride the medullary canal, for example, RIA or Pressure Sentinel [42]. Therefore, it must be borne in mind that all the clinical results of ACNs show at the same time the results of debridement and other therapeutic actions [43].

3.5. Nail Fabrication. Multiple techniques for the fabrication of the nails have been described, from manual rolling of the cement [34], through the use of chest tube as a temporary mould, which is peeled off once the cement hardens [12, 21, 23, 29, 35, 37, 38, 44], to using a reusable mould [45, 46].

Usually, a chest tube or another kind of drainage tube with an inner diameter similar to the outer diameter of the removed nail or the diameter of the last reamer used is selected and closed at one end, for example, with Kocher forceps. Some kind of guide wire (*K*-wire, Ender nail, etc.) is selected and cut a little bit longer than the tube and its end is bent to facilitate later extraction from the medullary canal. It can also be bent to adapt to the dead space, for example, with the Herzog angle in case of replacing a tibia nail. Later, antibiotic powder is mixed with poly(methyl methacrylate) powder. The next step is to add liquid monomer, usually

Table 1: Literature review of antibiotic cement nail cases.

First author	Year	Number of cases	Anatomical site	Mean age (range)	Follow-up (range)	Nail formulation per 40 g PMMA	Results
Case series							
Kanakaris [28]	2014	24	14 femurs 10 tibias	47 (17–75) years	19 (8–36) months	0.5 g gentamicin 2 g vancomycin, antifungals	4% recurrence 5% failure in nail removal
Asloum [29]	2014	28	3 femurs 25 tibias	43 (19–70) years	48 (4–96) months	Unknown	7% recurrence 7% complications
Dhanasekhar [30]	2013	18	Femurs and tibias	Unknown	Unknown	2 g vancomycin 0.5 gentamicin	0% recurrence
Wasko [23]	2013	10	10 tibias	42 (20–59) years	72 (60–84) months	2.5 gentamicin	0% recurrence 0% complications
Selhi [31]	2011	16	8 femurs 7 tibias 1 humerus	38 (18–54) years	Unknown	4 g vancomycin 0.5 gentamicin	31% recurrence 0% complications
Kanakaris [32]	2011	8	8 femurs	40 (22–76) years	12 (12–20) months	0.5 g gentamicin 2 g vancomycin	0% recurrence 0% complications
Bar-On [33]	2010	4	2 femurs 2 tibias	9 (5–14) years	41 (36–46) months	Unknown	0% recurrence 50% wound healing disturbances
Bhadra [13]	2009	30	Lower limb	47 (20–79) years	26 (4–40) months	1.2 mg tobramycin 1 g vancomycin	Unknown
Shyam [34]	2009	25	23 femurs 2 tibias	33 (21–58) years	29 (18–40) months	2 g vancomycin 2 g gentamicin	20% recurrence 0% complications
Sancineto [27]	2008	18	4 femurs 14 tibias	37 (18–52) years	12 (10–54) months	4 g vancomycin Various others	6% recurrence 6% intolerance to nail
Qiang [35]	2007	19	5 femurs 14 tibias	38 (22–78) years	16 (6–28) months	2 g vancomycin	0% recurrence 5% complications
Paley [21]	2002	9	6 femurs 2 tibias 1 humerus	30 (8–70) years	41 (32–48) months	2.4 tobramycin 2 g vancomycin	0% recurrence 10% rod fracture
Case reports							
Mauffrey [36]	2014	1	1 femur	58 years	2 months	0.5 gentamicin 2.4 g tobramycin 2 g vancomycin	Unknown
Riel [37]	2010	1	1 tibia	±65 years	Unknown	0.5 g gentamicin	Unknown
Madanagopal [12]	2004	1	1 tibia	Unknown	Unknown	1.2 g tobramycin	0% recurrence
Ohtsuka [38]	2002	1	1 tibia	28 years	18 months	1.2 gentamicin	0% recurrence

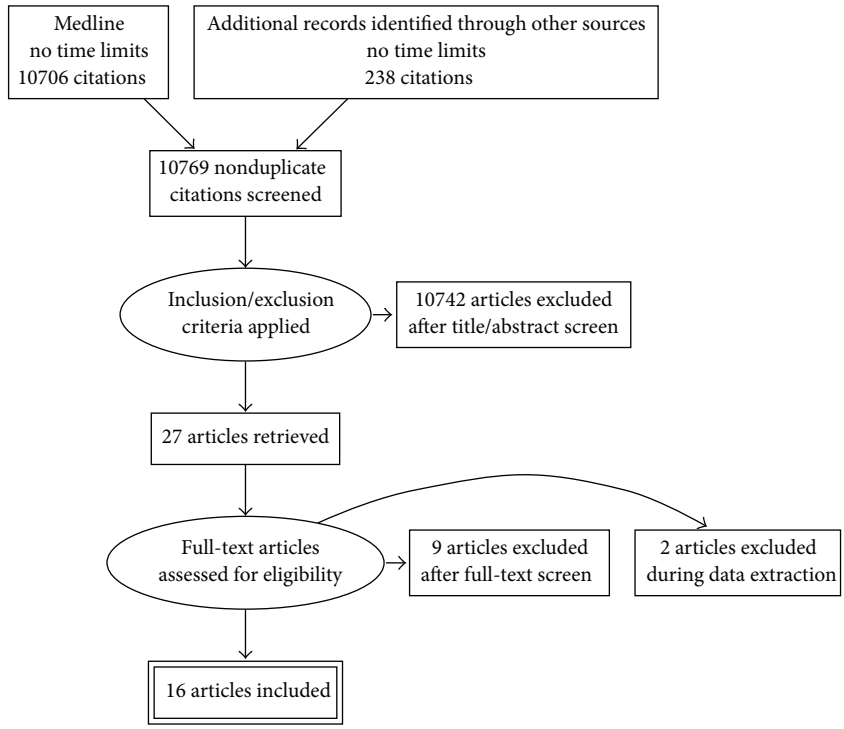

Figure 2: Article search strategy flow diagram for this paper.

more than would be used for the single batch of cement, to compensate for large volume of antibiotics. Next, the cement is poured into the cement gun and injected into the tube. The precut wire is inserted into the middle of the cement in the tube. At some point, either when the cement begins to harden and heats up or after the exothermic reaction, the tube is cut with surgical knife and peeled from the cement. Then the surgeon waits for the nail to cool and for the monomer to evaporate, which usually takes around 15 minutes. The nail can then be inserted into the medullary canal, with the bent/looped end extruding for easier retrieval.

3.6. Cement Type. When compared with other bone cements, Palacos cement showed highest elution rates, which was explained by its inherent porosity [48].

3.7. Mixing Techniques. It has been advocated that vacuum mixing the cement results in stable antibiotic elution [21], although this effect varies for different cement types [49]. On the other hand, there are papers arguing that vacuum mixing decreases cement's porosity and thus reduces the total elution of the antibiotic [50]. In-depth analysis was provided by Neut et al., who showed that vacuum-mixed gentamicin-loaded Palacos R released more gentamicin after one week *in vitro* than hand-mixed Palacos R did despite a reduction in the porosity, which theoretically should reduce elution [51]. The authors explained this discrepancy by the increase in the number and distribution of micropores smaller than one millimetre in the vacuum-mixing group, which occurred during cement polymerization by evaporation of the volatile monomer. On the other hand, the same article mentions that hand mixing with a spatula resulted in increased antibiotic release than hand mixing in a dedicated system (Cemvac) [51]. It has also been brought to attention that mixing systems in general are very heterogeneous in regard to resulting cement porosity, which probably influences the elution rates a great deal [52, 53].

3.8. Antibiotics

3.8.1. Antibiotics: General Considerations. To effectively eliminate bacteria in a biofilm, local antibiotic concentrations achieved must be 10 to 100 times the usual bactericidal concentration [5]. This usually cannot be achieved by safe doses of parenteral antibiotics, rendering this form of biofilm treatment ineffective [2]. Bone cement can deliver high concentrations of antibiotics, even to poorly vascularised and hypoxic environment, as it is independent of vascular supply [21, 54–56]. For the most popular antibiotics, bactericidal concentrations were found for up to six weeks after implanting PMMA beads [57]. Most likely, this observation would be applicable to the use of nails, since hip spacers show similar pharmacokinetics [58].

The antibiotics used for the fabrication of ACNs should be available in powder form and have a wide antibacterial spectrum with bactericidal activity at low concentrations [59]. Other desirable characteristics include high elution rate from PMMA over long periods of time and thermal stability with low influence for the mechanical properties of the cement [8]. Since they are eluted locally, they should not cause allergy or bind to serum protein easily, to maintain high

concentration [48, 54]. They should also have as minimal as possible inhibitory influence on new bone formation [60].

Liquid antibiotics elute larger amounts from bone cement than antibiotics in powder form [8]. However, they are not used in clinical practice since they negatively influence the mechanical properties of PMMA [61, 62]. Antibiotics in powder form are reported to have a rather negligible effect on the mechanical stability of bone cement as long as the antibiotic to cement ratio does not exceed 10%, which is a lower proportion than usually applied in the ACNs formulation [63].

3.8.2. Antibiotic Choice: Microorganism Sensibility. Nowadays, effective serum levels describe sensitivity of bacteria to the antibiotics. Most bacteria defined as resistant by these criteria might be sensitive when exposed to local antibiotics [7, 55, 64]. To guide the antimicrobial treatment properly, pathogens should be reconsidered to be either sensitive or resistant to the antibiotic levels achievable locally [7, 31, 55]. This is the case, for example, in classical Buchholz's work, where the antibiotic placed in the bone cement did not necessarily correlate with the culture-based sensitivity of the organisms [65]. On the other hand, there have been reports of changing patterns in microorganism resistance, partly as a result of widespread local and systemic prophylaxis [66]. Increasing numbers of gentamicin-resistant species are reported to cause deep infections, including medullary infections [67, 68]. One must remember that, even with antibiotics' concentrations as high as after adding up to 20% weight of the PMMA, colonization of the spacer/nail can still occur [69].

3.8.3. Antibiotics: Dosage. Acrylic bone cement was primarily developed as a fixation device for arthroplasty. Although the addition of more than two grams of any antibiotic per 40 g of cement reduces the cement's strength, this is not relevant to the infection treatment, as those devices are only temporary and only partially loaded mechanically [56]. To maintain elution rates and concentrations sufficient to treat an established musculoskeletal infection, at least 3.4 g of antibiotic should be used for 40 g batch of PMMA [70, 71].

3.8.4. Antibiotics: Elution. There are no papers on antibiotic elution from ACNs in English. The only report we were able to find was a Japanese article with no English translation [72]. However, there is a multitude of antibiotic elution studies on cement beads and spacers. Although the absolute values for drug release from ACNs might be different from beads and spacers, the general proportions between elution rates and processes governing the elution remain the same [73].

The first study on elution was performed by Marks et al., who showed that oxacillin, cefazolin, and gentamicin elute in a microbiologically active form from Palacos and Simplex bone cements [62]. Afterwards, it was established that elution of antibiotics from acrylic cement follows a biphasic pattern, with high elution rates early, followed by slower but sustained elution rates as time progresses [8]. Only a small portion of the antibiotic incorporated in bone cement is released; the amount of antibiotic released from cement shows an exponential decline after day 1 of implantation [49, 51, 74]. The hydrophobicity of ALBC permits roughly 10% of the added antibiotic to elute over a 6–8-week period [8].

The mechanism by which these drugs are released is not fully understood. First papers to tackle that issue suggested that the elution of antibiotics from bone cement was mainly by diffusion [75, 76]. The diffusion theory relies on the presence of pores and interconnected channels in bone cement, through which the circulating medium penetrates and dissolves the incorporated antibiotics which then slowly diffuse outwards [77]. However, Masri et al. argued that the data provided by the diffusion theory protagonists did not support this conclusion [78].

Nowadays, most of the research suggests that antibiotic release from PMMA is a passive phenomenon in which diffusion occurs out of pores, cracks, and voids in the cement [8, 79]. In support of this theory, studies show that elution is improved with increasing surface area and porosity of the cement. [62, 78–80]. van de Belt et al. studied the release of gentamicin as a function of time from six different gentamicin-loaded bone cements. They related elution to surface roughness, porosity, and wettability of the PMMA. The release kinetics of gentamicin in their study was controlled by surface roughness and porosity. They suggested that the initial release antibiotic from bone cement was mainly a surface phenomenon, while sustained release over several days was a bulk diffusion phenomenon [81]. This theory best accounts for the biphasic release characteristics of antibiotic bone cement [8].

The elution of antibiotic from PMMA would be therefore dependent on multiple variables: which cement is used [48, 54], which antibiotic is chosen [71], the amount of total antibiotic added [71], and how it is mixed [82]. Highly porous cement has been shown to elute more antibiotic and for a longer period of time relative to cement with less porosity [71].

Commercially manufactured antibiotic loaded drug delivery systems have more predictable elution patterns, compared to devices manufactured with a manual addition of an antibiotic (due to the more homogenous distribution of the incorporated antibiotic(s) in the cement powder). However, this is often the only way to make the bone cement appropriate to the sensitivity profile of the causative pathogen. Adding another antibiotic powder not only increases the activity spectrum but also increases the antibiotic elution rates. Most studies evaluating combinations of antibiotics have demonstrated a synergistic effect, in that adding a second antibiotic seems to increase the elution of both antibiotics [8, 54, 71, 83]. This is true for tobramycin and vancomycin [71, 84], teicoplanin and gentamicin [83], and linezolid and gentamicin [85]. However, two studies have reported that combining antibiotics results in decreased elution [86, 87]. No change in elution rate was reported when vancomycin and amikacin had been used together; elution rates were the same as when used individually [73]. On the other hand, with the use of another PMMA cement, different antibiotics ratio, and different testing conditions, one can find that release of one of the drugs is inhibited by the addition of another antibiotic [87]. Generally, when two

antibiotics are mixed into the same batch of bone cement, a phenomenon called passive opportunisms occurs; one of the substances acts as a soluble additive increasing porosity of the cement and increasing the total elution [71]. Thus, total antimicrobial effect of eluted substances is increased. This phenomenon seems to depend on the volume ratio between two antibiotics added to PMMA [8].

Díez-Peña et al. tried to predict the gentamicin elution from low- and high-loaded bone cement (containing up to 10 wt% of gentamicin sulfate and more than 20 wt% of gentamicin sulfate in relation to the weight of entire block of bone cement) by means of mathematical equations in an experimental model. They found out that each differently loaded PMMA has a different equation describing the release process. Moreover, for low-loaded cement, the release was mainly controlled by the imperfections of the matrix, whereas in the high-loaded PMMA an abrupt increase in the amount of drug released was evident allowing the almost complete release of the drug incorporated [88].

Lastly, the method used to mix the antibiotic seems to play an important role. Hand mixing with a spatula has been shown to increase the total antibiotic release when compared with mixing with a specialized cement mixer [51]. It is hypothesized that hand mixing introduces significant porosity to the cement, which in turn should increase antibiotic elution [8]. Other authors argue that hand mixing, in contrast to device mixing, does not crush the antibiotic crystals and thus may improve elution characteristic [50].

3.8.5. Antibiotics: Current Practice. The most used antibiotic for the fabrication of ACNs is gentamicin, followed by vancomycin [30, 44]. Concomitant use of these two agents can widen the spectrum of activity but also enhance the elution rates for both substances simultaneously [89].

3.8.6. Antibiotics: Complications. Only low serum concentrations and minor systemic toxicity are achieved while using ACNs and other local cement delivery devices [54, 90]. Research has consistently shown that antibiotics added to cement devices do not reach significant concentrations in the bloodstream, and there is no systemic toxicity in otherwise healthy individuals without hepatic or renal disease [55]. We found four case reports that have been published on acute renal failure after the use of high-dose ALBC for the treatment of deep periprosthetic sepsis, three total knees and two total hip patients [91–94]. Concurrent administration of IV antibiotics and significant comorbidities (e.g., preexisting renal disease) complicate all of these patient histories. On the other hand, a study from Mayo clinic by Springer et al. which retrospectively reviewed 36 knees in 34 patients treated with 4 g of vancomycin and 4.8 g of gentamicin per 40 g batch of PMMA reported only a single case of transient elevation in serum creatinine with no permanent systemic complications [95]. Noteworthily, the mean total dose of antibiotic per patient in that study was 10.5 g of vancomycin and 12.5 g of gentamicin, which is much higher than with any of the ACNs reported. Up to date, we were not able to find any report on renal or auditory complication in ACN patients. This might be due to the fact that the majority of those nails are put in trauma or posttraumatic patients, who tend to be younger and previously healthy compared to, for example, total joint replacement patient population. Multiple papers show that patients treated with local antibiotics are at no more risk and are probably at less risk of experiencing ototoxicity and nephrotoxicity than ones subjected to long-term parenteral antibiotics [96–98]. There are more adverse reactions due to the use of systemic antibiotics than to the use of local antibiotic-eluting spacers and nails [99].

Another important complication of ACNs is resistance induction. There are two articles describing ability of bacteria to adhere to and colonize gentamicin [69] and mixed gentamicin-vancomycin-loaded cement [100] after prolonged periods of implantation and even ability to develop gentamicin resistance despite preoperative susceptibility.

3.9. In Vitro and In Vivo Studies on ACNs. As far as the authors know, there is no report on the use of ACNs in an animal model. Most probably this is due to the technical difficulties and availability of similar models, that is, antibiotic-coated implants. Local application of a biodegradable coating with 10% gentamicin was shown to be effective in reducing implant-related infection in a rat model [101]. Similar data was found for fibrin sealant plus tobramycin, a combination which was as effective as poly(methyl methacrylate) beads plus tobramycin against methicillin-sensitive *Staphylococcus aureus* osteomyelitis in a rabbit model [102].

Elson et al. performed one of the most important early laboratory studies. They showed that when antibiotic loaded acrylic bone cement is placed next to cortical bone, dense cortical bone is penetrated by the eluted antibiotic and its concentration in the bone is much higher than what can be achieved safely by systemic administration [103].

3.10. ACNs Benefits and Risks. The benefits and risks of ACNs are summarised in Table 2. Since the benefits were thoroughly discussed in the previous sections of this paper, only ACNs' shortcomings are described below.

First and foremost, local antibiotic carriers have never been shown to be superior to intravenous administration of antibiotics in terms of cure rate. At the same time, most of them require some sort of repeat surgery, unless they biodegrade, which is not the case in ACNs [44].

There has been one report linking high failure rate to the use of ACNs in infected nonunion with bone defect exceeding 6 cm [34]. The authors suggested that when faced with a large bone defect, other alternative forms of treatment should be used. Unfortunately, they did not provide a multivariate analysis on risk factors that might influence their results.

One of the concerns with all the PMMA carriers for antibiotic is the emergence of resistance. There have been reports on induction of coagulase-negative staphylococci after applying gentamicin-loaded bone cement [69]. However, there are, to our knowledge, no reports on resistance after ACNs.

From the technical point of view, there is a possibility of debonding of the cement from the nail upon its introduction or removal from the medullary canal. However, this situation

Table 2: The benefits and drawbacks of antibiotic cement nails.

Benefits	Drawbacks
High concentration of local antibiotic elution: up to 200 times greater than with systemic drug administration, independent of vascular supply [21] Stability to the fracture/nonunion site, allowing for early weight bearing [23] Local antibiotic delivery independent of patient compliance [23] Systemic toxicity of antibiotics very rarely observed [8] Versatility of modifying antibiotic as per the culture report [27] Control of infection and stability is achieved with a single procedure [44] Alternative for patients refusing or not being right candidates for external fixation [13]	Local antibiotic carriers have never been shown to be superior to intravenous administration of antibiotics in terms of cure rate [21] Require repeat surgery [23] Possible emergence of resistance [13] Possible MMA toxicity [102, 103]

is usually quickly resolved with reaming or using long-reaching surgical tools and, in our experience, as with every surgical complication, the rate of debonding decreases with the familiarity with the technique and increasing expertise in nail fabrication [23, 46].

In the past, bone cement liquid monomer, methyl methacrylate (MMA), was believed to be carcinogenic. However, the lack of consistency in the results of various studies and the absence of dose response lead to the conclusion that MMA in not carcinogenic to humans under normal conditions of use [104]. Moreover, the evidence shows that even repeated mixing of PMMA bone cement does not pose an additional risk to operative theatres' personnel [105]. In a study comparing ionically dissolved or precipitated metals with MMA toxicity, MMA monomer toxicity was found to be low compared to metal toxicity [47]. The study of Elmaraghy et al. found that the presence of MMA monomer in femoral venous blood has no effect on the formation of fat emboli or their pulmonary haemodynamic outcome during cemented hip arthroplasty [106]. To our knowledge, there are no studies on MMA toxicity after the use of ACNs.

3.11. Alternatives. The novel concept of local antibiotic delivery by gentamicin-impregnated acrylic bone cement was introduced by Buchholz et al. in the early 1970s for the treatment of infected hip arthroplasty [65]. Antibiotic bead chains were introduced by Klemm in 1976 [24]. Later on, his team reported on the use of an antibiotic-impregnated cement "stick" [25, 107].

In a study of two cases, Tandon and Thomas were able to provide a proof of concept of using hollow, slotted nail with gentamicin cement beads. Based on the observation that commercially available beads are 7 mm in diameter, they argued that two to three strings of beads could be inserted into most intramedullary nails and effectively treat infection [108]. Unfortunately, their technique did not allow for the use of interlocking screws, as they would make extracting the beads without the nail impossible, and was never published on a larger series.

3.12. Outlook. It is perceived that with future developments local antibiotic delivery systems will likely supplant the traditional use of systemic antibiotics for the treatment of musculoskeletal infections [7, 109].

Another field of development is the MRI-compatible ACN. There has been only a single, short follow-up case report by Mauffrey et al. The authors claim that serum inflammatory markers might not always be reliable and that MRI monitoring of the infection might provide better insight into whether or not the infection has healed and one could move to the definitive fixation by a metallic nail [36]. On the other hand, the use of carbon fibre nail was estimated to incur an additional cost of $2,600, which is almost 30-fold higher than for most of the nails described in the literature [23].

Since 2005, there are also prefabricated interlocking antibiotic-coated titanium nails, which use polylactic acid (PLA) coating loaded with gentamicin and offer both sustained release kinetics and biodegradability. Promising 6-month results have been reported in primary fracture setting [110].

It is important to realize that as long as none of the ACNs is FDA-approved, which is the current state as of 2015, their use is off-label and prospective clinical trials cannot be undertaken [44].

There is only one short paediatric case series, in which ACNs have been used. It was found to be safe and effective in the treatment of chronic osteomyelitis, with special attention to protecting the epiphyseal growth plates of long bones. The authors believed also that using the nail instead of other forms of local antibiotic carrier enabled for prevention of further tissue loss [33]. We believe this patient group could benefit from the use of ACNs, but further clinical trials are necessary before introducing the ACNs into regular paediatric trauma/orthopaedic practice.

There are certain substances other than antibiotics, such as dextran, glycine, or xylitol, which could be used to impregnate PMMA for the enhancement of the antibiotic elution. However, the ideal filler material and amount of filler are yet to be established [8]. We are not aware of any studies beyond the laboratory phase on the PMMA fillers [111].

Another technical development is the introduction of the Reamer-Irrigator-Aspirator (RIA) system (Synthes, Inc., West Chester, Philadelphia) which, in animal models and cadaver studies, offers an advance on existing reaming devices, as it is less traumatic [32, 42]. It is used in the debridement and irrigation of the intramedullary canal of the femur and tibia [112]. Its use is very promising and could facilitate proper debridement of the medullary canal, which is the basic condition of intramedullary infection healing.

Ultrasound was also found to increase the transport of gentamicin across and within the biofilm of *P. aeruginosa* and *E. coli*. The other effect of ultrasound waves is presumably to

increase the transport of oxygen and other small molecules, which may increase the metabolic state and render cells more susceptible to antibiotics [113, 114]. The ultrasound may have also a positive effect on antibiotic elution characteristics [8]. Further laboratory, feasibility, and clinical studies are needed to explain the potential for enhanced antibiotic release from PMMA by ultrasound and translate those basic science findings into clinical practice.

4. Conclusions

Since the introduction of antibiotic loaded acrylic bone cement by Buchholz and Engelbrecht, it remains a golden standard in local antibiotic delivery. This is also true in case of long bone medullary infections, where antibiotic cement nails remain an important treatment option. The major advantage of ACNs is the local release of high antibiotic concentrations, which vastly exceed those after systemic administration with no or low systemic toxicity. At the same time, they are able to provide limited stability to the fracture/nonunion site, which promotes infection healing. They are used as a clinician directed application; therefore, there is no issue with availability and antibiotic specificity, as it can be based on preoperative culture. Antibiotic elution rates, mechanisms, and ways to improve total amount of drug delivered are still debated and researched. Despite promising short- and midterm results from clinical studies, further basic science and translational studies are desirable before routine use of ACNs in clinical practice.

Conflict of Interests

The authors declare that there is no conflict of interests regarding the publication of this paper.

References

[1] P. Stoodley, G. D. Ehrlich, P. P. Sedghizadeh et al., "Orthopaedic biofilm infections," *Current Orthopaedic Practice*, vol. 22, no. 6, pp. 558–563, 2011.

[2] C. L. Nelson, "The current status of material used for depot delivery of drugs," *Clinical Orthopaedics and Related Research*, no. 427, pp. 72–78, 2004.

[3] G. Cierny and J. Mader, "The surgical treatment of adult osteomyelitis," in *Surgery of the Musculoskeletal System*, pp. 4814–4834, Churchill Livingstone, New York, NY, USA, 1983.

[4] P. D. P. Lew and P. F. A. Waldvogel, "Osteomyelitis," *The Lancet*, vol. 364, no. 9431, pp. 369–379, 2004.

[5] P. S. Stewart and J. W. Costerton, "Antibiotic resistance of bacteria in biofilms," *The Lancet*, vol. 358, no. 9276, pp. 135–138, 2001.

[6] L. Lazzarini, J. T. Mader, and J. H. Calhoun, "Osteomyelitis in long bones," *The Journal of Bone and Joint Surgery—American Volume*, vol. 86, no. 10, pp. 2305–2318, 2004.

[7] A. D. Hanssen, "Local antibiotic delivery vehicles in the treatment of musculoskeletal infection," *Clinical Orthopaedics and Related Research*, no. 437, pp. 91–96, 2005.

[8] K. Anagnostakos and J. Kelm, "Enhancement of antibiotic elution from acrylic bone cement," *Journal of Biomedical Materials Research Part B: Applied Biomaterials*, vol. 90, no. 1, pp. 467–475, 2009.

[9] S. B. Rosslenbroich, M. J. Raschke, C. Kreis et al., "Daptomycin: local application in implant-associated infection and complicated osteomyelitis," *The Scientific World Journal*, vol. 2012, Article ID 578251, 9 pages, 2012.

[10] K. Makridis, T. Tosounidis, and P. Giannoudis, "Suppl 2: management of infection after intramedullary nailing of long bone fractures: treatment protocols and outcomes," *The Open Orthopaedics Journal*, vol. 7, pp. 219–226, 2013.

[11] M. J. Patzakis, J. Wilkins, and D. A. Wiss, "Infection following intramedullary nailing of long bones: diagnosis and management," *Clinical Orthopaedics and Related Research*, vol. 212, pp. 182–191, 1986.

[12] S. G. Madanagopal, D. Seligson, and C. S. Roberts, "The antibiotic cement nail for infection after tibial nailing," *Orthopedics*, vol. 27, no. 7, pp. 709–712, 2004.

[13] A. K. Bhadra and C. S. Roberts, "Indications for antibiotic cement nails," *Journal of Orthopaedic Trauma*, vol. 23, supplement 5, pp. S26–S30, 2009.

[14] P. J. Nowotarski, C. H. Turen, R. J. Brumback, and J. M. Scarboro, "Conversion of external fixation to intramedullary nailing for fractures of the shaft of the femur in multiply injured patients," *The Journal of Bone & Joint Surgery—American Volume*, vol. 82, no. 6, pp. 781–788, 2000.

[15] T. M. Scalea, S. A. Boswell, J. D. Scott, K. A. Mitchell, M. E. Kramer, and A. N. Pollak, "External fixation as a bridge to intramedullary nailing for patients with multiple injuries and with femur fractures: damage control orthopedics," *The Journal of Trauma—Injury, Infection and Critical Care*, vol. 48, no. 4, pp. 613–623, 2000.

[16] A. A. Parekh, W. R. Smith, S. Silva et al., "Treatment of distal femur and proximal tibia fractures with external fixation followed by planned conversion to internal fixation," *Journal of Trauma—Injury, Infection and Critical Care*, vol. 64, no. 3, pp. 736–739, 2008.

[17] M. Bernat, C. Lecoq, M. Lempidakis, G. Martin, R. Aswad, and D. G. Poitout, "Secondary internal osteosynthesis after external fixation for recent or old open fracture of the lower limb," *Revue de Chirurgie Orthopédique et Réparatrice de L'Appareil Moteur*, vol. 82, no. 2, pp. 137–144, 1996.

[18] D. J. Maurer, R. L. Merkow, and R. B. Gustilo, "Infection after intramedullary nailing of severe open tibial fractures initially treated with external fixation," *The Journal of Bone & Joint Surgery—American Volume*, vol. 71, no. 6, pp. 835–838, 1989.

[19] D. Paley, J. E. Herzenberg, and N. Bor, "Fixator-assisted nailing of femoral and tibial deformities," *Techniques in Orthopaedics*, vol. 12, no. 4, pp. 260–275, 1997.

[20] G. Oedekoven, D. Jansen, M. Raschke, and B. F. Claudi, "The monorail system—bone segment transport over unreamed interlocking," *Der Chirurg*, vol. 67, no. 11, pp. 1069–1079, 1996.

[21] D. Paley and J. E. Herzenberg, "Intramedullary infections treated with antibiotic cement rods: preliminary results in nine cases," *Journal of Orthopaedic Trauma*, vol. 16, no. 10, pp. 723–729, 2002.

[22] K. Tetsworth and G. Cierny III, "Osteomyelitis debridement techniques," *Clinical Orthopaedics and Related Research*, no. 360, pp. 87–96, 1999.

[23] M. K. Wasko and O. Borens, "Antibiotic cement nail for the treatment of posttraumatic intramedullary infections of the

tibia: midterm results in 10 cases," *Injury*, vol. 44, no. 8, pp. 1057–1060, 2013.

[24] K. Klemm, "Gentamicin-PMMA-beads in treating bone and tissue infections (author's transl)," *Zentralblatt für Chirurgie*, vol. 104, no. 14, pp. 934–942, 1979.

[25] D. Seligson and K. Klemm, "Treatment of infection following intramedullary nailing," in *The Science and Practice of Intramedullary Nailing*, vol. 2, pp. 317–333, Lippincott Williams & Wilkins, 1996.

[26] M. E. Miller, J. R. Ada, and L. X. Webb, "Treatment of infected nonunion and delayed union of tibia fractures with locking intramedullary nails," *Clinical Orthopaedics and Related Research*, no. 245, pp. 233–238, 1989.

[27] C. F. Sancineto and J. D. Barla, "Treatment of long bone osteomyelitis with a mechanically stable intramedullar antibiotic dispenser: nineteen consecutive cases with a minimum of 12 months follow-up," *The Journal of Trauma—Injury, Infection and Critical Care*, vol. 65, no. 6, pp. 1416–1420, 2008.

[28] N. Kanakaris, S. Gudipati, T. Tosounidis, P. Harwood, S. Britten, and P. V. Giannoudis, "The treatment of intramedullary osteomyelitis of the femur and tibia using the Reamer-Irrigator-Aspirator system and antibiotic cement rods," *The Bone & Joint Journal*, vol. 96-B, no. 6, pp. 783–788, 2014.

[29] Y. Asloum, G. Vergnenegre, B. Bedin et al., "L'enclouage cimenté transitoire en traumatologie. À propos de 26 cas," *Revue de Chirurgie Orthopédique et Traumatologique*, vol. 100, no. 4, pp. S91–S98, 2014.

[30] R. Dhanasekhar, P. Jacob, and J. Francis, "Antibiotic cement impregnated nailing in the management of infected non-union of femur and tibia," *Kerala Journal of Orthopaedics*, vol. 26, no. 2, pp. 93–97, 2013.

[31] H. S. Selhi, P. Mahindra, M. Yamin, D. Jain, W. G. De Long Jr., and J. Singh, "Outcome in patients with an infected nonunion of the long bones treated with a reinforced antibiotic bone cement rod," *Journal of Orthopaedic Trauma*, vol. 26, no. 3, pp. 184–188, 2012.

[32] N. K. Kanakaris, D. Morell, S. Gudipati, S. Britten, and P. V. Giannoudis, "Reaming irrigator aspirator system: early experience of its multipurpose use," *Injury*, vol. 42, no. 4, pp. S28–S34, 2011.

[33] E. Bar-On, D. M. Weigl, N. Bor et al., "Chronic osteomyelitis in children: treatment by intramedullary reaming and antibiotic-impregnated cement rods," *Journal of Pediatric Orthopaedics*, vol. 30, no. 5, pp. 508–513, 2010.

[34] A. K. Shyam, P. K. Sancheti, S. K. Patel, S. Rocha, C. Pradhan, and A. Patil, "Use of antibiotic cement-impregnated intramedullary nail in treatment of infected non-union of long bone," *Indian Journal of Orthopaedics*, vol. 43, no. 4, pp. 396–402, 2009.

[35] Z. Qiang, P. Z. Jun, X. J. Jie, L. Hang, L. J. Bing, and L. F. Cai, "Use of antibiotic cement rod to treat intramedullary infection after nailing: preliminary study in 19 patients," *Archives of Orthopaedic and Trauma Surgery*, vol. 127, no. 10, pp. 945–951, 2007.

[36] C. Mauffrey, G. W. Chaus, N. Butler, and H. Young, "MR-compatible antibiotic interlocked nail fabrication for the management of long bone infections: first case report of a new technique," *Patient Safety in Surgery*, vol. 8, no. 1, article 14, 2014.

[37] R. U. Riel and P. B. Gladden, "A simple method for fashioning an antibiotic cement-coated interlocking intramedullary nail," *The American Journal of Orthopedics*, vol. 39, no. 1, pp. 18–21, 2010.

[38] H. Ohtsuka, K. Yokoyama, K. Higashi et al., "Use of antibiotic-impregnated bone cement nail to treat septic nonunion after open tibial fracture," *Journal of Trauma-Injury, Infection and Critical Care*, vol. 52, no. 2, pp. 364–366, 2002.

[39] L. O. Conterno and M. D. Turchi, "Antibiotics for treating chronic osteomyelitis in adults," *The Cochrane Database of Systematic Reviews*, vol. 9, Article ID CD004439, 2013.

[40] J. Sanders and C. Mauffrey, "Long bone osteomyelitis in adults: fundamental concepts and current techniques," *Orthopedics*, vol. 36, no. 5, pp. 368–375, 2013.

[41] A. H. R. W. Simpson, M. Deakin, and J. M. Latham, "Chronic osteomyelitis. The effect of the extent of surgical resection on infection-free survival," *The Journal of Bone & Joint Surgery—British Volume*, vol. 83, no. 3, pp. 403–407, 2001.

[42] G. Goplen, J. A. Wilson, M. McAffrey, K. Deluzio, and R. Leighton, "A cadaver model evaluating femoral intramedullary reaming: a comparison between new reamer design (Pressure Sentinel) and a novel suction/irrigation reamer (RIA)," *Injury*, vol. 41, no. 2, pp. S38–S42, 2010.

[43] Y. Xu, Y. Zhu, X. Fan, T. Jin, Y. Li, and X. He, "Implant-related infection in the Tibia: surgical revision strategy with vancomycin cement," *The Scientific World Journal*, vol. 2014, Article ID 124864, 6 pages, 2014.

[44] J. W. Kim, D. O. Cuellar, J. Hao, D. Seligson, and C. Mauffrey, "Custom-made antibiotic cement nails: a comparative study of different fabrication techniques," *Injury*, vol. 45, no. 8, pp. 1179–1184, 2014.

[45] R. Thonse and J. Conway, "Antibiotic cement-coated interlocking nail for the treatment of infected nonunions and segmental bone defects," *Journal of Orthopaedic Trauma*, vol. 21, no. 4, pp. 258–268, 2007.

[46] R. Thonse and J. D. Conway, "Antibiotic cement-coated nails for the treatment of infected nonunions and segmental bone defects," *The Journal of Bone & Joint Surgery—American Volume*, vol. 90, no. 4, pp. 163–174, 2008.

[47] M. G. Shettlemore and K. J. Bundy, "Assessment of dental material degradation product toxicity using a bioluminescent bacterial assay," *Dental Materials*, vol. 18, no. 6, pp. 445–453, 2002.

[48] M. J. Penner, C. P. Duncan, and B. A. Masri, "The in vitro elution characteristics of antibiotic-loaded CMW and Palacos-R bone cements," *Journal of Arthroplasty*, vol. 14, no. 2, pp. 209–214, 1999.

[49] J. Meyer, G. Piller, C. A. Spiegel, S. Hetzel, and M. Squire, "Vacuum-mixing significantly changes antibiotic elution characteristics of commercially available antibiotic-impregnated bone cements," *The Journal of Bone & Joint Surgery—American Volume*, vol. 93, no. 22, pp. 2049–2056, 2011.

[50] T. A. Clyburn and Q. Cui, "Antibiotic laden cement: current state of the art," *AAOS Now*, 2007.

[51] D. Neut, H. van de Belt, J. R. van Horn, H. C. van der Mei, and H. J. Busscher, "The effect of mixing on gentamicin release from polymethylmethacrylate bone cements," *Acta Orthopaedica Scandinavica*, vol. 74, no. 6, pp. 670–676, 2003.

[52] H. Mau, K. Schelling, C. Heisel, J.-S. Wang, and S. J. Breusch, "Comparison of various vacuum mixing systems and bone cements as regards reliability, porosity and bending strength," *Acta Orthopaedica Scandinavica*, vol. 75, no. 2, pp. 160–172, 2004.

[53] A. Bistolfi, G. Massazza, E. Verné et al., "Antibiotic-loaded cement in orthopedic surgery: a review," *ISRN Orthopedics*, vol. 2011, Article ID 290851, 8 pages, 2011.

[54] D. Cerretani, G. Giorgi, P. Fornara et al., "The in vitro elution characteristics of vancomycin combined with imipenem-cilastatin in acrylic bone-cements: a pharmacokinetic study," *The Journal of Arthroplasty*, vol. 17, no. 5, pp. 619–626, 2002.

[55] W. W. Brien, E. A. Salvati, R. Klein, B. Brause, and S. Stern, "Antibiotic impregnated bone cement in total hip arthroplasty: an in vivo comparison of the elution properties of tobramycin and vancomycin," *Clinical Orthopaedics and Related Research*, no. 296, pp. 242–248, 1993.

[56] M. Baleani, C. Persson, C. Zolezzi, A. Andollina, A. M. Borrelli, and D. Tigani, "Biological and biomechanical effects of vancomycin and meropenem in acrylic bone cement," *The Journal of Arthroplasty*, vol. 23, no. 8, pp. 1232–1238, 2008.

[57] D. Seligson, G. J. Popham, K. Voos, S. L. Henry, and M. Faghri, "Antibiotic-leaching from polymethylmethacrylate beads," *The Journal of Bone & Joint Surgery—American Volume*, vol. 75, no. 5, pp. 714–720, 1993.

[58] E. Bertazzoni Minelli, A. Benini, B. Magnan, and P. Bartolozzi, "Release of gentamicin and vancomycin from temporary human hip spacers in two-stage revision of infected arthroplasty," *The Journal of Antimicrobial Chemotherapy*, vol. 53, no. 2, pp. 329–334, 2004.

[59] K. Anagnostakos, O. Fürst, and J. Kelm, "Antibiotic-impregnated PMMA hip spacers: current status," *Acta Orthopaedica*, vol. 77, no. 4, pp. 628–637, 2006.

[60] C. G. Zalavras, M. J. Patzakis, and P. Holtom, "Local antibiotic therapy in the treatment of open fractures and osteomyelitis," *Clinical Orthopaedics and Related Research*, no. 427, pp. 86–93, 2004.

[61] E. Ger, D. Dall, T. Miles, and A. Forder, "Bone cement and antibiotics," *South African Medical Journal*, vol. 51, no. 9, pp. 276–279, 1977.

[62] K. E. Marks, C. L. Nelson, and E. P. Lautenschlager, "Antibiotic-impregnated acrylic bone cement," *The Journal of Bone & Joint Surgery—American Volume*, vol. 58, no. 3, pp. 358–364, 1976.

[63] E. P. Lautenschlager, J. J. Jacobs, G. W. Marshall, and P. R. Meyer Jr., "Mechanical properties of bone cements containing large doses of antibiotic powders," *Journal of Biomedical Materials Research*, vol. 10, no. 6, pp. 929–938, 1976.

[64] A. D. Hanssen and M. J. Spangehl, "Practical applications of antibiotic-loaded bone cement for treatment of infected joint replacements," *Clinical Orthopaedics and Related Research*, no. 427, pp. 79–85, 2004.

[65] H. W. Buchholz, R. A. Elson, E. Engelbrecht, H. Lodenkämper, J. Röttger, and A. Siegel, "Management of deep infection of total hip replacement," *The Journal of Bone & Joint Surgery—British Volume*, vol. 63, no. 3, pp. 342–353, 1981.

[66] P. Anguita-Alonso, A. D. Hanssen, D. R. Osmon, A. Trampuz, J. M. Steckelberg, and R. Patel, "High rate of aminoglycoside resistance among staphylococci causing prosthetic joint infection," *Clinical Orthopaedics and Related Research*, no. 439, pp. 43–47, 2005.

[67] C.-E. Chen, J.-Y. Ko, J.-W. Wang, and C.-J. Wang, "Infection after intramedullary nailing of the femur," *The Journal of Trauma*, vol. 55, no. 2, pp. 338–344, 2003.

[68] M. M. Tunney, G. Ramage, S. Patrick, J. R. Nixon, P. G. Murphy, and S. P. Gorman, "Antimicrobial susceptibility of bacteria isolated from orthopedic implants following revision hip surgery," *Antimicrobial Agents and Chemotherapy*, vol. 42, no. 11, pp. 3002–3005, 1998.

[69] B. Thornes, P. Murray, and D. Bouchier-Hayes, "Development of resistant strains of *Staphylococcus epidermidis* on gentamicin-loaded bone cement in vivo," *The Journal of Bone and Joint Surgery—British Volume*, vol. 84, no. 5, pp. 758–760, 2002.

[70] W. A. Jiranek, A. D. Hanssen, and A. S. Greenwald, "Current concepts review: antibiotic-loaded bone cement for infection prophylaxis in total joint replacement," *The Journal of Bone & Joint Surgery—American Volume*, vol. 88, no. 11, pp. 2487–2500, 2006.

[71] M. J. Penner, B. A. Masri, and C. P. Duncan, "Elution characteristics of vancomycin and tobramycin combined in acrylic bone-cement," *The Journal of Arthroplasty*, vol. 11, no. 8, pp. 939–944, 1996.

[72] M. Tonegawa, A. Hashimoto, and M. Sekiguchi, "Release of gentamicin from acrylic bone cement spacer," *Kotsu Kansetsu Jintai*, vol. 11, pp. 1019–1024, 1998.

[73] D. K. Kuechle, G. C. Landon, D. M. Musher, and P. C. Noble, "Elution of vancomycin, daptomycin, and amikacin from acrylic bone cement," *Clinical Orthopaedics and Related Research*, no. 264, pp. 302–308, 1991.

[74] N. Greene, P. D. Holtom, C. A. Warren et al., "In vitro elution of tobramycin and vancomycin polymethylmethacrylate beads and spacers from Simplex and Palacos," *American Journal of Orthopedics*, vol. 27, no. 3, pp. 201–205, 1998.

[75] H. W. Buchholz, R. A. Elson, and K. Heinert, "Antibiotic-loaded acrylic cement: current concepts," *Clinical Orthopaedics and Related Research*, vol. 190, pp. 96–108, 1984.

[76] R. Bayston and R. D. G. Milner, "The sustained release of antimicrobial drugs from bone cement. An appraisal of laboratory investigations and their significance," *The Journal of Bone & Joint Surgery—British Volume*, vol. 64, no. 4, pp. 460–464, 1982.

[77] H. van de Belt, D. Neut, W. Schenk, J. R. Van Horn, H. C. Van der Mei, and H. J. Busscher, "Infection of orthopedic implants and the use of antibiotic-loaded bone cements," *Acta Orthopaedica Scandinavica*, vol. 72, no. 6, pp. 557–571, 2001.

[78] B. A. Masri, C. P. Duncan, C. P. Beauchamp, N. J. Paris, and J. Arntorp, "Effect of varying surface patterns on antibiotic elution from antibiotic-loaded bone cement," *The Journal of Arthroplasty*, vol. 10, no. 4, pp. 453–459, 1995.

[79] A. S. Baker and L. W. Greenham, "Release of gentamicin from acrylic bone cement. Elution and diffusion studies," *The Journal of Bone and Joint Surgery—American Volume*, vol. 70, no. 10, pp. 1551–1557, 1988.

[80] B. M. Wroblewski, "Leaching out from acrylic bone cement. Experimental evaluation," *Clinical Orthopaedics and Related Research*, no. 124, pp. 311–312, 1977.

[81] H. van de Belt, D. Neut, D. R. A. Uges et al., "Surface roughness, porosity and wettability of gentamicin-loaded bone cements and their antibiotic release," *Biomaterials*, vol. 21, no. 19, pp. 1981–1987, 2000.

[82] G. Lewis, S. Janna, and A. Bhattaram, "Influence of the method of blending an antibiotic powder with an acrylic bone cement powder on physical, mechanical, and thermal properties of the cured cement," *Biomaterials*, vol. 26, no. 20, pp. 4317–4325, 2005.

[83] K. Anagnostakos, J. Kelm, T. Regitz, E. Schmitt, and W. Jung, "In vitro evaluation of antibiotic release from and bacteria growth inhibition by antibiotic-loaded acrylic bone cement spacers," *Journal of Biomedical Materials Research Part B: Applied Biomaterials*, vol. 72, no. 2, pp. 373–378, 2005.

[84] B. A. Masri, C. P. Duncan, and C. P. Beauchamp, "Long-term elution of antibiotics from bone-cement: an in vivo study using the prosthesis of antibiotic-loaded acrylic cement (PROSTALAC) system," *The Journal of Arthroplasty*, vol. 13, no. 3, pp. 331–338, 1998.

[85] K. Anagnostakos, J. Kelm, S. Grün, E. Schmitt, W. Jung, and S. Swoboda, "Antimicrobial properties and elution kinetics of linezolid-loaded hip spacers in vitro," *Journal of Biomedical Materials Research—Part B Applied Biomaterials*, vol. 87, no. 1, pp. 173–178, 2008.

[86] M. E. Bertazzoni, C. Caveiari, and A. Benini, "Release of antibiotics from polymethylmethacrylate cement," *Journal of Chemotherapy*, vol. 14, no. 5, pp. 492–500, 2002.

[87] J. Klekamp, J. M. Dawson, D. W. Haas, D. DeBoer, and M. Christie, "The use of vancomycin and tobramycin in acrylic bone cement: biomechanical effects and elution kinetics for use in joint arthroplasty," *The Journal of Arthroplasty*, vol. 14, no. 3, pp. 339–346, 1999.

[88] E. Díez-Peña, G. Frutos, P. Frutos, and J. M. Barrales-Rienda, "Gentamicin sulphate release from a modified commercial acrylic surgical radiopaque bone cement. I. Influence of the gentamicin concentration on the release process mechanism," *Chemical & Pharmaceutical Bulletin*, vol. 50, no. 9, pp. 1201–1208, 2002.

[89] K.-H. Koo, J.-W. Yang, S.-H. Cho et al., "Impregnation of vancomycin, gentamicin, and cefotaxime in a cement spacer for two-stage cementless reconstruction in infected total hip arthroplasty," *The Journal of Arthroplasty*, vol. 16, no. 7, pp. 882–892, 2001.

[90] M. Kruger-Franke, C. Carl, and J. Haus, "Treatment of infection following intramedullary nailing. A comparison of various treatment regimens," *Aktuelle Traumatologie*, vol. 23, no. 2, pp. 72–76, 1993.

[91] J. M. Curtis, V. Sternhagen, and D. Batts, "Acute renal failure after placement of tobramycin-impregnated bone cement in an infected total knee arthroplasty," *Pharmacotherapy*, vol. 25, no. 6, pp. 876–880, 2005.

[92] S. Dovas, V. Liakopoulos, L. Papatheodorou et al., "Acute renal failure after antibiotic-impregnated bone cement treatment of an infected total knee arthroplasty," *Clinical Nephrology*, vol. 69, no. 3, pp. 207–212, 2008.

[93] B. N. Patrick, M. P. Rivey, and D. R. Allington, "Acute renal failure associated with vancomycin- and tobramycin-laden cement in total hip arthroplasty," *The Annals of Pharmacotherapy*, vol. 40, no. 11, pp. 2037–2042, 2006.

[94] T. M. van Raaij, L. E. Visser, A. G. Vulto, and J. A. N. Verhaar, "Acute renal failure after local gentamicin treatment in an infected total knee arthroplasty," *The Journal of Arthroplasty*, vol. 17, no. 7, pp. 948–950, 2002.

[95] B. D. Springer, G.-C. Lee, D. Osmon, G. J. Haidukewych, A. D. Hanssen, and D. J. Jacofsky, "Systemic safety of high-dose antibiotic-loaded cement spacers after resection of an infected total knee arthroplasty," *Clinical Orthopaedics and Related Research*, no. 427, pp. 47–51, 2004.

[96] D. E. Stabile and A. M. Jacobs, "Development and application of antibiotic-loaded bone cement beads," *Journal of the American Podiatric Medical Association*, vol. 80, no. 7, pp. 354–359, 1990.

[97] K. Klemm, "The use of antibiotic-containing bead chains in the treatment of chronic bone infections," *Clinical Microbiology and Infection*, vol. 7, no. 1, pp. 28–31, 2001.

[98] R. C. Haydon, J. D. Blaha, C. Mancinelli, and K. Koike, "Audiometric thresholds in osteomyelitis patients treated with gentamicin- impregnated methylmethacrylate beads (Septopal)," *Clinical Orthopaedics and Related Research*, no. 295, pp. 43–46, 1993.

[99] J. D. Blaha, J. H. Calhoun, C. L. Nelson et al., "Comparison of the clinical efficacy and tolerance of gentamicin PMMA beads on surgical wire versus combined and systemic therapy for osteomyelitis," *Clinical Orthopaedics and Related Research*, no. 295, pp. 8–12, 1993.

[100] K. Anagnostakos, P. Hitzler, D. Pape, D. Kohn, and J. Kelm, "Persistence of bacterial growth on antibiotic-loaded beads: is it actually a problem?" *Acta Orthopaedica*, vol. 79, no. 2, pp. 302–307, 2008.

[101] M. Lucke, G. Schmidmaier, S. Sadoni et al., "Gentamicin coating of metallic implants reduces implant-related osteomyelitis in rats," *Bone*, vol. 32, no. 5, pp. 521–531, 2003.

[102] J. T. Mader, C. M. Stevens, J. H. Stevens, R. Ruble, J. T. Lathrop, and J. H. Calhoun, "Treatment of experimental osteomyelitis with a fibrin sealant antibiotic implant," *Clinical Orthopaedics and Related Research*, no. 403, pp. 58–72, 2002.

[103] R. A. Elson, A. E. Jephcott, D. B. McGechie, and D. Verettas, "Antibiotic loaded acrylic cement," *The Journal of Bone and Joint Surgery—British Volume*, vol. 59, no. 2, pp. 200–205, 1977.

[104] J. A. Tomenson, A. V. Carpenter, and M. A. Pemberton, "Critical review of the epidemiology literature on the potential cancer risks of methyl methacrylate," *International Archives of Occupational and Environmental Health*, vol. 78, no. 8, pp. 603–612, 2005.

[105] U. J. Schlegel, M. Sturm, V. Ewerbeck, and S. J. Breusch, "Efficacy of vacuum bone cement mixing systems in reducing methylmethacrylate fume exposure: comparison of 7 different mixing devices and handmixing," *Acta Orthopaedica Scandinavica*, vol. 75, no. 5, pp. 559–566, 2004.

[106] A. W. Elmaraghy, B. Humeniuk, G. I. Anderson, E. H. Schemitsch, and R. R. Richards, "The role of methylmethacrylate monomer in the formation and haemodynamic outcome of pulmonary fat emboli," *The Journal of Bone and Joint Surgery—British Volume*, vol. 80, no. 1, pp. 156–161, 1998.

[107] K. Klemm, S. L. Henry, and D. Seligson, "The treatment of infection after interlocking nailing," *Techniques in Orthopaedics*, vol. 3, no. 3, pp. 54–61, 1988.

[108] S. C. Tandon and P. B. M. Thomas, "Persistent osteomyelitis of the femur-2 cases of exchange intramedullary nailing with gentamicin beads in the nail," *Acta Orthopaedica Scandinavica*, vol. 67, no. 6, pp. 620–622, 1996.

[109] K. Anagnostakos and K. Schröder, "Antibiotic-impregnated bone grafts in orthopaedic and trauma surgery: a systematic review of the literature," *International Journal of Biomaterials*, vol. 2012, Article ID 538061, 9 pages, 2012.

[110] T. Fuchs, R. Stange, G. Schmidmaier, and M. J. Raschke, "The use of gentamicin-coated nails in the tibia: preliminary results of a prospective study," *Archives of Orthopaedic and Trauma Surgery*, vol. 131, no. 10, pp. 1419–1425, 2011.

[111] L. Legout and E. Senneville, "Periprosthetic joint infections: clinical and bench research," *The Scientific World Journal*, vol. 2013, Article ID 549091, 17 pages, 2013.

[112] C. G. Zalavras and M. Sirkin, "Treatment of long bone intramedullary infection using the RIA for removal of infected tissue: indications, method and clinical results," *Injury*, vol. 41, no. 2, pp. S43–S47, 2010.

[113] J. C. Carmen, J. L. Nelson, B. L. Beckstead et al., "Ultrasonic-enhanced gentamicin transport through colony biofilms of *Pseudomonas aeruginosa* and *Escherichia coli*," *Journal of Infection and Chemotherapy*, vol. 10, no. 4, pp. 193–199, 2004.

[114] T. Lin, X.-Z. Cai, M.-M. Shi et al., "In vitro and in vivo evaluation of vancomycin-loaded PMMA cement in combination with ultrasound and microbubbles-mediated ultrasound," *BioMed Research International*, vol. 2015, Article ID 309739, 7 pages, 2015.

Hindawi Publishing Corporation
BioMed Research International
Volume 2015, Article ID 362564, 6 pages
http://dx.doi.org/10.1155/2015/362564

Research Article

Twelve-Month Results of a Single or Multiple Dexamethasone Intravitreal Implant for Macular Edema following Uncomplicated Phacoemulsification

Solmaz Abdolrahimzadeh,[1] Vito Fenicia,[2] Maurizio Maurizi Enrici,[2] Pasquale Plateroti,[2] Dora Cianfrone,[2] and Santi Maria Recupero[2]

[1]*Ophthalmology Unit, DAI Testa/Collo, Azienda Policlinico Umberto I, University of Rome "Sapienza", Viale del Policlinico 155, 00161 Rome, Italy*
[2]*Ophthalmology Unit, Sant'Andrea Hospital, NESMOS Department, University of Rome "Sapienza", Via di Grottarossa 1035-1039, 00189 Rome, Italy*

Correspondence should be addressed to Solmaz Abdolrahimzadeh; solmazzadeh@gmail.com

Received 9 January 2015; Accepted 17 February 2015

Academic Editor: Francesco Piraino

The clinical efficacy of one or two intravitreal injections of a continued deliverance dexamethasone 700 μg implant in ten patients with persistent macular edema following uncomplicated phacoemulsification was evaluated. Complete ophthalmological examination and spectral domain optical coherence tomography were carried out. Follow-up was at day 7 and months 1, 2, 4, 6, 8, and 12. At baseline mean best corrected visual acuity was 62 Early Treatment Diabetic Retinopathy Study Chart letters, which showed statistically significant improvement at each follow-up, except at month 6, to reach 79 letters at month 12 ($P = 0.018$). Prior to treatment mean central foveal thickness was 622 μm, which showed statistically significant improvement at each follow-up to reach a mean value of 282 μm ($P = 0.012$) at month 12. Five patients received a second dexamethasone implant at month 7. Two patients were excluded from the study at months 4 and 8. Intraocular pressure remained stable during the study period with the exception of mild increase in two patients requiring topical therapy. In conclusion there was statistically significant improvement of best corrected visual acuity and mean central foveal thickness with one or two intravitreal dexamethasone implants over 12 months.

1. Introduction

Cystoid macular edema (CME) or Irvine-Gass syndrome is the main motive for inauspicious visual acuity achievement following uncomplicated cataract extraction. The incidence of CME after phacoemulsification is reported between 0.1 and 2% [1, 2]. Numerous factors have been held accountable in the pathogenesis of CME but the phenomenon is still poorly understood. However, it has been suggested that macular edema arises due to increased vascular permeability following surgical procedures such as cataract removal and pars plana vitrectomy, which cause the release of prostaglandins and disruption of the blood-retinal barrier [3, 4]. Corticosteroids, nonsteroidal anti-inflammatory agents, and carbonic anhydrase inhibitors have been employed as common treatment procedures [3–5]. Recently, intravitreal administration of antivascular endothelial growth factor agents have also been tested [6]. Treatment is recommended only in patients with clinically significant macular edema, which is considered when visual acuity is 20/40 or less [7]. To date, there is no standard treatment protocol for the management of chronic pseudophakic CME.

Intravitreal pharmacological treatment has the advantage of bypassing the blood-ocular barriers. Furthermore, due to the particular anatomy of the eye, high intravitreal levels of drug can be obtained and the efficacy of treatment can be intensified by drug distribution close to the target site. The dexamethasone implant (Ozurdex, Allergan Inc., Irvine, CA, USA) is an innovative treatment alternative for noninfectious posterior uveitis and macular edema in retinal vein occlusion [8]. Diabetic macular edema and, recently,

prostaglandin-induced CME have also been treated with agreeable results [9–11]. This biodegradable implant measures 6.5 mm × 0.45 mm and is composed of a matrix consisting of a copolymer of lactic and glycolic acids and dexamethasone which dissolves completely into H_2O and CO_2 leaving no remnants. It is injected through the pars plana with a monouse 22-gauge injector and postimplantation sutures are not necessary. It furnishes continued deliverance of dexamethasone where peak doses are supplied for 2 months ensued by a slower release, altogether lasting for 6 months and providing 700 μg of dexamethasone [12].

The use of this implant has been reported in pseudophakic CME with short-term follow-up [13–16]. To our knowledge there are no reports of long-term results and the number of implants necessary in the management of pseudophakic CME. This study was carried out to evaluate the long-term clinical efficacy of the dexamethasone intravitreal implant in patients with persistent CME following uncomplicated phacoemulsification.

2. Materials and Methods

In the present study we assessed 10 patients who were diagnosed with CME due to decreased visual acuity and increase in central foveal thickness (CFT) ensuing unremarkable phacoemulsification. The patients were unresponsive to topical steroids and nonsteroidal anti-inflammatory agents and received treatment with the dexamethasone implant at the Ophthalmology Unit of the St. Andrea Hospital, University of Rome "Sapienza". According to the declaration of Helsinki, at the time of recruitment, informed consent to take part in the study was read and signed by all patients.

Exclusion criteria comprised patients with diabetes, uveitis, or other systemic diseases that could cause ocular involvement, patients who had undergone precedent surgical or parasurgical ocular procedures other than phacoemulsification, vitreomacular traction with epiretinal membrane or macular hole, age-related macular degeneration, retinal vascular pathologies, glaucoma, or elevated IOP. Furthermore, patients were also excluded if they were cortisone responders. Cataract extraction was performed with the divide and conquer technique and in-bag IOL implantation with no complications. Clinically significant CME was classified as visual acuity lower than 20/40 and CFT of more than 250 μm persisting for a period longer than 90 days.

The method was similar to precedent studies on CME (14–16) and the following were carried out for all patients: ophthalmological examination comprising best corrected visual acuity (BCVA) assessment using Early Treatment Diabetic Retinopathy Study (ETDRS) charts, ICare Tonometry [17], and OCT evaluation using spectral domain optical coherence tomography (SD-OCT) evaluation (Cross Line, MM5, 3D Macular, RTVue SD-OCT) with CFT measurement.

The intravitreal dexamethasone implant was injected in the operating theatre through a biplanar intrascleral path with a 22-gauge needle. All patients were then examined at day 7 and months 1, 2, 4, 6, 8, and 12. Patients requiring a second injection of dexamethasone were implanted at month 7.

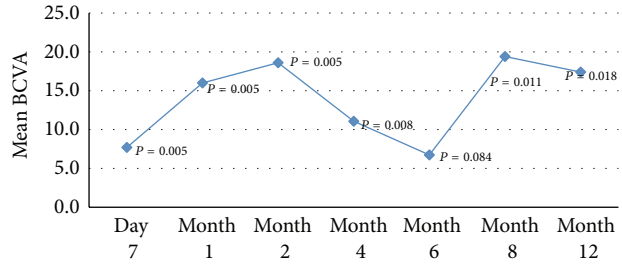

Figure 1: Mean change in best corrected visual acuity (BVCA) from baseline at each follow-up assessment.

2.1. Statistical Analysis. Statistical analysis was carried out with SPSS software package V.21 (SPSS, Inc., Chicago, Illinois, USA). Since the normality of data could not be assumed because of the small sample size, the (nonparametric) Wilcoxon signed-rank test was used to evaluate the differences in the median values of BCVA, CFT, and IOP between baseline and day 7 and months 1, 2, 4, 6, 8, and 12. A P value < 0.05 was considered significant, meaning that the median of the difference (i.e., baseline day 7 or baseline month 6) is not 0.

3. Results

Ten patients with persistent pseudophakic CME who received one or two implants of dexamethasone were selected. The details regarding patient characteristics are given in Table 1. The average persistence of macular edema before dexamethasone implantation was 3.1 months. One patient was excluded from the study due to arterial occlusion at month 4 and a second patient decided to discontinue follow-up at month 8.

Mean BCVA prior to treatment was 62 ETDRS letters. Following implantation, statistically significant improvement in BCVA was detected at day 7 and at each follow-up interval with the exception of month 6. Three patients did not require a second implant. In 5 eyes where visual acuity had declined and foveal thickness had increased, a second implant was injected at month 7. Mean BCVA was 79 ETDRS letters at 12 months ($P = 0.018$) (Table 1, Figure 1).

Prior to treatment the mean CFT was 622 μm; following dexamethasone implantation, statistically significant improvement was seen at day 7 and at each follow-up interval to improve to 282 μm ($P = 0.012$) at 12 months. A second implant was injected at month 7 in 5 patients who showed recurrence (Table 2, Figure 2).

Figure 3 shows optical coherence tomography images of CFT change over time and results of a second implant in one patient with recurrence.

There were two cases of intraocular pressure increase >25 mmHg, which were successfully managed with topical timolol 0.5% and intraocular pressure remained stable during the study period (Table 3).

Table 1: Patient characteristics and best corrected visual acuity (BCVA) values in study eye using ETDRS charts prior to treatment and at follow-up intervals.

Patient	Gender	Age	Baseline	Day 7	Mo. 1	Mo. 2	Mo. 4	Mo. 6	Mo. 8	Mo. 12
1	F	72	78	84	86	87	88	88	88	88
2	F	81	71	73	78	79	80	80	80	80
3[§]	M	78	36	58	70	78	—	—	—	—
4[§]	M	77	35	36	73	78	49	36	—	—
5	F	78	70	71	73	74	76	78	83	84
6[*]	M	81	65	80	83	84	75	66	78	65
7[*]	F	62	72	74	80	83	76	70	80	78
8[*]	F	65	59	60	70	73	68	67	72	74
9[*]	M	71	60	78	80	83	67	62	83	75
10[*]	M	71	70	79	83	83	75	68	84	88
Mean		73.6	61.6	69.3	77.6	80.2	72.7	68.3	81	79
Median		74.5	67.5	73.5	79	81	75	68	81.5	79
SD		6.5	14.9	14.4	5.8	4.5	10.8	14.6	4.8	7.8
Range		62–81	35–78	36–84	70–86	73–87	49–88	36–88	72–88	65–8
P value[†]				**0.005**	**0.005**	**0.005**	**0.008**	0.084	**0.011**	**0.018**
Delta[‡]				7.7	16	18.6	11.1	6.7	19.4	17.4

[*] Patients denoted with ∗ had a second implant at month 7.
[§] Patients dropped out from the study.
[†] *P* value refers to Wilcoxon signed-rank test on the median values with respect to the baseline.
[‡] Delta denotes the mean difference with the baseline.
Mo.: month.

Table 2: Central foveal thickness (CFT) prior to treatment and at follow-up intervals.

Patient	Baseline	Day 7	Mo. 1	Mo. 2	Mo. 4	Mo. 6	Mo. 8	Mo. 12
1	563	349	349	346	345	339	340	346
2	438	381	266	256	250	255	251	248
3[§]	852	361	221	220	—	—	—	—
4[§]	707	395	223	215	260	470	—	—
5	658	263	254	201	213	213	210	215
6[*]	630	312	279	266	295	309	250	369
7[*]	424	297	269	289	268	277	250	261
8[*]	808	397	270	263	278	280	273	268
9[*]	610	369	302	289	285	298	281	303
10[*]	526	331	305	289	290	293	282	249
Mean	621.6	345.5	273.8	263.4	276	303.8	267.1	282.4
Median	620	355	269.5	264.5	278	293	262	264.5
SD	142.2	44.3	38.5	43.4	36.0	71.5	37.5	52.7
Range	424–852	263–397	221–349	201–346	213–345	213–470	210–340	215–369
P value[†]		**0.005**	**0.005**	**0.005**	**0.008**	**0.008**	**0.012**	**0.012**
Delta[‡]		−276	−348	−358	−346	−318	−354	−339

[*] Patients denoted with ∗ had a second implant at month 7.
[§] Patients dropped out from the study.
[†] *P* value refers to Wilcoxon signed-rank test on the median values with respect to the baseline.
[‡] Delta denotes the mean difference with the baseline.
Mo.: month.

4. Discussion

In the present study on CME following uncomplicated phacoemulsification, mean BCVA and CFT improved following one or two injections of intravitreal dexamethasone implants over 12 months of follow-up. A second implant was required in five eyes whereas in three eyes results were maintained after only one implant throughout the follow-up period.

There have been few studies where the results of one intravitreal injection of dexamethasone have been evaluated with short-term follow-up in pseudophakic CME (13–16). Analysis of 8 patients with Irvine-Gass syndrome showed

Table 3: Intraocular pressure (mmHg) prior to treatment and at follow-up intervals.

	Baseline	Day 7	Mo. 1	Mo. 2	Mo. 4	Mo 6	Mo. 8	Mo. 12
1	17	14	14	14	14	14	13	14
2	11	16	13	13	13	13	13	13
3[§]	14	17	16	13	—	—	—	—
4[§]	13	21	21	20	18[t]	14[t]	—	—
5	14	16	12	12	14	13	13	16
6[*]	14	16	14	16	16	18	18	16
7[*]	14	16	20	17[t]	18[t]	15[t]	16[t]	16[t]
8[*]	15	19	19	18	16	15	20	16
9[*]	15	17	16	17	17	16	16	14
10[*]	15	16	17	16	16	17	17	17
Mean	14.2	16.8	16.2	15.6	15.8	15	15.8	16
Median	14	16	16	16	16	15	16	16
SD	1.5	1.9	3.0	2.5	1.8	1.7	2.6	1.4
Range	11–17	14–21	12–21	12–20	13–18	13–18	13–20	13–17
P value[†]		**0.031**	0.120	0.165	0.091	0.228	0.158	0.222
Delta[‡]		2.6	2.0	1.4	1.6	0.8	1.6	1.8

[*] Patients denoted with ∗ had a second implant at month 7.
[§] Patients dropped out from the study.
[†] P value refers to Wilcoxon signed-rank test on the median values with respect to the baseline.
[‡] Delta denotes the mean difference with the baseline.
[t] Patients who were prescribed topical intraocular pressure lowering medication.
Mo.: month.

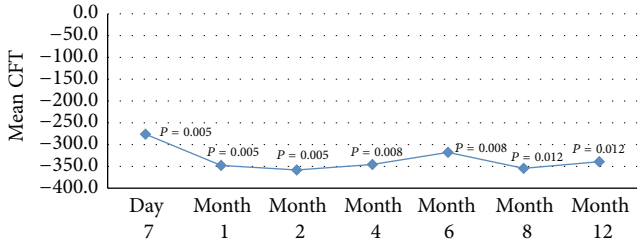

Figure 2: Mean change in central foveal thickness (CFT) from baseline at each follow-up assessment.

improvement of both BCVA and macular edema at 90 days from intravitreal injection of dexamethasone, which was maintained up to 180 days in 54% of eyes [13]. This is similar to our results where 50% of patients required a second implant after 6 months. Furino et al. and Al Zamil analyzed eyes with CME following uncomplicated phacoemulsification with a mean duration of 2.4 and 7.7 months, respectively, where a single injection of dexamethasone was performed and found significant reduction of macular edema and improvement of BCVA at 6 months [15, 16].

Medeiros et al. presented the outcome of a single dexamethasone implant in 9 patients with Irvine-Gass syndrome with a mean duration of 9.1 months. They reported peak effectiveness of the implant at 3 months from treatment and significant amelioration of macular thickness and BCVA during 6 months of follow-up [14]. In our study mean peak improvement of visual acuity was at 2 months following the first implant and at 8 months following the second implant. Mean peak improvement of CFT was at 2 months. Mean BCVA significantly improved at each follow-up except at month 6. According to the pharmacodynamics of the dexamethasone implant, this corresponds to the time when the release of dexamethasone is largely terminated. Nevertheless, at 12 months, following a second implant in 50% of patients, BCVA was significantly improved. As regarding CFT, there was a statistically significant improvement at each follow-up and the trend was more stable with respect to BCVA; however, even here there was a slight increase in CFT at 6 months (304 μm).

Corticosteroids diminish the amount of intraocular prostaglandins and other factors believed to have a role in postoperative CME. In a prospective randomized controlled trial Negi et al. compared topical and periocular corticosteroids following routine cataract surgery and found both safe and effective routes of administration [18]. However, topical and periocular administration have a short half-life and have been reported to reach significant systemic concentrations [19]. Intravitreal injection of triamcinolone acetonide has been demonstrated to produce visual improvement and reduction of CME [20, 21] but the use of triamcinolone is limited due to the requirement of multiple injections and the side effects in terms of increase in intraocular pressure and cataract formation [22], although even with the dexamethasone implant a repeat injection was required in 50% of our cases. While dexamethasone is a more potent corticosteroid, it has a shorter half-life, which restricts its clinical efficacy as an injectable suspension, thus the rationale for an implant with a continued deliverance method, which can provide drug release through long periods with a minor frequency of adverse effects.

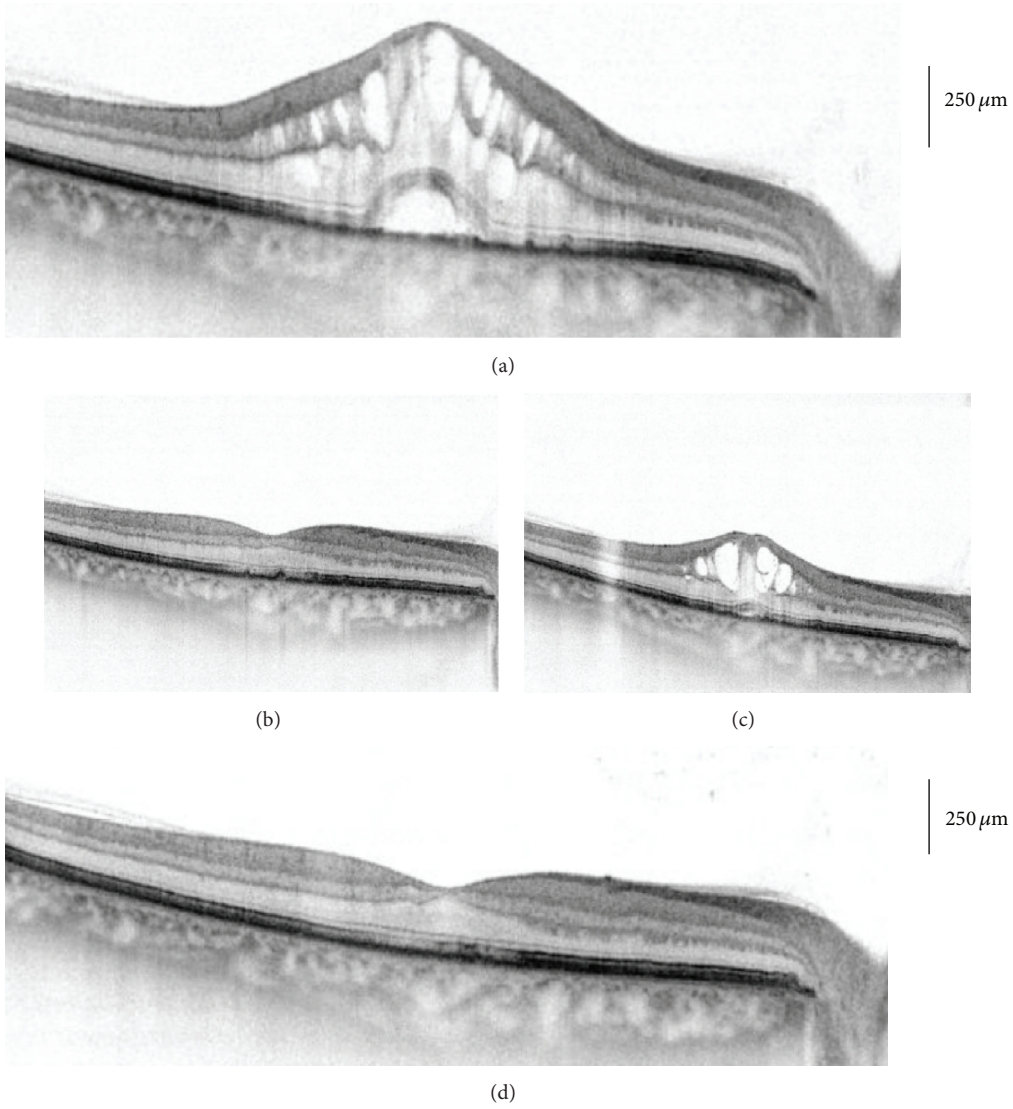

Figure 3: Optical coherence tomography of macular profile and thickness following dexamethasone implant at baseline and 7 months. (a) Before treatment, (b) 2 months following first dexamethasone implant, (c) 6 months following first dexamethasone implant, and (d) 12 months following second dexamethasone implant at month 7.

In two patients there was an increase in IOP > 25 which was successfully managed with topical treatment. This is in agreement with the reported trend following intravitreal dexamethasone administration where IOP is increased in 15% of patients with peak values at 60 days and returns to baseline at 6 months [23]. Patient 3 had retinal artery occlusion at month 4. We cannot be sure of the cause; however, in the judgment of the authors, it is unlikely that there was a reasonable possibility that this serious adverse effect was caused by the dexamethasone implant, the applicator, or the injection procedure. Furthermore, to our knowledge, arterial occlusion has not been reported in large patient population studies, which have also addressed the safety profile of the dexamethasone implant [9, 24]. There were no cases of cataract formation in any patient.

The limitations of our study were the retrospective description, the modest number of eyes, and the absence of a control group. The strength of our study was the long follow-up, which demonstrated the necessity for a second implant after 6 months in 50% of cases.

5. Conclusions

This is the first report on the long-term clinical results of the dexamethasone intravitreal implant in patients presenting CME following phacoemulsification. BCVA and CFT significantly improved at 12 months of follow-up although a second implant was required after 6 months in 50% of cases. Therefore, our studies suggest that single or multiple injections of the dexamethasone implant are an effective treatment option for patients with persistent CME ensuing uncomplicated cataract extraction with phacoemulsification.

Conflict of Interests

The authors declare that there is no conflict of interests regarding the publication of this paper.

Authors' Contribution

Solmaz Abdolrahimzadeh and Vito Fenicia contributed equally.

Acknowledgment

The authors are grateful to Alessia Mammone, Ph.D. in statistics, Centre for Biostatistics and Bioinformatics (CIBB), University of Rome "Tor Vergata", Rome, Italy, for the statistical analysis.

References

[1] S. Ray and D. J. D'Amico, "Pseudophakic cystoid macular edema," *Seminars in Ophthalmology*, vol. 17, no. 3-4, pp. 167–180, 2002.

[2] J. Mentes, T. Erakgun, F. Afrashi, and G. Kerci, "Incidence of cystoid macular edema after uncomplicated phacoemulsification," *Ophthalmologica*, vol. 217, no. 6, pp. 408–412, 2003.

[3] N. R. Benitah and J. G. Arroyo, "Pseudophakic cystoid macular edema," *International Ophthalmology Clinics*, vol. 50, no. 1, pp. 139–153, 2010.

[4] V. Romano, M. Angi, F. Scotti et al., "Inflammation and macular oedema after pars plana vitrectomy," *Mediators of Inflammation*, vol. 2013, Article ID 971758, 8 pages, 2013.

[5] S. Sivaprasad, C. Bunce, and R. Wormald, "Non-steroidal anti-inflammatory agents for cystoid macular oedema following cataract surgery: a systematic review," *British Journal of Ophthalmology*, vol. 89, no. 11, pp. 1420–1422, 2005.

[6] H. N. Shelsta and L. M. Jampol, "Pharmacologic therapy of pseudophakic cystoid macular edema: 2010 update," *Retina*, vol. 31, no. 1, pp. 4–12, 2011.

[7] M. Gharbiya, F. Cruciani, G. Cuozzo, F. Parisi, P. Russo, and S. Abdolrahimzadeh, "Macular thickness changes evaluated with spectral domain optical coherence tomography after uncomplicated phacoemulsification," *Eye*, vol. 27, no. 5, pp. 605–611, 2013.

[8] S. S. Lee, P. Hughes, A. D. Ross, and M. R. Robinson, "Biodegradable implants for sustained drug release in the eye," *Pharmaceutical Research*, vol. 27, no. 10, pp. 2043–2053, 2010.

[9] D. S. Boyer, Y. H. Yoon, R. Belfort Jr. et al., "Three-year, randomized, sham-controlled trial of dexamethasone intravitreal implant in patients with diabetic macular edema," *Ophthalmology*, vol. 121, pp. 1904–1914, 2014.

[10] J. A. Haller, B. D. Kuppermann, M. S. Blumenkranz et al., "Randomized controlled trial of an intravitreous dexamethasone drug delivery system in patients with diabetic macular edema," *Archives of Ophthalmology*, vol. 128, no. 3, pp. 289–296, 2010.

[11] M. Sacchi, E. Villani, F. Gilardoni, and P. Nucci, "Efficacy of intravitreal dexamethasone implant for prostaglandin-induced refractory pseudophakic cystoid macular edema: case report and review of the literature," *Clinical Ophthalmology*, vol. 8, pp. 1253–1257, 2014.

[12] A. Lambiase, S. Abdolrahimzadeh, and S. M. Recupero, "An update on intravitreal implants in use for eye disorders," *Drugs of Today*, vol. 50, no. 3, pp. 239–249, 2014.

[13] G. A. Williams, J. A. Haller, B. D. Kuppermann et al., "Dexamethasone posterior-segment drug delivery system in the treatment of macular edema resulting from uveitis or Irvine-Gass syndrome," *The American Journal of Ophthalmology*, vol. 147, no. 6, pp. 1048–1054, 2009.

[14] M. D. Medeiros, R. Navarro, J. Garcia-Arumí, C. Mateo, and B. Corcóstegui, "Dexamethasone intravitreal implant for treatment of patients with recalcitrant macular edema resulting from Irvine-Gass syndrome," *Investigative Ophthalmology and Visual Science*, vol. 54, no. 5, pp. 3320–3324, 2013.

[15] C. Furino, F. Boscia, N. Recchimurzo, C. Sborgia, and G. Alessio, "Intravitreal dexamethasone implant for macular edema following uncomplicated phacoemulsification," *European Journal of Ophthalmology*, vol. 24, no. 3, pp. 387–391, 2014.

[16] W. M. Al Zamil, "Short-term safety and efficacy of intravitreal 0.7-mg dexamethasone implants for pseudophakic cystoid macular edema," *Saudi Journal of Ophthalmology*, 2014.

[17] G. L. Scuderi, N. C. Cascone, F. Regine, A. Perdicchi, A. Cerulli, and S. M. Recupero, "Validity and limits of the rebound tonometer (ICare): clinical study," *European Journal of Ophthalmology*, vol. 21, no. 3, pp. 251–257, 2011.

[18] A. K. Negi, A. C. Browning, and S. A. Vernon, "Single perioperative triamcinolone injection versus standard postoperative steroid drops after uneventful phacoemulsification surgery: randomized controlled trial," *Journal of Cataract and Refractive Surgery*, vol. 32, no. 3, pp. 468–474, 2006.

[19] O. Weijtens, F. A. Van der Sluijs, R. C. Schoemaker et al., "Peribulbar corticosteroid injection: vitreal and serum concentrations after dexamethasone disodium phosphate injection," *The American Journal of Ophthalmology*, vol. 123, no. 3, pp. 358–363, 1997.

[20] M. D. Conway, C. Canakis, C. Livir-Rallatos, and G. A. Peyman, "Intravitreal triamcinolone acetonide for refractory chronic pseudophakic cystoid macular edema," *Journal of Cataract and Refractive Surgery*, vol. 29, no. 1, pp. 27–33, 2003.

[21] C. Koutsandrea, M. M. Moschos, D. Brouzas, E. Loukianou, and M. Apostolopoulos, "Intraocular triamcinolone acetonide for pseudophakic cystoid macular edema: optical coherence tomography and multifocal electroretinography study," *Retina*, vol. 27, no. 2, pp. 159–164, 2007.

[22] A. Sallam, S. R. J. Taylor, Z. Habot-Wilner et al., "Repeat intravitreal triamcinolone acetonide injections in uveitic macular oedema," *Acta Ophthalmologica*, vol. 90, no. 4, pp. e323–e325, 2012.

[23] W. Kiddee, G. E. Trope, L. Sheng et al., "Intraocular pressure monitoring post intravitreal steroids: a systematic review," *Survey of Ophthalmology*, vol. 58, no. 4, pp. 291–310, 2013.

[24] J. A. Haller, F. Bandello, R. Belfort Jr. et al., "Randomized, sham-controlled trial of dexamethasone intravitreal implant in patients with macular edema due to retinal vein occlusion," *Ophthalmology*, vol. 117, no. 6, pp. 1134–1146, 2010.

Hindawi Publishing Corporation
BioMed Research International
Volume 2015, Article ID 730105, 14 pages
http://dx.doi.org/10.1155/2015/730105

Research Article

A Comparison of the Process of Remodeling of Hydroxyapatite/Poly-D/L-Lactide and Beta-Tricalcium Phosphate in a Loading Site

Hiroyuki Akagi,[1] Hiroki Ochi,[2] Satoshi Soeta,[3] Nobuo Kanno,[1] Megumi Yoshihara,[4] Kenshi Okazaki,[4] Takuya Yogo,[1] Yasuji Harada,[1] Hajime Amasaki,[3] and Yasushi Hara[1]

[1]*Division of Veterinary Surgery, Department of Veterinary Science, Faculty of Veterinary Medicine, Nippon Veterinary and Life Science University, 1-7-1 Musashino, Tokyo 180-8602, Japan*
[2]*Division of Veterinary Microbiology, Department of Veterinary Science, Faculty of Veterinary Medicine, Nippon Veterinary and Life Science University, 1-7-1 Musashino, Tokyo 180-8602, Japan*
[3]*Division of Veterinary Anatomy, Department of Veterinary Science, Faculty of Veterinary Medicine, Nippon Veterinary and Life Science University, 1-7-1 Musashino, Tokyo 180-8602, Japan*
[4]*Medical Research Group, Development Department, Takiron Co., Ltd., 7-1-19, Minatojima Minamimachi, Chuo-ku, Kobe 650-0047, Japan*

Correspondence should be addressed to Hiroyuki Akagi; hiroyuki-akagi@hotmail.co.jp

Received 28 January 2015; Revised 9 May 2015; Accepted 18 May 2015

Academic Editor: Francesco Piraino

Currently, the most commonly used bioresorbable scaffold is made of beta-tricalcium phosphate (β-TCP); it is hoped that scaffolds made of a mixture of hydroxyapatite (HA) and poly-D/L-lactide (PDLLA) will be able to act as novel bioresorbable scaffolds. The aim of this study was to evaluate the utility of a HA/PDLLA scaffold compared to β-TCP, at a loading site. Dogs underwent surgery to replace a section of tibial bone with a bioresorbable scaffold. After the follow-up period, the scaffold was subjected to histological analysis. The HA/PDLLA scaffold showed similar bone formation and superior cell and tissue infiltration compared to the β-TCP scaffold, as seen after Villanueva Goldner staining. Moreover, silver staining and immunohistochemistry for Von Willebrand factor and cathepsin K demonstrated better cell infiltration in the HA/PDLLA scaffold. The fibrous tissue and cells that had infiltrated into the HA/PDLLA scaffold tested positive for collagen type I and RUNX2, respectively, indicating that the tissue and cells that had infiltrated into the HA/PDLLA scaffold had the potential to differentiate into bone. The HA/PDLLA scaffold is therefore likely to find clinical application as a new bioresorbable scaffold.

1. Introduction

In the field of veterinary orthopedics, bone transplantation has been generally applied for the large bone defect associated with the surgery for bone tumors, trauma, or infection. Bone grafts include autografts, allografts, demineralized bone matrix, and bioresorbable scaffolds. Autografts have been the gold standard of bone grafting, because of the superior osteoconductivity and osteoinductivity achieved, although retrieving autograft tissue causes pain at the surgical site and poses an infectious risk, and there are limits to the amount of material that can be retrieved. Thus, the development of an ideal bioresorbable scaffold has been an ongoing focus in orthopedic surgery.

From the 1980s, researches for development of bioresorbable scaffolds which have osteoconductive, osteoinductive, and bioresorptive properties have advanced [1]. Recently, an artificial bone, constructed from calcium phosphate and bioresorbable polymers, has been developed and applied in the regeneration of bone and cartilage [2–5].

One new form of porous artificial bone is mainly composed of hydroxyapatite (HA) and β-tricalcium phosphate (β-TCP). These porous scaffolds are highly biocompatible and show good osteoconductivity [6]. On the other hand,

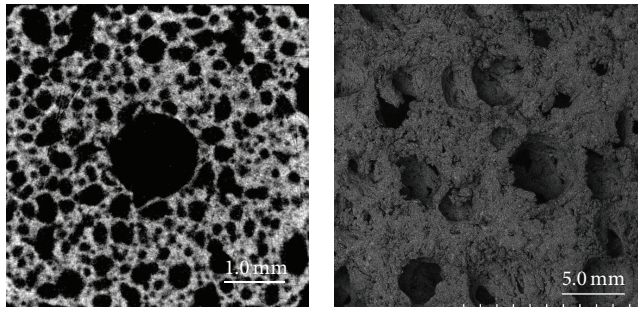

(a) (b)

Figure 1: Images of micro-CT and scanning electron microscope (SEM). (a) The micro-CT image of HA/PDLLA scaffold. (b) The SEM image of HA/PDLLA scaffold.

porous scaffolds take a long time to be absorbed, and some of them demonstrate low osteoinductive properties [7]. In general, HA has superior biocompatibility compared to β-TCP but shows delayed resorption *in vivo* [8].

Polyglycolic acid (PGA) and polylactic acid (PLA) are typical bioresorbable polymers. These bioresorbable polymers can be used in various shapes, like rods, pins, plates, and screws [9]. In clinical cases, osteosynthetic implants made of PLA and PGA have been used for the treatment of fractures at various sites, such as the femoral head, the condyle of the femur, the condyle of the humerus, and the carpal bone [10]. However, these bioresorbable polymers generally show low bioactivity, and the rate of resorption tends to be dependent on the capacity of the material [6, 11].

After 2000, new bioresorbable scaffolds, composed of a combination of calcium phosphate and bioresorbable polymers, have been developed, in order to utilize the advantages of both types of materials and to compensate for their drawbacks [12, 13]. The aim of this combination was to achieve appropriate structural strength and direct union with the host bone and to match the processes of regeneration of bone and scaffold resorption. We previously reported that HA/poly-L-lactide (PLLA) achieved complete remodeling into cortical bone, but that this was not the case with PLLA only [14]. Shikinami et al. and Sai and Fujii reported that HA/poly-L/D-lactide (PDLLA), containing 70 wt% unsintered-HA particles in 30 wt% PDLLA, demonstrated superior biocompatibility and good bioresorption in the medullary cavity of the rabbit [15, 16]. The HA/PDLLA scaffold demonstrated good remodeling at an unloaded site, but the remodeling process at a loaded site was not then investigated.

The aim of this study was to evaluate the usefulness of the HA/PDLLA scaffold in a loaded site, by analyzing the remodeling process in comparison to that achieved with a β-TCP scaffold.

2. Material and Methods

2.1. Bioresorbable Scaffold. The HA/PDLLA scaffold was composed of 70 wt% unsintered HA and 30 wt% PDLLA (Mv: 77 kDa; D/L: 50/50 mol%) matrix and was prepared by hot-compression moulding of nonwoven composite fibers. Manufacturing involved the scaffold fiber precipitation method, following the report by Shikinami et al. [15]. The HA/PDLLA scaffold (Comporus: Takiron, Osaka, Japan) had 70% porosity, a 40–480 μm (average: 170 μm) interconnected pore size, and 4.1 ± 0.4 MPa compressive strength [15]. The structure of the HA/PDLLA scaffold, identified using scanning electron microscope (SEM) and micro-CT, was shown in Figure 1. The control material, that is, the β-TCP scaffold (Osferion60; Olympus Terumo Biomaterials, Tokyo, Japan) had 60% porosity, 10 MPa compressive strength, and 100–165 μm pore size. Both biomaterial scaffolds were prepared to a cuboid of size 10 × 10 × 15 mm, and the center area had a 3.0 mm hole.

2.2. Animals. Nine healthy male beagles were included in the study. All dogs were 11.4 ± 0.5 (mean ± SD) months of age at the beginning of the experiment and their average weight was 9.6 ± 0.9 kg. Surgical treatment and postoperative management of the dogs were performed in accordance with the Guidelines for Care and Use of Laboratory Animals of the Nippon Veterinary and Life Science University. Dogs were randomly divided into three groups: 1-, 3-, and 12-month group, with three dogs per group.

2.3. Surgical Treatment. The dogs received preanesthetic injections of droperidol (0.25 mg/kg, i.m.), and general anesthesia was induced with propofol (7 mg/kg, i.v.). Each dog was intratracheally intubated, and anesthesia was maintained with isoflurane and oxygen. All anesthetized dogs received epidural injections of buprenorphine hydrochloride (5 μg/kg) and bupivacaine hydrochloride (0.5 mg/kg). A surgical approach was made via the right medial side to expose the tibial diaphysis. The tibial length was measured prior to the operation; a 15-mm region of the central tibia was removed using an oscillating bone saw. A bridging plate fixation was applied using an 81 mm 9-hole locking compression plate (Synthes, SE) and φ 2.7 mm × 16 mm locking head screws (Synthes), using three screws to each of the proximal and distal region of the tibia (Figure 2(a)). Thereafter, the HA/PDLLA scaffold was inserted into the space (HP group;

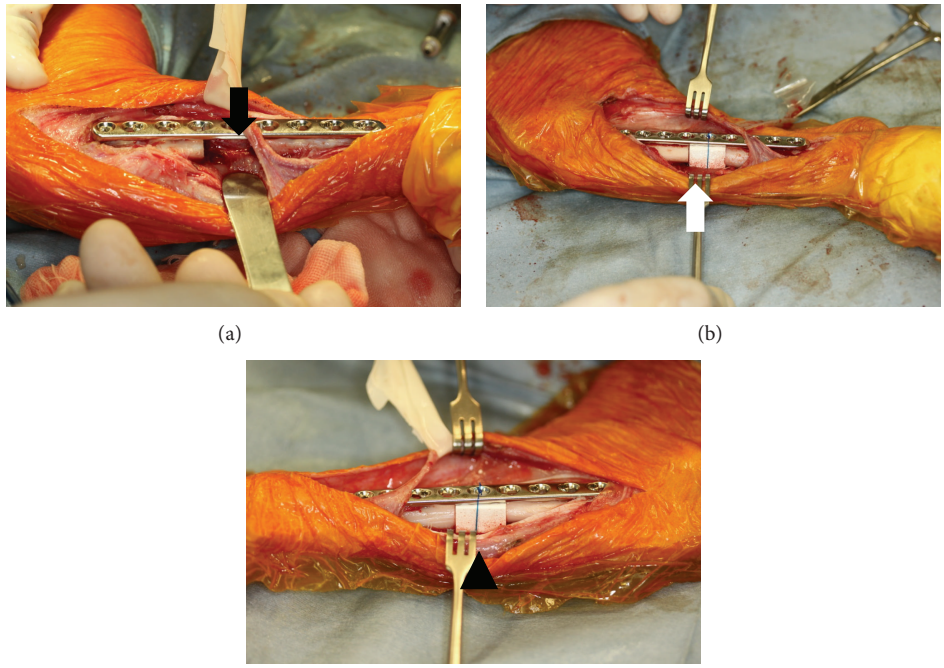

(a) (b)

(c)

Figure 2: Images of surgery. (a) The central region of the tibia was removed using an oscillating bone saw (black arrow). (b) The HA/PDLLA composite was inserted into the space created (white arrow). (c) The β-TCP composite was inserted into the space created (black arrow head).

Figure 2(b)). The wound was closed routinely. The same procedure was used to implant a β-TCP scaffold into the left limb (TCP group; Figure 2(c)).

Animals were treated using a Robert–Jones bandage up to 14 days, with limited physical activity. Postoperative analgesic management was achieved by administration of buprenorphine (0.02 mg/kg, i.m.; q 12 h) for 14 days. Each dog received cefamezin (25 mg/kg, p.o., q 12 h) for 14 days after the operation. Animals were kept in a cage to rest during the follow-up period. Dogs were euthanized via administration of an overdose of sodium pentobarbital after the indicated time.

2.4. Radiographic Analysis. Craniocaudal radiographics were obtained at 1, 3, 6, 9, and 12 months. Radiographic analysis was conducted to assess the union of the bioresorbable scaffold and host bone, and the condition of the scaffold and the fixation system.

2.5. $Ca_2(PO_4)_3$ Content. After euthanasia, all plates and screws were removed, and computed tomography (CT; Asteion, Toshiba Medical Systems Corporation, Tokyo, Japan) imaging performed. CT images of the full length of the tibia were obtained at 120 kV, 100 mA, and with 1.0 mm slice thickness, in a prone position. The DICOM data was retrieved to commercial image analysis software (Image J analysis software; NIH, Bethesda, MD). While obtaining CT images, standard bone mineral phantom (B-MAS 200, Kyoto Kagaku, Japan) was used to measure the CT value of both scaffolds. The $Ca_2(PO_4)_3$ content was measured at the axial site of the central portion of the scaffold.

2.6. Histological Analysis. After CT analysis, both tibias of each dog were retrieved and fixed using 10% neutral buffered formalin for 7 days. A sample was cut at the axial center, and the proximal portion was decalcified with 10% EDTA. Thereafter, each specimen was embedded in paraffin. The central plane of the specimens was sectioned parallel to the sagittal plane at a thickness of 5 μm, and stained hematoxylin and eosin (HE), and silver impregnation. The sections were randomly chosen and stained according to following protocol.

The distal portion was dehydrated in serial concentrations of ethanol (30, 50, 70, 80, 90, and 100% v/v; 2 days per concentration) and then embedded in LR White resin (London Resin Company Ltd., London, UK). The specimens were sectioned using a band saw (BS-300CP, EXAKT Apparatebau GmbH) parallel to the sagittal plane of the sample. Then, the surface of specimens was polished with diamond paper (MG-4000, EXAKT Apparatebau GmbH) and subjected to Villanueva Goldner (VG) staining, which was then observed under a light microscope.

2.7. Immunohistochemistry Staining

2.7.1. Collagen Type 1 (COL1). The proximal section of HA/PDLLA scaffolds and β-TCP scaffolds were cut into 5 μm thick sections. The sections were stained with a polyclonal rat-anti-rabbit-COL1 (1 : 5000, Cosmo Bio, Tokyo, Japan)

followed by a rabbit IgG antibody (CosmoBio), which served as secondary antibody. The complex was detected using 3,3′-diaminobenzidine, tetrahydrochloride (DAB; DAKO, Glostrup, Denmark).

2.7.2. Von Willebrand (VW) Factor. The sections were stained with a polyclonal rat-anti-rabbit-VW factor (1 : 2000, Cosmo Bio) followed by anti-rabbit IgG antibody (Cosmo Bio), which served as secondary antibody. The complex was detected using DAB (DAKO).

2.7.3. Cathepsin K. The sections were stained with a polyclonal human anti-goat cathepsin K antibody (1 : 300, Santa Cruz Biotechnology, Santa Cruz, CA) followed by anti-goat IgG antibody (Nichirei Biosciences, Inc., Tokyo Japan), as secondary antibody. The complex was detected using DAB (DAKO).

2.7.4. RUNX2. The sections were stained with a polyclonal human anti-goat RUNX2 antibody (1 : 100, Santa Cruz Biotechnology), followed by anti-goat IgG antibody (Nichirei Biosciences, Inc.), as secondary antibody. The complex was detected using DAB (DAKO).

2.8. Qualitative and Quantitative Analysis. Qualitative and quantitative analysis was conducted as detailed in Table 1. Each image was taken using a BX51 microscope (Olympus, Tokyo, Japan) and saved as TIFF files. The images were analyzed using image J software (NIH, Bethesda, MD).

2.9. Statistical Analysis. Differences between HA/PDLLA and β-TCP were analyzed using the Mann-Whitney test. The temporal change in each scaffold was analyzed using Tukey's honestly significant difference test. These tests were performed using SPSS statistical software (SPSS, Japan Inc., Tokyo, Japan). Differences were considered significant at values of $p < 0.05$.

Table 1: Qualitative and quantitative analysis method.

Staining method	Magnification	Number of views	Aim
Silver impregnation	40	6	Area of fibrous tissue
COL 1	100	1	Identifying the fibrous tissue
Von Willebrand	100	10	Number of vessel cavities
Cathepsin K	200	10	Number of osteoclast-like cells
Runx2	200	10	Number of positive cells
VG staining	20	2	Bone, residual composite, osteoid

3. Results

3.1. Radiographic Analysis. Figure 3 shows the craniocaudal view of specimens, showing temporal radiographic changes. In the craniocaudal view, the TCP group indicated higher radiopacity compared to the HP group. At the 9-month follow-up, the border between the scaffold and host bone was unclear in the HP group (Figure 3(k)), indicating the continuousness of the HA/PDLLA scaffold and host bone; in contrast, the borders of the site and host bone could still be clearly seen at 12 months (Figure 3(l)).

3.2. $Ca_3(PO_4)_2$ Content. The differences in $Ca_3(PO_4)_2$ content are shown in Figure 4. The 12-month HP group indicated a significantly higher $Ca_3(PO_4)_2$ content compared to the 1- and 3-month groups. The 12-month TCP group had a significantly lower $Ca_3(PO_4)_2$ content compared to the 1- and 3-month TCP groups; the TCP groups also demonstrated a significantly higher $Ca_3(PO_4)_2$ content compared to the HP group at 1 and 3 months. However, the TCP and HA groups were not significantly different at 12 months.

3.3. Histological Analysis. HE stained specimens are shown in Figure 5. At low magnification, the HP and TCP groups demonstrated the same level of bone formation, although the HP group showed earlier scaffold hydrolyzed than absorbed the TCP group. Moreover, the process of remodeling was observed to be markedly different between the HP group and the TCP group. Specifically, the HP group demonstrated significant fibrous tissue infiltration, whereas the TCP group did not.

3.4. Area of Bone Formation, Residual Scaffold, and Osteoid Tissue. The areas representing bone formation (Figure 6(g)), residual scaffold (Figure 6(h)), and osteoid tissue (Figure 6(i)) was measured in specimens after VG staining. Both scaffolds indicated bone formation; in particular, the bone formation was significantly increased between 3 months and 12 months (Figure 6(g)). Both scaffolds indicated a lowering in the residual scaffold material over time; again, the residual scaffold was significantly reduced between 3 and 12 months (Figure 6(h)), with the HP group showing a significantly smaller area of residual scaffold than did the TCP group during the follow-up period. Both groups showed little osteoid tissue formation at 1 and 3 months, although both groups showed a significantly higher level of osteoid formation at 12 months (Figure 6(i)).

3.5. Fibrous Tissue. Specimens that had been stained by silver impregnation are shown in Figures 7(a)–7(f). The fibrous tissue areas are represented in Figure 7(g). There was little fibrous tissue infiltration in the TCP group (Figures 7(a), 7(c), and 7(e)), but the HP group showed greater infiltration of fibrous tissue (Figures 7(b), 7(d), and 7(f)). More specifically, there was less fibrous tissue infiltration in the caudal side compared to the cranial side (data not shown). There was a significant difference between the HA group and the TCP group during the follow-up period; the HP group showed a significant reduction in fibrous tissue infiltration over time.

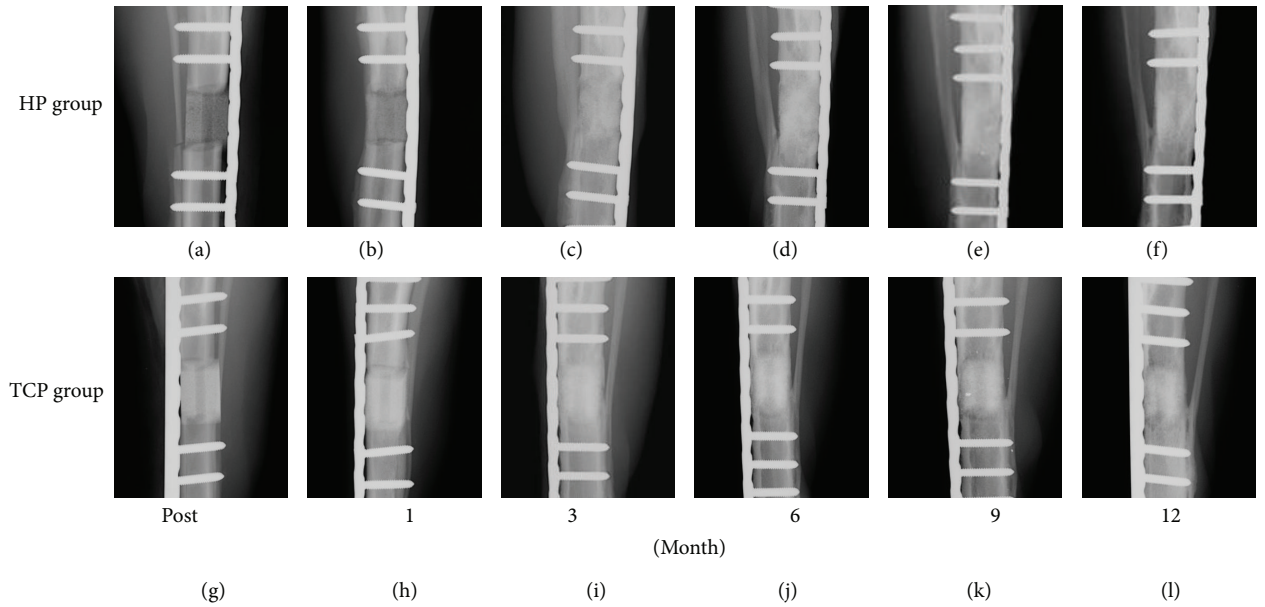

Figure 3: Craniocaudal view of the bioresorbable scaffold. ((a)–(f)) HP group. ((g)–(l)) TCP group. ((a), (g)) Postsurgery. ((b), (h)) 1 month. ((c), (i)) 3 months. ((d), (j)) 6 months, ((e), (k)) 9 months, and ((f), (l)) 12 months. Fibula fractures were found in six dogs, including three limbs in the TCP group and five limbs in the HP group, at 1- to 3-month follow-up. After 3 months, no fractures or refractures were observed. No fractures or displacement of the scaffold or fixation was seen.

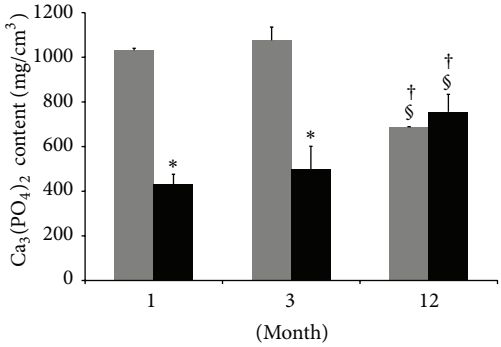

Figure 4: $Ca_3(PO_4)_2$ content of the specimens. β-TCP (grey box), HA/PDLLA (black box). The 12-month HP group indicated a significantly higher $Ca_3(PO_4)_2$ content compared to the 1- and 3-month groups. The 12-month TCP group had a significantly lower $Ca_3(PO_4)_2$ content compared to the 1- and 3-month TCP groups; the TCP group also demonstrated a significantly higher $Ca_3(PO_4)_2$ content compared to the HP group at 1 and 3 months. However, the TCP and HA groups were not significantly different at 12 months. $*$: $p < 0.05$ versus TCP group. †: $p < 0.05$ versus 1 month. §: $p < 0.05$ versus 3 months.

3.6. COL1. Specimens that had been stained for COL1 by immunohistochemistry are shown in Figures 8(a)–8(f). Most of the infiltrated tissue in the bioresorbable scaffolds was positive for COL1. As the TCP group did not show much fibrous tissue infiltration, there was little COL1-positive tissue in this group. In contrast, as the HP group demonstrated markedly more fibrous tissue infiltration, this group also showed more COL1-positive tissue. Specifically, the 1- and 3-month HP groups showed markedly more fibrous tissue infiltration, which was also positive for COL1 (Figures 8(b) and 8(d)).

3.7. Vessel Cavity Measurement. Figures 9(a)–9(f) show specimens stained for VW factor by immunohistochemistry. The number of vessel cavities positive for VW factor is shown in Figure 9(g). The HP groups showed a significantly higher number of vessel cavities than did the TCP groups during the follow-up period. Particularly, the 1-month HP group showed a markedly higher number of vessel cavities than did the 3- and 12-month HP groups. The TCP groups showed a significantly higher number of vessel cavities at 3 months compared to that at 1 month; however, this number decreased significantly by 12 months.

3.8. Osteoclast-Like Cells. Cathepsin K-positive specimens are shown in Figures 10(a)–10(f), and the results of measurement of the positive regions are shown in Figure 10(g). The HP group showed significantly more cathepsin K-positive

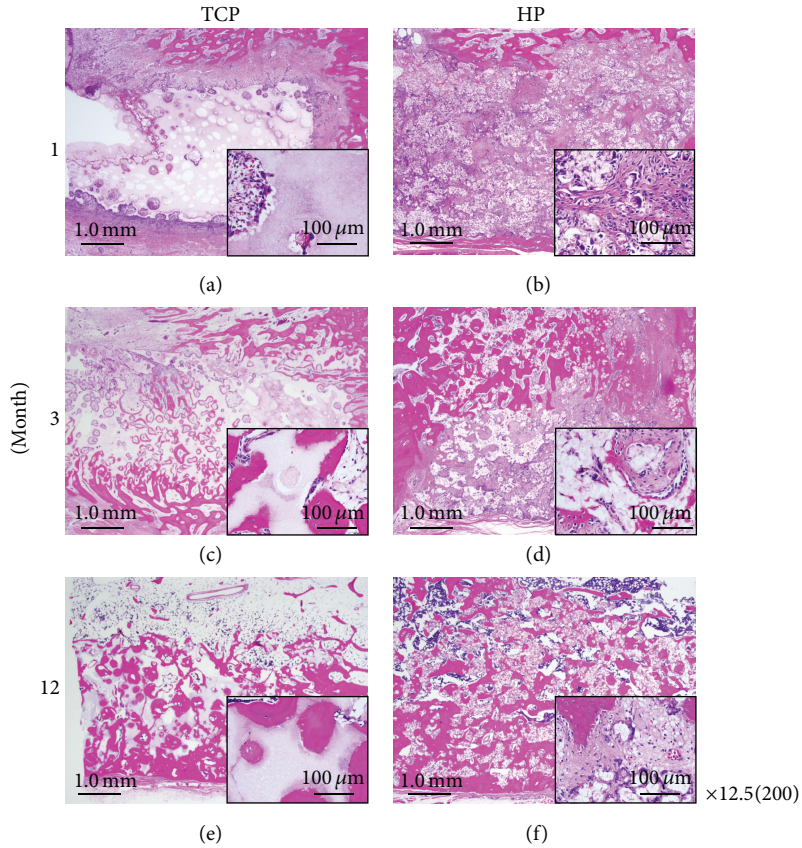

Figure 5: Tissue sections were stained with hematoxylin and eosin and viewed at ×12.5 and ×200 (insets) magnification. ((a), (c), and (e)) TCP group. ((b), (d), and (f)) HP group. ((a), (b)) 1 month. ((c), (d)) 3 months. ((e), (f)) 12 months. The HP group and TCP group showed the same level of bone formation. The HP group showed earlier scaffold resorption than did the TCP group. The process of remodeling was observed to be markedly different between the HP group and the TCP group. In particular, the HP group demonstrated significant fibrous tissue infiltration, whereas the TCP group did not. Scale bars: 1.0 mm and 100 μm.

cells than the TCP group during the follow-up period. In the HP group, the positive cells reduced significantly over time. In the TCP group, the 3-month group showed significantly more cathepsin K-positive cells compared to the 1- and 12-month groups.

3.9. RUNX2. The RUNX2-positive specimens are shown in Figures 11(a)–11(f) and the results of measurement of the corresponding areas are shown in Figure 11(g). Most of the spindle-shaped cells that were often observed in the HP group were positive for RUNX2. The HP group showed significantly more RUNX2-positive cells compared to the TCP group during the follow-up period. In the HP group, specimens at 1 and 3 months demonstrated significantly more RUNX2-positive cells compared to the 12-month group. In the TCP group, the 3-month group showed significantly more RUNX2-positive cells than did the 1- and 12-month groups.

4. Discussion

The aim of this study was to evaluate the usefulness of the HA/PDLLA scaffold compared to β-TCP scaffold, which is currently considered the most popular bioresorbable scaffold. The β-TCP scaffold has been reported to have superior osteoinduction and osteoconduction [16, 17]. Cutright et al. previously reported that implantation of β-TCP scaffold into rat tibia resulted in 95% of the scaffold being absorbed and formation of a medullary cavity after 48 days [18]. These results indicated that the β-TCP scaffold demonstrates good bioresorptive qualities, although the TCP group retained a clear scaffold form during the follow-up period. This is influenced by the scaffold porosity and pore size [19]. On the other hand, in our study, the border between the HA/PDLLA scaffold and host bone was not recognizable by 9 months. Examination of β-TCP scaffold implanted into rabbit femur resulted in a gradual increase in radiolucency [20]. In our study, the radiolucency gradually decreased, until the radiolucency of the β-TCP scaffold and the host bone was similar at 9 months. Differences in the species and examination procedures used may be responsible for differences in each result. However, obtaining equal radiolucency with the host cortical bone was a common result between previous reports and this study.

Upon histological analysis, the HP group and the TCP group indicated equal bone formation. Although the feature

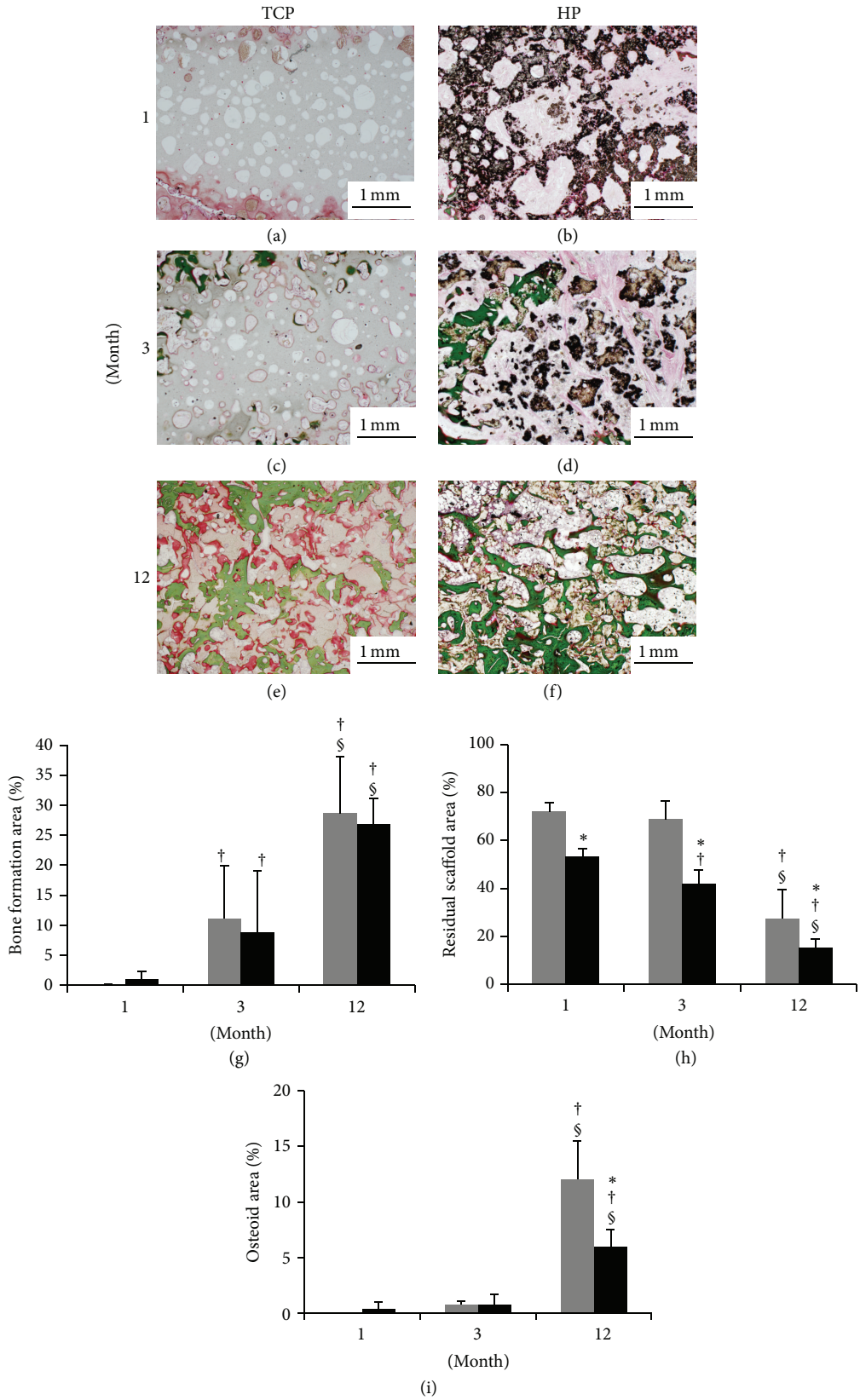

Figure 6: Tissue sections were stained with Villanueva Goldner (VG) stain and viewed at ×20 magnification. ((a), (c), and (e)) TCP group. ((b), (d), and (f)) HP group. ((a), (b)) 1 month. ((c), (d)) 3 months. ((e), (f)) 12 months. (g) Area of bone formation. (h) Area of residual composite. (i) Area of osteoid formation. β-TCP (grey box), HA/PDLLA (black box). (g) The HP and TCP groups showed the same level of bone formation, and both groups showed significant increases of bone formation over time. (h) The HP group represented superior scaffold resorption. (i) Both groups demonstrated a low level of osteoid formation at 1 and 3 months, although both groups showed significantly higher osteoid formation at 12 months. $*$: $p < 0.05$ versus TCP group. †: $p < 0.05$ versus 1 month. §: $p < 0.05$ versus 3 months. Scale bars: 1.0 mm.

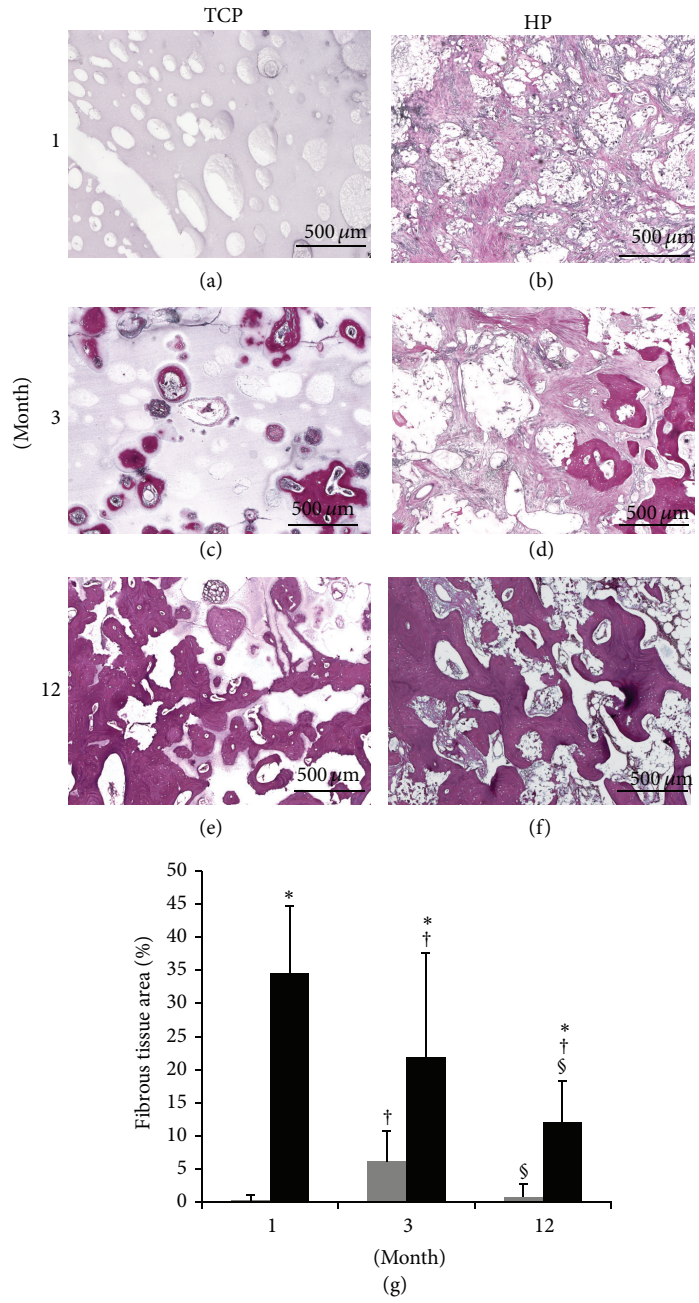

Figure 7: Tissue sections were stained by silver impregnation and observed at ×40 magnification. ((a), (c), and (e)) TCP group. ((b), (d), and (f)) HP group. ((a), (b)) 1 month. ((c), (d)) 3 months. ((e), (f)) 12 months. (g) Measurements of the infiltrated fibrous tissue. β-TCP (grey box), HA/PDLLA (black box). (g) The TCP group showed little fibrous tissue infiltration during the follow-up period. On the other hand, the HP group showed a stronger fibrous tissue infiltration than did the TCP group. $*$: $p < 0.05$ versus TCP group. †: $p < 0.05$ versus 1 month. §: $p < 0.05$ versus 3 months. Scale bars: 500 μm.

of bone formation were different between HA/PDLLA scaffold and β-TCP scaffold, the HP group showed significantly less residual scaffold than did the TCP group. Moreover, the HA/PDLLA scaffold indicated superior utility compared to the TCP scaffold. The HP group showed strong fibrous tissue infiltration, while the TCP group showed little fibrous tissue infiltration. These results indicated a difference in the remodeling process between the HA/PDLLA scaffold and β-TCP scaffold. In a study in which β-TCP scaffold was implanted into the canine dorsal region, the pattern of bone formation suggested intramembrane ossification [21]. In this study, the results obtained using the β-TCP scaffolds indicated slight fibrous tissue infiltration and significant osteoid tissue formation at 12 months. Thus, the remodeling

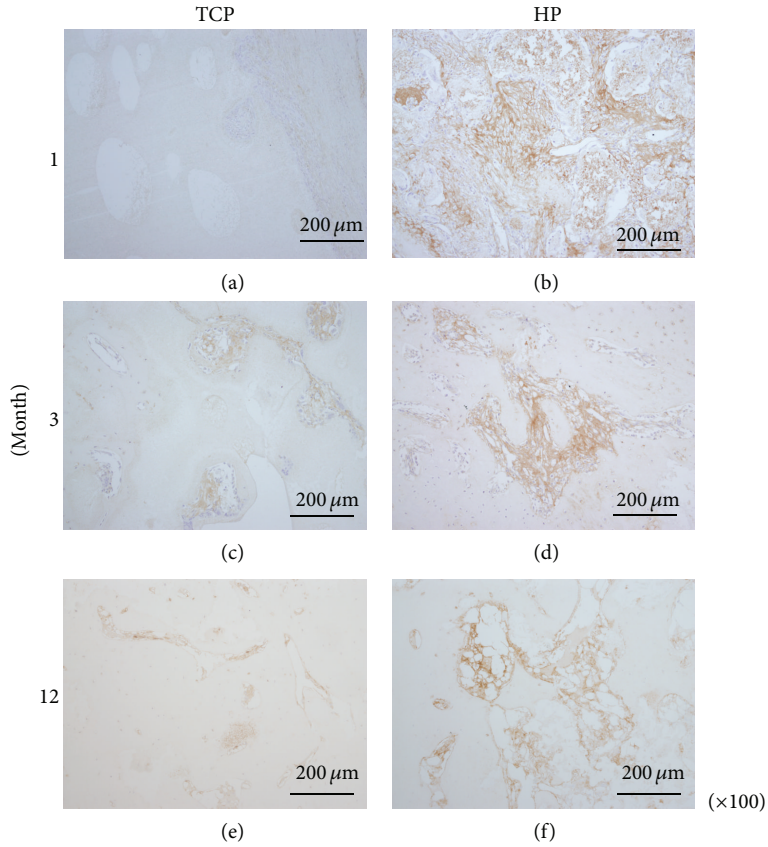

Figure 8: Tissue sections were stained for COL 1 and observed at ×200 magnification. ((a), (c), and (e)) TCP group. ((b), (d), and (f)) HP group. ((a), (b)) 1 month. ((c), (d)) 3 months. ((e), (f)) 12 months. Most of the infiltrated fibrous tissue in the bioresorbable scaffolds was positive for COL1. The HP groups showed COL1-positive tissue infiltration; particularly, the 1- and 3-month HP groups showed marked COL1-positive tissue infiltration. On the other hand, the TCP groups did not show much fibrous tissue infiltration. Scale bars: 200 μm.

process observed in this study was likely to involve intramembrane ossification. On the other hand, the HP group showed marked fibrous tissue infiltration, which gradually became calcified.

The VW factor is specifically expressed in vascular endothelial cells [22, 23]. Vessel formation plays an important role in both endochondral ossification and intramembrane ossification and for delivery of some cytokines, oxygen, nutrition, and various cells from the host site to the site of the bioresorbable scaffold [24, 25]. Moreover, lack of a blood supply causes delayed healing and lack of union at the fracture site [26]. In our study, the HP group demonstrated a significantly higher degree of vessel formation compared to that in the TCP group.

The results of silver staining and VW factor immunohistochemistry indicated that the HA/PDLLA scaffold demonstrated superior infiltration compared to the β-TCP scaffold.

The vessel cavity formed in the scaffold transports various types of cells. In particular, infiltration of osteoclast-like cells, which plays a role in scaffold resorption, is very important. Chazono et al. previously reported that bone formation occurs after scaffold resorption [27]. Cathepsin K is expressed in osteoclast cells [28–30]. The HP group showed a significantly higher number of cathepsin K-positive cells compared to the TCP group; this indicated that the HA/PDLLA scaffold was more likely to be resorbed by osteoclast-like cells than was the β-TCP scaffold. Additionally, more PDLLA is degraded by hydrolysis, so that the HA/PDLLA scaffold is likely to be useful in patients with osteopetrosis and diabetes [31].

The infiltrated fibrous tissue was positive for COL1 and most of the infiltrated cells were positive for RUNX2. RUNX2 plays a role in differentiation of mesenchymal cells into osteoblasts, activation of COL1 expression, and is also related to vessel formation [32–36]. RUNX2 influences not only bone formation, but also bone resorption [37–39]. Compared to the TCP group, the HP group had significantly higher numbers of RUNX2-positive cells throughout the entire follow-up period, suggesting that both bone formation and the remodeling process of bone resorption had been activated. The size of pore and interconnection pore were critical factors for biomaterial scaffolds [40–43]. Tsuruga et al. reported that for cell adhesion, differentiation, growth of osteoblasts, and vascularization, the optimal pore size was approximately 300–400 μm [40]. Lu et al. recommended the favorable interconnection pore size to be over 50 μm, while Xiao et al. reported that the 150 μm interconnection pore size showed significant greater vascularization compared to

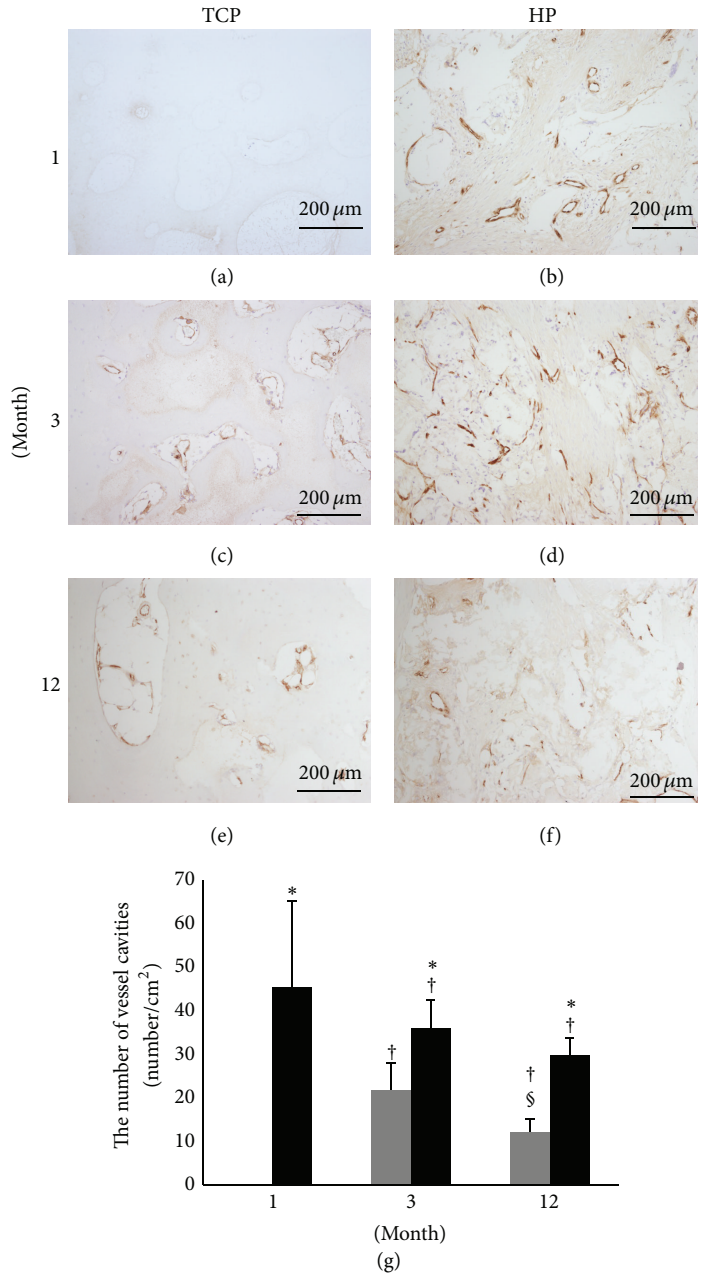

Figure 9: Tissue sections were stained for Von Willebrand (VW) factor and observed at ×100 magnification. ((a), (c), and (e)) TCP group. ((b), (d), and (f)) HP group. ((a), (b)) 1 month. ((c), (d)) 3 months. ((e), (f)) 12 months. (g) Measurement of the number of infiltrating vessels. β-TCP (grey box), HA/PDLLA (black box). Most of the vessel cavities were present in the infiltrated fibrous tissue; the HP groups showed significantly more vessel cavities than did the TCP groups during the follow-up period. ∗: $p < 0.05$ versus TCP group. †: $p < 0.05$ versus 1 month. §: $p < 0.05$ versus 3 months. Scale bars: 200 μm.

100 and 120 μm [43, 44]. From these researches, it can be said that the HA/PDLLA scaffold was sufficient in both the pore size and interconnection pore size.

In generally, a bioresorbable scaffold does not have sufficient mechanical strength to be used at a loading site. However, Liu et al. reported that it was possible to apply bioresorbable scaffolds to a loading site while using a proper fixation system, although they reported that using β-TCP-only scaffold did not result in good bone formation [45]. In other words, a wide range of bone injuries could not be healed by transplantation of only cancellous bone [45]. In our study, using a particular bioresorbable scaffold alone resulted in good bone formation. We hypothesized that this was due to the animal species used, the porosity and pore size of the material used, and the medullary-like cavity created in the bioresorbable scaffold. In a previous study of a bioresorbable scaffold implanted subcutaneously into rabbit, cartilage tissue and chondrocytes were observed by 3 months [46];

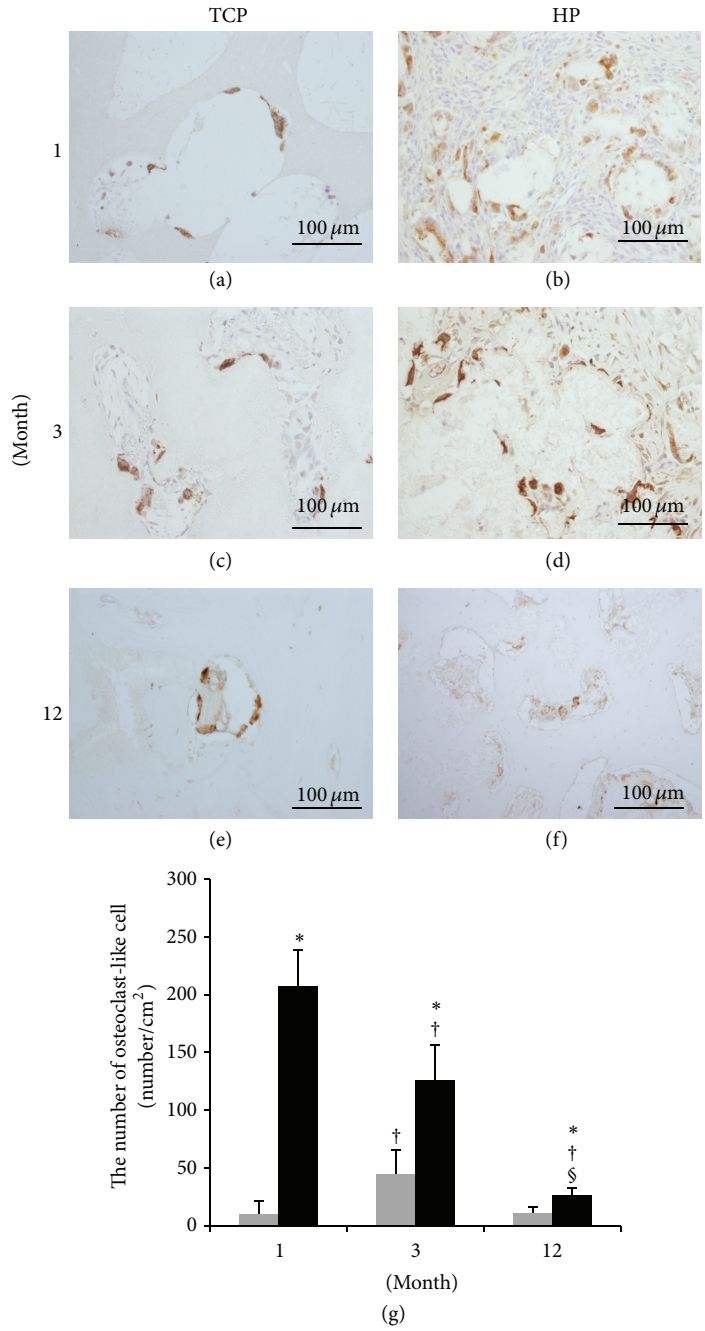

Figure 10: Tissue sections were stained for cathepsin K and viewed at ×200 magnification. ((a), (c), and (e)) TCP group. ((b), (d), and (f)) HP group. ((a), (b)) 1 month. ((c), (d)) 3 months. ((e), (f)) 12 months. (g) Number of osteoclast-like cells present after implantation of bioresorbable materials. β-TCP (grey box), HA/PDLLA (black box). The number of cathepsin K-positive cells was measured. We defined osteoclast-like cells as cells that were cathepsin K-positive and possessed more than five nuclei. HP groups showed significantly more osteoclast-like cells compared to the TCP groups during the follow-up period. In the HP group, the positive cells reduced significantly over time. In the TCP group, the 3-month group showed a significant more cathepsin K-positive cells compared to the 1- and 12-month groups. $*$: $p < 0.05$ versus TCP group. †: $p < 0.05$ versus 1 month. §: $p < 0.05$ versus 3 months. Scale bars: 100 μm.

however, we did not observe these features in our study, and the reason for this is not immediately clear.

Ozawa et al. reported a study in which 167 clinical cases received β-TCP scaffold implants and observed good remodeling radiologically [47]. However, the β-TCP scaffold could not be remolded easily to replace the defect site. In contrast, the HA/PDLLA scaffold could be formed into various shapes, using a scalpel and thermal modification, to fill the defect site optimally [15, 46], thereby offering easy intraoperative manipulation by the surgeon.

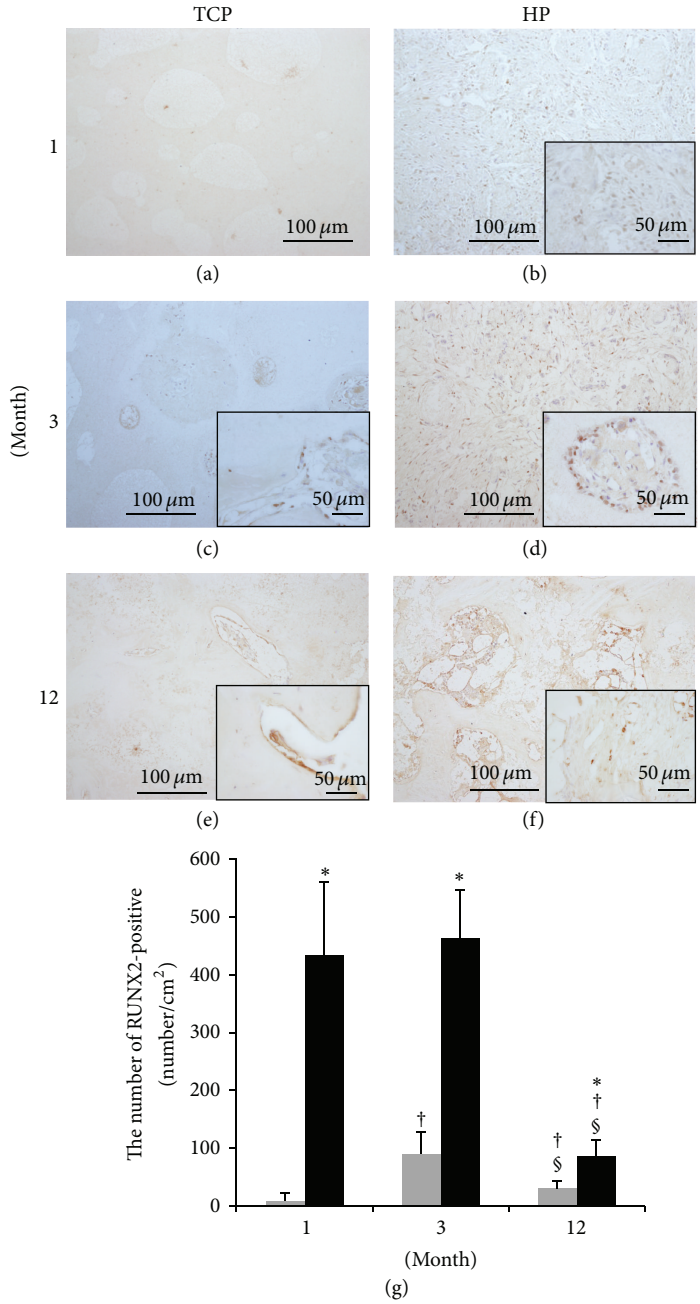

Figure 11: Tissue sections were stained for RUNX2 and viewed at ×100 and ×400 (insets) magnification. ((a), (c), and (e)) TCP group. ((b), (d), and (f)) HP group. ((a), (b)) 1 month. ((c), (d)) 3 months. ((e), (f)) 12 months. (g) The number of cells positive for RUNX2. β-TCP (grey box), HA/PDLLA (black box). Most of the spindle-shaped cells that were frequently observed in the HP group were positive for RUNX2. The HP group showed significantly more RUNX2-positive cells than did the TCP group during the follow-up period. In the HP group, specimens at 1 and 3 months demonstrated significantly more RUNX2-positive cells compared to the 12-month group. In the TCP group, the 3-month group demonstrated significantly more RUNX2-positive cells compared to the 1- and 12-month groups. $*$: $p < 0.05$ versus TCP group. †: $p < 0.05$ versus 1 month. §: $p < 0.05$ versus 3 months. Scale bars: 100 μm and 50 μm.

5. Conclusion

The results of this study showed that the HA/PDLLA scaffold is equal to the β-TCP scaffold in terms of bone formation and shows fine hydrolysis and operability. This study used 12 months as the follow-up period, but neither scaffold had achieved complete replacement by that period. The residual scaffold evoked pain and dysfunction. The result of immunohistochemistry staining showed that the HA/PDLLA scaffold had significantly higher infiltration and activation of the bone remodeling process than did the β-TCP scaffold; thus, the HA/PDLLA scaffold indicated a lower risk of residual

scaffold. It is likely that the HA/PDLLA scaffold will find clinical application as a new bioresorbable scaffold.

Conflict of Interests

The authors declare that there is no conflict of interests.

Acknowledgments

The authors thank the orthopedic team members, Drs. Munetaka Iwata, Hirokazu Amimoto, Tomu Ichinohe, Yuuta Hayashi, Takaharu Hakozaki, Yoshiyuki Ochi, Mariko Ozawa, Mitsunobu Kawazu, Yukari Nagahiro, Norihiro Muroi, Koutatou Kawakita, Yukino Suyama, Shouko Terashima, Hitoshi Mukaitouge, and Daichi Katori, for their technical support.

References

[1] M. Navarro, A. Michiardi, O. Castaño, and J. A. Planell, "Biomaterials in orthopaedics," *Journal of the Royal Society Interface*, vol. 5, no. 27, pp. 1137–1158, 2008.

[2] M. A. Slivka, N. C. Leatherbury, K. Kieswetter, and G. G. Niederauer, "Porous, resorbable, fiber-reinforced scaffolds tailored for articular cartilage repair," *Tissue Engineering*, vol. 7, no. 6, pp. 767–780, 2001.

[3] S. Yang, K.-F. Leong, Z. Du, and C.-K. Chua, "The design of scaffolds for use in tissue engineering. Part I. Traditional factors," *Tissue Engineering*, vol. 7, no. 6, pp. 679–689, 2001.

[4] Y. Doi, T. Horiguchi, Y. Moriwaki, H. Kitago, T. Kajimoto, and Y. Iwayama, "Formation of apatite-collagen complexes," *Journal of Biomedical Materials Research*, vol. 31, no. 1, pp. 43–49, 1996.

[5] T. Watanabe, S. Ban, T. Ito, S. Tsuruta, T. Kawai, and H. Nakamura, "Biocompatibility of composite membrane consisting of oriented needle-like apatite and biodegradable copolymer with soft and hard tissues in rats," *Dental Materials Journal*, vol. 23, no. 4, pp. 609–612, 2004.

[6] G. Daculsi, O. Laboux, O. Malard, and P. Weiss, "Current state of the art of biphasic calcium phosphate bioceramics," *Journal of Materials Science: Materials in Medicine*, vol. 14, no. 3, pp. 195–200, 2003.

[7] K. Kurashina, H. Kurita, Q. Wu, A. Ohtsuka, and H. Kobayashi, "Ectopic osteogenesis with biphasic ceramics of hydroxyapatite and tricalcium phosphate in rabbits," *Biomaterials*, vol. 23, no. 2, pp. 407–412, 2002.

[8] Y. Doi, H. Iwanaga, T. Shibutani, Y. Moriwaki, and Y. Iwayama, "Osteoclastic responses to various calcium phosphates in cell cultures," *Journal of Biomedical Materials Research*, vol. 47, no. 3, pp. 424–433, 1999.

[9] W. J. Ciccone II, C. Motz, C. Bentley, and J. P. Tasto, "Bioabsorbable implants in orthopaedics: new developments and clinical applications," *Journal of the American Academy of Orthopaedic Surgeons*, vol. 9, no. 5, pp. 280–288, 2001.

[10] P. U. Rokkanen, "Bioabsorbable fixation devices in orthopaedics and traumatology," *Scandinavian Journal of Surgery*, vol. 87, no. 1, pp. 13–20, 1998.

[11] Y. Wan, C. Tu, J. Yang, J. Bei, and S. Wang, "Influences of ammonia plasma treatment on modifying depth and degradation of poly(L-lactide) scaffolds," *Biomaterials*, vol. 27, no. 13, pp. 2699–2704, 2006.

[12] T. Kasuga, H. Maeda, K. Kato, M. Nogami, K.-I. Hata, and M. Ueda, "Preparation of poly(lactic acid) composites containing calcium carbonate (vaterite)," *Biomaterials*, vol. 24, no. 19, pp. 3247–3253, 2003.

[13] C. Kunze, T. Freier, E. Helwig et al., "Surface modification of tricalcium phosphate for improvement of the interfacial compatibility with biodegradable polymers," *Biomaterials*, vol. 24, no. 6, pp. 967–974, 2003.

[14] H. Akagi, M. Iwata, T. Ichinohe et al., "Hydroxyapatite/poly-L-lactide acid screws have better biocompatibility and femoral burr hole closure than does poly-L-lactide acid alone," *Journal of Biomaterials Applications*, vol. 28, no. 6, pp. 954–962, 2014.

[15] Y. Shikinami, K. Okazaki, M. Saito et al., "Bioactive and bioresorbable cellular cubic-composite scaffolds for use in bone reconstruction," *Journal of the Royal Society Interface*, vol. 3, no. 11, pp. 805–821, 2006.

[16] S. Sai and K. Fujii, "β-tricalcium phosphate as a bone graft substitute," *Jikeikai Medical Journal*, vol. 52, pp. 47–54, 2005.

[17] P. Müller, U. Bulnheim, A. Diener et al., "Calcium phosphate surfaces promote osteogenic differentiation of mesenchymal stem cells," *Journal of Cellular and Molecular Medicine*, vol. 12, no. 1, pp. 281–291, 2008.

[18] D. E. Cutright, S. N. Bhaskar, J. M. Brady, L. Getter, and W. R. Posey, "Reaction of bone to tricalcium phosphate ceramic pellets," *Oral Surgery, Oral Medicine, Oral Pathology*, vol. 33, no. 5, pp. 850–856, 1972.

[19] V. Karageorgiou and D. Kaplan, "Porosity of 3D biomaterial scaffolds and osteogenesis," *Biomaterials*, vol. 26, no. 27, pp. 5474–5491, 2005.

[20] S. Hasegawa, J. Tamura, M. Neo et al., "In vivo evaluation of a porous hydroxyapatite/poly-DL-lactide composite for use as a bone substitute," *Journal of Biomedical Materials Research Part A*, vol. 75, no. 3, pp. 567–579, 2005.

[21] N. Kondo, A. Ogose, K. Tokunaga et al., "Osteoinduction with highly purified β-tricalcium phosphate in dog dorsal muscles and the proliferation of osteoclasts before heterotopic bone formation," *Biomaterials*, vol. 27, no. 25, pp. 4419–4427, 2006.

[22] R. D. McComb, T. R. Jones, S. V. Pizzo, and D. D. Bigner, "Specificity and sensitivity of immunohistochemical detection of factor VIII/von Willebrand factor antigen in formalin-fixed paraffin-embedded tissue," *Journal of Histochemistry and Cytochemistry*, vol. 30, no. 4, pp. 371–377, 1982.

[23] N. Weidner, "Current pathologic methods for measuring intratumoral microvessel density within breast carcinoma and other solid tumors," *Breast Cancer Research and Treatment*, vol. 36, no. 2, pp. 169–180, 1995.

[24] J. Harper and M. Klagsbrun, "Cartilage to bone—angiogenesis leads the way," *Nature Medicine*, vol. 5, no. 6, pp. 617–618, 1999.

[25] J. Lienau, K. Schmidt-Bleek, A. Peters et al., "Differential regulation of blood vessel formation between standard and delayed bone healing," *Journal of Orthopaedic Research*, vol. 27, no. 9, pp. 1133–1140, 2009.

[26] M. R. Hausman, M. B. Schaffler, and R. J. Majeska, "Prevention of fracture healing in rats by an inhibitor of angiogenesis," *Bone*, vol. 29, no. 6, pp. 560–564, 2001.

[27] M. Chazono, T. Tanaka, H. Komaki, and K. Fujii, "Bone formation and bioresorption after implantation of injectable β-tricalcium phosphate granules-hyaluronate complex in rabbit bone defects," *Journal of Biomedical Materials Research Part A*, vol. 70, no. 4, pp. 542–549, 2004.

[28] A. J. Littlewood-Evans, G. Bilbe, W. B. Bowler et al., "The osteoclast-associated protease cathepsin K is expressed in human breast carcinoma," *Cancer Research*, vol. 57, no. 23, pp. 5386–5390, 1997.

[29] S. Sai and K. Fujii, "Mater Res Aphosphate as a bone graft substitute," *Jikeikai Medical Journal*, vol. 52, pp. 47–54, 2005.

[30] K.-I. Tezuka, Y. Tezuka, A. Maejima et al., "Molecular cloning of a possible cysteine proteinase predominantly expressed in osteoclasts," *The Journal of Biological Chemistry*, vol. 269, no. 2, pp. 1106–1109, 1994.

[31] V. Maquet, A. R. Boccaccini, L. Pravata, I. Notingher, and R. Jérôme, "Preparation, characterization, and in vitro degradation of bioresorbable and bioactive composites based on Bioglass-filled polylactide foams," *Journal of Biomedical Materials Research A*, vol. 66, no. 2, pp. 335–346, 2003.

[32] M. Inada, T. Yasui, S. Nomura et al., "Maturational disturbance of chondrocytes in Cbfa1-deficient mice," *Developmental Dynamics*, vol. 214, no. 4, pp. 279–290, 1999.

[33] H. Itoh, Y. Hara, M. Tagawa et al., "Evaluation of the association between runt-related transcription factor 2 expression and intervertebral disk aging in dogs," *The American Journal of Veterinary Research*, vol. 73, no. 10, pp. 1553–1559, 2012.

[34] I. S. Kim, F. Otto, B. Zabel, and S. Mundlos, "Regulation of chondrocyte differentiation by Cbfa1," *Mechanisms of Development*, vol. 80, no. 2, pp. 159–170, 1999.

[35] T. Komori, "Regulation of osteoblast differentiation by transcription factors," *Journal of Cellular Biochemistry*, vol. 99, no. 5, pp. 1233–1239, 2006.

[36] T. Komori, "Regulation of skeletal development by the Runx family of transcription factors," *Journal of Cellular Biochemistry*, vol. 95, no. 3, pp. 445–453, 2005.

[37] H. Enomoto, S. Shiojiri, K. Hoshi et al., "Induction of osteoclast differentiation by Runx2 through receptor activator of nuclear factor-κB ligand (RANKL) and osteoprotegerin regulation and partial rescue of osteoclastogenesis in Runx2$^{-/-}$ mice by RANKL transgene," *Journal of Biological Chemistry*, vol. 278, no. 26, pp. 23971–23977, 2003.

[38] H. Hsu, D. L. Lacey, C. R. Dunstan et al., "Tumor necrosis factor receptor family member RANK mediates osteoclast differentiation and activation induced by osteoprotegerin ligand," *Proceedings of the National Academy of Sciences of the United States of America*, vol. 96, no. 7, pp. 3540–3545, 1999.

[39] N. Nakagawa, M. Kinosaki, K. Yamaguchi et al., "RANK is the essential signaling receptor for osteoclast differentiation factor in osteoclastogenesis," *Biochemical and Biophysical Research Communications*, vol. 253, no. 2, pp. 395–400, 1998.

[40] E. Tsuruga, H. Takita, H. Itoh, Y. Wakisaka, and Y. Kuboki, "Pore size of porous hydroxyapatite as the cell-substratum controls BMP-induced osteogenesis," *Journal of Biochemistry*, vol. 121, no. 2, pp. 317–324, 1997.

[41] M. Mastrogiacomo, S. Scaglione, R. Martinetti et al., "Role of scaffold internal structure on in vivo bone formation in macroporous calcium phosphate bioceramics," *Biomaterials*, vol. 27, no. 17, pp. 3230–3237, 2006.

[42] J. X. Lu, B. Flautre, K. Anselme et al., "Role of interconnections in porous bioceramics on bone recolonization in vitro and in vivo," *Journal of Materials Science: Materials in Medicine*, vol. 10, no. 2, pp. 111–120, 1999.

[43] F. Bai, Z. Wang, J. Lu et al., "The correlation between the internal structure and vascularization of controllable porous bioceramic materials in vivo: a quantitative study," *Tissue Engineering, Part A*, vol. 16, no. 12, pp. 3791–3803, 2010.

[44] X. Xiao, W. Wang, D. Liu et al., "The promotion of angiogenesis induced by three-dimensional porous beta-tricalcium phosphate scaffold with different interconnection sizes via activation of PI3K/Akt pathways," *Scientific Reports*, vol. 5, article 9409, 2015.

[45] G. Liu, L. Zhao, W. Zhang, L. Cui, W. Liu, and Y. Cao, "Repair of goat tibial defects with bone marrow stromal cells and β-tricalcium phosphate," *Journal of Materials Science: Materials in Medicine*, vol. 19, no. 6, pp. 2367–2376, 2008.

[46] S. Hasegawa, M. Neo, J. Tamura et al., "In vivo evaluation of a porous hydroxyapatite/poly-DL-lactide composite for bone tissue engineering," *Journal of Biomedical Materials Research: Part A*, vol. 81, no. 4, pp. 930–938, 2007.

[47] M. Ozawa, T. Tanaka, S. Morikawa, M. Chazono, and K. Fujii, "Clinical study of the pure β-tricalcium phosphate-reports of 167 cases," *Journal of the Eastern Japan Association of Orthopaedics and Traumatology*, vol. 12, pp. 409–413, 2000.

Hindawi Publishing Corporation
BioMed Research International
Volume 2015, Article ID 821279, 15 pages
http://dx.doi.org/10.1155/2015/821279

Review Article

Chitosan and Its Potential Use as a Scaffold for Tissue Engineering in Regenerative Medicine

Martin Rodríguez-Vázquez, Brenda Vega-Ruiz, Rodrigo Ramos-Zúñiga, Daniel Alexander Saldaña-Koppel, and Luis Fernando Quiñones-Olvera

Translational Neurosciences Institute, Department of Neurosciences, University Center of Health Sciences CUCS, Universidad de Guadalajara, 44340 Guadalajara, JAL, Mexico

Correspondence should be addressed to Rodrigo Ramos-Zúñiga; rodrigorz13@gmail.com

Received 2 March 2015; Revised 26 April 2015; Accepted 13 May 2015

Academic Editor: Francesco Piraino

Tissue engineering is an important therapeutic strategy to be used in regenerative medicine in the present and in the future. Functional biomaterials research is focused on the development and improvement of scaffolding, which can be used to repair or regenerate an organ or tissue. Scaffolds are one of the crucial factors for tissue engineering. Scaffolds consisting of natural polymers have recently been developed more quickly and have gained more popularity. These include chitosan, a copolymer derived from the alkaline deacetylation of chitin. Expectations for use of these scaffolds are increasing as the knowledge regarding their chemical and biological properties expands, and new biomedical applications are investigated. Due to their different biological properties such as being biocompatible, biodegradable, and bioactive, they have given the pattern for use in tissue engineering for repair and/or regeneration of different tissues including skin, bone, cartilage, nerves, liver, and muscle. In this review, we focus on the intrinsic properties offered by chitosan and its use in tissue engineering, considering it as a promising alternative for regenerative medicine as a bioactive polymer.

1. Introduction

Currently, regenerative medicine is one of the most popular scientific fields and the future of life sciences, where new technology and today's public health challenges converge.

Regenerative medicine is defined as the association of tissue engineering, stem cells research, gene therapy, and therapeutic cloning, as important strategies for regenerative medicine in the present and future.

Recently, research on biomaterials has pointed to the design, development, and improvement of scaffolds as new drug release systems and bioactive molecules for regenerative medicine [1].

All of this has been possible because of dramatic advances in the field of tissue engineering during the last 10 years, offering potential regeneration of almost all tissues and organs of the human body.

Tissue engineering is an important therapeutic strategy for present and future medicine. Therefore, the goal in tissue engineering is to restore, regenerate, maintain, or improve function in defective tissue or lost tissue due to different disease conditions. This may be possible by using the development of biologic substitutes or by rebuilding structural scaffolds that induce tissue regeneration. Tissue engineering is defined as the use of isolated cells or cell substitutes, tissue inducers, and cells placed on or in a matrix to repair and regenerate tissue [2]. Strategies can be classified into three groups: (1) isolated cell implants or cell substitutes in the body, (2) tissue inducer substances (such as growth factors), and (3) cells placed on or in different matrices or substrates that work as a vehicle or scaffold that induce tissue regeneration [3].

Thus, the focus on tissue engineering points to the use of structures used to repair injured tissue or tissue with structural malformations and also reinforce and, in certain cases, organize regenerating tissue that would work as a scaffolding to restore or regenerate the damaged tissue [4].

Table 1: Characteristics that must contain a biomaterial for use in tissue engineering and regenerative medicine.

Characteristics	Description of the characteristic
Biocompatibility	They must be accepted by the receptor and must not lead to rejection mechanisms because of its presence
Absorbability and degradability	Absorbable, with controllable degradation and resorption rate to be the same as the in vitro and in vivo cell/tissue growth
Not to be toxic or carcinogenic	Its degradation products cannot cause local or systemic adverse effect on a biological system
Chemically stable	Chemical modifications not being present in a biological system implant or biodegradable in nontoxic products, at least during the scheduled time to regenerate tissue
Chemically adequate surface	To have a chemically adequate surface for cell access, proliferation and cell differentiation
Adequate resistance and mechanical properties	Resistance and mechanical properties, superficial characteristics, fatigue time, and weight, according to the receptor tissue needs, as well
The proper design, size, and shape of the scaffolding	Which allows having a structure with properties according to the needs of the receiving tissue to regenerate or repair.

2. The Scaffolding

Scaffolding is defined as 3D porous solid biomaterials, designed for the following functions: (1) promoting cell-biomaterial interactions, cell adhesion, and extracellular matrix deposits (ECMD), (2) allowing for sufficient transport of gases, nutrients, and regulatory factors to allow for cell survival, proliferation, and differentiation, (3) breaking down at a controllable rate that is close to the regeneration rate of the tissue of interest, and (4) creating minimal inflammation [5].

Biomaterials used as scaffolds in tissue engineering must meet certain requirements or characteristics in order that they can perform the above functions (Table 1) [23]. This scaffolding composed of natural or synthetic materials is commonly used as scaffolds to interact with biological systems to accomplish desirable medical outcomes in modern healthcare, providing alternatives to overcome the limitations and restrictions imposed by the use of autograft and allograft tissues [23].

Polymers are biocompatible biomaterials for application in regenerative medicine and tissue engineering. They can be natural, synthetic biodegradable, and synthetic non-biodegradable. Among them, the polymers that are mostly used as biomaterials are the natural and synthetic biodegradable ones, which have attracted significant interest because of their flexibility in terms of chemical manipulation and the ability to break down into low molecular weight fragments that can be eliminated or resorbed by the human body [24, 25].

Natural polymers can be considered as the first biodegradable biomaterials used in human clinical conditions [24]. These natural materials, due to their bioactive properties, tend to have greater biological interaction with the cells, which allow them to have better performance in the biological system. Natural polymers can be classified as proteins (silk, collagen, fibrinogen, elastin, cheratin, actin, and myosin) and polysaccharides (cellulose, amylose, dextran, chitin, and glycosaminoglycans) or polynucleotides (DNA, RNA) [26].

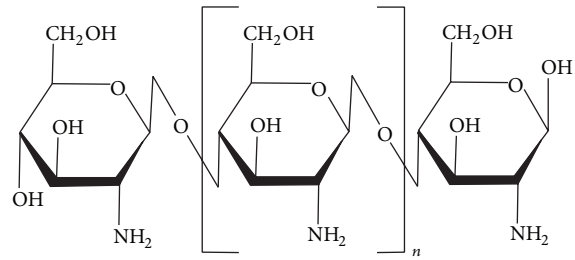

Figure 1: Chemical structure of chitosan [poly-(β-1/4)-2-amino-2-deoxy-D-glucopyranose].

Currently, polymers have been widely used as biomaterials for manufacturing medical devices and scaffolds in tissue engineering [27, 28]. In biomedical applications, the selection criteria of polymer materials used as biomaterials are based on certain features such as chemical composition, molecular weight, solubility, shape and structure, hydrophilicity/hydrophobicity, surface energy, water absorption capacity, breakdown, and erosion mechanism. Polymer scaffolds are attracting a great deal of attention due to their unique features, such as the high surface-volume ratio, great porosity on the surface with a very small pore size, ability to control biodegradation, and mechanical properties. They have several biocompatibility benefits, versatility in surface chemistry, and biological properties that are important in tissue engineering application and organ replacement in regenerative medicine [29]. In this context, chitosan has drawn a lot of attention.

3. Chitosan Characteristics

Chitosan [poly-(β-1/4)-2-amino-2-deoxy-D-glucopyranose] [30] is a copolymer made of D-glucosamine and N-acetyl-D-glucosamine bonds and β bonds (1–4) (Figure 1), in which glucosamine is the predominant repeating unit in its structure; it is a derivative of the alkaline deacetylation of chitin, and the glucosamine content is named according to

the degree of deacetylation (DD). Depending on the procedure of origin and preparation, molecular weight may vary from 300 kD to over 1,000 kD, with a deacetylation between 30% and 95% in the available commercial preparations. Chitosan has been the best version of the chitin polymer because it is readily soluble in diluted organic acids, thereby having greater availability to be used in chemical reactions [27, 28, 31–33].

Chitosan properties are very much affected by the conditions in which the material is processed because the manufacturing process conditions are the ones that control the resulting amount of deacetylation. The DD in chitosan is a key feature that determines its physical, chemical, and biological characteristics. The DD is determined by the amount of free amino groups in the polymer chain, and this free amino group confers a positive charge to chitosan. The amino group and the hydroxyl group provide functionality, so chitosan turns out to be a highly reactive polysaccharide. The positive charge in chitosan allows for many electrostatic interactions with negatively charged molecules. The processing conditions, as well as the amount of functional groups created by deacetylation, allow for coupling of the groups, having an impact on the crystallinity of chitosan which in turn is directly associated with the ability of chitosan to be soluble in aqueous acid solutions, resulting in one of its main features for processing [34].

Chitosan has many physical and chemical properties conferred by its functional groups (amino NH2 and hydroxyl OH), as well as biological properties coming from its chemical composition. Solubility, biodegradability, reactivity, and absorption of many of its substrates depend on the amount of protonated amino groups in the polymer chain and thus in the rate of acetylated or nonacetylated glucosamine [35, 36]. All of these features make it an attractive option for several applications in science such as food/nutrition, medicine, microbiology, immunology, agriculture, and veterinary medicine [37].

4. Physicochemical Properties

4.1. pH Dependence and Solubility. Chitosan solubility depends on the distribution of free amino and N-acetyl groups. In diluted acid solutions (pH $\leq$ 6) the free amino groups are protonated and confer a polycationic behavior and the molecule becomes soluble [4]. From the pka standpoint, similarly, the amino groups (pka 6.2–7.0) are completely protonated in acids with a pka less than 6.2, making chitosan soluble, remaining so until reaching a pH near 6.2, when, at a higher pH (>de 6.5) the amines in chitosan deprotonate and chitosan become insoluble, after which precipitates, such as hydrated gels, are formed. Chitosan is insoluble in water, aqueous solutions, concentrated acids, and common organic solvents, but it is totally soluble when stirred into aqueous solutions such as acetic acid, nitric acid, hydrochloric acid, perchloric acid, lactic acid, and phosphoric acid [36, 38, 39].

4.2. Degree of Deacetylation (DD). The degree of deacetylation (DD) represents the rate of D-glucosamine units with respect to the total amount of N-acetyl-D-glucosamine that makes the chitosan molecule, since this unit is found in the amino group created from the elimination of the acetyl group. A deacetylated chitin over 60 or 70% is already considered to be chitosan. The DD is a structural parameter that determines some physical and chemical properties such as solubility limit in acid solutions (pH 2–6), molecular weight, and mechanical properties (elasticity and traction resistance). The deacetylation process turning chitin into chitosan will transform the acetyl group into a primary amino group, which is more hydrophilic than the preceding molecule; thereby, the DD in chitosan increases the water content in samples taken from chitosan samples, tending to have an impact on the ability to absorb water and limiting the ability to have maximum swelling [40].

The DD also has an impact on biological properties, such as the in vitro and in vivo biodegradation. It has been proven that, at a greater DD (between 84 and 90%), the degradation process is delayed. Highly deacetylated chitosan (over 85%) shows a low degradation index in the aqueous environment and will degrade after a few months, and a lower DD (between 82 and 65%) would lead to a faster degradation. The commercially available preparations have a DD between 60 and 90%. This feature has an impact on some biological properties in chitosan, such as healing capacity, increase in osteogenesis, and a breakdown process by lysozymes in biological systems [41, 42].

The DD plays a key role in cell adhesion and proliferation but does not change the cytocompatibility of chitosan. "In vitro" studies have shown that the lower the DD in chitosan, the lower the cell adhesion in the films. It has been found that keratinocytes attached to the chitosan film may change their adhesion and cell growth depending on their deacetylation degree (DD), but proliferation is not promoted. Thus, DD affects growth of cells in the same way as cell adhesion.

4.3. Molecular Weight. Depending on where and how the preparation procedure is done, the molecular weight may change from 300 to over 1000 kD [4]; viscosity and molecular weight are inversely proportional to the degree of acetylation. Therefore, the greater the molecular weight is, the chitosan membranes tend to be more viscous, thus allowing for controlling fluidity in them, an important feature in tissue interaction. Due to its high molecular weight and its lineal nonbranched structure, chitosan is a strong viscosity-building agent in acid mediums and behaves as a pseudoplastic material, where viscosity depends on agitation [43].

It has also been proven that the molecular weight has an indirect effect or is inversely proportional to the swelling capacity and/or hydration of chitosan membranes, and when the molecular weight is greater and the DD is higher, the swelling or permeability is less in chitosan membranes [44].

There is a direct association between molecular weight and DD. These two parameters have a direct effect on the biodegradation process of chitosan, since at a greater molecular weight the degradation process is delayed in "in vitro" as well as "in vivo" systems [45].

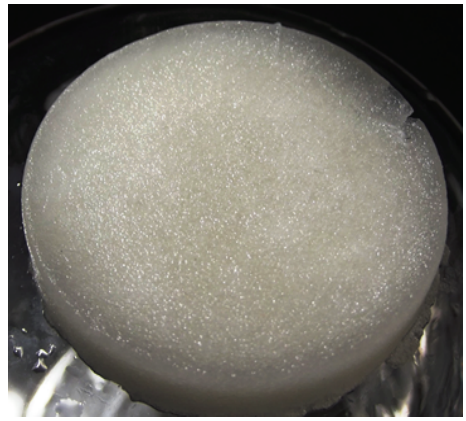

(a)

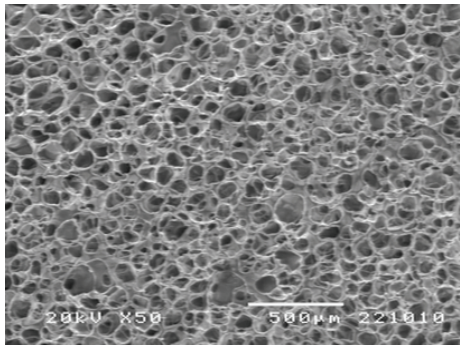

(b)

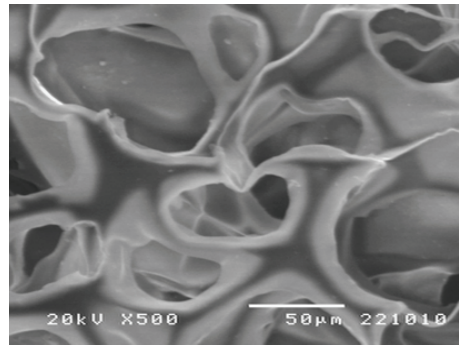

(c)

Figure 2: Macroscopic photographs (a) and micrographs (SEM) ((b) and (c)) of porous chitosan scaffold. Micrographs show low and high magnification.

After oral administration in mice and rats, the molecular weight decrease in chitosan leads to greater absorption. When low molecular weight chitosan was absorbed, it was found to extend to several inspected organs, that is, liver, kidney, spleen, thymus, heart, and lung and it was also easily metabolized [44, 46].

4.4. Porosity. Porosity is a feature in polymers used as scaffolding. Porous scaffolds serve to provide support in tissue engineering because they act as a platform and provide necessary support to physically guide differentiation and proliferation of cells for tissue growth "in vivo" and "in vitro." The porous scaffolding must be similar to MEC present in tissue, allowing for organized cell growth and neovascularization. For all these reasons, these polymers such as chitosan have been extensively investigated for such applications, specifically for soft tissue replacement because porous scaffolding can retain water in its polymeric structure as well as retaining bioactive proteins [47].

In order for chitosan scaffolding to be used as structural support in tissue regeneration, it should be highly porous so as to have the proper cell proliferation in the action site and also have enough surface area for live cells to accommodate adequately, have the correct pore size so that the growing cells can penetrate and proliferate, and have highly interconnected pore structures that allow cells to grow and to have proper transport of nutrients (Figure 2) [48].

Several methods are used to prepare 3D porous scaffolds, among which we find that of thermally induced phase separation (TIPS) in which temperature is reduced to freezing conditions to induce phase separation in a degradable homogenous polymer. Since chitosan is a polymer, it can produce porous membranes to be used as scaffolds [49].

Porous scaffoldings resulting from the TIPS method can synthetize different structures that contain somewhat different pores with size ranges from 1 to 250 μm and that vary according to temperature and water content. For example, the lower the temperature and the greater the water content, the smaller the pore size; porosity in chitosan membranes has a direct effect on its surface size. Hydrated porous chitosan membranes have been shown to have at least twice more surface size and volume compared to nonporous chitosan membranes, but their elasticity and resistance to traction are ten times smaller than nonporous membranes used as controls [50]. The porous structure can be stabilized adding glutaraldehyde, polyethylenglycol, heparin, or collagen, allowing the structure to become more resistant and to maintain elasticity. These compounds can make chitosan turn insoluble in acid solutions and consequently form closed pore structures [51, 52].

Currently, ideal scaffolding should have 80 to 90% porosity with a pore size of 50 to 250 μm. Its pores should be interconnected so as to provide physical support to cells and

guide their proliferation and differentiation, also facilitating neovascularization. The pore sizes recommended for skin scaffolding should be greater than 160 μm, varying between 15–100 μm and 100–200 μm, with a desired 90% porosity to provide the necessary space and enough surface to grow cells and create priority temporary scaffolds for implantation allowing for regeneration or damaged tissue repair [53].

4.5. Water Absorption Capacity. When placed in liquid media, chitosan membranes can swell and retain a given water volume absorbed from the medium in their three-dimensional network. In order to be used for biomedical purposes, they should absorb fluid from the body for cell transference, plus they should allow for an adequate distribution of nutrients, metabolites, and growth factors, through extracellular media [47].

4.6. Mechanical Properties. Considering the appropriate mechanical properties we can state that chitosan membranes have a disadvantage when used for support in tissue engineering because these membranes are very stiff and brittle; that is, they have low mechanical resistance [23]. So then, in order to optimize resistance and elasticity, crosslinking agents are used with at least two functional reactive groups that allow for making bridges between polymeric chains with formaldehyde, epoxides reacting with polyethyleneglycol, dialdehydes (glutaraldehyde and glyoxal), and starch [54]. In cross-linked hydrogels the polymeric chains are bound by the crosslinking agent, building a 3D network. Their nature will mainly depend on the density or crosslinking degree, named according to the ratio of moles in the agent with the moles in the repeat units of the polymer. Among the reactions to the crosslinks in chitosan with some other materials we can find the aldehyde-amine reaction with polyethylene glycol, which is used because it is hydrophilic, with low toxicity and good biocompatibility. Studies have been conducted showing the effectiveness of the chitosan-DiepoxyPEG (Diepoxy-polyethylene glycol) crosslinking, resulting in an improvement of the mechanical properties of the crosslinked compound [54, 55].

4.7. Biological Properties. Chitosan has many beneficial biomedical properties, such as biocompatibility, biodegradability, and no toxicity. Biological activity of chitosan is closely related to its solubility and therefore molecular weight and DD [56].

4.8. Biodegradability. The process of biodegradation of chitosan can be through various media both physical (thermal degradation) and chemical (enzymatic degradation); the rate of degradation of the chitosan is inversely proportional to the degree of crystallinity of the polymer and therefore the DD and, thus, can manipulate the degradation rate by controlling the DD which occurs during processing [41, 57].

There is a broad range of hydrolytic enzymes such as lysozyme, which is the primary enzyme responsible for chitosan degradation in "in vivo systems" and that is found in lymphoid human and animal tissue and that can be used to naturally degrade chitosan [58, 59]. Inside the body it leads to the release of amino sugars that can be processed and released by the metabolic system. Chitosan degradation is an important property assuming that the end processes and applications it will ultimately be given can agree with the resulting design [35].

Some of the specific enzymes that degrade chitin and chitosan have a clearly identified structure but their action mechanisms are still unknown. In mammals, these enzymes seem to be completely absent; however, when chitosan is implanted, it will eventually disappear completely after some time and the degradation speed seems to depend on DD [35].

Through enzymatic hydrolysis mechanisms chitosan may be easily depolymerized due to susceptibility β bonds (1–4) mediated by different hydrolases including lysozymes, pectinase, cellulases, hemicellulases, lipases, and amylases among others, which means that chitosan has a peculiar vulnerability to other enzymes that are different from chitinases. Its degradation products are oligosaccharides or monosaccharides, natural metabolites of glycosaminoglycans or glycoaminoproteins. Lysozyme is an unspecific proteolytic enzyme common in mammals. It can hydrolyze chitosan, but this action quickly disappears when chitosan has a degree of acetylation (DA) below 30% [41].

When chitosan is fully acetylated, it is totally insensitive to this enzyme. Moreover, it seems that at least three consecutive N-acetylated groups are necessary to be recognized by this enzyme and, in spite of depending on the amine content in chitin and chitosan the unspecific enzymes that degrade these polymers are inactivated, and such degradation can be found in in vivo implants. It has been proven that whatever the circumstances may be, biodegradation of chitosan takes place depending on many and diverse factors, especially the degree of acetylation, molecular weight, degree of crystallinity, water content, and also the shape and condition of the surface on the material, aside from its microstructure [41].

4.9. Biocompatibility. Biomaterials should be biocompatible; that is, contact with the body should not result in adverse reactions, so they must be capable of recognizing and cooperate harmoniously with structures and cells of the human body, without producing unspecific reactions [60]. Clinical tests conducted so far have not reported any inflammatory or allergic reactions after implantation, injection, topical application, or ingestion of chitosan in the human body [40]. This is due to the fact that chitosan is made of GlcN and GlcNac that are natural components of mammalian tissues [61].

There are studies that support the biocompatibility of the material and the direct relationship of this property with its DD material used. In the first reports that determined toxicity, none of the materials were chitosan films using a standard "in vivo" toxicity tests to assess their safety [62]. The biocompatibility of chitosan films has also been shown with different DD; studies where a model of subcutaneous implantation in rats is applied showed that the films of chitosan with DD between 69 and 74% induced a relatively acute inflammatory reaction by rapid biodegradation, with almost complete resorption after 4 weeks of implantation; DD films with high (between 74 to 90%) resulted in

a mild inflammatory reaction in tissue degradation rate and a slower rate. This is in agreement with the well-known fact that rapidly biodegradable biomaterials elicit an acute inflammation reaction due to a significantly large production of low-molecular-weight compounds within a short time. Therefore it was determined that films with ≥ 84% DD showed reaction to softer tissue because these were degraded more slowly [45].

4.10. Non Toxic. Several studies have proven that, so far, clinical tests conducted with chitosan have not reported adverse inflammatory or allergic reactions when used in tissue engineering or as a vehicle in drugs, nor after implantation, injection, or topical application in the human body or for oral application. This property is due to the fact that chitosan is made of GlcN and GlcNAc, natural components of mammalian tissue [41, 42, 63].

5. Cytocompatibility

A wide number of cells have been successfully cultured on 2D and 3D chitosan matrices envisaging cell-based regenerative therapies, among them keratinocytes, chondrocytes, osteoblasts, hepatocytes, and Schwann cells [40, 64–68]. Some studies found that the DD was an important parameter affecting cell adhesion, by promoting high adhesion. This effect was reported for a number of anchorage-dependent cells, such as keratinocytes, fibroblasts, dorsal root ganglion neurons, and Schwann cells [69–71].

In other studies the effect of DD concerning behavior of the osteogenic cells and chitosan films was investigated in porous matrices, using DD in the range of 96–51%. These studies revealed a trend that determines that there is an increase of cell adhesion related to an increase in the DD, and the differences showed that a DD greater than 91% can be critical in terms of osteogenic response from chitosan [72, 73].

6. Nonimmunogenic

Chitosan and its oligomers stimulate macrophage activity increasing nitric oxide, reactive oxygen species, TNF-α, interferon, and IL-1, as well as TGF-β1 and PDGF. However, since there are no proteins and lipids in its structure, it is not possible to develop specific antibodies against it, unless it is coupled with other substances such as albumin. The conclusion from all the studies on the subject indicates that chitosan is hypoallergenic and only transiently stimulates the immune system because when impregnated with tissue fluids in the receptor body it ultimately becomes biotolerated and metabolized [41, 63, 74].

7. Antimicrobial and Antifungal

Chitosan inhibits growth of many types of fungi, yeasts, and bacteria. In solutions made of acid dilutions the positive loads in them interact with the negatively charged residues of macromolecules on the cell surface of microorganisms, supposedly competing against the Ca+2 for the electronegative sites in the membrane, but without conferring dimensional stability, compromising the membrane integrity and making it weak [75]. Among the antimicrobial effects of chitosan are those related to *Candida albicans*, *Enterobacter cloacae*, *Enterococcus faecalis*, *Escherichia coli*, *Klebsiella pneumoniae*, *Pseudomonas aeruginosa*, *Staphylococcus aureus*, and *Streptococcus pyogenes*.

This property is of special significance because it has been proven that the antimicrobial agents such as bandaging materials and dressings generally lead to cytotoxicity, delaying the healing process, or leading to pathogen resistance. In the case of chitosan, since the antimicrobial effects come directly from the membrane, there is almost no need to use antibacterial substances or change bandages, the implants themselves, or dressings when they are applied [63].

8. Tissue Repair and Regenerative Medicine

In regenerative medicine applications of biomaterials for tissue repair and regeneration include their use as orthopedic implants and, as bone fillers, adhesives for tissue repair and the use of scaffolds for tissue engineering; the latter are used for repair and/or regeneration of skin, bone, cartilage and nerve tissues, since these tissues have been the focus of greater research in regenerative medicine. This involves the use of chitosan as a scaffolding material or as an analog or extracellular matrix (ECMD), which works as support for the regeneration of damaged tissue (Table 2) [6–22, 76].

The popularity of chitosan for tissue repair and regeneration is due to the fact that it can be easily processed and manufactured in a variety of forms including fibers, films, sponges, and hydrogels. This provides the ability to mimic the shape of the receiving tissue or biomaterial tissue interface. Moreover, the similarity of its chemical structure to some polysaccharides and ECM constituents offers the possibility of being chemically modified to adapt structurally and functionally to the host tissue, due to its previously described properties that allow for the ability to regenerate primary tissue cells and even stem cells. Thus its potential is to be used in regenerative medicine [4, 33, 77, 78].

9. Chitosan and Tissue Engineering

9.1. Skin, Nerves, and Soft Tissues. The generation of scaffolds with porous structures is important in the engineering of epithelial and soft tissues. Chitosan can be manufactured in a porous structure to allow for cell seeding. This space created by the porous structure allows for cell proliferation, migration, and the exchange of nutrients. In addition, the controllable porosity of chitosan scaffolds is beneficial to angiogenesis, which is fundamental in supporting the survival and function of the regenerated soft tissues [50, 79]. Chitosan scaffolds have shown both cytocompatibility in vitro and biocompatibility in vivo. Generally, chitosan evokes only a minimal foreign body reaction in vivo, and implanted chitosan scaffolds seldom induce chitosan-specific reactions [32].

Table 2: Applications of chitosan-based scaffolds for tissue engineering.

Chitosan combination	Scaffold obtained	Experimental model	Tissue application	Reference
Chitosan + hyaluronan	Hybrid polymer fiber	Fibroblasts from patellar tendon of Japanese white rabbit	Ligament	[6]
Collagen-chitosan + fibrin glue	Asymmetric porous scaffold	Human dermal fibroblasts and keratinocytes	Skin	[7]
Chitosan + alginate	Polyelectrolyte multilayer film	C2C12 myoblasts	Muscle	[8]
Chitosan + aloe vera	Blended membrane	Bovine articular chondrocytes and mesenchymal stem cells	Skin	[9]
Chitosan alone	Membrane	Embryonal submandibular gland cells	Salivary gland	[10]
Chitosan + layer of chitosan/gelatin	Sandwich tubular scaffold	Vascular smooth muscle cells from rabbit aorta	Blood vessel	[11]
Genipin-crosslinked chitosan, chitosan-nanohydroxyapatite	Framework	Human periodontal ligament tissue, periodontal ligament stem cells	Bone	[12]
Chitosan + collagen	Hydrogel	Epididymal fat pads cells, and subcutaneous pocket of male Lewis rat	Adipose tissue	[13]
Chitosan + polyester	Compressed porous disc	Bovine articular chondrocytes	Cartilage	[14]
Chitosan + collagen + genipin	Crosslinked porous membrane	Rabbit articular chondrocytes	Cartilage	[15]
Chitosan + chondroitin sulphate	Bidimensional glass surfaces or 3D packet of paraffin	Bovine articular chondrocytes and human mesenchymal stem cells culture	Cartilage	[16]
Chitosan + adipose-derived stem cells	Tube nerve conduit	Male, Sprague-Dawley rats sciatic nerve transection	Nerve	[17]
Chitosan alone	Tube	Male, beagle dogs phrenic nerve resection	Nerve	[18]
Chitosan alone	Viscous solution and a monolayer rigid physical hydrogel	Female minipigs third-degree burns	Skin	[19]
Chitosan + silk fibroin	Thin blended film	Female guinea pigs ventral hernia	Muscle	[20]
Chitosan + β-sodium glycerophosphate + hydroxyethyl cellulose	Hydrogel	Male and female sheep articular defect	Cartilage	[21]
Chitosan + calcium phosphate cement	Chitosan microspheres inside cement paste	Male rabbit femoral defect	Bone	[22]

Due to the fact that some chitin-based biomaterials do not provide a friendly interface for cell adhesion of some specific tissue types, other biomaterials, such as collagen or fibronectin with tissue-specific binding sequence, should be blended with chitosan to produce scaffolds with higher cell affinity. Also, chitosan is blended with other biomaterials to create scaffolds that are more appropriate for directing the desired cell behaviors and to mechanically strengthen the tissues engineering of tissues such as the skeletal system [80, 81]. The biological activity beneficial to tissue regeneration can be introduced through the entrapment of bioactive agents in the scaffolds through physical adsorption [6]. For example, trimethylated chitosan has been reported to be efficient in gene transfection without increasing cytotoxicity [82].

Specifically speaking about the difference in tissues, there is evidence that chitin-based materials support neuronal growth. In addition, many different substrates and bioactive molecules have been added into chitin-based scaffold to increase their affinity with nerve cells [83]. A chitosan tube immobilized with laminin peptides can facilitate proximal nerve sprouting and regenerate axon bridging [84]. In 2004, a study showed that chitosan fibers supported the adhesion, migration, and proliferation of Schwann cells, which allowed for axonal regeneration in the peripheral nervous system [68]. Whenever there is a peripheral nerve lesion, the current standard treatment is to use an autologous nerve graft to bridge the neural gap and facilitate nerve regeneration and reconnection; however, since there have been frequent and severe complications, several attempts have been made over the last decades to overcome this problem by using different biomaterials but functional recovery is still far from being acceptable [85]. Nevertheless, different scaffolds were fabricated in a study by cross-linking chitosan with acetic acid and chitosan with γ-glycidoxypropyltrimethoxysilane, which would later be cultivated with N1E-115 cells, derived from mouse neuroblastoma C-1300. The resulting hybrid membranes presented good cytocompatibility besides the fact that, when cultured in the presence of dimethylsulfoxide (DMSO) or cyclic AMP (cAMP), they show characteristics from neural cells, such as ceased multiplication, extensive neurite outgrowth, and polarization of cellular membranes, being able to locally produce and deliver nerve growth factors, essential in the reconstruction of peripheral nerve lesions. In vivo studies suggest that these chitosan-based membranes show promising results regarding its applications in peripheral nerve engineering due to their porous structure, their chemical modifications, and high affinity to cellular systems [85]. These modifications make chitin-based materials more diverse and functional for soft tissue regeneration. In the same manner, it was found that in the regeneration of ligaments, chitosan-hyaluronic hybrid polymers can provide appropriate environments for cellular adhesion, proliferation, and extracellular membrane (ECM) production, as well as facilitating the biological effects of seeded cells [6].

For vascular tissues, in order to mimic the morphological and mechanical properties of blood vessels and improve long-term patency rates, collagen has been crosslinked with chitosan to generate a tubular scaffold. This biocompatible scaffold proved to have desirable porosity and pliability, enhanced cell adhesion, proliferation, and ECM production [86, 87]. In addition to vascular applications, chitosan/collagen blended scaffolds have also been employed in adipose tissue regeneration. When adipocytes were seeded, the in vitro cytocompatibility and in vivo biocompatibility of scaffolds were confirmed experimentally [88].

Chitosan also has a potential use in skin repair and regeneration subsequent to injuries or burns. A study was performed in which chitosan was cross-linked with silica particles (SiO2), used as a porogen agent and the extractions from the developed membranes demonstrated no cytotoxicity against L-929 cells 24 hours after the culture. In addition, the macroporous membrane exhibited excellent cellular adhesion and proliferation after 24 and 48 hours of culturing, which is why the developed scaffold might be adequate for skin tissue engineering [89]. Chitin-based materials have also demonstrated their potential in maintaining and inducing cell phenotypes used in culturing melanocytes, corneal keratinocytes, and skin keratinocytes [90, 91]. Even in the salivary gland, the morphogenetic efficacy of mesenchyme-derived growth factors is dramatically augmented with the assistance of chitosan. The effects of epithelial morphogenetic factors, such as fibroblast growth factors 7 (FGF7), fibroblast growth factor 10 (FGF10), and hepatocyte growth factor (HGF), have been upregulated in the presence of chitosan [88].

Furthermore, chitosan use in the design of new tissue adhesives was motivated by the fact that it can bind to collagen due to hydrogen bonding and polyanionic–polycationic interactions [88]. There is evidence that hydrogels and meshes of chitosan cross-linked with other biomaterials are useful in the prevention of postoperative abdominal adhesions. A study was developed in which they used thermosensitive hydroxybutyl chitosan (HBC) in a rat side-wall defect-cecum abrasion model for prevention of postoperative abdominal adhesions. HBC is a new derivative of chitosan whose main character is the intelligent response to changing temperature. HBC demonstrated antiadhesive activity as well as being easy to handle during the operation. Therefore, it may be effective in prevention of postoperative adhesions [92]. Another protocol was performed where they compared 3 different types of meshes: Dynamesh-IPoM mesh, a simple polypropylene mesh, and a polypropylene/chitosan mesh. The results were that the polypropylene/chitosan mesh proved to be the least irritating for the recipient's tissue as well as surrounding tissues, as evidenced by the lowest rate of inflammatory reaction within the connective tissue, which guarantees the implant acceptance and the least extensive adhesion to internal organs, and thus the lowest rate of complications [93]. Finally, there was another protocol in which they determined that a chitosan-gelatin modified film modified chitosan film is effective on preventing peritoneal adhesions induced by wound, ischemia, and infection, but the effect is not apparent in foreign body-induced adhesion [94].

Due to the properties that chitosan has shown in reduction and prevention of postoperative intraperitoneal adhesions, it is also widely being studied for its use in repair and regeneration of the abdominal wall in ventral hernias. A study was conducted to investigate the feasibility of using silk

fibroin and chitosan blend scaffolds for ventral hernia repair in guinea pigs [20]. This blended scaffold was compared to a biodegradable human acellular dermal matrix and a nonbiodegradable polypropylene mesh. The investigators concluded that the silk fibroin and chitosan blend scaffold, unlike the mesh and the matrix, showed tissue remodeling in all 3 dimensions, with seamless integration at the interface with adjacent native tissue, the repair sites remained intact, and their mechanical strength was similar to that of the native abdominal wall. Additionally, the scaffold promoted the deposition of new extracellular matrix, uniform vascularization, and cellular infiltration in the repair sites, which contributed to the increase in mechanical strength of the regenerated tissue. Thus, this scaffold is potentially useful in reconstruction and regeneration of the abdominal wall [20]. Furthermore, due to its utility in ventral hernia repair, it might also have a potential use in inguinal hernias and other types of herniation. It might even be useful in the repair of certain congenital defects such as omphalocele or gastroschisis, although to date there are still no apparent models that prove its effectiveness for application in humans for these types of defects.

Specifically speaking about intestinal tissue, its engineering is an emerging field due to a growing demand for intestinal lengthening and replacement procedures secondary to massive bowel resections [95, 96]. Intestinal transplantation is a common treatment but its limitation resides in the high incidence of rejection, availability of donor organs, and the size of the donor graft. The biocompatibility of chitosan was investigated by growing rabbit colonic circular smooth muscle cells on chitosan-coated plates [95]. The cells maintained their spindle-like morphology and preserved their smooth muscle phenotypic markers. Tubular scaffolds were manufactured with central openings composed of chitosan and collagen in a 1 : 1 ratio. Concentrically aligned 3D circular muscle constructs were bioengineered using fibrin-based hydrogel seeded with the colonic circular smooth muscle cells from the rabbit. The muscle constructs contracted in response to acetylcholine (Ach) and potassium chloride (KCl) and they relaxed in response to vasoactive intestinal peptide (VIP). These results demonstrate that chitosan is a biomaterial possibly suitable for intestinal tissue engineering applications [95].

In conclusion, it is safe to say that chitosan has great potential in applications for soft tissue engineering, whether it is used for wound closure or for its potential use in generating specific tissue grafts. Nonetheless, there is still much research to be done in terms of their properties and formation of scaffolds. Next generation scaffolds should be able to carry many different bioactive factors and release them in specific order. To this end, decisions on how to control the separate loading capacity, kinetics of drug release, and rate of substrate degradation are the major challenges to be faced [88].

10. Potential Applications Supported by Its Biological Activity

10.1. Hemostatic Properties. Chitosan is capable of promoting platelet adhesion by initializing a cascade of intracellular signaling which activates glycoproteins IIb/IIa as well as thromboxane A2/ADP, increasing platelet spreading and strengthening the stability of adhesion [97]. Chitosan is available in different presentations, including films, fibers, and hydrogels, and each one of them offers specific advantages in terms of absorption depending in its therapeutic use.

Several studies have proven efficacy of chitosan as a hemostatic agent. However, it has been reported that the hemostatic mechanisms of chitosan are separate from the classic coagulation cascade [62]. The hemostatic effect in chitosan is achieved from the direct interaction with platelets, mainly in alpha granules. The intracellular signaling induces PDGF-AB and TGF-β1 release. An increased rate in the PDGF-AB has been found, as much as up to 130%, with the use of chitosan compared to a control group [98]. Chitosan can be used in medical and surgical procedures by direct application on bleeding surfaces, using several presentations such as powder, solutions, coatings, films, hydrogels, compounded filaments, and more. Nevertheless, its clinical use will depend on the application technique used as well as the type of wound that it is applied on. Many investigators have described the hemostatic applications for chitosan; however, different presentations have been used in each study; that is, why results should be analyzed according to the different groups, depending on the physical form of the material [99].

10.2. Liver Repair Application. There are three crucial factors for successful use of chitosan in surgery: it must be placed in the intra-abdominal cavity, it must have good bonding to the surface of the lesion, and it must be able to maintain proper hemostasis.

A study compared the effectiveness of a freeze-dry chitosan graft versus the use of sponge gauze in a venous bleeding due to a severe liver lesion in a pig model. The animal model involves extensive vascular damage, as well as damage to the liver parenchyma. Several vascular lesions of approximately 1 cm in diameter were made. The outcome reported with the chitosan graft had less blood loss ($p < 0.01$) compared to the group of sponges (264 mL and 2,879 mL, resp.) [100].

In further investigations the hemostatic effects of chitosan as a solution have been previously analyzed. The results of a lingual incision in a heparinized animal model according to the evaluations with electron microscopy concluded that the incisions treated with chitosan showed a disturbance in the morphology of red cells, as well as an unusual affinity among the red cells. It was reported that the red cell fractions that interacted with chitosan reduced bleeding in 60%, reaching hemostasis at 800 μg/mL [99].

10.3. Healing Properties. In another study it was found that, by means of chitosan hydrogel application on skin wounds in diabetic mice, the wound shrinking speed improved and wound closure was significantly faster. The chitosan hydrogel combined with fibroblast growth factor type 2 was seen to accelerate the closing process even further. Histology examination showed that the combination of chitosan and fibroblast growth factor type 2 fostered the formation of granulation tissue, capillary network, and epithelialization [101].

The regenerative properties of chitosan are based on a matrix building capacity that is adequate for growth and activation of macrophages and proliferative cells in three-dimensional tissue. A comparative study between wounds treated with chitosan and a control group treated only with saline solution was conducted in a dog animal model. The wounds were clinically assessed throughout the study and inspected histologically once the animal was euthanized. Clinically, complete healing was achieved in the chitosan-treated group after three weeks, while in the control group it took four weeks. A complete repair of epidermal cells with a keratin layer associated with connective tissue proliferation was seen. In the chitosan group a collagen network of fibers produced by fibroblasts was found, which surrounded the neovasculature of the wound, while in the control group hyalinosis of subcutaneous tissue occurred [102].

10.4. Chitosan Composites for Bone and Cartilage Regeneration. Chitosan composites have been synthesized for hard tissue regeneration, as in the case of bone and cartilage.

Evaluation of chitosan composites for bone tissue regeneration is based on physicochemical and biological characterizations. Physicochemical characterization comprises the study of homogeneity, purity, percentage composition, chemical bonding, thermic stability, mechanical tests, and incubation on simulated body fluid [103, 104]. On the other hand biological evaluation includes the test in in vitro culture cells (MC-3T3, hFOB, MG63, and bone marrow stem cells) [105–108]. These assays evaluate composite cytocompatibility and cytotoxicity, in addition to its intinsic capacity of induction of cellular differentiation [109]. Finally the efficacy in the treatment of surgical defects on animal models is evaluated [21, 107, 110].

In the first place, chitosan as a matrix allows for biocompatibility of an implantable material, and in the second, it allows for the interaction or combination with inducer materials for tissue regeneration. In this sense, the use of chitosan composites for tissue regeneration in experimental models is a promising strategy for treatment of skeletal and joint diseases [76, 111, 112].

In the case of bone tissue engineering, chitosan matrices have been combined with osteogenic materials, like hydroxyapatite [103, 108, 109, 111], calcium phosphate and sulfate [113, 114], and others [115–117]. The purpose of the combination of those biomaterials is to obtain organic and inorganic composites that simulate the bone structure [118].

The evaluation of chitosan composites in osteoblast culture is an important factor to identify its biocompatibility. In in vitro assays with the MC3T3 cell line, which comes from calvarial murine osteoblasts, cross-linked membrane of chitosan with tripolyphosphate showed the same values in MTT assay of cell viability compared to controls; results were observed in composites compound of chitosan with calcium phosphate, and chitosan with the release of bone morphogenic protein type-2, concluding that those membranes are biocompatible with osteoblasts. Additionally it has mechanical properties that make it a good implantable composite in bone defects [113, 119].

When bone tissue is damaged by trauma, cancer, or infection, a source of autogenous bone tissue or replacement materials is needed to regenerate the compromised tissue. Experimental animal models are a good resource to understand how biological and pathological conditions participate in the healing of bone tissue. In this sense, chitosan composites can be used to induce bone healing and regeneration.

Chitosan composites have been tested in bone defects in experimental models successfully for bone regeneration. Chitosan hydrogel, gelifiable by blue light, was used for BMP-2 release and showed good bone regeneration in a femoral defect in rat [120]. Similar results were observed with the use of a lyophilized porous membrane, a compound of chitosan and hydroxyapatite, in a calvarial defect in rat, the composite membrane filled up the defect as compared to a control, in addition, the presence of osteogenic markers was more abundant in the experimental group [121].

Osteogenesis is the process where osteoblast cells proliferate from mesenchymal cells and deposit extracellular matrix; at the end of the bone defect these cells differentiate into mature osteocytes. All of this tissue process includes the expression of multiple bone markers and enzymes involved in cell maturation and bone calcification.

Chitosan/nanohydroxyapatite composites have been more relevant for tissue engineering, because of its ability to induce a good proliferative response in osteoblasts, and in a tibial defect in a rabbit it showed good bone regeneration at 8 weeks seen by microcomputarized tomography [122].

Joint defects are common in elderly people, caused by rheumatoid arthritis and dehydration of cartilage tissue in the entire body or by the lifting of heavy loads with the corresponding joint wear, leading to the total dependence of joint replacement therapy.

In the case of cartilage tissue regeneration, chitosan composites have been designed to form hydrogels. These composites allow for the inclusion of cells and molecules for cartilage regeneration. The most combined inducer agent of cartilage regeneration is collagen type II, this is the main protein in cartilage tissue, and it enhances the adhesion and formation of clusters of chondrocytes in vitro [15, 123, 124], a requirement for cartilage regeneration. Collagen II and chondroitin sulfate in chitosan hydrogels stimulate chondrocytes attachment in a blue light gelification composite, it also induces the mesenchymal stem cells differentiation to chondrocytes in vitro [125], and similar results have been observed with chitosan hydrogel with alginate and fibroin. In order to follow the seeding cells on chitosan composites, the next step in regeneration is the formation of functional tissue; collagen II expression by chondroblasts and chondrocytes is a determinant factor in cartilage formation, and it has been observed in the glycerophosphate-chitosan hydrogel with silk fibrils, where chondrocyte phenotype is maintained for the expression of glycosaminoglycans and type II collagen in vitro [126], as obtained with alginate and fibroin in chitosan hydrogels [127]. These findings suggest that chitosan can support the addition of an inducer material and also is a biocompatible material for cartilage tissue engineering. Extracellular matrix deposition is a key factor to recognize

biocompatibility and normal cell function, in addition a 3D matrix for growth tissue by proliferation and differentiation of precursor cells. In the case of chondroblast and chondrocytes, production of collagen II is a functional tissue determinant, and this has been found in glycerophosphate-chitosan hydrogel and silk fibrils, which stimulates the production of collagen II and glycosaminoglycans by chondrocytes in vitro [126].

The polylactide acid-chitosan membranes with collagen provide a laminate matrix with mechanical properties similar to cartilage, but in addition they have worked as a support for chondrocytes from rabbit cartilage [128], and this opens the possibility to use chitosan composites in the regeneration of cartilage defects [21], as in the case of arthritis or joint cartilage damage from aging.

A biomaterial combination of chitosan with polycaprolactone [112, 124, 129], silk fibrils [126], genipin [15], chondroitin sulfate [130], and polyester [14] has been designed with the purpose of obtaining composites with properties that resemble those of cartilage, and it also provides a proper environment for extracellular matrix deposition, cell viability, and differentiation.

This perspective allows for understanding the potential properties of chitosan composites in hard tissue regeneration. In summary, chitosan composites provide physical and chemical and mechanical support, cell attachment, proliferation, and differentiation, with the corresponding biocompatibility to induce the bone and cartilage tissue regeneration.

11. Conclusions

Regenerative medicine is facing new challenges in the way to induce tissue repair in live tissue. Advances have led to the availability of bioactive compounds for damaged tissue. Such compounds must have a regenerative effect and foster wound repair, with the least possible morbidity and with high biocompatibility conditions. Chitosan polymers have been proven to serve as scaffolds that induce tissue regeneration, but beyond that, they are considered to be an ideal polymer for making bioactive compounds [131]. This is possible because there is a potential synergy in their byproducts, when combined with growth factors and stem cells, either of mesenchymal origin or neural origin. Additional studies should try to confirm the translational issues on the role of bioactive polymers and their real impact on regenerative medicine.

Abbreviations

DD: Degree of deacetylation
TIPS: Thermally induced phase separation
ECMD: Extracellular matrix deposits
ECM: Extracellular membrane.

Conflict of Interests

The authors report no conflict of interests.

References

[1] C. Shi, Y. Zhu, X. Ran, M. Wang, Y. Su, and T. Cheng, "Therapeutic potential of chitosan and its derivatives in regenerative medicine," *Journal of Surgical Research*, vol. 133, no. 2, pp. 185–192, 2006.

[2] Y. Fung, "A proposal to the National science Foundation for an Engineering Research Centre at USCD," UCSD 865023, Center for the Engineering of Living Tissues, 2001.

[3] R. Langer and J. P. Vacanti, "Tissue engineering," *Science*, vol. 260, no. 5110, pp. 920–926, 1993.

[4] I.-Y. Kim, S.-J. Seo, H.-S. Moon et al., "Chitosan and its derivatives for tissue engineering applications," *Biotechnology Advances*, vol. 26, no. 1, pp. 1–21, 2008.

[5] R. Langer and D. A. Tirrell, "Designing materials for biology and medicine," *Nature*, vol. 428, no. 6982, pp. 487–492, 2004.

[6] T. Funakoshi, T. Majima, N. Iwasaki et al., "Novel chitosan-based hyaluronan hybrid polymer fibers as a scaffold in ligament tissue engineering," *Journal of Biomedical Materials Research Part A*, vol. 74, no. 3, pp. 338–346, 2005.

[7] C.-M. Han, L.-P. Zhang, J.-Z. Sun, H.-F. Shi, J. Zhou, and C.-Y. Gao, "Application of collagen-chitosan/fibrin glue asymmetric scaffolds in skin tissue engineering," *Journal of Zhejiang University Science B*, vol. 11, no. 7, pp. 524–530, 2010.

[8] S. G. Caridade, C. Monge, F. Gilde, T. Boudou, J. F. Mano, and C. Picart, "Free-standing polyelectrolyte membranes made of chitosan and alginate," *Biomacromolecules*, vol. 14, no. 5, pp. 1653–1660, 2013.

[9] S. S. Silva, S. G. Caridade, J. F. Mano, and R. L. Reis, "Effect of crosslinking in chitosan/aloe vera-based membranes for biomedical applications," *Carbohydrate Polymers*, vol. 98, no. 1, pp. 581–588, 2013.

[10] T.-L. Yang and T.-H. Young, "The enhancement of submandibular gland branch formation on chitosan membranes," *Biomaterials*, vol. 29, no. 16, pp. 2501–2508, 2008.

[11] L. Zhang, Q. Ao, A. Wang et al., "A sandwich tubular scaffold derived from chitosan for blood vessel tissue engineering," *Journal of Biomedical Materials Research Part A*, vol. 77, no. 2, pp. 277–284, 2006.

[12] S. Ge, N. Zhao, L. Wang et al., "Bone repair by periodontal ligament stem cell-seeded nanohydroxyapatite-chitosan scaffold," *International Journal of Nanomedicine*, vol. 7, pp. 5405–5414, 2012.

[13] X. Wu, L. Black, G. Santacana-Laffitte, and C. W. Patrick Jr., "Preparation and assessment of glutaraldehyde-crosslinked collagen–chitosan hydrogels for adipose tissue engineering," *Journal of Biomedical Materials Research Part A*, vol. 81, no. 1, pp. 59–65, 2007.

[14] M. L. A. da Silva, A. Crawford, J. M. Mundy et al., "Chitosan/polyester-based scaffolds for cartilage tissue engineering: assessment of extracellular matrix formation," *Acta Biomaterialia*, vol. 6, no. 3, pp. 1149–1157, 2010.

[15] L.-P. Yan, Y.-J. Wang, L. Ren et al., "Genipin-cross-linked collagen/chitosan biomimetic scaffolds for articular cartilage tissue engineering applications," *Journal of Biomedical Materials Research, Part A*, vol. 95, no. 2, pp. 465–475, 2010.

[16] J. M. Silva, N. Georgi, R. Costa et al., "Nanostructured 3D constructs based on chitosan and chondroitin sulphate multilayers for cartilage tissue engineering," *PLoS ONE*, vol. 8, no. 2, Article ID e55451, 2013.

[17] Y.-Y. Hsueh, Y.-J. Chang, T.-C. Huang et al., "Functional recoveries of sciatic nerve regeneration by combining chitosan-coated conduit and neurosphere cells induced from adipose-derived stem cells," *Biomaterials*, vol. 35, no. 7, pp. 2234–2244, 2014.

[18] N. Tanaka, I. Matsumoto, M. Suzuki et al., "Chitosan tubes can restore the function of resected phrenic nerves," *Interactive CardioVascular and Thoracic Surgery*, 2015.

[19] N. Boucard, C. Viton, D. Agay et al., "The use of physical hydrogels of chitosan for skin regeneration following third-degree burns," *Biomaterials*, vol. 28, no. 24, pp. 3478–3488, 2007.

[20] A. S. Gobin, C. E. Butler, and A. B. Mathur, "Repair and regeneration of the abdominal wall musculofascial defect using silk fibroin-chitosan blend," *Tissue Engineering*, vol. 12, no. 12, pp. 3383–3394, 2006.

[21] T. Hao, N. Wen, J.-K. Cao et al., "The support of matrix accumulation and the promotion of sheep articular cartilage defects repair in vivo by chitosan hydrogels," *Osteoarthritis and Cartilage*, vol. 18, no. 2, pp. 257–265, 2010.

[22] D. Meng, L. Dong, Y. Wen, and Q. Xie, "Effects of adding resorbable chitosan microspheres to calcium phosphate cements for bone regeneration," *Materials Science and Engineering: C*, vol. 47, pp. 266–272, 2015.

[23] M. A. Lizarbe, "Sustitutivos de tejidos: de los biomateriales a la ingeniería tisular," *Revista de la Real Academia de Ciencias Exactas, Físicas y Naturales*, vol. 101, no. 1, pp. 227–249, 2007.

[24] L. S. Nair and C. T. Laurencin, "Biodegradable polymers as biomaterials," *Progress in Polymer Science*, vol. 32, no. 8-9, pp. 762–798, 2007.

[25] S. Ramakrishna, J. Mayer, E. Wintermantel, and K. W. Leong, "Biomedical applications of polymer-composite materials: a review," *Composites Science and Technology*, vol. 61, no. 9, pp. 1189–1224, 2001.

[26] B. D. Ratner, *Biomaterials Science: An Introduction to Materials in Medicine*, Academic Press, 2004.

[27] E. Khor and L. Y. Lim, "Implantable applications of chitin and chitosan," *Biomaterials*, vol. 24, no. 13, pp. 2339–2349, 2003.

[28] R. A. Muzzarelli, C. Jeuniaux, and G. W. Gooday, *Chitin in Nature and Technology*, Springer, 1986.

[29] B. Dhandayuthapani, Y. Yoshida, T. Maekawa, and D. S. Kumar, "Polymeric scaffolds in tissue engineering application: a review," *International Journal of Polymer Science*, vol. 2011, Article ID 290602, 19 pages, 2011.

[30] G. Lodhi, Y.-S. Kim, J.-W. Hwang et al., "Chitooligosaccharide and its derivatives: preparation and biological applications," *BioMed Research International*, vol. 2014, Article ID 654913, 13 pages, 2014.

[31] K. Rudall, "Chitin and its association with other molecules," *Journal of Polymer Science C: Polymer Symposia*, vol. 28, no. 1, pp. 83–102, 1969.

[32] P. J. VandeVord, H. W. T. Matthew, S. P. Desilva, L. Mayton, B. Wu, and P. H. Wooley, "Evaluation of the biocompatibility of a chitosan scaffold in mice," *Journal of Biomedical Materials Research*, vol. 59, no. 3, pp. 585–590, 2002.

[33] M. N. V. R. Kumar, "A review of chitin and chitosan applications," *Reactive and Functional Polymers*, vol. 46, no. 1, pp. 1–27, 2000.

[34] D. W. Lee, H. Lim, H. N. Chong, and W. S. Shim, "Advances in chitosan material and its hybrid derivatives: a review," *The Open Biomaterials Journal*, vol. 1, no. 1, pp. 10–20, 2009.

[35] N. H. Foda, H. M. El-Laithy, and M. I. Tadros, "Implantable biodegradable sponges: effect of interpolymer complex formation of chitosan with gelatin on the release behavior of tramadol hydrochloride," *Drug Development and Industrial Pharmacy*, vol. 33, no. 1, pp. 7–17, 2007.

[36] M. Rinaudo, "Chitin and chitosan: properties and applications," *Progress in Polymer Science*, vol. 31, no. 7, pp. 603–632, 2006.

[37] K. V. Harish Prashanth and R. N. Tharanathan, "Chitin/chitosan: modifications and their unlimited application potential—an overview," *Trends in Food Science & Technology*, vol. 18, no. 3, pp. 117–131, 2007.

[38] A. Chenite, C. Chaput, D. Wang et al., "Novel injectable neutral solutions of chitosan form biodegradable gels in situ," *Biomaterials*, vol. 21, no. 21, pp. 2155–2161, 2000.

[39] H. Yi, L.-Q. Wu, W. E. Bentley et al., "Biofabrication with chitosan," *Biomacromolecules*, vol. 6, no. 6, pp. 2881–2894, 2005.

[40] C. Chatelet, O. Damour, and A. Domard, "Influence of the degree of acetylation on some biological properties of chitosan films," *Biomaterials*, vol. 22, no. 3, pp. 261–268, 2001.

[41] R. A. A. Muzzarelli, "Human enzymatic activities related to the therapeutic administration of chitin derivatives," *Cellular and Molecular Life Sciences*, vol. 53, no. 2, pp. 131–140, 1997.

[42] K. Tomihata and Y. Ikada, "In vitro and in vivo degradation of films of chitin and its deacetylated derivatives," *Biomaterials*, vol. 18, no. 7, pp. 567–575, 1997.

[43] D. K. Singh and A. R. Ray, "Biomedical applications of chitin, chitosan, and their derivatives," *Journal of Macromolecular Science C: Polymer Reviews*, vol. 40, no. 1, pp. 69–83, 2000.

[44] L. Zeng, C. Qin, W. Wang, W. Chi, and W. Li, "Absorption and distribution of chitosan in mice after oral administration," *Carbohydrate Polymers*, vol. 71, no. 3, pp. 435–440, 2008.

[45] X.-G. Chen, L. Zheng, Z. Wang, C.-Y. Lee, and H.-J. Park, "Molecular affinity and permeability of different molecular weight chitosan membranes," *Journal of Agricultural and Food Chemistry*, vol. 50, no. 21, pp. 5915–5918, 2002.

[46] S. Y. Chae, M.-K. Jang, and J.-W. Nah, "Influence of molecular weight on oral absorption of water soluble chitosans," *Journal of Controlled Release*, vol. 102, no. 2, pp. 383–394, 2005.

[47] A. Sánchez, M. R. S. Ballesteros, J. R. Vega-Baudrit, and M. Rojas, "Utilización de soportes de hidrogel de quitosano obtenidos a partir de desechos del camarón langostino (*Pleuroncodes planipes*) para el crecimiento 'in vitro' de fibroblastos humanos," *Revista Iberoamericana de Polímeros*, vol. 8, no. 5, pp. 347–362, 2007.

[48] M.-H. Ho, P.-Y. Kuo, H.-J. Hsieh et al., "Preparation of porous scaffolds by using freeze-extraction and freeze-gelation methods," *Biomaterials*, vol. 25, no. 1, pp. 129–138, 2004.

[49] D. W. Hutmacher, "Scaffolds in tissue engineering bone and cartilage," *Biomaterials*, vol. 21, no. 24, pp. 2529–2543, 2000.

[50] S. V. Madihally and H. W. T. Matthew, "Porous chitosan scaffolds for tissue engineering," *Biomaterials*, vol. 20, no. 12, pp. 1133–1142, 1999.

[51] L. Ma, C. Gao, Z. Mao et al., "Collagen/chitosan porous scaffolds with improved biostability for skin tissue engineering," *Biomaterials*, vol. 24, no. 26, pp. 4833–4841, 2003.

[52] I. J. Roh and I.-C. Kwon, "Fabrication of a pure porous chitosan bead matrix: influences of phase separation on the microstructure," *Journal of Biomaterials Science, Polymer Edition*, vol. 13, no. 7, pp. 769–782, 2002.

[53] H. Liu, F. Yao, Y. Zhou et al., "Porous poly (DL-lactic acid) modified chitosan-gelatin scaffolds for tissue engineering,"

Journal of Biomaterials Applications, vol. 19, no. 4, pp. 303–322, 2005.

[54] H. Kiuchi, W. Kai, and Y. Inoue, "Preparation and characterization of poly(ethylene glycol) crosslinked chitosan films," *Journal of Applied Polymer Science*, vol. 107, no. 6, pp. 3823–3830, 2008.

[55] I. Adekogbe and A. Ghanem, "Fabrication and characterization of DTBP-crosslinked chitosan scaffolds for skin tissue engineering," *Biomaterials*, vol. 26, no. 35, pp. 7241–7250, 2005.

[56] J. Stefan, B. Lorkowska-Zawicka, K. Kaminski, K. Szczubialka, M. Nowakowska, and R. Korbut, "The current view on biological potency of cationically modified chitosan," *Journal of Physiology and Pharmacology*, vol. 65, no. 3, pp. 341–347, 2014.

[57] T. Dvir, O. Tsur-Gang, and S. Cohen, "'Designer' scaffolds for tissue engineering and regeneration," *Israel Journal of Chemistry*, vol. 45, no. 4, pp. 487–494, 2005.

[58] S. Şenel and S. J. McClure, "Potential applications of chitosan in veterinary medicine," *Advanced Drug Delivery Reviews*, vol. 56, no. 10, pp. 1467–1480, 2004.

[59] A. Di Martino, M. Sittinger, and M. V. Risbud, "Chitosan: a versatile biopolymer for orthopaedic tissue-engineering," *Biomaterials*, vol. 26, no. 30, pp. 5983–5990, 2005.

[60] J. Jagur-Grodzinski, "Biomedical application of functional polymers," *Reactive and Functional Polymers*, vol. 39, no. 2, pp. 99–138, 1999.

[61] T. A. Khan, K. K. Peh, and H. S. Ch'ng, "Mechanical, bioadhesive strength and biological evaluations of chitosan films for wound dressing," *Journal of Pharmacy & Pharmaceutical Sciences*, vol. 3, no. 3, pp. 303–311, 2000.

[62] S. B. Rao and C. P. Sharma, "Use of chitosan as a biomaterial: studies on its safety and hemostatic potential," *Journal of Biomedical Materials Research*, vol. 34, no. 1, pp. 21–28, 1997.

[63] H. Ueno, T. Mori, and T. Fujinaga, "Topical formulations and wound healing applications of chitosan," *Advanced Drug Delivery Reviews*, vol. 52, no. 2, pp. 105–115, 2001.

[64] S. M. Oliveira, D. Q. Mijares, G. Turner, I. F. Amaral, M. A. Barbosa, and C. C. Teixeira, "Engineering endochondral bone: *in vivo* studies," *Tissue Engineering Part A*, vol. 15, no. 3, pp. 635–643, 2009.

[65] I. F. Amaral, P. L. Granja, and M. A. Barbosa, "Chemical modification of chitosan by phosphorylation: an XPS, FT-IR and SEM study," *Journal of Biomaterials Science, Polymer Edition*, vol. 16, no. 12, pp. 1575–1593, 2005.

[66] I. F. Amaral, M. Lamghari, S. R. Sousa, P. Sampaio, and M. A. Barbosa, "Rat bone marrow stromal cell osteogenic differentiation and fibronectin adsorption on chitosan membranes: the effect of the degree of acetylation," *Journal of Biomedical Materials Research Part A*, vol. 75, no. 2, pp. 387–397, 2005.

[67] A. Lahiji, A. Sohrabi, D. S. Hungerford, and C. G. Frondoza, "Chitosan supports the expression of extracellular matrix proteins in human osteoblasts and chondrocytes," *Journal of Biomedical Materials Research*, vol. 51, no. 4, pp. 586–595, 2000.

[68] Y. Yuan, P. Zhang, Y. Yang, X. Wang, and X. Gu, "The interaction of Schwann cells with chitosan membranes and fibers in vitro," *Biomaterials*, vol. 25, no. 18, pp. 4273–4278, 2004.

[69] M. Prasitsilp, R. Jenwithisuk, K. Kongsuwan, N. Damrongchai, and P. Watts, "Cellular responses to chitosan in vitro: the importance of deacetylation," *Journal of Materials Science: Materials in Medicine*, vol. 11, no. 12, pp. 773–778, 2000.

[70] T. Freier, H. S. Koh, K. Kazazian, and M. S. Shoichet, "Controlling cell adhesion and degradation of chitosan films by N-acetylation," *Biomaterials*, vol. 26, no. 29, pp. 5872–5878, 2005.

[71] T. Freier, R. Montenegro, H. S. Koh, and M. S. Shoichet, "Chitin-based tubes for tissue engineering in the nervous system," *Biomaterials*, vol. 26, no. 22, pp. 4624–4632, 2005.

[72] I. F. Amaral, A. L. Cordeiro, P. Sampaio, and M. A. Barbosa, "Attachment, spreading and short-term proliferation of human osteoblastic cells cultured on chitosan films with different degrees of acetylation," *Journal of Biomaterials Science, Polymer Edition*, vol. 18, no. 4, pp. 469–485, 2007.

[73] I. F. Amaral, P. Sampaio, and M. A. Barbosa, "Three-dimensional culture of human osteoblastic cells in chitosan sponges: the effect of the degree of acetylation," *Journal of Biomedical Materials Research, Part A*, vol. 76, no. 2, pp. 335–346, 2006.

[74] K. Nishimura, S. Nishimura, N. Nishi, S. Tokura, and I. Azuma, "Immunological activity of chitin derivatives," in *Chitin in Nature and Technology*, R. Muzzarelli, C. Jeuniaux, and G. Gooday, Eds., pp. 477–483, Springer, New York, NY, USA, 1986.

[75] T. Mori, M. Murakami, M. Okumura, T. Kadosawa, T. Uede, and T. Fujinaga, "Mechanism of macrophage activation by chitin derivatives," *Journal of Veterinary Medical Science*, vol. 67, no. 1, pp. 51–56, 2005.

[76] S. Ge, N. Zhao, L. Wang et al., "Bone repair by periodontal ligament stem cell-seeded nanohydroxyapatite-chitosan scaffold," *International Journal of Nanomedicine*, vol. 7, pp. 5405–5414, 2012.

[77] J. M. Dang and K. W. Leong, "Natural polymers for gene delivery and tissue engineering," *Advanced Drug Delivery Reviews*, vol. 58, no. 4, pp. 487–499, 2006.

[78] R. A. A. Muzzarelli, "Chitins and chitosans for the repair of wounded skin, nerve, cartilage and bone," *Carbohydrate Polymers*, vol. 76, no. 2, pp. 167–182, 2009.

[79] Y.-G. Ko, N. Kawazoe, T. Tateishi, and G. Chen, "Preparation of chitosan scaffolds with a hierarchical porous structure," *Journal of Biomedical Materials Research Part B: Applied Biomaterials*, vol. 93, no. 2, pp. 341–350, 2010.

[80] S.-J. Lin, S.-H. Jee, W.-C. Hsaio, S.-J. Lee, and T.-H. Young, "Formation of melanocyte spheroids on the chitosan-coated surface," *Biomaterials*, vol. 26, no. 12, pp. 1413–1422, 2005.

[81] T.-W. Huang, Y.-H. Young, P.-W. Cheng, Y.-H. Chan, and T.-H. Young, "Culture of nasal epithelial cells using chitosan-based membranes," *The Laryngoscope*, vol. 119, no. 10, pp. 2066–2070, 2009.

[82] T. Kean, S. Roth, and M. Thanou, "Trimethylated chitosans as non-viral gene delivery vectors: cytotoxicity and transfection efficiency," *Journal of Controlled Release*, vol. 103, no. 3, pp. 643–653, 2005.

[83] A. Matsuda, H. Kobayashi, S. Itoh, K. Kataoka, and J. Tanaka, "Immobilization of laminin peptide in molecularly aligned chitosan by covalent bonding," *Biomaterials*, vol. 26, no. 15, pp. 2273–2279, 2005.

[84] S. Itoh, A. Matsuda, H. Kobayashi, S. Ichinose, K. Shinomiya, and J. Tanaka, "Effects of a laminin peptide (YIGSR) immobilized on crab-tendon chitosan tubes on nerve regeneration," *Journal of Biomedical Materials Research, Part B: Applied Biomaterials*, vol. 73, no. 2, pp. 375–382, 2005.

[85] M. J. Simões, A. Gärtner, Y. Shirosaki et al., "In vitro and in vivo chitosan membranes testing for peripheral nerve reconstruction," *Acta Medica Portuguesa*, vol. 24, no. 1, pp. 43–52, 2011.

[86] C. Zhu, D. Fan, Z. Duan et al., "Initial investigation of novel human-like collagen/chitosan scaffold for vascular tissue engineering," *Journal of Biomedical Materials Research Part A*, vol. 89, no. 3, pp. 829–840, 2009.

[87] H. Shi, C. Han, Z. Mao, L. Ma, and C. Gao, "Enhanced angiogenesis in porous collagen-chitosan scaffolds loaded with angiogenin," *Tissue Engineering Part A*, vol. 14, no. 11, pp. 1775–1785, 2008.

[88] M. A. Barbosa, A. P. Pêgo, and I. F. Amaral, "2.213—Chitosan," in *Comprehensive Biomaterials*, P. Ducheyne, Ed., pp. 221–237, Elsevier, Oxford, UK, 2011.

[89] L. Mei, D. Hu, J. Ma, X. Wang, Y. Yang, and J. Liu, "Preparation, characterization and evaluation of chitosan macroporous for potential application in skin tissue engineering," *International Journal of Biological Macromolecules*, vol. 51, no. 5, pp. 992–997, 2012.

[90] J. S. Choi and H. S. Yoo, "Pluronic/chitosan hydrogels containing epidermal growth factor with wound-adhesive and photo-crosslinkable properties," *Journal of Biomedical Materials Research, Part A*, vol. 95, no. 2, pp. 564–573, 2010.

[91] Y.-H. Chen, I.-J. Wang, and T.-H. Young, "Formation of keratocyte spheroids on chitosan-coated surface can maintain keratocyte phenotypes," *Tissue Engineering Part A*, vol. 15, no. 8, pp. 2001–2013, 2009.

[92] C. Wei, C. Hou, Q. Gu, L. Jiang, B. Zhu, and A. Sheng, "Efficacy of thermosensitive hydroxybutyl chitosan in prevention of post-operative abdominal adhesions in a rat model," *Iranian Polymer Journal*, vol. 18, no. 5, pp. 355–364, 2009.

[93] P. Ławniczak, B. Grobelski, and Z. Pasieka, "Properties comparison of intraperitoneal hernia meshes in reconstruction of the abdominal wall—animal model study," *Polish Journal of Surgery*, vol. 83, no. 1, pp. 19–26, 2011.

[94] X.-L. Zhou, S.-W. Chen, G.-D. Liao et al., "Preventive effect of gelatinizedly-modified chitosan film on peritoneal adhesion of different types," *World Journal of Gastroenterology*, vol. 13, no. 8, pp. 1262–1267, 2007.

[95] E. Zakhem, S. Raghavan, R. R. Gilmont, and K. N. Bitar, "Chitosan-based scaffolds for the support of smooth muscle constructs in intestinal tissue engineering," *Biomaterials*, vol. 33, no. 19, pp. 4810–4817, 2012.

[96] T.-L. Yang, "Chitin-based materials in tissue engineering: applications in soft tissue and epithelial organ," *International Journal of Molecular Sciences*, vol. 12, no. 3, pp. 1936–1963, 2011.

[97] C.-C. Wu, F.-N. Ko, T.-F. Huang, and C.-M. Teng, "Mechanisms-regulated platelet spreading after initial platelet contact with collagen," *Biochemical and Biophysical Research Communications*, vol. 220, no. 2, pp. 388–393, 1996.

[98] H. Mercy, A. Halim, and A. Hussein, "Chitosan-derivatives as hemostatic agents: their role in tissue regeneration," *Regenerative Research*, vol. 1, no. 1, pp. 38–46, 2012.

[99] H. S. Whang, W. Kirsch, Y. H. Zhu, C. Z. Yang, and S. M. Hudson, "Hemostatic agents derived from chitin and chitosan," *Journal of Macromolecular Science, Part C: Polymer Reviews*, vol. 45, no. 4, pp. 309–323, 2005.

[100] A. E. Pusateri, S. J. McCarthy, K. W. Gregory et al., "Effect of a chitosan-based hemostatic dressing on blood loss and survival in a model of severe venous hemorrhage and hepatic injury in swine," *The Journal of Trauma-Injury Infection & Critical Care*, vol. 54, no. 1, pp. 177–182, 2003.

[101] K. Obara, M. Ishihara, T. Ishizuka et al., "Photocrosslinkable chitosan hydrogel containing fibroblast growth factor-2 stimulates wound healing in healing-impaired db/db mice," *Biomaterials*, vol. 24, no. 20, pp. 3437–3444, 2003.

[102] N. E.-H. Inas and A. A. Kawkab, "Application of chitosan for wound repair in dogs," *Life Science Journal*, vol. 1, no. 9, article 2201, 2012.

[103] K. R. Mohamed, Z. M. El-Rashidy, and A. A. Salama, "In vitro properties of nano-hydroxyapatite/chitosan biocomposites," *Ceramics International*, vol. 37, no. 8, pp. 3265–3271, 2011.

[104] L. Kong, Y. Gao, W. Cao, Y. Gong, N. Zhao, and X. Zhang, "Preparation and characterization of nano-hydroxyapatite/chitosan composite scaffolds," *Journal of Biomedical Materials Research Part A*, vol. 75, no. 2, pp. 275–282, 2005.

[105] Y. Chen, Z. Huang, X. Li et al., "In vitro biocompatibility and osteoblast differentiation of an injectable chitosan/nano-hydroxyapatite/collagen scaffold," *Journal of Nanomaterials*, vol. 2012, Article ID 401084, 6 pages, 2012.

[106] K. R. Mohamed, H. H. Beherei, and Z. M. El-Rashidy, "In vitro study of nano-hydroxyapatite/chitosan-gelatin composites for bio-applications," *Journal of Advanced Research*, vol. 5, no. 2, pp. 201–208, 2014.

[107] S. W. Whu, K.-C. Hung, K.-H. Hsieh, C.-H. Chen, C.-L. Tsai, and S.-H. Hsu, "In vitro and in vivo evaluation of chitosan-gelatin scaffolds for cartilage tissue engineering," *Materials Science & Engineering C*, vol. 33, no. 5, pp. 2855–2863, 2013.

[108] C. Xianmiao, L. Yubao, Z. Yi, Z. Li, L. Jidong, and W. Huanan, "Properties and in vitro biological evaluation of nano-hydroxyapatite/chitosan membranes for bone guided regeneration," *Materials Science and Engineering C*, vol. 29, no. 1, pp. 29–35, 2009.

[109] S. M. Zo, D. Singh, A. Kumar, Y. W. Cho, T. H. Oh, and S. S. Han, "Chitosan-hydroxyapatite macroporous matrix for bone tissue engineering," *Current Science*, vol. 103, no. 12, pp. 1438–1446, 2012.

[110] J. G. Saltarrelli Junior and D. P. Mukherjee, "In vivo testing of a bone graft containing chitosan, calcium sulfate and osteoblasts in a paste form in a critical size defect model in rats," *Journal of Biomedical Science and Engineering*, vol. 02, pp. 24–29, 2009.

[111] J. Zhang, G. Liu, Q. Wu, J. Zuo, Y. Qin, and J. Wang, "Novel mesoporous hydroxyapatite/chitosan composite for bone repair," *Journal of Bionic Engineering*, vol. 9, no. 2, pp. 243–251, 2012.

[112] S. C. Neves, L. S. Moreira Teixeira, L. Moroni et al., "Chitosan/Poly(ε-caprolactone) blend scaffolds for cartilage repair," *Biomaterials*, vol. 32, no. 4, pp. 1068–1079, 2011.

[113] M. D. Weir and H. H. K. Xu, "Osteoblastic induction on calcium phosphate cement-chitosan constructs for bone tissue engineering," *Journal of Biomedical Materials Research, Part A*, vol. 94, no. 1, pp. 223–233, 2010.

[114] K. Dahlan, S. U. Dewi, A. Nurlaila, and D. Soejoko, "Synthesis and characterization of calcium phosphate/chitosan composites," *International Journal of Basic & Applied Sciences*, vol. 12, no. 1, pp. 50–57, 2012.

[115] G.-J. Lai, K. T. Shalumon, S.-H. Chen, and J.-P. Chen, "Composite chitosan/silk fibroin nanofibers for modulation of osteogenic differentiation and proliferation of human mesenchymal stem cells," *Carbohydrate Polymers*, vol. 111, pp. 288–297, 2014.

[116] J. H. Lee and B. O. Jeong, "The effect of hyaluronate-carboxymethyl cellulose on bone graft substitute healing in a rat spinal fusion model," *Journal of Korean Neurosurgical Society*, vol. 50, no. 5, pp. 409–414, 2011.

[117] M. Lee, W. Li, R. K. Siu et al., "Biomimetic apatite-coated alginate/chitosan microparticles as osteogenic protein carriers," *Biomaterials*, vol. 30, no. 30, pp. 6094–6101, 2009.

[118] A. Anitha, S. Sowmya, P. T. S. Kumar et al., "Chitin and chitosan in selected biomedical applications," *Progress in Polymer Science*, vol. 39, no. 9, pp. 1644–1667, 2014.

[119] S. Ma, Z. Chen, F. Qiao et al., "Guided bone regeneration with tripolyphosphate cross-linked asymmetric chitosan membrane," *Journal of Dentistry*, vol. 42, no. 12, pp. 1603–1612, 2014.

[120] S. Kim, K. Bedigrew, T. Guda et al., "Novel osteoinductive photo-cross-linkable chitosan-lactide-fibrinogen hydrogels enhance bone regeneration in critical size segmental bone defects," *Acta Biomaterialia*, vol. 10, no. 12, pp. 5021–5033, 2014.

[121] Y. H. Kang, S. H. Shin, and K. C. Kim, "Osteoconductive effect of chitosan/hydroxyapatite composite matrix on rat skull defect," *Tissue Engineering and Regenerative Medicine*, vol. 8, no. 1, pp. 23–31, 2011.

[122] J. S. Lee, S. D. Baek, J. Venkatesan et al., "*In vivo* study of chitosan-natural nano hydroxyapatite scaffolds for bone tissue regeneration," *International Journal of Biological Macromolecules*, vol. 67, pp. 360–366, 2014.

[123] B. Choi, S. Kim, B. Lin et al., "Visible-light-initiated hydrogels preserving cartilage extracellular signaling for inducing chondrogenesis of mesenchymal stem cells," *Acta Biomaterialia*, vol. 12, pp. 30–41, 2015.

[124] Y. Zhu, H. Wu, S. Sun, T. Zhou, J. Wu, and Y. Wan, "Designed composites for mimicking compressive mechanical properties of articular cartilage matrix," *Journal of the Mechanical Behavior of Biomedical Materials*, vol. 36, pp. 32–46, 2014.

[125] B. Choi, S. Kim, B. Lin, B. M. Wu, and M. Lee, "Cartilaginous extracellular matrix-modified chitosan hydrogels for cartilage tissue engineering," *ACS Applied Materials & Interfaces*, vol. 6, no. 22, pp. 20110–20121, 2014.

[126] F. Mirahmadi, M. Tafazzoli-Shadpour, M. A. Shokrgozar, and S. Bonakdar, "Enhanced mechanical properties of thermosensitive chitosan hydrogel by silk fibers for cartilage tissue engineering," *Materials Science and Engineering C*, vol. 33, no. 8, pp. 4786–4794, 2013.

[127] E. J. Sheehy, T. Mesallati, T. Vinardell, and D. J. Kelly, "Engineering cartilage or endochondral bone: a comparison of different naturally derived hydrogels," *Acta Biomaterialia*, vol. 13, pp. 245–253, 2015.

[128] D. Yin, H. Wu, C. Liu et al., "Fabrication of composition-graded collagen/chitosan–polylactide scaffolds with gradient architecture and properties," *Reactive and Functional Polymers*, vol. 83, pp. 98–106, 2014.

[129] C. Li, L. Wang, Z. Yang, G. Kim, H. Chen, and Z. Ge, "A viscoelastic chitosan-modified three-dimensional porous poly (L-lactide-co-ε-caprolactone) scaffold for cartilage tissue engineering," *Journal of Biomaterials Science, Polymer Edition*, vol. 23, no. 1–4, pp. 405–424, 2012.

[130] C. Kuo, C. Chen, C. Hsiao, and J. Chen, "Incorporation of chitosan in biomimetic gelatin/chondroitin-6-sulfate/hyaluronan cryogel for cartilage tissue engineering," *Carbohydrate Polymers*, vol. 117, pp. 722–730, 2015.

[131] J. H. Sandoval-Sánchez, R. Ramos-Zúñiga, S. L. de Anda et al., "A new bilayer chitosan scaffolding as a dural substitute: experimental evaluation," *World Neurosurgery*, vol. 77, no. 3-4, pp. 577–582, 2012.

Hindawi Publishing Corporation
BioMed Research International
Volume 2015, Article ID 168294, 10 pages
http://dx.doi.org/10.1155/2015/168294

Research Article

Potential of Newborn and Adult Stem Cells for the Production of Vascular Constructs Using the Living Tissue Sheet Approach

Jean-Michel Bourget,[1,2,3,4,5] Robert Gauvin,[1,2,3,6] David Duchesneau,[1,2,3] Murielle Remy,[7] François A. Auger,[1,2,3] and Lucie Germain[1,2,3]

[1] *Université Laval Experimental Organogenesis Center/LOEX, Enfant-Jesus Hospital, 1401 18th rue, Québec, QC, Canada G1J 1Z4*
[2] *Regenerative Medicine Section, CHU de Québec Research Centre, Québec, QC, Canada G1J 1Z4*
[3] *Department of Surgery, Faculty of Medicine, Université Laval, Québec, QC, Canada G1V 0A6*
[4] *Maisonneuve-Rosemont Hospital Research Center, 415 Assomption boulevard, Montreal, QC, Canada H1T 2M4*
[5] *Department of Ophthalmology, University of Montreal, Montreal, QC, Canada H3T 1J4*
[6] *Quebec Center for Functional Materials (CQMF), Office 2634, Alexandre-Vachon Building, Université Laval, Québec, QC, Canada G1V 0A6*
[7] *Bordeaux Segalen University, INSERM-U1026, 146 Léo Saignat Street, 33000 Bordeaux, France*

Correspondence should be addressed to Lucie Germain; lucie.germain@fmed.ulaval.ca

Received 19 February 2015; Revised 23 April 2015; Accepted 24 April 2015

Academic Editor: Magali Cucchiarini

Bypass surgeries using native vessels rely on the availability of autologous veins and arteries. An alternative to those vessels could be tissue-engineered vascular constructs made by self-organized tissue sheets. This paper intends to evaluate the potential use of mesenchymal stem cells (MSCs) isolated from two different sources: (1) bone marrow-derived MSCs and (2) umbilical cord blood-derived MSCs. When cultured *in vitro*, a proportion of those cells differentiated into smooth muscle cell- (SMC-) like cells and expressed contraction associated proteins. Moreover, these cells assembled into manipulable tissue sheets when cultured in presence of ascorbic acid. Tubular vessels were then produced by rolling those tissue sheets on a mandrel. The architecture, contractility, and mechanical resistance of reconstructed vessels were compared with tissue-engineered media and adventitia produced from SMCs and dermal fibroblasts, respectively. Histology revealed a collagenous extracellular matrix and the contractile responses measured for these vessels were stronger than dermal fibroblasts derived constructs although weaker than SMCs-derived constructs. The burst pressure of bone marrow-derived vessels was higher than SMCs-derived ones. These results reinforce the versatility of the self-organization approach since they demonstrate that it is possible to recapitulate a contractile media layer from MSCs without the need of exogenous scaffolding material.

1. Introduction

Cardiovascular diseases (CVD) are the leading cause of mortality in the United States (US) [1]. Half of the CVD-associated fatalities are attributed to myocardial infarct caused by obstruction of a coronary artery [1]. The gold standard for vascular bypass surgeries of small diameter/low blood flow vessels is the transplantation of an autologous vein or artery [2]. However, these vessels are limited in availability and could be pathologic [3–5]. Therefore, there is an urgent need for the development of an alternative conduit that could be nonthrombogenic and nonimmunogenic and present proper mechanical properties as well as vasoreactivity [6, 7]. Such vessels can be engineered from autologous cells using the self-organization approach, which takes advantage of the capability of mesenchymal cells to produce and assemble their own extracellular matrix (ECM) when cultured in presence of ascorbic acid [8, 9]. In a seminal paper by L'Heureux et al. [9] the adventitia was recapitulated using adult dermal fibroblasts (DFs) while the media layer was engineered from umbilical vein smooth muscle cells (SMCs) and the intima from umbilical vein endothelial cells. However, this source

of SMCs is not compatible with a fully autologous approach. In order to fulfill this expectancy, it would be preferable to have access to another potential source of SMCs.

Previous studies have focused on the evaluation of alternative cell sources for media reconstruction by the self-organization approach (formerly called the self-assembly approach). Grenier et al. [10] developed a protocol for the isolation of the 3 vascular cell types (endothelial, SMC, and fibroblast) from a single vein biopsy. This interesting approach faces, however, the potential problems, for some patients, of the cells taken from a pathologic vessel such as the saphenous vein. Moreover, it is an invasive approach since it requires surgery and an available vein, which can be difficult to access for patients with history of multiple autologous vascular bypass grafts. Additionally, tissue-engineered vessels produced from cells isolated from veins have demonstrated inferior mechanical properties than those reconstructed from arterial cells [11].

The use of adult mesenchymal stem cells (MSCs) could overcome the challenge of using cells from pathologic tissues. MSCs are known to be able to differentiate into multiple mesenchymal cell types (cardiomyocytes, osteocytes, chondrocytes, myocytes, fibroblasts, and adipocytes) [12]. They can also spontaneously differentiate into smooth muscle cells when cultured for several passages [13]. Moreover, those cells possess paracrine effects such as immunomodulation, antiapoptosis, antiscarring, and chemoattraction [12]. They can be obtained from different sources including adipose tissue, the umbilical cord, bone marrow, and the dermis [14–16]. The current theory on the MSCs niche is that these cells are located around capillaries and correspond to pericytes [17–19].

Previous work demonstrated the potential of those cells for tissue engineering applications using the self-organization approach. Hayward et al. have demonstrated that umbilical cord Wharton's jelly-derived MSCs can be used to reconstruct dermal and vascular constructs [20, 21]. Vermette et al. [22] and Rousseau et al. [23] have also used adipose tissue-derived stromal cell containing MSCs for engineered adipose tissue and bladder wall, respectively.

In order to find a suitable alternative source of cells, we studied the potential of bone marrow mesenchymal stem cells (BMSCs) and umbilical cord blood mesenchymal stem cells (UCB-MSCs) to differentiate in SMCs, assemble extracellular matrix, produce manipulable cell sheets, and form a cohesive vascular media substitute.

2. Materials and Methods

2.1. Cell Isolation and Culture. All protocols were approved by the institutional committee for the protection of human subjects (Comité d'Éthique de la Recherche du Centre Hospitalier Universitaire de Québec) and conducted in accordance with the Declaration of Helsinki.

Umbilical cord blood mesenchymal stem cells (UCB-MSCs) were isolated from the mononuclear fraction of samples of freshly collected human umbilical cord blood samples (50–80 mL), using an adaptation of the previously described protocol by Kaushal et al. [24]. Briefly, after elimination of the plasma and platelets by centrifugation, the erythrocytes were sedimented in 6% dextran (Sigma-Aldrich, Oakville, Ontario, Canada). The mononuclear fraction was then isolated by centrifugation through a Ficoll-Paque gradient (Amersham Biosciences, Piscataway, NJ, USA) and resuspended in phosphate buffered saline (PBS). Cells were centrifuged and resuspended in M199 medium (Sigma-Aldrich) supplemented with 20% newborn calf serum (FetalClone II, HyClone, Logan, UT, USA), endothelial cell growth supplement (20 μg/mL; Sigma-Aldrich), glutamine (333 μg/mL; Life Technologies, Burlington, Ontario, Canada), heparin (40 U/mL; LEO Pharma Inc., Thornhill, Ontario, Canada), and antibiotics: 100 U/mL penicillin G (Sigma-Aldrich) and 25 g/mL of gentamicin (Schering, Pointe-Claire, QC, Canada). This mononuclear fraction obtained from cord blood was then plated in a Petri dish coated with 0.2% gelatin (Fisher Scientific, Ottawa, Ontario, Canada). Cells were allowed to adhere to the dish for 3 hours in M199 medium at 37°C to select the population of adherent cells. After 20 days, two distinct cell populations were visible in the flask, angioblastic-like cells and mesenchymal-like cells. These two populations were separated by differential trypsinization (trypsin; Life Technologies). The mesenchymal population was then cultured in Dulbecco's modified Eagle medium (DMEM, Life Technologies) and Ham's F12 (Life Technologies) in a 3 : 1 ratio (DMEM-Ham), 20% fetal calf serum (FCS; HyClone), and antibiotics.

Bone marrow mesenchymal stem cells (BMSCs) were bought from Lonza (Lonza, Walkersville, MD, USA) and cultured as prescribed by the manufacturer. This cell line has been characterized previously (CD105+, CD66+, CD29+, CD44+, CD34−, CD14−, and CD45−) and can be differentiated into adipogenic, chondrogenic, and osteogenic cells [25].

Human DFs were isolated from a healthy donor following breast surgery and cell isolation was performed as described previously [26]. Briefly, a small portion of skin was incubated at 37°C for 2 hours in a thermolysin (500 μg/mL, Sigma-Aldrich)/HEPES buffer (pH 7.4, MP Biomedicals, Montreal, QC, Canada) solution. The dermis and epidermis were then separated using fine forceps. The dermis was cut into small pieces and incubated at 37°C for 20 hours in a collagenase H solution (0.125 U/mL, Roche, Laval, QC, Canada) in order to isolate fibroblasts from the connective tissue. Fibroblasts were centrifuged (300 ×g, 10 min), plated into culture flasks, and cultured in DMEM with 10% FCS and antibiotics.

Human arterial SMCs were isolated from an umbilical cord artery using the explants method of Ross [27, 28]. Briefly, the artery was longitudinally opened and the endothelium was removed by gentle scraping with a sterile gauze soaked in a PBS solution. Strips of the media layer were dissected, cut into small pieces, and allowed to adhere to a gelatin-coated 6-well plate (BD Bioscience, Mississauga, Ontario, Canada) containing culture medium: DMEM-Ham, 20% FCS, and antibiotics. After 2 weeks in culture, SMCs migrated out of the explants and were allowed to proliferate for two more weeks. SMCs were detached from the tissue culture plastic using trypsin/EDTA and further plated at a density of 10^4 cells/cm^2 in tissue culture flasks to allow for expansion.

All cell types were grown in an incubator at 8% CO_2, 95% relative humidity (RH), and 37°C and the culture medium was changed 3 times a week.

2.2. Production of Tissue-Engineered Vascular Constructs. The tissue-engineered vascular constructs were produced using the self-organization technique previously described [9, 29]. Briefly, cells were seeded on tissue culture flask (T75, BD Bioscience) in DME-Ham (3 : 1), supplemented with 10% FCS and 50 μg/mL ascorbic acid. After 3 weeks in culture, cell sheets were peeled off the flask and rolled around mandrels (4.5 mm diameter) to generate a vascular construct. These were cultured for an additional three weeks in DMEM-Ham supplemented with 10% FetalClone II serum, antibiotics, and 50 μg/mL of sodium ascorbate.

2.3. Immunostaining. For immunostaining on coverslips, cells were fixed in 100% methanol (−20°C, 10 min) and rinsed in PBS. For immunostaining of cross sections, segments of tissue-engineered vessels were embedded in optimal cutting temperature compound (OCT, Tissue-Tek/Somagen, Edmonton, Alberta, Canada) and frozen at −80°C. OCT embedded tissues were cut orthogonal to the length of the vascular construct in 5 μm sections using a cryostat (Leica Canada, Montreal, QC, Canada), fixed in 100% acetone (−20°C, 10 min), and rinsed in PBS. Primary antibodies used were mouse monoclonal antibodies (IgG) against α-smooth muscle actin (clone 1A4; Dako, Burlington, Ontario, Canada; 1/200), calponin (clone hCP; Sigma-Aldrich; 1/200), h-caldesmon (clone hHCD; Sigma-Aldrich; 1/100), and keratin-18 (clone KS18.174; ARP, Waltham, MA, USA; 1/100). Secondary antibody was goat polyclonal antibody against mouse IgG conjugated with Alexa 594 (Life Technologies; 1/800).

2.4. Histology. Segments of constructs were fixed in 3,7% formaldehyde (VWR, Montreal, QC, Canada) and embedded in paraffin. Five-micrometer thick cross sections were cut using a microtome and stained with Masson's trichrome [30, 31] using Weigert's haematoxylin, fuchsin-ponceau, and aniline blue stains.

2.5. Burst Pressure Test. Burst pressure measurements were performed by gradually inflating the tissue-engineered constructs until failure, while recording the internal pressure, using a custom-built experimental setup described previously [32]. Briefly, tissues were cannulated and loaded in a PBS containing chamber maintained at 37°C. Pressurization of vascular constructs with PBS was ensured by a syringe pump activated by a stepper motor (Excitron, Boulder, CO, USA) and controlled by a LabView virtual instrument (National Instruments, Austin, TX), at a constant flow rate of 4 mL/min. Pressure data were recorded by a pressure transducer (68846-series; Cole Parmer, Montreal, QC, Canada) connected to an acquisition card (NI PCI-6221; National Instruments) and acquired using the previously described virtual instrument [32]. Burst pressure was considered to be the highest pressure value recorded prior to failure of the construct.

2.6. Uniaxial Tensile Test. Mechanical properties of the vascular constructs were evaluated by ring tensile testing using an Tytron 250 Microforce Testing System (MTS Corporation, Eden Prairies, MN, USA) as previously described [32, 33]. Briefly, five-millimetre-long ring samples were cut from the different constructs and mounted between hooks linked to a 10 N load cell. The hooks were pulled apart at the constant speed of 0.2 mm/s until failure of the specimen.

2.7. Vasoconstriction. The contractile properties of the tissue-engineered vessels were evaluated by recording their response to histamine (Sigma-Aldrich) as previously described [34, 35]. Briefly, the different constructs were cut into five-millimetre-long ring sections, rinsed in physiological salt Krebs solution (119 mM NaCl, 4.7 mM KCl, 1.2 mM KH_2PO_4, 25 mM $NaHCO_3$, 1.2 mM $MgSO_4$, 2.5 mM $CaCl_2$, and 10 mM glucose), mounted between two anchors for isometric contractile force measurements (Radnoti, Harvard Apparatus, Montreal, QC, Canada), and submerged in isolated organ baths containing Krebs solution maintained at 37°C and oxygenated with a mixture of 95% O_2 and 5% CO_2 (pH 7.4). After 30 minutes of equilibration, each ring was passively stretched until a stable preload of 500 mg was obtained. The maximal contractile capability of each ring was determined by a single dose of histamine (10^{-4} M).

3. Results

3.1. Cultured MSCs Express SMC Differentiation Markers In Vitro. In order to evaluate the extent of the differentiation of UCB-MSCs and BMSCs into SMCs, cells were characterized for expression of SMC markers by immunofluorescence at different passages and compared to SMCs and DFs (Figure 1). At passage 10, both types of MSCs were positive for the expression of α-smooth muscle actin (α-SMA) (Figures 1(a)–1(d)) and calponin (Figures 1(e)–1(h)), two early SMC markers. Similarly, DFs also stained positive for calponin which can be explained by a transition of those cells toward a myofibroblastic phenotype in culture. Expression of h-caldesmon (Figures 1(i)–1(l)), a later stage SMC marker, was also tested. This protein was expressed by a small proportion of UCB-MSCs (30% of cells) but was present in each cell population tested. Expression of h-caldesmon was high in BMSCs (100% of cells) (Figure 1(j)). Most SMCs stained positive for this marker although some of them did not express h-caldesmon (Figure 1(k)), since SMCs are known to dedifferentiate from their contractile phenotype to a proliferative phenotype when cultured *in vitro* [36]. Keratin-18 is known to be expressed by SMCs but not by dermal fibroblasts [37–39]. This protein was expressed by a small proportion of UCB-MSCs (9%) and BMSCs (14%) but by a high proportion of SMCs (87%). As expected, DFs were negative for this marker.

3.2. MSCs Capability to Form Cell Sheets. The BMSCs and UCB-MSCs were cultured in presence of ascorbic acid in order to evaluate their capability to secrete and assemble collagen using a previously described protocol [26]. Both types

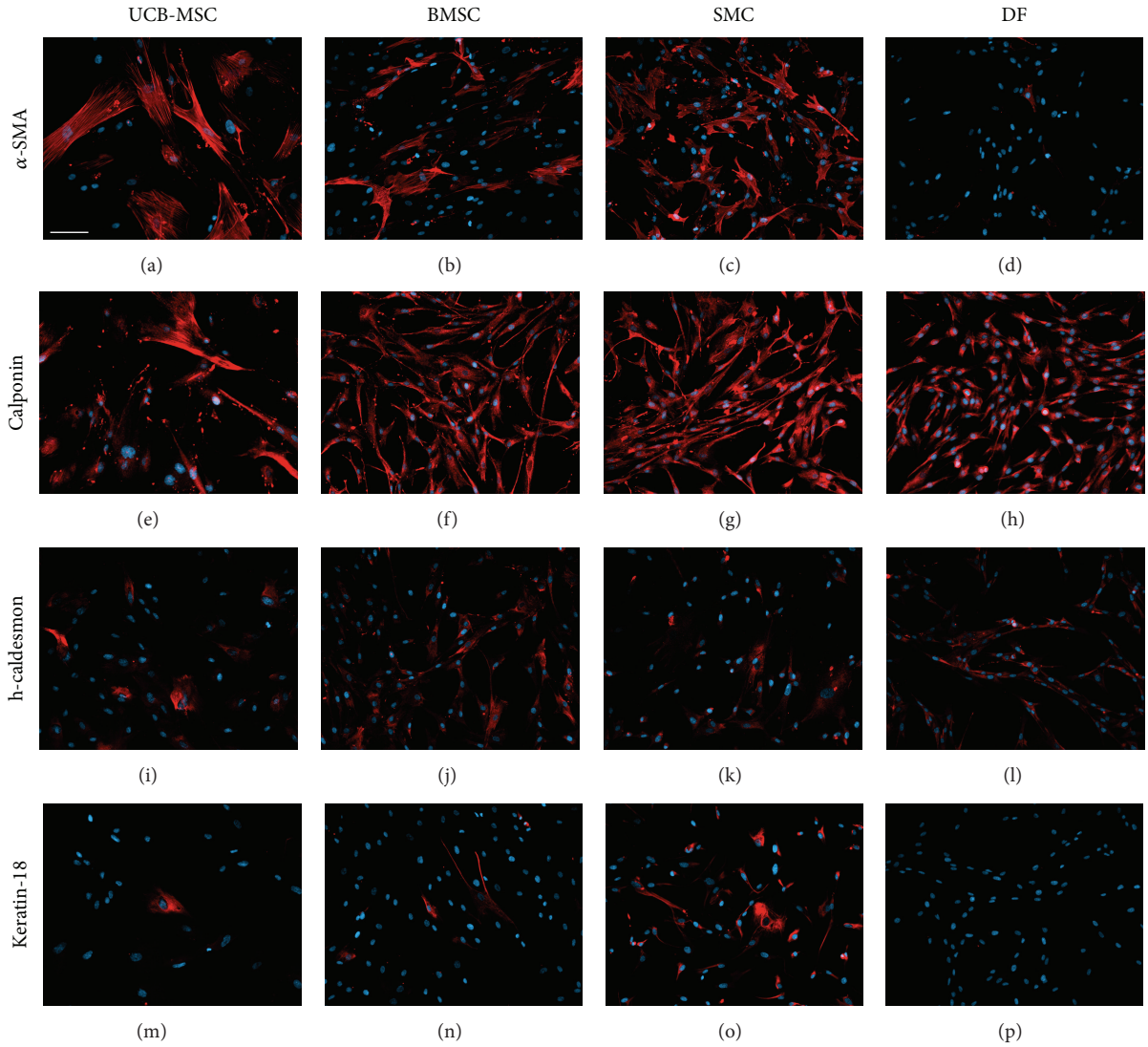

Figure 1: Cultured MSCs express smooth muscle cell markers. Expression of smooth muscle cell markers by various cell types in culture, UCB-MSCs (a, e, i, and m) and BMSCs (b, f, j, and n), as well as control cells, SMCs (c, g, k, and o) and DFs (d, h, l, and p). Immunostaining against (red) α-smooth muscle (SM) actin (a–d), calponin (e–h), h-caldesmon (i–l), and keratin-18 (m–p). Nuclei were counterstained with Hoechst (blue); scale bar: 100 μm.

of MSCs secreted a sufficient amount of extracellular matrix to form cell sheets. However, UCB-MSCs formed fragile cell sheets that were hard to manipulate in comparison with their counterparts. MSCs-derived sheets were rolled around a mandrel to form vascular constructs. Those constructs and control ones (SMCs- and DFs-derived) were stained with Masson's trichrome to visualize cells and ECM (Figure 2). All cell types formed tubular constructs comprising cells embedded into a dense collagenous ECM. UCB-MSCs-derived vessels were much thinner than the others. This finding correlates with the previous observation of a thin and fragile cell sheet. However, all four types of constructs could be slit out from their support mandrel into culture medium and were able to maintain their internal lumen geometry without collapsing.

3.3. Vascular Constructs Produced from Stem Cells Express Contractile SMC Proteins. In order to evaluate the expression of SMC markers in the vascular constructs derived from all four cells types, cross sections of tissue-engineered vessels were immunostained with the same markers as 2D cultures presented in Figure 1. SMCs-derived constructs stained positive for all four markers, namely, α-SMA, calponin, h-caldesmon, and keratin-18 (Figures 3(c), 3(g), 3(k), and 3(o)) while DFs-derived ones turned out to be negative for the same four markers (Figures 3(d), 3(h), 3(l), and 3(p)). MSCs-derived constructs, from UCB-MSCs (Figures 3(a), 3(e), 3(i), and 3(m)) and from BMSCs (Figures 3(b), 3(f), 3(j), and 3(n)), displayed an intermediate phenotype with a level of expression of SMC markers between the SMCs- and DFs-derived constructs.

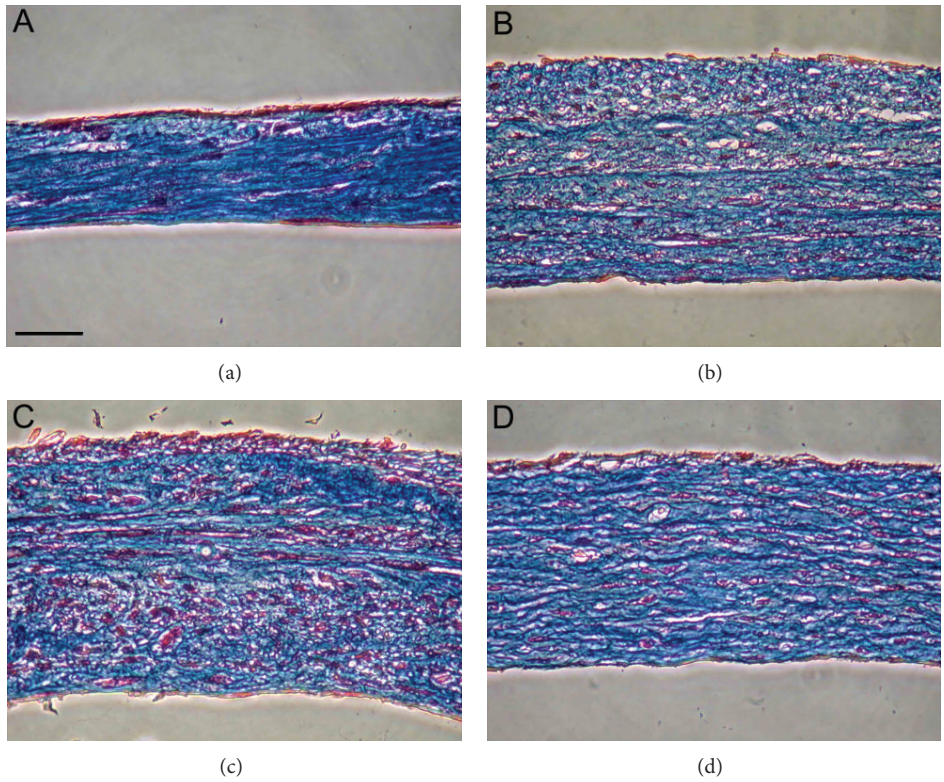

Figure 2: Cultured stem cells produce ECM and form cell sheets that can be later rolled into vascular constructs. Cross sections of tissue-engineered vessels made from cultured UCB-MSCs (a), BMSCs (b), SMCs (c), or DFs (d) were stained with Masson's trichrome in order to visualize collagen (blue) and cells (red). Scale bar: 50 μm.

3.4. Evaluation of the Contractile Capability of Stem Cell Derived Media. We have previously demonstrated that media produced by self-organization of tissue sheets from SMCs can contract in response to different agonist [34]. This contractile capability is paramount to proper function of this blood vessel layer. Being able to dilate or contract in response to local increases in pressure or blood flow might have significant impact on vascular functionality. Therefore, we evaluated the contractile response of the different engineered media to histamine. This molecule is known to induce the contraction of SMCs-derived constructs and has been previously validated by our group [35, 40–43]. The UCB-MSCs- and BMSCs-engineered vascular media produced a low level of contraction as compared to the SMCs-engineered media. The contraction of BMSCs-derived media was higher than UCB-MSCs-derived media. Still, the contraction monitored for those MSCs-derived media was higher than the contraction of the control, DFs-derived vessels (Figure 4). The agonist-dependent response of MSCs-derived media demonstrates that their contractile apparatus is functional and that they express the histamine receptor.

3.5. Evaluation of the Mechanical Properties of Stem Cell Derived Vascular Construct. Suitable mechanical properties of a vascular substitute intended for transplantation are paramount. In order to evaluate those properties in the different constructs, tissues were subjected to two types of mechanical tests: uniaxial tensile tests (Figures 5(a), 5(b), and 5(c)) and burst pressure tests (Figure 5(d)). Mechanical resistance of UCB-MSCs-derived constructs was too low to be determined accurately. Results have shown that BMSCs could lead to vascular construct displaying mechanical properties within the same order of magnitude when compared to SMCs and DFs.

4. Discussion

We have shown that it is possible to engineer a contractile media layer from adult and newborn MSCs. Those constructs expressed SMCs differentiation markers and formed a cohesive tubular construct. Adult MSCs isolated from the bone marrow presented superior properties over UCB-MSCs since their contractile capability was found to be closer to SMCs-derived constructs and they present a higher mechanical resistance than UCB-MSCs.

Nowadays, use of MSCs in tissue engineering and regenerative medicine is quite common [44–49]. These cells have been used for vascular tissue engineering [50] in scaffold based approaches such as ECM-based scaffold (fibrin) [51], decellularized tissue [52, 53], and biodegradable scaffolds [54–56], including electrospun of nanofibers [57–59], as well as scaffold-free approach such as cell sheet engineering [60] and the present paper.

Ren et al. [61] have shown that MSCs cell sheets seeded with endothelial cells promote the formation of a microvascular network in the construct. This is quite interesting since

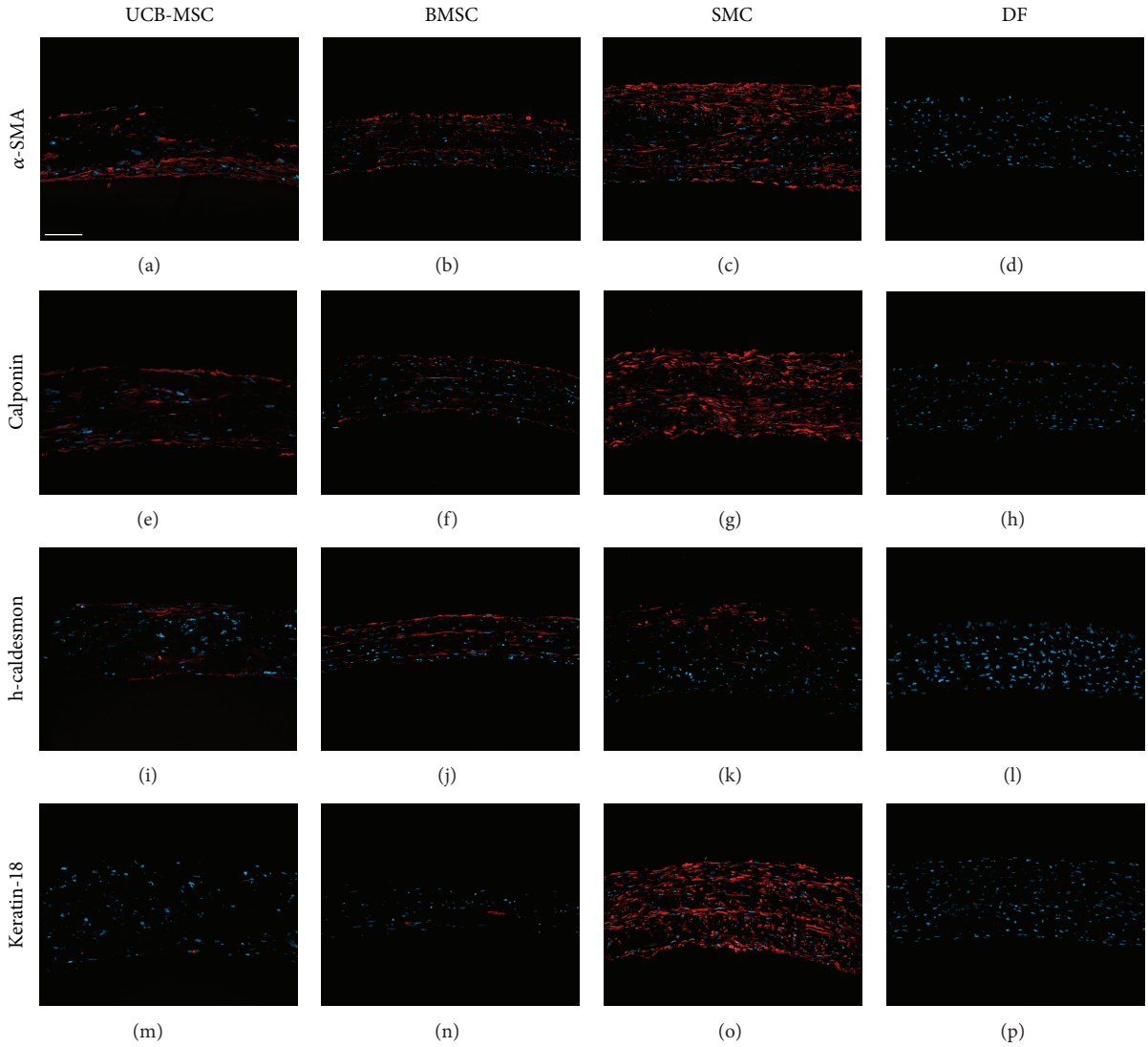

Figure 3: Expression of SMC differentiation markers in MSCs-derived vessels. Cross sections of tissue-engineered vessels made from cultured UCB-MSCs (a, e, i, and m), BMSCs (b, f, j, and n), SMCs (c, g, k, and o), or DFs (d, h, l, and p) were immunostained (red) for α-SMA (a–d), calponin (e–h), h-caldesmon (i–l), and keratin-18 (m–p). Nuclei were counterstained with Hoechst (blue); scale bar: 100 μm.

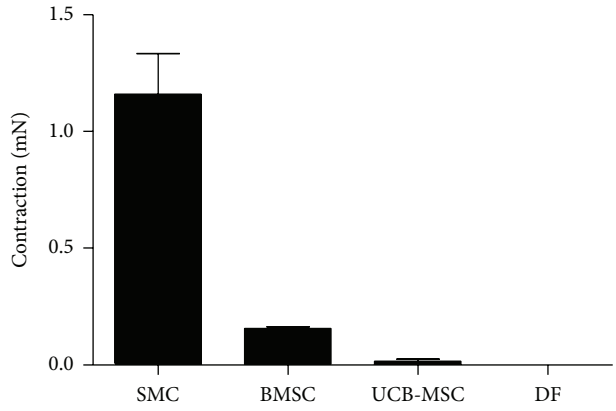

Figure 4: MSCs-derived media responsiveness to contractile agonist. Vasoreactivity of different tissue-engineered vessels. Recording of the maximal contraction to histamine (10^{-4} M).

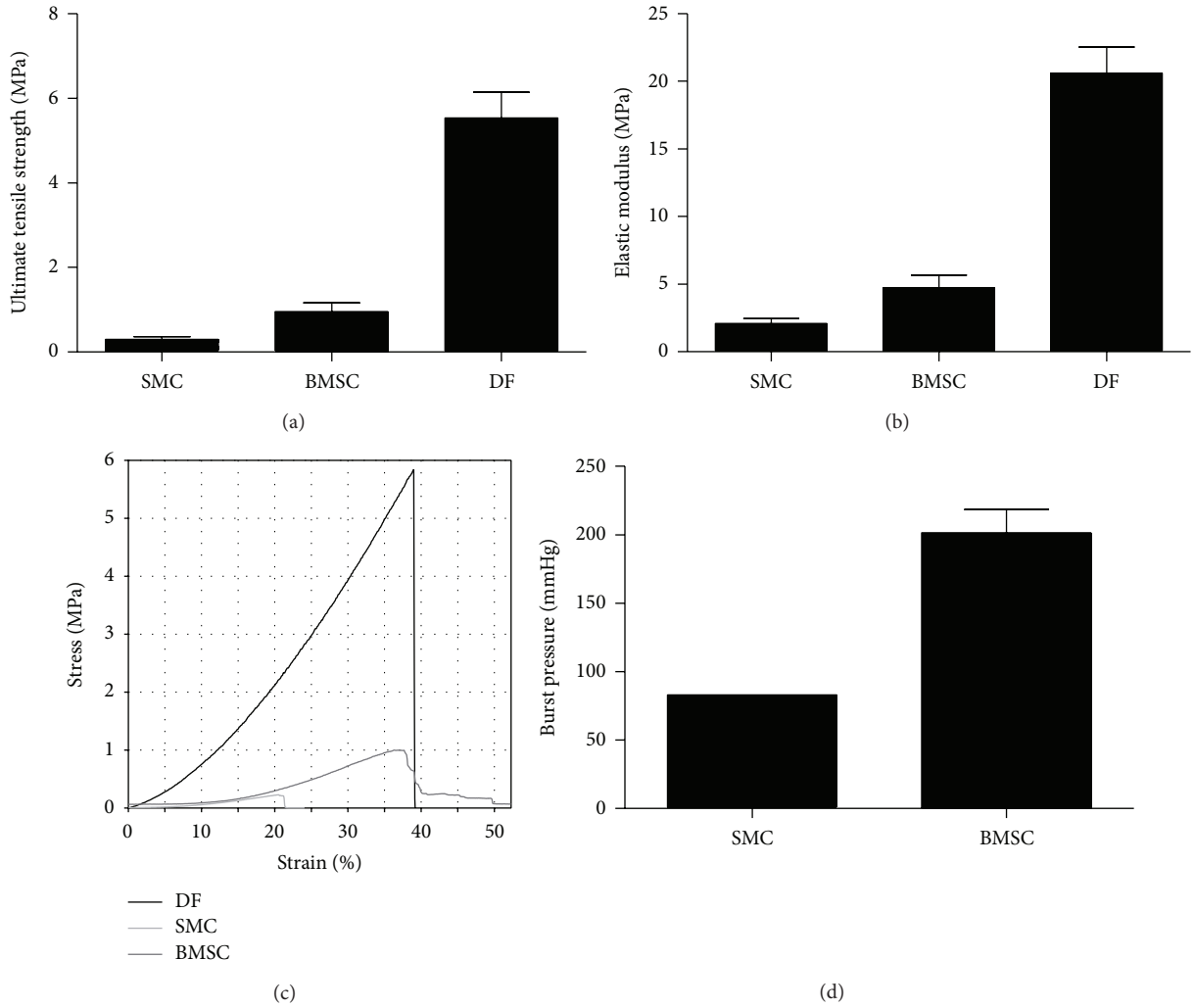

Figure 5: BMSCs-derived media present higher mechanical resistance than SMCs-derived media. Ultimate tensile stress (a) and elastic modulus (b) were determined by uniaxial tensile testing. A representative stress-strain curve is shown in (c). Burst pressure was evaluated on whole tissue-engineered vessels (d).

the formation of a vasa vasorum in the vascular adventitia of tissue-engineered vessels [62] and tissue-engineered skin [63], using dermal fibroblasts, improves the graft integration and inosculation.

There are advantages of using mesenchymal stem cells for reconstruction of the vascular media. Mechanical resistance of BMSCs construct was found to be higher than SMCs-derived constructs. The BMSCs are readily available from a simple bone marrow biopsy and can be expanded *in vitro*. They are also available commercially for research purposes. They form cell sheets that can improve capillary formation. However, there is also inherent drawback to take into account. Contractile response to vasocontractile agonist is lower than SMCs-derived constructs. Interestingly, contraction intensity seems to correlate with the expression of SMC contractile apparatus proteins. Indeed, more cells expressed h-caldesmon in BMSCs culture than UCB-MSCs. Accordingly, BMSCs-derived media present a higher contractile capability. It is also likely that mechanical stimulation of the construct might be able to improve the contractile response after grafting [33]. This mechanical stimulation could also be simulated *in vitro* in a bioreactor. Indeed, previous studies have shown that applying cyclic strain to SMC tissue sheets increased mechanical resistance and contractility [64]. Uniaxial mechanical stimulation of DF tissue sheets also increased ultimate tensile strength [65]. The same phenomenon could probably be observed for tissue sheets engineered using BMSCs, since cell type is known to be influenced by mechanical stimulation [66, 67].

5. Conclusion

This study demonstrated the feasibility of producing a contractile media layer *in vitro* from adult and newborn MSCs using the self-organization approach. The cohesive tubular construct contained cells expressing SMCs differentiation markers. Adult BMSCs were found to be preferable to replace SMCs isolated from the vessels, compared to UCB-MSCs, to

reconstruct a media layer. Contractile capability of BMSCs was closer to SMCs-derived constructs and they presented a higher mechanical resistance when compared to UCB-MSCs. Those cells could potentially be isolated from the patients' bone marrow in an autologous approach. The use of MSCs in tissue engineering might be the key autologous reconstruction of blood vessels, especially for patients lacking available healthy tissue for bypass surgeries.

Conflict of Interests

The authors declare that there is no conflict of interests regarding the publication of this paper.

Authors' Contribution

Jean-Michel Bourget, Robert Gauvin, and David Duchesneau contributed equally to this work.

Acknowledgments

This work was supported by the Canadian Institutes for Health Research (CIHR), the Fonds de Recherche du Québec en Santé (FRQS), and ThéCell Network: Réseau de Thérapie Cellulaire et Tissulaire du FRQS. Jean-Michel Bourget is recipient of a Postdoctoral Training Award from the FRQS. Lucie Germain holds the Canadian Research Chair in Stem Cells and Tissue Engineering from CIHR.

References

[1] D. Mozaffarian, E. J. Benjamin, A. S. Go et al., "Executive summary: heart disease and stroke statistics-2015 update: a report from the american heart association," *Circulation*, vol. 131, no. 4, pp. 434–441, 2015.

[2] K. A. Eagle, R. A. Guyton, R. Davidoff et al., "ACC/AHA 2004 guideline update for coronary artery bypass graft surgery: a report of the American College of Cardiology/American Heart Association Task Force on Practice Guidelines (Committee to Update the 1999 Guidelines for Coronary Artery Bypass Graft Surgery)," *Circulation*, vol. 110, no. 14, pp. e340–e437, 2004.

[3] R. E. Harskamp, R. D. Lopes, C. E. Baisden, R. J. De Winter, and J. H. Alexander, "Saphenous vein graft failure after coronary artery bypass surgery: pathophysiology, management, and future directions," *Annals of Surgery*, vol. 257, no. 5, pp. 824–833, 2013.

[4] A. Morishita, T. Shimakura, M. Miyagishima, J. Kawamoto, and H. Morimoto, "Minimally invasive direct redo coronary artery bypass grafting," *Annals of Thoracic and Cardiovascular Surgery*, vol. 8, no. 4, pp. 209–212, 2002.

[5] W. S. Weintraub, M. V. Grau-Sepulveda, J. M. Weiss et al., "Comparative effectiveness of revascularization strategies," *The New England Journal of Medicine*, vol. 366, no. 16, pp. 1467–1476, 2012.

[6] L. E. Niklason, J. Gao, W. M. Abbott et al., "Functional arteries grown in vitro," *Science*, vol. 284, no. 5413, pp. 489–493, 1999.

[7] B. V. Udelsman, M. W. Maxfield, and C. K. Breuer, "Tissue engineering of blood vessels in cardiovascular disease: moving towards clinical translation," *Heart*, vol. 99, no. 7, pp. 454–460, 2013.

[8] F. A. Auger, M. Rémy-Zolghadri, G. Grenier, and L. Germain, "Review: the self-assembly approach for organ reconstruction by tissue engineering," *e-biomed: The Journal of Regenerative Medicine*, vol. 1, no. 5, pp. 75–86, 2000.

[9] N. L'Heureux, S. Pâquet, R. Labbé, L. Germain, and F. A. Auger, "A completely biological tissue-engineered human blood vessel," *The FASEB Journal*, vol. 12, no. 1, pp. 47–56, 1998.

[10] G. Grenier, M. Rémy-Zolghadri, R. Guignard et al., "Isolation and culture of the three vascular cell types from a small vein biopsy sample," *In Vitro Cellular & Developmental Biology—Animal*, vol. 39, no. 3-4, pp. 131–139, 2003.

[11] R. Gauvin, M. Guillemette, T. Galbraith et al., "Mechanical properties of tissue-engineered vascular constructs produced using arterial or venous cells," *Tissue Engineering Part A*, vol. 17, no. 15-16, pp. 2049–2059, 2011.

[12] N. G. Singer and A. I. Caplan, "Mesenchymal stem cells: mechanisms of inflammation," *Annual Review of Pathology*, vol. 6, pp. 457–478, 2011.

[13] M. C. Galmiche, V. E. Koteliansky, J. Briere, P. Herve, and P. Charbord, "Stromal cells from human long-term marrow cultures are mesenchymal cells that differentiate following a vascular smooth muscle differentiation pathway," *Blood*, vol. 82, no. 1, pp. 66–76, 1993.

[14] A. I. Caplan, "Mesenchymal stem cells," *Journal of Orthopaedic Research*, vol. 9, no. 5, pp. 641–650, 1991.

[15] A. I. Caplan, "Review: mesenchymal stem cells: cell-based reconstructive therapy in orthopedics," *Tissue Engineering*, vol. 11, no. 7-8, pp. 1198–1211, 2005.

[16] A. I. Caplan, "Adult mesenchymal stem cells for tissue engineering versus regenerative medicine," *Journal of Cellular Physiology*, vol. 213, no. 2, pp. 341–347, 2007.

[17] L. D. S. Meirelles, A. I. Caplan, and N. B. Nardi, "In search of the in vivo identity of mesenchymal stem cells," *Stem Cells*, vol. 26, no. 9, pp. 2287–2299, 2008.

[18] A. I. Caplan, "All MSCs are pericytes?" *Cell Stem Cell*, vol. 3, no. 3, pp. 229–230, 2008.

[19] M. Crisan, S. Yap, L. Casteilla et al., "A perivascular origin for mesenchymal stem cells in multiple human organs," *Cell Stem Cell*, vol. 3, no. 3, pp. 301–313, 2008.

[20] C. J. Hayward, J. Fradette, T. Galbraith et al., "Harvesting the potential of the human umbilical cord: isolation and characterisation of four cell types for tissue engineering applications," *Cells Tissues Organs*, vol. 197, no. 1, pp. 37–54, 2012.

[21] C. J. Hayward, J. Fradette, P. Morissette Martin, R. Guignard, L. Germain, and F. A. Auger, "Using human umbilical cord cells for tissue engineering: a comparison with skin cells," *Differentiation*, vol. 87, no. 3-4, pp. 172–181, 2014.

[22] M. Vermette, V. Trottier, V. Ménard, L. Saint-Pierre, A. Roy, and J. Fradette, "Production of a new tissue-engineered adipose substitute from human adipose-derived stromal cells," *Biomaterials*, vol. 28, no. 18, pp. 2850–2860, 2007.

[23] A. Rousseau, J. Fradette, G. Bernard, R. Gauvin, V. Laterreur, and S. Bolduc, "Adipose-derived stromal cells for the reconstruction of a human vesical equivalent," *Journal of Tissue Engineering and Regenerative Medicine*, 2013.

[24] S. Kaushal, G. E. Amiel, K. J. Guleserian et al., "Functional small-diameter neovessels created using endothelial progenitor cells expanded ex vivo," *Nature Medicine*, vol. 7, no. 9, pp. 1035–1040, 2001.

[25] M. F. Pittenger, A. M. Mackay, S. C. Beck et al., "Multilineage potential of adult human mesenchymal stem cells," *Science*, vol. 284, no. 5411, pp. 143–147, 1999.

[26] D. Larouche, C. Paquet, J. Fradette, P. Carrier, F. A. Auger, and L. Germain, "Regeneration of skin and cornea by tissue engineering," *Methods in Molecular Biology*, vol. 482, pp. 233–256, 2009.

[27] R. Ross, "The smooth muscle cell. II. Growth of smooth muscle in culture and formation of elastic fibers," *The Journal of Cell Biology*, vol. 50, no. 1, pp. 172–186, 1971.

[28] J.-M. Bourget, R. Gauvin, D. Larouche et al., "Human fibroblast-derived ECM as a scaffold for vascular tissue engineering," *Biomaterials*, vol. 33, no. 36, pp. 9205–9213, 2012.

[29] K. Laflamme, C. J. Roberge, S. Pouliot, P. D'Orléans-Juste, F. A. Auger, and L. Germain, "Tissue-engineered human vascular media produced in vitro by the self-assembly approach present functional properties similar to those of their native blood vessels," *Tissue Engineering*, vol. 12, no. 8, pp. 2275–2281, 2006.

[30] L. G. Luna, *Manual of Histologic Staining Methods of the Armed Forces Institute of Pathology*, Blakiston Division, McGraw-Hill, New York, NY, USA, 1968.

[31] P. Masson, "Some histological methods: trichrome staining and their preliminary technique," *Journal of Technical Methods—Bulletin of the International Association of Medical Museums*, vol. 12, no. 75, 1929.

[32] R. Gauvin, T. Ahsan, D. Larouche et al., "A novel single-step self-assembly approach for the fabrication of tissue-engineered vascular constructs," *Tissue Engineering Part A*, vol. 16, no. 5, pp. 1737–1747, 2010.

[33] D. Seliktar, R. A. Black, R. P. Vito, and R. M. Nerem, "Dynamic mechanical conditioning of collagen-gel blood vessel constructs induces remodeling in vitro," *Annals of Biomedical Engineering*, vol. 28, no. 4, pp. 351–362, 2000.

[34] N. L'Heureux, J.-C. Stoclet, F. A. Auger, G. J.-L. Lagaud, L. Germain, and R. Andriantsitohaina, "A human tissue-engineered vascular media: a new model for pharmacological studies of contractile responses," *The FASEB Journal*, vol. 15, no. 2, pp. 515–524, 2001.

[35] M. Pricci, J.-M. Bourget, H. Robitaille et al., "Applications of human tissue-engineered blood vessel models to study the effects of shed membrane microparticles from T-lymphocytes on vascular function," *Tissue Engineering Part A*, vol. 15, no. 1, pp. 137–145, 2009.

[36] M. R. Alexander and G. K. Owens, "Epigenetic control of smooth muscle cell differentiation and phenotypic switching in vascular development and disease," *Annual Review of Physiology*, vol. 74, pp. 13–40, 2012.

[37] B. L. Bader, L. Jahn, and W. W. Franke, "Low level expression of cytokeratins 8, 18 and 19 in vascular smooth muscle cells of human umbilical cord and in cultured cells derived therefrom, with an analysis of the chromosomal locus containing the cytokeratin 19 gene," *European Journal of Cell Biology*, vol. 47, no. 2, pp. 300–319, 1988.

[38] H. Bär, F. Bea, E. Blessing et al., "Phosphorylation of cytokeratin 8 and 18 in human vascular smooth muscle cells of atherosclerotic lesions and umbilical cord vessels," *Basic Research in Cardiology*, vol. 96, no. 1, pp. 50–58, 2001.

[39] L. Jahn, J. Kreuzer, E. von Hodenberg et al., "Cytokeratins 8 and 18 in smooth muscle cells: detection in human coronary artery, peripheral vascular, and vein graft disease and in transplantation-associated arteriosclerosis," *Arteriosclerosis, Thrombosis, and Vascular Biology*, vol. 13, no. 11, pp. 1631–1639, 1993.

[40] C. Su and J. A. Bevan, "The electrical response of pulmonary artery muscle to acetylcholine, histamine and serotonin," *Life Sciences*, vol. 4, no. 10, pp. 1025–1029, 1965.

[41] P. M. Hudgins and G. B. Weiss, "Differential effects of calcium removal upon vascular smooth muscle contraction induced by norepinephrine, histamine and potassium," *The Journal of Pharmacology and Experimental Therapeutics*, vol. 159, no. 1, pp. 91–97, 1968.

[42] H. A. Mostefai, J.-M. Bourget, F. Meziani et al., "Interleukin-10 controls the protective effects of circulating microparticles from patients with septic shock on tissue-engineered vascular media," *Clinical Science*, vol. 125, no. 2, pp. 77–85, 2013.

[43] S. J. Hill, C. R. Ganellin, H. Timmerman et al., "International union of pharmacology. XIII. Classification of histamine receptors," *Pharmacological Reviews*, vol. 49, no. 3, pp. 253–278, 1997.

[44] J. J. Bara, R. G. Richards, M. Alini, and M. J. Stoddart, "Concise review: bone marrow-derived mesenchymal stem cells change phenotype following in vitro culture: implications for basic research and the clinic," *Stem Cells*, vol. 32, no. 7, pp. 1713–1723, 2014.

[45] F. Bortolotti, L. Ukovich, V. Razban et al., "In vivo therapeutic potential of mesenchymal stromal cells depends on the source and the isolation procedure," *Stem Cell Reports*, vol. 4, no. 3, pp. 332–339, 2015.

[46] D. L. Coutu, W. Mahfouz, O. Loutochin, J. Galipeau, and J. Corcos, "Tissue engineering of rat bladder using marrow-derived mesenchymal stem cells and bladder acellular matrix," *PLoS ONE*, vol. 9, no. 12, Article ID e111966, 2014.

[47] D. Kai, M. P. Prabhakaran, G. Jin, L. Tian, and S. Ramakrishna, "Potential of VEGF-encapsulated electrospun nanofibers for in vitro cardiomyogenic differentiation of human mesenchymal stem cells," *Journal of Tissue Engineering and Regenerative Medicine*, 2015.

[48] V. Savkovic, H. Li, J. K. Seon, M. Hacker, S. Franz, and J. C. Simon, "Mesenchymal stem cells in cartilage regeneration," *Current Stem Cell Research & Therapy*, vol. 9, no. 6, pp. 469–488, 2014.

[49] J. F. Stoltz, D. Bensoussan, L. Zhang et al., "Stem cells and applications: a survey," *Bio-Medical Materials and Engineering*, vol. 25, no. 1, supplement, pp. 3–26, 2015.

[50] H. Huang and S. Hsu, "Current advances of stem cell-based approaches to tissue-engineered vascular grafts," *OA Tissue Engineering*, vol. 1, no. 1, 2013.

[51] E. D. O'Cearbhaill, M. Murphy, F. Barry, P. E. McHugh, and V. Barron, "Behavior of human mesenchymal stem cells in fibrin-based vascular tissue engineering constructs," *Annals of Biomedical Engineering*, vol. 38, no. 3, pp. 649–657, 2010.

[52] L. Dainese, A. Guarino, I. Burba et al., "Heart valve engineering: decellularized aortic homograft seeded with human cardiac stromal cells," *The Journal of Heart Valve Disease*, vol. 21, no. 1, pp. 125–134, 2012.

[53] C. Quint, Y. Kondo, R. J. Manson, J. H. Lawson, A. Dardik, and L. E. Niklason, "Decellularized tissue-engineered blood vessel as an arterial conduit," *Proceedings of the National Academy of Sciences of the United States of America*, vol. 108, no. 22, pp. 9214–9219, 2011.

[54] L. Soletti, Y. Hong, J. Guan et al., "A bilayered elastomeric scaffold for tissue engineering of small diameter vascular grafts," *Acta Biomaterialia*, vol. 6, no. 1, pp. 110–122, 2010.

[55] A. Nieponice, L. Soletti, J. Guan et al., "In Vivo assessment of a tissue-engineered vascular graft combining a biodegradable

elastomeric scaffold and muscle-derived stem cells in a rat model," *Tissue Engineering—Part A*, vol. 16, no. 4, pp. 1215–1223, 2010.

[56] H. L. Sang, S.-W. Cho, J.-C. Park et al., "Tissue-engineered blood vessels with endothelial nitric oxide synthase activity," *Journal of Biomedical Materials Research Part B: Applied Biomaterials*, vol. 85, no. 2, pp. 537–546, 2008.

[57] L. Jia, M. P. Prabhakaran, X. Qin, and S. Ramakrishna, "Stem cell differentiation on electrospun nanofibrous substrates for vascular tissue engineering," *Materials Science & Engineering C*, vol. 33, no. 8, pp. 4640–4650, 2013.

[58] M. P. Prabhakaran, L. Ghasemi-Mobarakeh, and S. Ramakrishna, "Electrospun composite nanofibers for tissue regeneration," *Journal of Nanoscience and Nanotechnology*, vol. 11, no. 4, pp. 3039–3057, 2011.

[59] F. Wang, Z. Li, and J. Guan, "Fabrication of mesenchymal stem cells-integrated vascular constructs mimicking multiple properties of the native blood vessels," *Journal of Biomaterials Science Polymer Edition*, vol. 24, no. 7, pp. 769–783, 2013.

[60] J. Zhao, L. Liu, J. Wei et al., "A novel strategy to engineer small-diameter vascular grafts from marrow-derived mesenchymal stem cells," *Artificial Organs*, vol. 36, no. 1, pp. 93–101, 2012.

[61] L. Ren, D. Ma, B. Liu et al., "Preparation of three-dimensional vascularized MSC cell sheet constructs for tissue regeneration," *BioMed Research International*, vol. 2014, Article ID 301279, 10 pages, 2014.

[62] M. D. Guillemette, R. Gauvin, C. Perron, R. Labbé, L. Germain, and F. A. Auger, "Tissue-engineered vascular adventitia with vasa vasorum improves graft integration and vascularization through inosculation," *Tissue Engineering Part A*, vol. 16, no. 8, pp. 2617–2626, 2010.

[63] P.-L. Tremblay, V. Hudon, F. Berthod, L. Germain, and F. A. Auger, "Inosculation of tissue-engineered capillaries with the host's vasculature in a reconstructed skin transplanted on mice," *American Journal of Transplantation*, vol. 5, no. 5, pp. 1002–1010, 2005.

[64] G. Grenier, M. Rémy-Zolghadri, D. Larouche et al., "Tissue reorganization in response to mechanical load increases functionality," *Tissue Engineering*, vol. 11, no. 1-2, pp. 90–100, 2005.

[65] R. Gauvin, R. Parenteau-Bareil, D. Larouche et al., "Dynamic mechanical stimulations induce anisotropy and improve the tensile properties of engineered tissues produced without exogenous scaffolding," *Acta Biomaterialia*, vol. 7, no. 9, pp. 3294–3301, 2011.

[66] Z. Gong and L. E. Niklason, "Small-diameter human vessel wall engineered from bone marrow-derived mesenchymal stem cells (hMSCs)," *The FASEB Journal*, vol. 22, no. 6, pp. 1635–1648, 2008.

[67] T. M. Maul, D. W. Chew, A. Nieponice, and D. A. Vorp, "Mechanical stimuli differentially control stem cell behavior: morphology, proliferation, and differentiation," *Biomechanics and Modeling in Mechanobiology*, vol. 10, no. 6, pp. 939–953, 2011.

Hindawi Publishing Corporation
BioMed Research International
Volume 2015, Article ID 108571, 14 pages
http://dx.doi.org/10.1155/2015/108571

Research Article

In Vitro Evaluation of Scaffolds for the Delivery of Mesenchymal Stem Cells to Wounds

Elizabeth A. Wahl,[1] Fernando A. Fierro,[2] Thomas R. Peavy,[3] Ursula Hopfner,[1] Julian F. Dye,[4] Hans-Günther Machens,[1] José T. Egaña,[1,5] and Thilo L. Schenck[1]

[1]*Department of Plastic Surgery and Hand Surgery, University Hospital Klinikum rechts der Isar, Technical University Munich, 81675 Munich, Germany*
[2]*Institute for Regenerative Cures, UC Davis, Sacramento, CA 95817, USA*
[3]*Department of Biological Sciences, California State University, Sacramento, CA 95819, USA*
[4]*Institute of Biomedical Engineering, UCL, The Royal Institution, London W1S 4BS, UK*
[5]*FONDAP Center for Genome Regulation, Faculty of Sciences, University of Chile, 7800024 Santiago, Chile*

Correspondence should be addressed to José T. Egaña; tomasega@gmail.com

Received 18 February 2015; Revised 2 April 2015; Accepted 9 April 2015

Academic Editor: Robert Gauvin

Mesenchymal stem cells (MSCs) have been shown to improve tissue regeneration in several preclinical and clinical trials. These cells have been used in combination with three-dimensional scaffolds as a promising approach in the field of regenerative medicine. We compare the behavior of human adipose-derived MSCs (AdMSCs) on four different biomaterials that are awaiting or have already received FDA approval to determine a suitable regenerative scaffold for delivering these cells to dermal wounds and increasing healing potential. AdMSCs were isolated, characterized, and seeded onto scaffolds based on chitosan, fibrin, bovine collagen, and decellularized porcine dermis. *In vitro* results demonstrated that the scaffolds strongly influence key parameters, such as seeding efficiency, cellular distribution, attachment, survival, metabolic activity, and paracrine release. Chick chorioallantoic membrane assays revealed that the scaffold composition similarly influences the angiogenic potential of AdMSCs *in vivo*. The wound healing potential of scaffolds increases by means of a synergistic relationship between AdMSCs and biomaterial resulting in the release of proangiogenic and cytokine factors, which is currently lacking when a scaffold alone is utilized. Furthermore, the methods used herein can be utilized to test other scaffold materials to increase their wound healing potential with AdMSCs.

1. Introduction

Mesenchymal stem cells (MSCs) have been shown to improve tissue regeneration *in vitro* and *in vivo*. Clinical data corroborates their beneficial regenerative effects in several organs and tissues, such as the heart, nerves, bone, and skin [1–4]. In order to administer MSCs to patients, cells have been introduced systemically and locally. While MSCs do have a homing capability to migrate to injured tissue, it has been claimed that after systemic administration only a fraction of the cells can migrate to the target tissue, while the majority of cells accumulate in the kidneys and lungs [5, 6]. In the case of local injections, a large number of these cells are required and while a substantial proportion of the cells remain in the area, another quantity is flushed out into the blood circulation [2, 7]. In an attempt to increase the retention rate of the cells, MSCs have been applied in association with biomaterials; for example, fibrin sprays and microbeads have been used for chronic skin wounds [8, 9], while meshes and three-dimensional scaffolds have been used to treat ischemic heart tissue [10] and diabetic ischemic ulcers [11].

Engrafted MSCs can release a series of cytokines and growth factors by interacting with local tissue to enhance repair and regeneration [5, 12]. Recent studies indicate that MSCs modulate the regenerative microenvironment by means of a controlled release of several paracrine factors related to key processes, such as angiogenesis, cell homing, immunomodulation, tissue remodeling, and fibrosis [13–15].

Thus, MSCs may impact regeneration primarily by releasing paracrine factors necessary for wound healing [16–18] rather than tissue replacement.

While MSCs have been found to exist in nearly every adult tissue [19–24], the proliferation rate of MSCs derived from adipose tissue (AdMSCs) is not affected by donor age [25–27], making it possible to use them in an autologous manner in elderly patients in regenerative medicine. A high quantity of MSCs can be obtained from a small amount of fat tissue (at least 1×10^6 AdMSCs can be obtained from 200 mL of lipoaspirates) with more than 90% viability and virtually no harm to the donor [28, 29]. Furthermore, as vasculature is believed to be rich in MSCs, it is not surprising that a large quantity of AdMSCs can be isolated from a small amount of adipose tissue, which is highly vascularized [30, 31].

Several studies have shown the immunosuppressive properties of AdMSCs, which has allowed for xenogeneic transplantation into immunocompetent recipients for various disease models evidencing significant improvement without suppressing the immune system [31, 32]. Furthermore, clinical and preclinical studies have determined that allogeneic transplants of AdMSCs do not usually result in graft-versus-host disease (GvHD). These transplants have been used to treat GvHD after hematopoietic stem cell transplantation [32–34].

The positive effects of the use of MSCs are well established for various tissues; however, several regulatory and practical issues make chronic ulcers an attractive target for the clinical use of MSCs. More importantly, chronic ulcers remain an eminent clinical problem negatively impacting patients' quality of life and simultaneously representing a substantial expenditure for the healthcare system. In the US, these problems affect more than 8 million people with annual costs of around $20 billion [35]. With an aging population and the likelihood that the majority of the healthcare costs will come from patients over 65, the costs are almost certain to increase [36].

Several studies have proposed the combined use of scaffolds for dermal regeneration with stem cells for the treatment of chronic skin ulcers. In those studies, it has been shown that after seeding cells are able to survive in scaffolds, releasing several bioactive molecules that enhance skin regeneration *in vivo* [7, 37–39]. Although the results of preclinical trials are robust, several issues have to be clarified and optimized before clinical translation. In the case of chronic wounds, the cells must produce optimum amounts of paracrine factors in order to achieve the quantity necessary for healing. The addition of AdMSCs to the scaffold should support the healing process by creating a proregenerative microenvironment in the wound area. The key issue of determining the best combination of cells with a biomaterial and the development of an optimized composite material with increased regenerative capacity remains to be addressed.

Scaffolds alone are currently being used to treat chronic wounds in clinics and are composed of a variety of materials. In this study, we chose three scaffolds that are currently being used in clinics and one that is under development, all comprised of different biomaterials, to incorporate AdMSCs. BioPiel is a film-like scaffold derived from crustacean chitosan. Smart Matrix, currently under development, consists of a fibrin-alginate composite. Integra Dermal Regenerative Template (DRT) is a bilayer scaffold composed of type I bovine collagen and chondroitin-6-sulfate with a thin silicon layer and Strattice is derived from decellularized porcine dermis.

In this study, we analyzed and compared the behavior of AdMSCs in four distinct scaffolds, which were chosen because of their differences in the construction, material, and protein composition. The seeding efficiency, cellular distribution, attachment, survival, metabolic activity, and paracrine release of the seeded cells were analyzed *in vitro* as were the angiogenic effects *in vivo*.

2. Materials and Methods

2.1. Cell Isolation and Culture. Adipose tissue was derived from lipoaspirates obtained from donors who had given informed consent to participate in the study. The aspirated fraction was added to 50 mL Falcon tubes with an equal volume of 0.3 U/mL collagenase A (Roche, Basel, Switzerland) and incubated for 30 min at 37°C. After centrifugation, the resulting stromal vascular fraction was plated under standard conditions in Dulbecco's Modified Eagle's Medium with 4.0 mg glucose/L, stable glutamine, phenol red (DMEM; Biochrom, Berlin, Germany), supplemented with 10% fetal calf serum (FCS; PAA, Pasching, Austria), and 1% penicillin/streptomycin (P/S; Biochrom) under standard cell culture conditions (37°C, 5% CO_2) and medium was changed every 3-4 days. In all experimental settings, cells from passage 3 were used with three donors ($N = 3$) and performed in triplicate ($n = 3$).

2.2. Cell Characterization. For analysis of cell surface markers by flow cytometry, AdMSCs were detached from the culture flasks with trypsin-EDTA solution (Biochrom), rinsed with phosphate buffered saline (PBS; Biochrom) and incubated for 45 min with Phycoerythrin- (PE-) conjugated antibodies raised against CD45, CD73, CD90, CD105, and CD146 at 4°C (1 : 100 dilution) ($N = 3$, $n = 3$). As isotype controls, IgG-PE was used (all antibodies from BD Biosciences, San Jose, CA). Samples were examined with a Cytomics FC500 (Beckman Coulter, Brea, CA).

To test the osteogenic differentiation potential of the AdMSCs, 80–90% confluent cells were cultured for 18 d in either control medium (alpha-MEM (Biochrom) + 10% FCS and 1% P/S) or osteogenic medium (hMSC osteogenic differentiation BulletKit, Lonza, Basel, Switzerland) in 6-well plates with a medium change every 3-4 d. Then, cells were fixed with 10% v/v formalin solution for 15 min, rinsed with PBS, stained with 0.5% w/v Alizarin Red S indicator (Ricca Chemicals Company, Arlington, TX) 30 min with gentle shaking, washed 3 times with PBS, and imaged for calcium deposition.

To test adipogenic differentiation of AdMSCs, cells were seeded in 6-well plates to 80–90% confluence. Medium was changed to either control medium (alpha-MEM + 10% FCS

and 1% P/S) or adipogenic induction medium (hMSC adipogenic differentiation BulletKit, Lonza). For Oil Red O staining, cells were fixed after 14 d with 10% v/v formalin solution, rinsed with PBS, and stained with Oil Red O (Electron Microscopy Sciences, Hatfield, PA), and adipocytes were imaged (Nikon Eclipse TS100 Inverted Microscope).

Chondrogenic differentiation potential was carried out with three-dimensional pellet cultures in 15 mL polypropylene conical tubes. The initial pellets contained 2.5×10^5 cells and were cultivated for 21 d in either control medium or chondrogenic induction medium (hMSC chondrogenic differentiation BulletKit, Lonza) supplemented with TGF Beta 3 (Lonza). After collection, pellets were rinsed with PBS and fixed in formalin. Pellets were sectioned (5 μm) in paraffin and stained with Alcian Blue to visualize acetic mucins and acid mucosubstances and counterstained with Nuclear Fast Red (both from Sigma-Aldrich, St. Louis, MO, USA) before imaging. All stainings were carried out with $N = 3$ and $n = 3$.

2.3. Scaffolds. Four scaffolds, based on different biomaterials, were tested in this study. Here we compared BioPiel (chitosan film), Smart Matrix (fibrin matrix), Integra DRT (collagen-glycosaminoglycan matrix), and Strattice (decellularized dermis). BioPiel (Recalcine, Santiago, Chile) is a commercially available wound dressing with hemostatic and bacteriostatic properties composed of chitosan. Smart Matrix (RAFT, Northwood, Middlesex, UK) is a porous cross-linked fibrin-alginate composite biomaterial and is not yet commercially available. Integra DRT (Integra Life Sciences, Plainsboro, NJ, USA) is a commonly used, FDA approved, biodegradable porous scaffold based on bovine type I collagen fibers that are cross-linked by glycosaminoglycans (GAG) with a protective silicon layer. Strattice (LifeCell Corporation, Branchburg, NJ, USA) is an FDA approved porcine decellularized dermal matrix. In all experiments, 6 mm (in diameter) discs, as created with a biopsy punch, were used.

2.4. Fluid Capacity of the Scaffolds. In order to determine the maximum seeding volume, the fluid uptake of each scaffold was determined. Dried matrices were placed in DMEM and their fluid capacity was calculated ($n = 8$) [41]:

$$\text{Hydrophilicity} = \frac{\text{wet weight} - \text{dry weight}}{\text{dry weight}}. \quad (1)$$

2.5. Structural Analysis of the Scaffolds. The micro- and macrostructures of the scaffolds were analyzed by scanning electron microscopy (SEM) and optical microscopy, respectively. Scaffolds were dehydrated with graded ethanol, air-dried, and sputter-coated with gold for 80 sec at 40 mA (Sputter Coating Device SCD 005, Bal-Tec AG, Liechtenstein). Analysis was performed at 5 kV accelerating voltage in a scanning electron microscope (Jeol JSM-5400, Japan). For macroanalysis, scaffolds were imaged using a stereoscope (Zeiss, Jena, Germany) from the side and top view.

2.6. Cell Seeding of Scaffolds. Scaffolds were placed in 24-well plates and 1.8×10^5 AdMSCs were seeded dropwise with defined volumes of DMEM, supplemented with 10% FCS and 1% P/S according to the fluid capacity of the scaffold (Chitosan film: 35 μL, Fibrin matrix: 25 μL, Collagen-GAG matrix: 40 μL and, Decellularized dermis: 22 μL). AdMSCs were suspended in DMEM and seeded dropwise directly onto the scaffold. After 1 h, 1 mL of additional medium was added to the scaffolds, which were further cultured under standard conditions.

2.7. Cell Seeding Efficiency on Scaffolds. The percentage of cells incorporated into the scaffolds ($n = 3$, $N = 4$) was quantified by counting the cells attached to the culture dish one hour after seeding, that is, cells that did not attach to the scaffold. The scaffolds were removed and the remaining cells were detached from the well plates with trypsin-EDTA solution and counted in a Neubauer chamber. Seeding efficiency was calculated as the percentage of cells in the scaffold from the total number of seeded cells.

2.8. Cellular Distribution throughout Scaffolds. AdMSC-containing scaffolds were rinsed with PBS, fixed (3.7% paraformaldehyde, 0.1% Triton in PBS) on ice for 30 min, and blocked in 2% BSA in PBS at 4°C overnight ($N = 3$, $n = 3$). Scaffolds were then incubated in a blocking solution containing 2 U/mL Texas Red-X Phalloidin (Life Technologies, Grand Island, NY) to stain polymerized actin and 3.5 μM To-Pro-3 (Life Technologies) to stain DNA. After washing 4 times with PBS (10 min each), scaffolds were dried with sterile gauze, mounted in Vectashield Mounting Medium (Vector Labs, Burlingame, CA) on glass bottom culture dishes (MatTek Corp., Ashland, MA), and imaged using an Olympus Fluoview FV10i confocal microscope (Olympus, Tokyo, Japan). Chitosan films were z-section imaged from top to bottom with the drop side facing down on the glass bottom, in 4 independent locations (one center and 3 periphery locations). As the fibrin matrix, collagen-GAG matrix, and decellularized dermis are too thick for visualization by confocal microscopy from top to bottom, they were sectioned using a razor blade and rotated onto their sides in order to generate z-section images from cross sections. Image analysis to assess cell morphology, number, and distribution was performed using Olympus FV10-ASW software (Olympus).

2.9. Metabolic Activity and Cytotoxicity in the Scaffold. On days 1, 3, 7, and 14 after seeding, the metabolic activity of the seeded cells was evaluated by precipitation of tetrazolium salt (WST-1). Cellular death was measured by the release of lactate dehydrogenase (LDH) from the cells on days 1, 3, and 7 (both from Roche, Mannheim, Germany) ($n = 3$, $N = 3$). As the medium needed to be changed after 7 d, the total LDH activity could not be measured over a 14 d period. Seeded scaffolds were incubated in DMEM and WST-1 solution (1 : 10 ratio) for 1 h. The absorbance of the resulting formazan dye was measured at 450 nm with a reference wavelength of 620 nm. For the measurement of LDH,

supernatants were harvested from the same scaffolds used for WST-1 assay and the analysis was performed according to the manufacturer's instructions. In short, the absorbance was measured at 490 nm and a reference wavelength of 620nm with controls including medium alone (background), cells in well plates without scaffolds (spontaneous LDH release), and cells in well plates without scaffolds with Triton X-100 in the medium (maximum LDH release). The resulting value was then calculated with the equation: cytotoxicity (%) = (experimental value – spontaneous LDH release)/(maximum LDH release – spontaneous LDH release) × 100.

2.10. Characterization of Secretion Profile. Supernatants were collected from AdMSC seeded on scaffolds or tissue culture plastic ($n = 3$, $N = 3$; 1.8×10^5 cells/scaffold) after 48 h under standard cell culture conditions, shock frozen with liquid nitrogen, and stored at −80°C until analysis. Human Cytokine and Angiogenesis Array Kits (R&D Systems, Abingdon OX, UK) were used to characterize the release of multiple cytokines and angiogenesis related proteins, respectively. Membranes were imaged using a Peqlab Fusion FX7 chemiluminescence system (Erlangen, Germany) and the spot intensity was quantified with ImageJ software [42] using the MicroArray Profile plugin (OptiNav, Inc.). Scaffolds without cells served as controls.

2.11. Hypoxia-Inducible Factor-1α Expression. Seeded scaffolds ($n = 3$, $N = 3$) were incubated in standard (21% O_2, 5% CO_2) or hypoxic conditions (1% O_2, 5% CO_2) and collected at 4, 8, and 16 h. Then scaffolds were washed two times with sterile PBS. Three scaffolds from each time point, oxygen condition, and type were briefly sonicated in 500 μL lysis buffer; the HIF-1α expression was analyzed using a Human Total HIF-1α ELISA kit (R&D Systems), and the optical density was measured at 450 nm using a Mithras LB 940 Microplate Reader. The total protein concentration was determined using a Pierce BCA Protein Assay Kit (Thermo Scientific, Rockford, IL) and the absorbance was measured at 560 nm.

2.12. Chicken Chorioallantoic Membrane (CAM) Assay. Research grade fertilized eggs (SPF, Valo Biomedia GmbH, Osterholz-Scharmbeck, Germany) were placed on a rotating egg tray for 3 days after fertilization at 37°C and 60–70% humidity. On day 3, a small window was made in the shell under aseptic conditions and the contents of the egg were gently placed into a 200 mL plastic dish. The dish was further placed into a petri dish with 50 mL of distilled water, 1% P/S, and 1% partricin and incubated at 70–80% humidity to prevent drying of the membrane. On day 10, autoclaved filter paper punches (5 mm) were added to the CAM directly followed by 10 μL of conditioned media collected from serum-free cell seeded scaffolds after 48 h in culture, DMEM, PBS, or 20 ng of VEGF, which was reapplied daily for 3 days [43]. The applied filter paper punches were imaged daily using a Canon EOS 20D digital SLR camera with a Canon EF 50 mm f/1.8 II Standard AutoFocus Lens. Samples were quantified ($n = 3$, $N = 6$) by being given arbitrary values based on the distribution and density of CAM vessels around the filter paper punch [40].

2.13. Statistical Analysis. Results were analyzed with GraphPad Prism version 6.0e for Mac OSX (GraphPad Software, San Diego, CA USA) and are shown as mean ± standard deviation. Significant differences between sample groups were determined by analysis of variance (ANOVA) with a Bonferroni posttest where $p < 0.05$ was considered statistically significant.

3. Results

Mesenchymal stem cells were isolated from human adipose tissue and characterized in terms of their immune phenotypes and differentiation potential. Fluorescence-activated cell sorting analysis showed that AdMSCs do not express pan-hematopoietic marker CD45 but are positive for CD73, CD90, and CD105 (Figure 1(a)). Interestingly, AdMSCs expressed very low levels of the pericyte marker CD146. Moreover, the cells showed a strong differentiation potential towards osteoblasts, adipocytes, and chondrocytes after culturing in their respective differentiation conditions (Figure 1(b)). Calcium deposits were stained with Alizarin Red S for AdMSCs exposed to osteoblast differentiation medium. Lipid vacuoles from adipogenic differentiation were stained with Oil Red O. Chondrogenic pellets were stained with Alcian Blue to show chondrocyte growth.

In this work, four different scaffolds were compared for their usability with AdMSCs in dermal regeneration (Table 1). We evaluated and compared the macro- and microstructure of the four scaffolds, observing important differences (Figure 2). The dry thickness of the scaffold varies from a minimum of 0.12 mm for chitosan films to 3.8 mm for fibrin matrices (Figure 2(a)). When wet, the structure of the fibrin matrices collapses to a fibrous mesh decreasing the measurable thickness. The decellularized dermis had the thickest structure at 1.5 mm, while the collagen-GAG matrix was 0.20 mm thick (Table 1). Compared to the other scaffolds, the chitosan has a film-like appearance, while the fibrin and collagen-GAG present a more mesh-like structure and exhibited high porosity throughout the scaffolds. The decellularized dermis exhibited much tighter pores and the chitosan did not have any visible porosity (Figure 2(b)).

Scaffold porosity and the degree to which the pores are interconnected determine the loading capacity of the scaffolds. After AdMSCs were seeded and allowed to attach to the scaffold for one hour the seeding efficiency was evaluated. A seeding efficiency of almost 90% was observed in the fibrin matrix (88.6 ± 2.9), collagen-GAG matrices (86.5 ± 3.8), and the decellularized dermis (89.2 ± 3.8), which was significantly higher than the chitosan films (60.1% ± 5.9%) ($p < 0.05$).

Differences in the mechanical properties should influence the cell behavior when seeded. For that, a detailed view into the interaction and distribution of the seeded cells in the scaffold was obtained by confocal microscopy. Except for the decellularized dermis, the AdMSCs were highly attached to the material, showing fibroblastic morphology, creating a

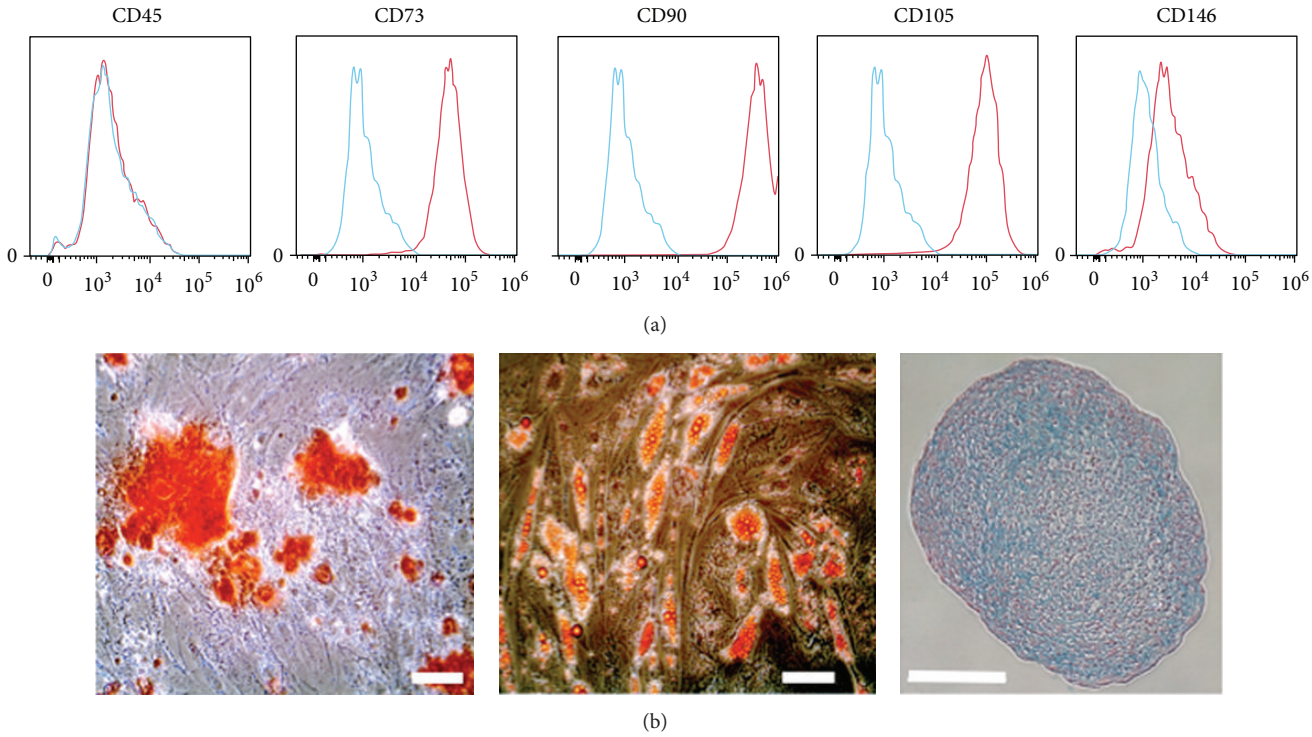

Figure 1: AdMSC characterization. The immune phenotype of the cells was evaluated by labeling cells with Phycoerythrin-conjugated antibodies for flow cytometry. The blue histogram indicates the isotype control (a). In order to evaluate their differentiation potential, AdMSCs were cultured with control (not shown), osteogenic, adipogenic, or chondrogenic medium (b). Calcium precipitation as a result of osteogenic differentiation was confirmed by Alizarin Red S staining (left panel), triglyceride-containing vacuoles emerging from adipogenic differentiation were stained used Oil Red O (middle panel), and cartilaginous glycosaminoglycans and mucins were stained using Alcian Blue with a Nuclear Fast Red nucleic cross stain. Staining was performed after 21 d in culture. Scale bars represent 100 μm. $n = 3$, $N = 3$.

Table 1: Comparison of scaffold properties. The general properties of the scaffolds show a broad variation in weight, size, fluid capacity, and price of material. As the fibrin matrix is currently not commercially available some information could not be divulged.

	Commercial name	Company	Price [USD/cm^2]	FDA approval	Dry weight [mg/cm^2]	Fluid capacity [μL/cm^2]	Dry thickness (mm)
Chitosan film	**BioPiel**	Recalcine	10	Yes	4 ± 0.3	123 ± 14.8	0.12
Fibrin matrix	**Smart Matrix**	RAFT	—	N/A	12 ± 1.5	87 ± 9.0	3.8–1.8
Collagen-GAG matrix	**Integra DRT**	Integra Life Sciences	3	Yes	10 ± 1.4	143 ± 5.6	0.20
Decellularized dermis	**Strattice**	LifeCell	26	Yes	148 ± 2.9	77 ± 4.1	1.5

complex tridimensional arrangement between the cells and the scaffold (Figure 3(a)). The images were analyzed to give quantitative, spatial information on the cellular distribution throughout the scaffold (Figure 3(b)). The AdMSCs formed a layer on the seeding surface of chitosan films, showing almost no cells in the core. In the case of the fibrin matrix, cells were observed throughout the scaffold with a tendency to accumulate at the inner core of the material. Cells seeded on collagen-GAG matrices also showed a different distribution pattern creating a cell gradient from the seeding side to the bottom. In the decellularized dermis, AdMSCs were more concentrated on the seeding side while migration through the scaffold was limited.

The distribution of the AdMSCs is an important indicator for biocompatibility with the different scaffold materials. However, secretion activity relies on cell survival beyond the initial seeding, which was measured by means of their metabolic activity. Interestingly, there was no correlation between the metabolic activity and seeding efficiency. Twenty-four hours after seeding, the formation of formazan blue, as an indicator of metabolic activity, was the highest in fibrin and collagen-GAG matrices, while AdMSCs seeded on the chitosan film and decellularized dermis showed comparable values initially (Figure 4(a)). In order to evaluate if these differences were due to increases in cellular death, lactate dehydrogenase (LDH) activity was measured from the supernatants. It can be seen that the decellularized dermis had a high rate of cytotoxicity (almost 100%), even after only one day in culture, whereas the collagen-GAG matrix had virtually no cytotoxic effect (Figure 4(b)).

The long-term viability of the AdMSCs seeded on the scaffolds was measured and compared at further time points

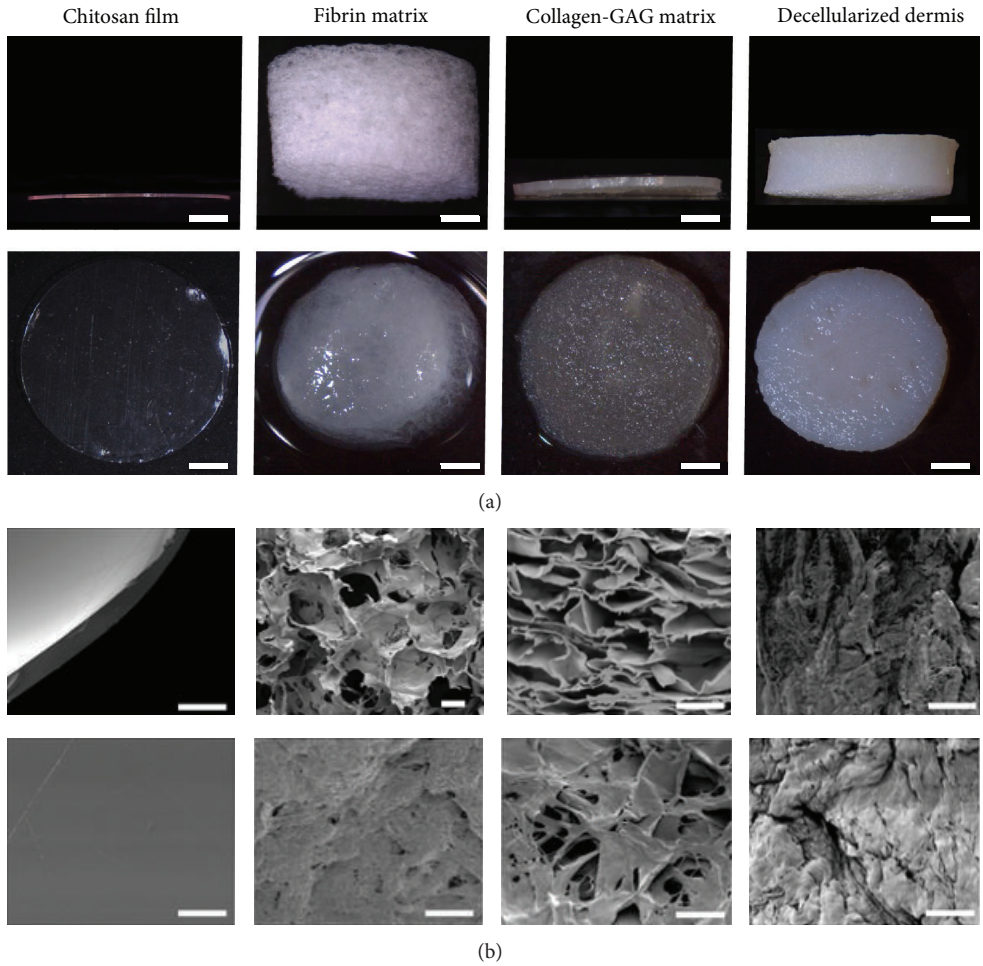

Figure 2: Scaffold characterization. The thickness and general structure of the scaffolds (6 mm in diameter) were analyzed macroscopically from the side (dry, top row) and the top (wet, bottom row). The thickness of the scaffolds remains the same except for the fibrin matrix, which collapses into a mesh of fibers. Scale bars represent 1 mm (a). The pore structure and texture of the scaffolds were analyzed by SEM micrographs from the transverse sections (top row) and top view (bottom row). Note the complete absence of pores in the chitosan film in comparison to the other scaffolds. Scale bars represent 100 μm (b).

after seeding. Results show that while the chitosan film and decellularized dermis have comparable metabolic activity through day 7, 14 days after seeding the chitosan film exhibited similar results to the fibrin and collagen-GAG matrices (Figure 4(a)). The collagen-GAG matrix showed steady metabolic activity throughout the 14 days, while the fibrin matrix showed an increase in activity through day 7 after which the activity decreased at day 14. Cellular death results showed a general increase in cytotoxicity as the metabolic activity of the cells increased, except for in day 7 of the fibrin and collagen-GAG matrix where the metabolic activity peaked. The highest percentage of cytotoxicity was seen in the decellularized dermis being close to 100% (Figure 4(b)).

The differences detected between scaffolds in relation to the behavior of AdMSCs lead to the conclusion that depending on the physical and chemical conditions, the factors secreted from the AdMSCs can also vary considerably. Here, the secretion of 91 different angiogenic, cytokine, and chemokine factors were analyzed to obtain a characteristic secretion profile for each scaffold. Among the detected factors, the most prevalent one was macrophage migration inhibitory factor (MIF), plasminogen activator inhibitor 1 (Serpin E1), interleukin 6 (IL-6), interleukin 8 (IL-8), chemokine (C-X-C motif) ligand 1 (CXCL1), placental growth factor (PlGF), and vascular endothelial growth factor (VEGF) (Figure 5). Due to the low viability of the cells observed after seeding, decellularized dermis scaffolds were excluded for this assay.

Compared to AdMSCs seeded directly onto tissue culture plastic, the scaffold condition itself significantly induces the release of PlGF while it reduces the release of VEGF ($p < 0.05$). Compared among the scaffolds, we observed that the release of angiogenesis inducing IL-8 was similar between fibrin matrices and two-dimensional cultures, while chitosan films and collagen-GAG matrices show a dramatic decrease ($p < 0.05$). The release of inflammation regulating IL-6 was elevated in supernatants from cells seeded on collagen-GAG matrices while chitosan films showed the highest expression of Serpin E1. MIF and CXCL1 did not show any significant differences between scaffolds or control conditions.

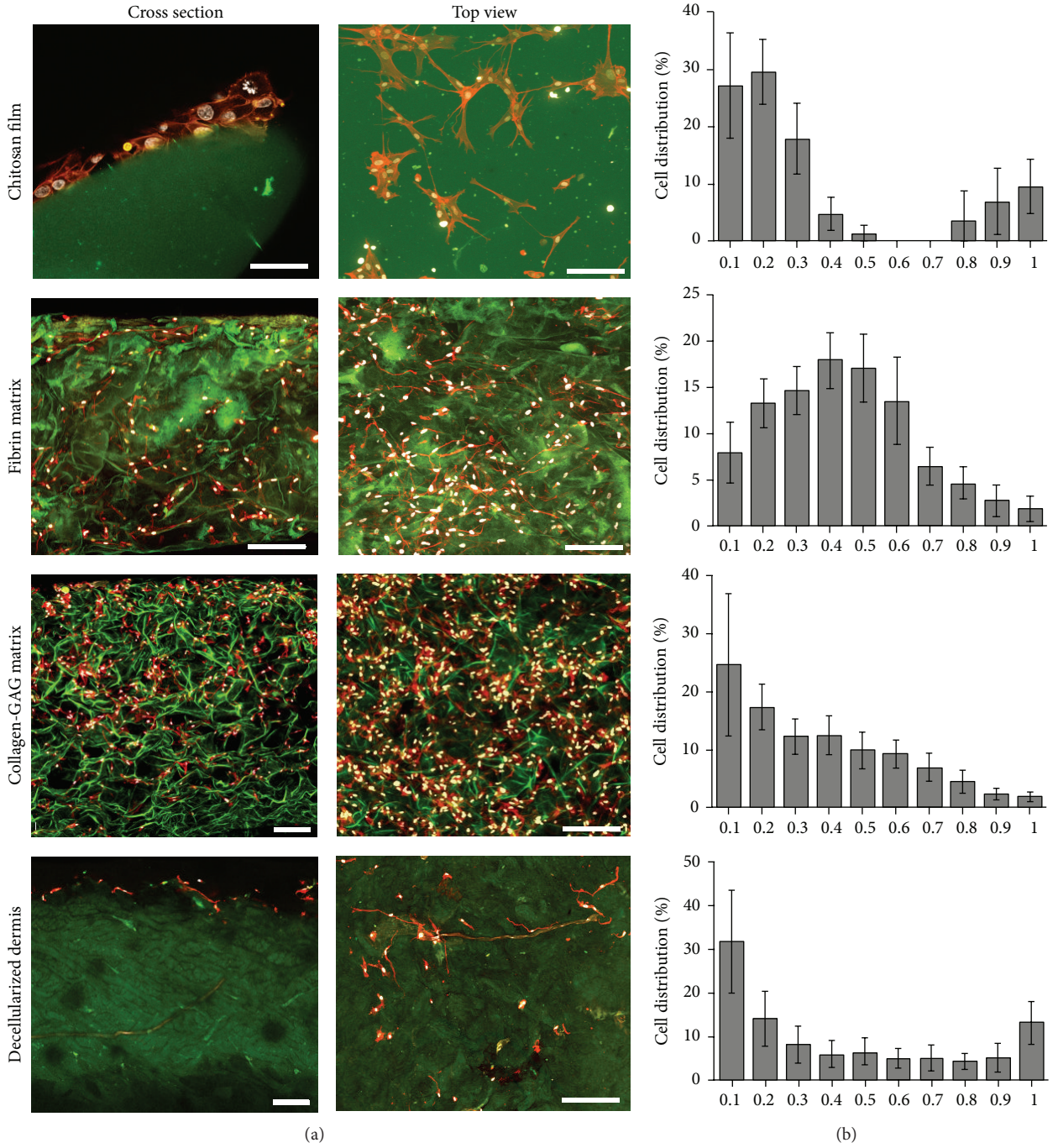

Figure 3: Cellular distribution and attachment of cells on scaffolds. After seeding, the distribution and attachment of the cells was evaluated by LSM. In all cases, except for the decellularized dermis, AdMSCs (To-Pro-3 (white)/phalloidin (red)) adhered to the scaffold (green autofluorescence) showing a fibroblast like morphology. As can be seen in the first column, cells formed a layer over chitosan films while the others cells were able to migrate further into the scaffold. Cross section (right) and top view (left) of scaffolds. Scale bar represents 150 μm (a). Quantification of the cellular densities after 1 d throughout sections, ranging from the top (0.1) to the bottom (1) of the scaffolds as seen in confocal imaging (b). $n = 3$, $N = 3$.

A major problem in wound healing is the limited oxygen concentrations inhibiting healing. We used hypoxia inducible factor-1α (HIF-1α) to investigate if the scaffolds inhibit the cells from gaining access to oxygen levels. At time points 4, 8, and 16 h no noticeable traces of HIF-1α could be detected (data not shown). We concluded that all scaffolds allow proper gas exchange with the environment.

Finally, we evaluated the biological effects of conditioned medium in an *in vivo* CAM assay model. The chicken chorioallantoic membrane assay is an established method to

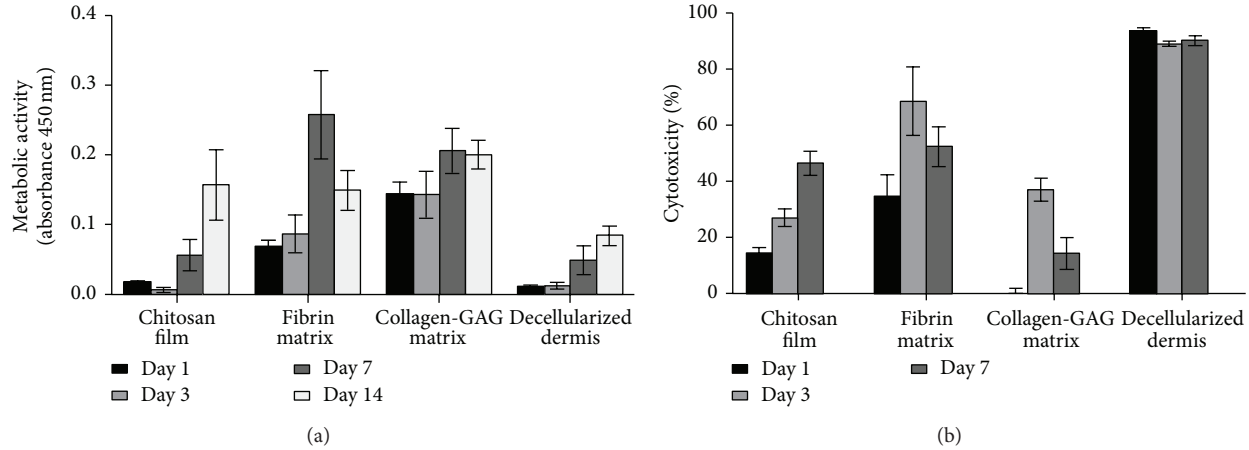

Figure 4: Cellular survival within the scaffold. The metabolic activity (WST-1) and cellular death (LDH) were measured and compared after seeding. Results show that the metabolic activity of the cells increased over time, indicating that the cells were able to proliferate within the scaffolds (a). The LDH released by the cells was measured as an indicator of cellular death. The highest mortality was observed after only 1 d in the decellularized dermis indicating a poor biocompatibility with the AdMSCs (b). $n = 3$, $N = 3$.

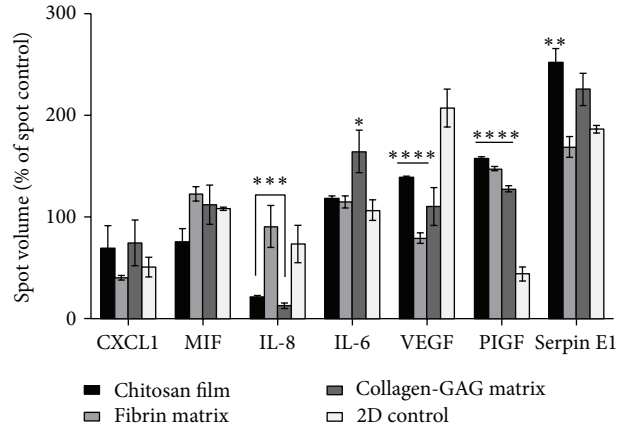

Figure 5: Secretion profile of AdMSC seeded scaffolds. Human cytokine and angiogenesis arrays were utilized in order to analyze supernatants after a 48 h incubation to detect if there is an effect of the scaffolds interaction with the cells on paracrine factor release. Decellularized dermis scaffolds were excluded as previous data revealed that it did not provide a compatible environment for the cells to migrate and flourish. Chitosan films and collagen-GAG matrices show a decrease in expression of IL-8 in comparison to fibrin matrices, which is similar to two-dimensional conditions. Collagen-GAG matrices had a significant release of IL-6, while chitosan films had an increase of Serpin E1 release over all other conditions. There are significant differences in release of PIGF and VEGF from all scaffolds in comparison to two-dimensional cultures. $^{*}p < 0.05$; $^{**}p < 0.01$; $^{***}p < 0.001$; $^{****}p < 0.0001$ when compared to 2D control. $n = 3$, $N = 3$.

monitor *de novo* vessel formation. Here, conditioned medium was pipetted onto autoclaved filter paper punches in order to determine if there was an enhanced effect from the factors secreted from the AdMSCs that was due to the composition of the scaffold or if the scaffold alone had any angiogenic potential. In order to minimize irritation to the CAM and avoid affecting the result, the scaffolds themselves were not utilized. In the positive control (VEGF), large existing vessels showed a tendency to move toward the filter paper, while this was not evident in the samples exposed to the AdMSC conditioned medium, suggesting that the supernatant of the cells was not as proangiogenic as pure VEGF (Figure 6(a)). Nevertheless, as seen in the *in vitro* data, the highest instance of neovascularization in small vessel convergence and growth occurred with medium that was obtained from collagen-GAG matrices followed by fibrin matrices and, finally, chitosan films (Figure 6). The quantification is based on arbitrary points given for *de novo* small vessel formation up to reorganization of existing vessels (Figure 6(b)) [40]. These results suggest that the composition of the scaffold has a direct effect on the angiogenic factors released from the AdMSCs. No significant differences appeared between PBS, conditioned medium without cells, and DMEM alone (data not shown for the medium exposed samples).

4. Discussion

Although various stem cell populations have been suggested for therapeutic use, MSCs are particularly attractive as they are well discerned and ongoing clinical trials have shown promising results in wounded tissue [4, 44–46]. Furthermore, there is great potential for using AdMSCs in regenerative medicine [1]. They are easy to isolate, are accessible with minimally invasive procedures, and contain a high number of cells within a small amount of tissue, and the age of the donor does not affect their proliferation rate or differentiation potential [26, 27], making them ideal for clinical procedures.

For clinical application, administration, and effectiveness are key factors in describing the efficacy of a given treatment. In the case of AdMSCs, this encompasses the viability of the cells under the given conditions and their ability to release beneficial growth factors to the damaged tissue. To minimize migration, which reduces the utility of the method, dermal

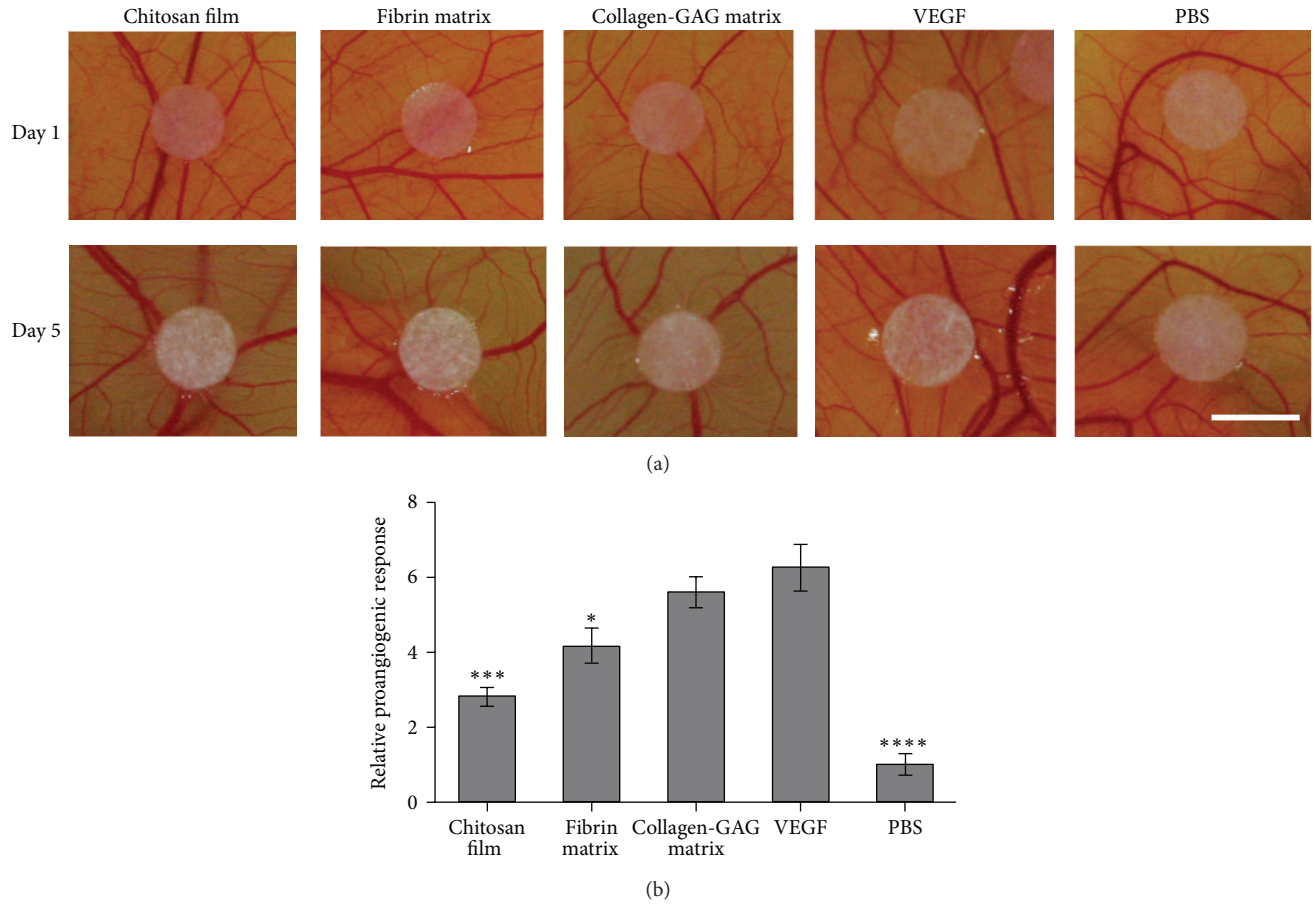

Figure 6: Chicken chorioallantoic membrane *in vivo* analysis. Autoclaved filter paper punches with conditioned medium from scaffolds after 48 h in culture were observed over a five-day period for neovascularization of the CAM. Note the increase in small vessel convergence from the scaffold, specifically in VEGF, collagen-GAG, and fibrin matrices (a). Samples exposed to conditioned medium without cells are not pictured, as they did not differ from the negative control (PBS). Growth was analyzed from 6 replicates per treatment based on an arbitrary scoring system dealing with new small vessel formation and the behavior of existing vessels as observed daily according to [40]. Briefly, a value was assigned for each 5 d ranging from (0) unchanged to slight changes in density and convergence towards filter paper punch (1) and further increases in density and convergence (up to 5) (b). 5 mm scale bar. $^{*}p < 0.05$, $^{***}p < 0.001$, $^{***}p < 0.0001$ when compared to VEGF positive control.

scaffolds were used. The scaffolds examined here were of particular interest as they are currently in use or being tested for use in clinics, although their healing effectiveness to date has been subpar due to slow tissue revascularization. Furthermore, the scaffolds chosen were substantially different in structure (Figure 2) and composition (Table 1). The viability, migration, and growth factor release, especially of the angiogenic growth factors, were of particular interest in this study.

After analyzing the AdMSCs (Figure 1) and scaffolds (Figure 2) for individual characteristics, the distribution and attachment of the seeded cells was analyzed and compared. As expected, AdMSCs adhered to all of the scaffolds but due to their composition and properties, their distribution varied greatly.

4.1. Chitosan Films. Consistent with the lack of porosity detected in chitosan films (Figure 2(b)), the AdMSCs created a single layer on the seeding side with virtually no penetration into the material (Figure 3). A level of porosity must be available in order for cells to be able to penetrate the scaffold and form a network for cells to communicate without overcrowding. Other chitosan derived scaffolds contain artificial pores in order to facilitate cell migration [47, 48]. The seeding side is critical for chitosan-based scaffolds to generate either a superficial cell layer or to create an AdMSC interface between the scaffold and the wound bed. As there is only a layer of cells, these may migrate out of the scaffold soon after transplantation and the effects of the AdMSCs on the wound bed may be beneficial for a short time in order to start a pathway towards healing. While metabolic activity increased over time, an overcrowding of the cells could limit the potential of the AdMSCs to release healing factors. The antimicrobial properties of chitosan makes it a beneficial treatment for superficial wounds and burns, to minimize scarring, decrease pain sensation, and reduce inflammation [49].

4.2. Collagen-GAG and Fibrin Matrices. In contrast to the chitosan film, the AdMSCs seeded onto the fibrin and collagen-GAG matrices showed better penetration into the material (Figure 3), with distribution in fibrin matrices peaking at the center of the scaffold. This effect may be due to the apparent unevenness of the porosity at the center of the fibrin matrix, showing a larger pore structure on the top and bottom of the scaffold, in comparison to the center, which might inhibit the cells from migrating throughout the scaffold (Figure 2). MSCs have been shown to possess a strong attachment to fibrin by way of small binding domains with the cell membrane, something not found with other cell types [50]. The cellular gradient observed in collagen-GAG matrices showed a higher concentration at the seeding side with a steady amount of migration throughout the scaffold. As collagen is the main component of the ECM, the cells were expected to be able to attach and distribute throughout the scaffold. Beyond their porosity, as both collagen and fibrin are dominant in the ECM, it is no surprise that they demonstrate a high cellular bond. Furthermore, AdMSCs isolated from lipoaspirates have previously shown a high affinity for binding to ECM proteins [51]. Beyond that, AdMSCs seeded in collagen-GAG matrices exhibited the highest level of metabolic activity and lowest level of cytotoxicity on day one.

The fibrin and collagen-GAG matrices showed the highest amount of cell migration of the four scaffolds, though at different distributions, which could be attributed to differences in cellular adhesion and migration triggered by the material itself [52, 53]. Throughout the observation, the cells seeded on the collagen-GAG matrix evidenced the steadiest rate of metabolic activity and the lowest rate of cellular death indicating the most compatible relationship between cells and biomaterial.

4.3. Decellularized Dermis. Although AdMSCs seeded onto the decellularized dermis were able to migrate through the material, a strong decrease in metabolic activity was seen soon after seeding, indicating that it may not provide adequate space for the cells to thrive or may even induce cell death (Figure 4). This might be particularly important for the decellularized dermis as it went through cell removal during preparation. The decellularized dermis utilized here, Strattice, has been used successfully as an internally placed scaffold for treatment of subcostal hernia repair [54] and breast reconstruction [55, 56]. Mirastschijski et al. have found that the decellularized dermis may be best suited for dermal wound beds that require a higher mechanical load than in those previously mentioned [57]. While residual porosity does facilitate some AdMSC migration, the high mortality rate would make this an unsuitable scaffold for a cell seeded dermal wound treatment. This high mortality rate may be due to residual chemicals from the decellularization process that cannot be easily washed away before cell seeding. However, the low cellular infiltration that we observed *in vitro* is in line with previous data showing similar results after subcutaneous implantation of the scaffold in a rat model [58].

Although the metabolic activity increased over time in the decellularized dermis, despite the initial rate of cellular death, of the four examined it seems to be the least compatible combination of the AdMSCs and biomaterial. This may be a result of cell overcrowding, due to tight porosity, and could limit the number of cells able to flourish. In addition, pore sizes in the decellularized dermis were not uniform enough in size for the cell-cell interaction necessary for the cells to thrive. Furthermore, the low metabolic activity observed over two weeks of seeding correlates with a high count of cell death only one day after seeding.

4.4. Scaffold-AdMSC Secretion Profile. During the first days after wounding, the release of paracrine factors is crucial for healing [59]. Independent of their differentiation capacity, MSCs have been shown to act as anti-inflammatory and immunoregulatory agents [59, 60], promote cell migration and proliferation and angiogenesis, and improve scarring [4]. The application of AdMSC seeded scaffolds to wounds could, therefore, be beneficial in all the three phases of wound healing: inflammation, proliferation, and tissue remodeling.

The physical and chemical conditions experienced by the cell can alter the cell behavior, in general, and the secretion profile, specifically. In addition, there can be further influences by exposure to biomolecules on the scaffolds, such as peptides and proteins, either artificially or intrinsically [61, 62]. Although the four scaffolds' chitosan is the only material that is not found in the human body, it has been employed successfully in wound healing treatments [49]. Surprisingly, the chitosan film released significantly higher levels of Serpin E1 than the control cells and fibrin matrices. Serpin E1 is known to regulate extracellular matrix (ECM) remodeling [63], which is why a high level of expression from the collagen-GAG matrices is expected (Figure 5).

VEGF and PlGF work together to induce angiogenesis, endothelial cell growth, and promote cell proliferation and migration. VEGF expression is dependent on PlGF while the PlGF/VEGF heterodimer induces pathological angiogenesis [64–66]. In general, the scaffolds had a significant effect in reducing VEGF and increasing PlGF expression relative to the two-dimensional culture (Figure 5). As little difference was found between the release of these factors from cells on each scaffold, this may imply that the scaffold itself upregulated the angiogenic potential of AdMSCs.

An increase in IL-6 may accelerate wound healing by increasing rates of angiogenesis and epithelial cell migration [18]. The scaffold composition did not seem to affect the release of this cytokine, except in the case of the collagen-GAG matrix where it was upregulated. IL-6 is known to induce collagen and GAG production [67] and a similar increase in IL-6 can be seen with primary human dermal fibroblasts seeded on a collagen-GAG matrix [68]. IL-6 also functions in pro- and anti-inflammatory situations and is a major regulator of acute phase reactions, which indicates a wound-like stimulation *in vitro*. IL-8 had a much lower expression rate in the chitosan film and collagen-GAG matrices. Fibrin is known to induce IL-8 expression in human umbilical vein endothelial cells (HUVECs) [69] and a relatively high expression of IL-8 was found in a previous study utilizing primary human dermal fibroblasts on the fibrin matrix [68]. IL-6 has been linked to angiogenesis by

increasing VEGF expression [70], while IL-8 has been shown to upregulate VEGF in endothelial cells [71] and bone marrow derived MSCs [72] via signaling pathways.

A hypoxic environment creates cell stress and triggers AdMSCs to release angiogenic factors via an upregulation of HIF-1α [73]. No HIF-1α expression could be detected in cells seeded on scaffolds implying that the scaffolds themselves do not create a hypoxic environment. In the case of the chitosan scaffold, there was little cellular penetration creating a two-dimensional like environment. The pore sizes in both the fibrin and collagen-GAG matrix were likely connected and large enough for proper gas exchange. While most of the cells died quickly that were seeded on the decellularized dermis, it is hard to gauge if the scaffold itself would create a hypoxic environment.

The results suggest that the scaffold allows for proper gas exchange, which is most likely explained by the thickness of the scaffolds. Proper gas exchange should not be hindered in a scaffold less than 200 μm [74]. In larger three-dimensional scaffolds, oxygen was depleted after 7 days [75]. As Strattice is 1.5 mm thick (Table 1) this could also pose a problem for the survival of the cells. The other three scaffolds should not be affected as the thickness after cell seeding is less than 200 μm. Furthermore, MIF and VEGF are both regulated by HIF-1α [73]. Even though the control shows a higher release of VEGF, there were no significant differences between the scaffolds and controls with MIF. Therefore, there is little chance of the scaffolds creating a hypoxic environment.

The cells released factors into the medium that contributed to increased angiogenesis *in vivo* as tested in the well-established CAM assay. The CAM offers an exceptional model, as there is no immune system and the vascular networks are exposed. The conditioned medium from the collagen-GAG matrix showed no significant difference in small vessel convergence and growth from that of the VEGF positive control (Figure 6(a)). The medium from the scaffolds themselves did not differ from the observed vascular growth when using PBS, indicating that the synergistic effects of the AdMSCs with the scaffolds were the main component in the increased rates of angiogenesis. Interestingly, the high levels of VEGF and PIGF released from the chitosan film *in vitro* did not seem to have a strong effect here. As the cell seeded scaffolds were not used directly on the CAM, to prevent irritation, there could still be an effect from the other factors released by the cells on the chitosan film that inhibits vascular growth. This may also indicate inhibitory effects from the material of the chitosan film.

These results are remarkable as they show that scaffolds not only can be designed to harbor AdMSCs but also should be optimized to work synergistically with the cells in order to enhance the release of necessary and desirable factors to enhance wound healing by promoting angiogenesis, reducing healing time, and minimizing scar tissue.

5. Conclusions

In this work, a suitable delivery vehicle for AdMSCs to the wound that can secrete factors to facilitate healing was evaluated. AdMSCs in conjunction with the different scaffold types examined released angiogenic factors and chemokines necessary for wound healing. Although the decellularized dermis (Strattice) is used in clinical settings, its lack of porosity and the poor environment it creates for the AdMSCs do not make it an ideal candidate for a cell seeded, topically applied wound treatment. Cells seeded on the chitosan film secreted factors that are helpful in wound healing although the scaffold lacked the capability to let cells migrate throughout, leaving a crowded film of cells at the seeding side which could be lost upon transplantation. The ability for the scaffold to provide (i) an ideal environment for the cells to migrate, (ii) porosity that facilitates cell migration and crosstalk, and (iii) a biocompatible material are necessary to achieve proper healing *in vivo*. Through our investigative efforts, the collagen-GAG and fibrin matrices proved to have the best potential under the applied conditions as a platform for AdMSCs to enhance wound healing *in vitro*. The *in vivo* CAM data correlates with the *in vitro* data to further show the collagen-GAG and fibrin matrices are superior in working with the AdMSCs to promote angiogenesis and thus speed healing.

Conflict of Interests

The authors declare that there is no conflict of interests regarding the publication of this paper.

Acknowledgments

This project was supported by a grant from the CIRM-BMBF Early Translational II Award to José T. Egaña and Fernando A. Fierro and the FONDAP Center for Genome regulation (no. 15090007) to José T. Egaña. The authors acknowledge the efforts by Ravneet S. Kang from the Department of Biological Sciences, California State University, Sacramento, in analyzing confocal images for seeding efficiencies of the matrices.

References

[1] H. Mizuno, M. Tobita, and A. C. Uysal, "Concise review: adipose-derived stem cells as a novel tool for future regenerative medicine," *Stem Cells*, vol. 30, no. 5, pp. 804–810, 2012.

[2] K. Bieback, P. Wuchter, D. Besser et al., "Mesenchymal stromal cells (MSCs): science and f(r)iction," *Journal of Molecular Medicine*, vol. 90, no. 7, pp. 773–782, 2012.

[3] E. Zomorodian and M. Baghaban Eslaminejad, "Mesenchymal stem cells as a potent cell source for bone regeneration," *Stem Cells International*, vol. 2012, Article ID 980353, 9 pages, 2012.

[4] S. Maxson, E. A. Lopez, D. Yoo, A. Danilkovitch-Miagkova, and M. A. LeRoux, "Concise review: role of mesenchymal stem cells in wound repair," *Stem Cells Translational Medicine*, vol. 1, no. 2, pp. 142–149, 2012.

[5] S. K. Kang, I. S. Shin, M. S. Ko, J. Y. Jo, and J. C. Ra, "Journey of mesenchymal stem cells for homing: strategies to enhance efficacy and safety of stem cell therapy," *Stem Cells International*, vol. 2012, Article ID 342968, 11 pages, 2012.

[6] I. M. Barbash, P. Chouraqui, J. Baron et al., "Systemic delivery of bone marrow-derived mesenchymal stem cells to the infarcted

myocardium: feasibility, cell migration, and body distribution," *Circulation*, vol. 108, no. 7, pp. 863–868, 2003.

[7] M. F. Pittenger, "Multilineage potential of adult human mesenchymal stem cells," *Science*, vol. 284, pp. 143–147, 1999.

[8] V. Falanga, S. Iwamoto, M. Chartier et al., "Autologous bone marrow-derived cultured mesenchymal stem cells delivered in a fibrin spray accelerate healing in murine and human cutaneous wounds," *Tissue Engineering*, vol. 13, no. 6, pp. 1299–1312, 2007.

[9] M. W. Xie, R. Gorodetsky, E. D. Micevicz et al., "Marrow-derived stromal cell delivery on fibrin microbeads can correct radiation-induced wound-healing deficits," *Journal of Investigative Dermatology*, vol. 133, no. 2, pp. 553–561, 2013.

[10] Y. Xing, A. Lv, L. Wang, X. Yan, W. Zhao, and F. Cao, "Engineered myocardial tissues constructed in vivo using cardiomyocyte-like cells derived from bone marrow mesenchymal stem cells in rats," *Journal of Biomedical Science*, vol. 19, p. 6, 2012.

[11] C. Hou, L. Shen, Q. Huang et al., "The effect of heme oxygenase-1 complexed with collagen on MSC performance in the treatment of diabetic ischemic ulcer," *Biomaterials*, vol. 34, no. 1, pp. 112–120, 2013.

[12] S. Ma, N. Xie, W. Li, B. Yuan, Y. Shi, and Y. Wang, "Immunobiology of mesenchymal stem cells," *Cell Death & Differentiation*, vol. 21, no. 2, pp. 216–225, 2014.

[13] M. R. Reagan and D. L. Kaplan, "Concise review: mesenchymal stem cell tumor-homing: detection methods in disease model systems," *Stem Cells*, vol. 29, no. 6, pp. 920–927, 2011.

[14] P. R. Baraniak and T. C. McDevitt, "Stem cell paracrine actions and tissue regeneration," *Regenerative Medicine*, vol. 5, no. 1, pp. 121–143, 2010.

[15] D. F. Anthony and P. G. Shiels, "Exploiting paracrine mechanisms of tissue regeneration to repair damaged organs," *Transplantation Research*, vol. 2, article 10, 2013.

[16] G. Broughton II, J. E. Janis, and C. E. Attinger, "The basic science of wound healing," *Plastic and Reconstructive Surgery*, vol. 117, no. 7, 2006.

[17] L. Chen, E. E. Tredget, P. Y. G. Wu, and Y. Wu, "Paracrine factors of mesenchymal stem cells recruit macrophages and endothelial lineage cells and enhance wound healing," *PLoS ONE*, vol. 3, no. 4, Article ID e1886, 2008.

[18] T.-L. Yew, Y.-T. Hung, H.-Y. Li et al., "Enhancement of wound healing by human multipotent stromal cell conditioned medium: the paracrine factors and p38 MAPK activation," *Cell Transplantation*, vol. 20, no. 5, pp. 693–706, 2011.

[19] L. da Silva Meirelles, P. C. Chagastelles, and N. B. Nardi, "Mesenchymal stem cells reside in virtually all post-natal organs and tissues," *Journal of Cell Science*, vol. 119, no. 11, pp. 2204–2213, 2006.

[20] S. A. Steigman and D. O. Fauza, "Isolation of mesenchymal stem cells from amniotic fluid and placenta," *Current Protocols in Stem Cell Biology*, chapter 1, unit 1E.2, 2007.

[21] M. J. Branch, K. Hashmani, P. Dhillon, D. R. E. Jones, H. S. Dua, and A. Hopkinson, "Mesenchymal stem cells in the human corneal limbal stroma," *Investigative Ophthalmology and Visual Science*, vol. 53, no. 9, pp. 5109–5116, 2012.

[22] A. Atala, F. Kurtis Kasper, and A. G. Mikos, "Engineering complex tissues," *Science Translational Medicine*, vol. 4, no. 160, Article ID 160rv12, 2012.

[23] G. Akpinar, M. Kasap, A. Aksoy, G. Duruksu, G. Gacar, and E. Karaoz, "Phenotypic and proteomic characteristics of human dental pulp derived mesenchymal stem cells from a natal, an exfoliated deciduous, and an impacted third molar tooth," *Stem Cells International*, vol. 2014, Article ID 457059, 19 pages, 2014.

[24] G. Chen, A. Yue, Z. Ruan et al., "Human umbilical cord-derived mesenchymal stem cells do not undergo malignant transformation during long-term culturing in serum-free medium," *PLoS ONE*, vol. 9, no. 6, Article ID e98565, 2014.

[25] L. J. Harris, P. Zhang, H. Abdollahi et al., "Availability of adipose-derived stem cells in patients undergoing vascular surgical procedures," *The Journal of Surgical Research*, vol. 163, no. 2, pp. e105–e112, 2010.

[26] A. Mirsaidi, K. N. Kleinhans, M. Rimann et al., "Telomere length, telomerase activity and osteogenic differentiation are maintained in adipose-derived stromal cells from senile osteoporotic SAMP6 mice," *Journal of Tissue Engineering and Regenerative Medicine*, vol. 6, no. 5, pp. 378–390, 2012.

[27] H.-T. Chen, M.-J. Lee, C.-H. Chen et al., "Proliferation and differentiation potential of human adipose-derived mesenchymal stem cells isolated from elderly patients with osteoporotic fractures," *Journal of Cellular and Molecular Medicine*, vol. 16, no. 3, pp. 582–593, 2012.

[28] L. Aust, B. Devlin, S. J. Foster et al., "Yield of human adipose-derived adult stem cells from liposuction aspirates," *Cytotherapy*, vol. 6, no. 1, pp. 7–14, 2004.

[29] B. M. Strem, K. C. Hicok, M. Zhu et al., "Multipotential differentiation of adipose tissue-derived stem cells," *The Keio Journal of Medicine*, vol. 54, no. 3, pp. 132–141, 2005.

[30] D. L. Crandall, G. J. Hausman, and J. G. Kral, "A review of the microcirculation of adipose tissue: anatomic, metabolic, and angiogenic perspectives," *Microcirculation*, vol. 4, no. 2, pp. 211–232, 1997.

[31] C.-S. Lin, Z.-C. Xin, C.-H. Deng, H. Ning, G. Lin, and T. F. Lue, "Defining adipose tissue-derived stem cells in tissue and in culture," *Histology and Histopathology*, vol. 25, no. 6, pp. 807–815, 2010.

[32] C.-S. Lin, G. Lin, and T. F. Lue, "Allogeneic and xenogeneic transplantation of adipose-derived stem cells in immunocompetent recipients without immunosuppressants," *Stem Cells and Development*, vol. 21, no. 15, pp. 2770–2778, 2012.

[33] F. Baron and R. Storb, "Mesenchymal stromal cells: a new tool against graft-versus-host disease?" *Biology of Blood and Marrow Transplantation*, vol. 18, no. 6, pp. 822–840, 2012.

[34] E.-J. Kim, N. Kim, and S.-G. Cho, "The potential use of mesenchymal stem cells in hematopoietic stem cell transplantation," *Experimental & Molecular Medicine*, vol. 45, no. 1, p. e2, 2013.

[35] H. Brem, J. Maggi, D. Nierman et al., "High cost of stage IV pressure ulcers," *The American Journal of Surgery*, vol. 200, no. 4, pp. 473–477, 2010.

[36] L. Gould, P. Abadir, H. Brem et al., "Chronic wound repair and healing in older adults: current status and future research," *Wound Repair and Regeneration*, vol. 23, no. 1, pp. 1–13, 2015.

[37] J. T. Egaña, F. A. Fierro, S. Krüger et al., "Use of human mesenchymal cells to improve vascularization in a mouse model for scaffold-based dermal regeneration," *Tissue Engineering Part A*, vol. 15, no. 5, pp. 1191–1200, 2009.

[38] N. Zippel, M. Schulze, and E. Tobiasch, "Biomaterials and mesenchymal stem cells for regenerative medicine," *Recent Patents on Biotechnology*, vol. 4, no. 1, pp. 1–22, 2010.

[39] S. Danner, M. Kremer, A. E. Petschnik et al., "The use of human sweat gland-derived stem cells for enhancing vascularization during dermal regeneration," *Journal of Investigative Dermatology*, vol. 132, no. 6, pp. 1707–1716, 2012.

[40] D. Ribatti, B. Nico, A. Vacca, and M. Presta, "The gelatin sponge-chorioallantoic membrane assay," *Nature Protocols*, vol. 1, no. 1, pp. 85–91, 2006.

[41] T. Thomson, "Product development," in *Design and Applications of Hydrophilic Polyurethanes Medical, Agricultural, and Other Applications*, Technomic Publishing Co., Lancaster, Pa, USA, 2000, http://marc.crcnetbase.com/isbn/9781420012897.

[42] C. A. Schneider, W. S. Rasband, and K. W. Eliceiri, "NIH Image to ImageJ: 25 years of image analysis," *Nature Methods*, vol. 9, no. 7, pp. 671–675, 2012.

[43] D. S. Dohle, S. D. Pasa, S. Gustmann et al., "Chick ex ovo culture and ex ovo CAM assay: how it really works," *Journal of Visualized Experiments*, no. 33, 2009.

[44] W. M. Jackson, L. J. Nesti, and R. S. Tuan, "Concise review: clinical translation of wound healing therapies based on mesenchymal stem cells," *Stem Cells Translational Medicine*, vol. 1, no. 1, pp. 44–50, 2012.

[45] L. Shin and D. A. Peterson, "Human mesenchymal stem cell grafts enhance normal and impaired wound healing by recruiting existing endogenous tissue stem/progenitor cells," *Stem Cells Translational Medicine*, vol. 2, no. 1, pp. 33–42, 2013.

[46] S. N. Dash, N. R. Dash, B. Guru, and P. C. Mohapatra, "Towards reaching the target: clinical application of mesenchymal stem cells for diabetic foot ulcers," *Rejuvenation Research*, vol. 17, no. 1, pp. 40–53, 2014.

[47] T. Ma, W. L. Grayson, M. Fröhlich, and G. Vunjak-Novakovic, "Hypoxia and stem cell-based engineering of mesenchymal tissues," *Biotechnology Progress*, vol. 25, no. 1, pp. 32–42, 2009.

[48] S. Tully-Dartez, H. E. Cardenas, and P.-F. S. Sit, "Pore characteristics of chitosan scaffolds studied by electrochemical impedance spectroscopy," *Tissue Engineering Part C: Methods*, vol. 16, no. 3, pp. 339–345, 2010.

[49] T. Dai, M. Tanaka, Y.-Y. Huang, and M. R. Hamblin, "Chitosan preparations for wounds and burns: antimicrobial and wound-healing effects," *Expert Review of Anti-Infective Therapy*, vol. 9, no. 7, pp. 857–879, 2011.

[50] M. W. Xie, R. Gorodetsky, E. D. Micewicz et al., "Marrow-derived stromal cell delivery on fibrin microbeads can correct radiation-induced wound-healing deficits," *Journal of Investigative Dermatology*, vol. 133, pp. 553–561, 2013.

[51] P. J. Amos, A. M. Bailey, H. Shang, A. J. Katz, M. B. Lawrence, and S. M. Peirce, "Functional binding of human adipose-derived stromal cells: Effects of extraction method and hypoxia pretreatment," *Annals of Plastic Surgery*, vol. 60, no. 4, pp. 437–444, 2008.

[52] B. A. C. Harley, H.-D. Kim, M. H. Zaman, I. V. Yannas, D. A. Lauffenburger, and L. J. Gibson, "Microarchitecture of three-dimensional scaffolds influences cell migration behavior via junction interactions," *Biophysical Journal*, vol. 95, no. 8, pp. 4013–4024, 2008.

[53] H. Yasuda, S. Kuroda, H. Shichinohe, S. Kamei, R. Kawamura, and Y. Iwasaki, "Effect of biodegradable fibrin scaffold on survival, migration, and differentiation of transplanted bone marrow stromal cells after cortical injury in rats: laboratory investigation," *Journal of Neurosurgery*, vol. 112, no. 2, pp. 336–344, 2010.

[54] J. King, J. D. Hayes, and B. Richmond, "Repair of giant subcostal hernia using porcine acellular dermal matrix (Strattice) with bone anchors and pedicled omental flap coverage: a case report," *Journal of Medical Case Reports*, vol. 7, article 258, 2013.

[55] S. B. Glasberg and D. Light, "AlloDerm and strattice in breast reconstruction: a comparison and techniques for optimizing outcomes," *Plastic and Reconstructive Surgery*, vol. 129, no. 6, pp. 1223–1233, 2012.

[56] J. N. Pozner, J. B. White, and M. I. Newman, "Use of porcine acellular dermal matrix in revisionary cosmetic breast augmentation," *Aesthetic Surgery Journal*, vol. 33, no. 5, pp. 681–690, 2013.

[57] U. Mirastschijski, C. Kerzel, R. Schnabel, S. Strauss, and K.-H. Breuing, "Complete horizontal skin cell resurfacing and delayed vertical cell infiltration into porcine reconstructive tissue matrix compared to bovine collagen matrix and human dermis," *Plastic and Reconstructive Surgery*, vol. 132, no. 4, pp. 861–869, 2013.

[58] G. A. Monteiro, N. L. Rodriguez, A. I. Delossantos, and C. T. Wagner, "Short-term in vivo biological and mechanical remodeling of porcine acellular dermal matrices," *Journal of Tissue Engineering*, vol. 4, no. 1, pp. 1–11, 2013.

[59] N. G. Singer and A. I. Caplan, "Mesenchymal stem cells: mechanisms of inflammation," *Annual Review of Pathology: Mechanisms of Disease*, vol. 6, pp. 457–478, 2011.

[60] R. E. Newman, D. Yoo, M. A. LeRoux, and A. Danilkovitch-Miagkova, "Treatment of inflammatory diseases with mesenchymal stem cells," *Inflammation and Allergy—Drug Targets*, vol. 8, no. 2, pp. 110–123, 2009.

[61] C. J. Bishop, J. Kim, and J. J. Green, "Biomolecule delivery to engineer the cellular microenvironment for regenerative medicine," *Annals of Biomedical Engineering*, vol. 42, pp. 1557–1572, 2014.

[62] U. Hersel, C. Dahmen, and H. Kessler, "RGD modified polymers: biomaterials for stimulated cell adhesion and beyond," *Biomaterials*, vol. 24, no. 24, pp. 4385–4415, 2003.

[63] K. M. Providence, S. P. Higgins, A. Mullen et al., "SERPINE1 (PAI-1) is deposited into keratinocyte migration 'trails' and required for optimal monolayer wound repair," *Archives of Dermatological Research*, vol. 300, no. 6, pp. 303–310, 2008.

[64] P. Carmeliet, L. Moons, A. Luttun et al., "Synergism between vascular endothelial growth factor and placental growth factor contributes to angiogenesis and plasma extravasation in pathological conditions," *Nature Medicine*, vol. 7, no. 5, pp. 575–583, 2001.

[65] S. P. Blaber, R. A. Webster, C. J. Hill et al., "Analysis of in vitro secretion profiles from adipose-derived cell populations," *Journal of Translational Medicine*, vol. 10, no. 1, article 172, 2012.

[66] M. Tjwa, A. Luttun, M. Autiero, and P. Carmeliet, "VEGF and PlGF: two pleiotropic growth factors with distinct roles in development and homeostasis," *Cell and Tissue Research*, vol. 314, no. 1, pp. 5–14, 2003.

[67] M. R. Duncan and B. Berman, "Stimulation of collagen and glycosaminoglycan production in cultured human adult dermal fibroblasts by recombinant human interleukin 6," *Journal of Investigative Dermatology*, vol. 97, no. 4, pp. 686–692, 1991.

[68] E. García-Gareta, N. Ravindran, V. Sharma, S. Samizadeh, and J. F. Dye, "A novel multiparameter *in vitro* model of three-dimensional cell ingress into scaffolds for dermal reconstruction to predict *in vivo* outcome," *BioResearch Open Access*, vol. 2, no. 6, pp. 412–420, 2013.

[69] J. Qi, S. Goralnick, and D. L. Kreutzer, "Fibrin regulation of interleukin-8 gene expression in human vascular endothelial cells," *Blood*, vol. 90, no. 9, pp. 3595–3602, 1997.

[70] T. Cohen, D. Nahari, L. W. Cerem, G. Neufeld, and B.-Z. Levin, "Interleukin 6 induces the expression of vascular endothelial growth factor," *The Journal of Biological Chemistry*, vol. 271, no. 2, pp. 736–741, 1996.

[71] D. Martin, R. Galisteo, and J. S. Gutkind, "CXCL8/IL8 stimulates vascular endothelial growth factor (VEGF) expression

and the autocrine activation of VEGFR2 in endothelial cells by activating NFkappaB through the CBM (Carma3/Bcl10/Malt1) complex," *The Journal of Biological Chemistry*, vol. 284, no. 10, pp. 6038–6042, 2009.

[72] Y. Hou, C. H. Ryu, J. A. Jun, S. M. Kim, C. H. Jeong, and S.-S. Jeun, "IL-8 enhances the angiogenic potential of human bone marrow mesenchymal stem cells by increasing vascular endothelial growth factor," *Cell Biology International*, vol. 38, pp. 1050–1059, 2014.

[73] Y. Asare, M. Schmitt, and J. Bernhagen, "The vascular biology of macrophage migration inhibitory factor (MIF): expression and effects in inflammation, atherogenesis and angiogenesis," *Thrombosis and Haemostasis*, vol. 109, no. 3, pp. 391–398, 2013.

[74] R. E. McClelland and R. N. Coger, "Use of micropathways to improve oxygen transport in a hepatic system," *Journal of Biomechanical Engineering*, vol. 122, no. 3, pp. 268–273, 2000.

[75] E. Volkmer, S. Otto, H. Polzer et al., "Overcoming hypoxia in 3D culture systems for tissue engineering of bone in vitro using an automated, oxygen-triggered feedback loop," *Journal of Materials Science: Materials in Medicine*, vol. 23, no. 11, pp. 2793–2801, 2012.